

Ph.D. Thesis

**REALISATION OF A TARGET CLASSIFIER FOR NOISE
SOURCES IN THE OCEAN**

Submitted to

THE COCHIN UNIVERSITY OF SCIENCE AND TECHNOLOGY

in partial fulfilment of the requirement for the award of the degree of

Doctor of Philosophy

by

SUPRIYA M.H.

Under the guidance of

Prof. (Dr.) P. R. S. Pillai

DEPARTMENT OF ELECTRONICS
COCHIN UNIVERSITY OF SCIENCE AND TECHNOLOGY
COCHIN – 682 022, INDIA

OCTOBER 2007

REALISATION OF A TARGET CLASSIFIER FOR NOISE SOURCES IN THE OCEAN

Ph.D. Thesis in the field of Ocean Electronics

Author

Supriya M.H.

Lecturer

DEPARTMENT OF ELECTRONICS

COCHIN UNIVERSITY OF SCIENCE AND TECHNOLOGY

Cochin,– 682 022, India

e-mail: supriya@cusat.ac.in

Research Advisor

Dr. P. R. S. Pillai

Professor

DEPARTMENT OF ELECTRONICS

COCHIN UNIVERSITY OF SCIENCE AND TECHNOLOGY

Cochin,– 682 022, India

e-mail : prspillai@cusat.ac.in

October, 2007



COCHIN UNIVERSITY OF SCIENCE AND TECHNOLOGY
DEPARTMENT OF ELECTRONICS
Thrissakka, Cochin – 682 022

CERTIFICATE

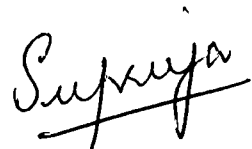
This is to certify that this thesis entitled, *Realisation of a Target Classifier for Noise Sources in the Ocean* is a bonafide record of the research work carried out by Ms. Supriya M.H. under my supervision in the Department of Electronics, Cochin University of Science and Technology. The result presented in this thesis or parts of it have not been presented for any other degree(s).

Prof. (Dr.) P.R.S. Pillai
Supervising Guide

Cochin - 682022
26th October 2007

DECLARATION

I hereby declare that the work presented in this thesis entitled *Realisation of a Target Classifier for Noise Sources in the Ocean* is a bonafide record of the research work carried out by me under the supervision of Dr. P.R.S. Pillai, Professor, in the Department of Electronics, Cochin University of Science and Technology. The result presented in this thesis or parts of it have not been presented for other degree.



SUPRIYA M.H.

Cochin – 22
26th October 2007

Acknowledgements

I would like to express my deepest sense of gratitude to my research guide, **Prof. (Dr.) P.R.S. Pillai**, Professor, Department of Electronics, Cochin University of Science and Technology for his excellent guidance and incessant encouragement. It has been a great pleasure and privilege to work under him and he was always there when I needed help.

I am much grateful to **Prof, (Dr.) K. Vasudevan**, Prof. & Head, Department of Electronics, Cochin University of Science and Technology, for the whole hearted support and constant encouragement.

I would like to express my sincere thanks to **Prof (Dr). K. G. Nair and Prof.(Dr.) K.G. Balakrishnan**, former Heads, Department of Electronics for their valuable suggestions and constant support and encouragement rendered to me.

Sincere thanks are due to **Prof. (Dr.) K.T. Mathew, Prof.(Dr.) P.Mohanan, and Dr. C. K. Aanandan**, Department of Electronics, Cochin University of Science and Technology, for providing adequate help and fruitful suggestions.

I take this opportunity to express my sincere thanks to **Dr. Tessamma Thomas, Mr. James Kurian**, Readers, Department of Electronics, for the constant encouragement rendered to me.

I immensely acknowledge the financial assistance rendered by Naval Research Board, New Delhi for carrying out some of the activities reported in this thesis and special thanks are also due to **CMDE R Bhushan**, Secy NRB and **CDR S K Thakur**, Dy Dir NRB and for their encouragements for carrying out my work.

I would like to give a special word of thanks to the research fellows in the *Centre for Ocean Electronics (CUCENTOL)*, Mr. Mohan Kumar K., Mr. Jinto George, Mr. Prajas John, Mr. Ananthakrishnan V., Ms. C. Prabha and Mr. S. Maheswaran.

A word of mention is deserved by Dr. Lethakumari B., Mr. Shaheer K., Mr. Mahendran M.G., Ms. Presty Joseph, Mr. Deepu V., Dr. Mani T.K., Dr. Bindu G., and Ms. Sreedevi K. Menon who all were there for me as a good support throughout my research period.

I thankfully bear in mind the sincere co-operation and support I received from the **library and administrative staff** of the Department.

I also take this opportunity to thank all the **M.Tech. and M.Sc. students**, Department of Electronics, Cochin University of Science and Technology who contributed and helped me in completing my thesis.

Last, but not least, it is beyond words to express my gratitude to my family members especially to my husband **Mr. Subash Chandra Bose M. R.** and my kids **Hari** and **Govind** for their sacrifice in connection with preparation of my thesis. I am sure I could not have completed this great task without their support and cooperation.

SUPRIYA M.H
26th October 2007.

Contents

Page No

<i>Acknowledgements</i>	<i>ix</i>
<i>Contents</i>	<i>xi</i>
<i>List of Figures</i>	<i>xv</i>
<i>List of Tables</i>	<i>xix</i>
<i>Abbreviations</i>	<i>xxi</i>
CHAPTER 1	1
INTRODUCTION	1
1.1 Definition of Sonar	1
1.2 Types of Sonar Systems	2
1.2.1 Active Sonar	2
1.2.2 Passive Sonar.....	6
1.3 Sonar Equations	7
1.3.1 Active and Passive Sonar Equations	9
1.4 Factors Affecting the Sonar Performance	11
1.4.1 Environmental Factors	11
1.4.2 Reverberation	12
1.4.3 Target Characteristics	12
1.4.4 Other Noises.....	13
1.5 Noise Sources in the ocean	13
1.5.1 Natural Sources of Ambient Noise	13
1.5.2 Manmade Noises	15
1.6 Types of Underwater Noises	17
1.6.1 Sources of Radiated Noise.....	18
1.7 Classifiers	19
1.8 Summary	22
CHAPTER 2	23
REVIEW OF PAST WORK	23
2.1 Introduction	23
2.2 Characteristic Signatures of Typical Ocean Noise	25
2.3 Classes of features	30
2.3.1 Spectral Features	30
2.3.2 Cepstral Features	37
2.3.3 Bispectral Features	45
2.4 Classifiers	50
2.4.1 Statistical Classifiers	50
2.4.2 Expert System Classifiers.....	51
2.4.3 Neural Network Classifiers	52
2.4.4 Fuzzy Classifiers	60
2.4.5 Sonar Signal Processor based Classifiers	61
2.4.6 Recent Trends.....	62
2.5 Summary	66

CHAPTER 3	67
METHODOLOGY	67
3.1 Introduction	68
3.2 Basic Model of the Proposed Classifier	70
3.3 Extraction of source signatures	71
3.3.1 Spectral Features	71
3.3.2 Cepstral Features	73
3.3.3 Bispectral Features	75
3.4 Compilation of Knowledge Base	76
3.5 Inference System	77
3.5.1 Feature Vector	77
3.5.2 Feature Selection	77
3.6 Summary	79
CHAPTER 4	80
Spectral and Cepstral Analysis	80
4.1 Introduction	81
4.1.1 Sources of Ambient Noise	82
4.2 Power spectral estimation	83
4.2.1 Definitions and Basics	84
4.3 Spectral Estimation Methods	86
4.3.1 Classical Methods.....	86
4.3.2 Parametric Estimators.....	87
4.3.3 AR Spectral Estimation	92
4.3.4 ARMA Spectral Estimation.....	98
4.4 Analysis of Noise Signals on the Spectral Perspective	98
4.5 Spectral Features	115
4.6 Cepstral Analysis	117
4.6.1 Cepstral Plots.....	120
4.7 Mel Frequency Cepstral Coefficients	127
4.7.1 MFCC Estimation	127
4.7.2 Window function	131
4.7.3 Vector Quantization	132
4.8 Cepstral Features	135
4.9 Summary	138
CHAPTER 5	139
BISPECTRAL ESTIMATION	139
5.1 Introduction	140
5.1.1 Theory and Definitions.....	140
5.2 Bispectrum	145
5.2.1 Energy Dependence of Bispectrum	146
5.3 Bicoherence	147
5.3.1 Linear and Gaussian Models	148
5.4 Properties of Bispectrum	150

5.5	Bispectral Estimators	153
5.5.1	Conventional Bispectral Estimators	154
5.6	Quadratic Phase Coupling (QPC).....	156
5.6.1	Theoretical Background	156
5.7	Data Analysis and Results.....	161
5.8	Bispectral Features	164
5.9	Summary	165
CHAPTER 6		167
THE TARGET CLASSIFIER.....		167
6.1	Introduction	168
6.2	Knowledge Base	170
6.2.1	Noise Data	170
6.2.2	Data Analysis	178
6.2.3	Updating of Knowledge Base.....	178
6.3	Generation of Feature Vector.....	179
6.4	Generation of Target Feature Record	180
6.5	Prototype Target Classifier.....	181
6.5.1	Feature Vector based Identifier	182
6.5.2	Hidden Markov Model Based Classifier	186
6.6	Decision System.....	198
6.6.1	Degenerative Unmixing Estimations Technique	198
6.7	Results and Discussions.....	199
6.8	Summary	208
CHAPTER 7		210
Conclusions.....		210
7.1	Highlights of the Thesis	211
7.1.1	Need and Requirement of a Computer Assisted Classifier.....	211
7.1.2	Preparation of a State-of-the-art Literature.....	211
7.1.3	Feature Vector Based Classifier	212
7.1.4	Extraction of Spectral Features	212
7.1.5	Extraction of Cepstral Features	212
7.1.6	Extraction of Bispectral Features	213
7.1.7	Generation of Target Feature Record	213
7.1.8	Classifier Based on Hierarchical Target Trimming Approach.	213
7.1.9	Towards Improving the Performance of the Classifier.....	214
7.1.10	DUET Algorithm for Resolving Contentions.....	214
7.2	Future Scope for Research.....	214
7.2.1	Prototype System.....	214
7.2.2	Realistic Field Data	215
7.2.3	Real-time Target Classifiers	215
7.2.4	Hardware Based Feature Vector Generator	215
7.2.5	Handling Multiple Target Scenario	216
7.2.6	Modeling other features using HMM	216
7.3	Summary	216

Page No

References..... 217
Publications brought out in the field of research..... 231
Other Publications..... 233
Subject Index 236

List of Figures

	Page No
Fig. 1.1 Principle of Active Sonar	3
Fig. 1.2 Scenario using Active sonar	4
Fig. 1.3 Scenario using Passive sonar	8
Fig. 3.1 Target Classifier	70
Fig. 4.1 Conceptual Diagram of sources of Ambient Noise	82
Fig. 4.2 Flow chart for the generic estimation of AR PSD	95
Fig. 4.3 Flowchart for the Generic MA PSD Estimation	97
Fig. 4.4 Flowchart for the Generic ARMA PSD Estimation	99
Fig. 4.5 GUI of the Spectral Estimator	100
Fig. 4.6 AR Spectrum of a Merchant Vessel using Yule Walker	102
Fig. 4.7 MA Spectrum of a Merchant Vessel using Yule Walker	103
Fig. 4.8 ARMA Spectrum of Merchant Vessel using Yule Walker	104
Fig. 4.9 AR Spectrum of a Merchant Vessel using Burg	104
Fig. 4.10 AR Spectrum of a Merchant Vessel using Covariance	105
Fig. 4.11 Spectrum of a Merchant Vessel using Mod. Covariance	105
Fig. 4.12 AR Spectrum of a Commercial Vessel using Yule Walker	105
Fig. 4.13 AR Spectrum of a Commercial Vessel using Burg	106
Fig. 4.14 AR Spectrum of a Commercial Vessel using Cov.Algo	106
Fig. 4.15 AR Spectrum of a Commercial Vessel using Mod. Cov	107
Fig. 4.16 MA Spectrum of a Commercial Vessel using Yule-Walker	107
Fig. 4.17 AR Spectrum of a Tug Boat using Yules	108
Fig. 4.18 MA Spectrum of a Tug Boat using Yules	109
Fig. 4.19 ARMA Spectrum of a Tug Boat using Yules	109
Fig. 4.20 AR Spectrum of a Torpedo using Yule Walker	110
Fig. 4.21 AR Spectrum of a Humpback Whale using Yule Walker	111
Fig. 4.22 MA Spectrum of a Humpback Whale using Yule Walker	111
Fig. 4.23 ARMA Spectrum of a Humpback Whale using Yule Walker	112
Fig. 4.24 AR Spectrum of a Pinnipeds using Yule Walker	113
Fig. 4.25 ARMA Spectrum of a Pinnipeds using Yule Walker	113
Fig. 4.26 AR Spectrum of a Beluga Whale using Yule Walker	114

Fig. 4.27 AR Spectrum of a Lightning using Yule Walker	114
Fig. 4.28 Illustration of Extraction of Spectral Features	116
Fig. 4.29 Steps involved in computing Real Cepstrum	119
Fig. 4.30 Steps involved in getting the complex cepstrum	120
Fig. 4.31 Characterisation of 3 Blade Engine Noise	121
Fig. 4.32 Characterisation of a Commercial Vessel	121
Fig. 4.33 Characterisation of Merchant Vessel	122
Fig. 4.34 Characterisation of Tug Boat	122
Fig. 4.35 Characterisation of an Engine	123
Fig. 4.36 Characterisation of Torpedo	123
Fig. 4.37 Characterisation of Blue Grunt (a marine mammal)	124
Fig. 4.38 Characterisation of Whale (a marine mammal)	124
Fig. 4.39 Characterisation of Humpback Whale (a marine mammal)	125
Fig. 4.40 Characterisation of Pinnipeds	125
Fig. 4.41 Characterisation of Rain	126
Fig. 4.42 Characterisation of Seal	126
Fig. 4.43 The Mel-scale	128
Fig. 4.44 Mel-Frequency filter bank on a linear frequency (Hz) scale	129
Fig. 4.45 Procedure for vector quantization	134
Fig. 4.46 Illustration of the steps involved in estimation of MFCC	136
Fig. 5.1 Bispectrum of Gaussian Noise	146
Fig. 5.2 (a) Bispectrum of the Gaussian signal amplified by 2	147
Fig. 5.2 (b) Bispectrum of the Gaussian signal amplified by 100	147
Fig. 5.3(a) Bicoherence of the signal amplified by 2	148
Fig. 5.3(b) Bicoherence of the signal amplified by 100	148
Fig. 5.4 (a) Symmetry regions of third-order moments	151
Fig. 5.4 (b) Symmetry regions of Bispectrum	151
Fig. 5.5 Model of a Nonlinear System	156
Fig. 5.6 Flowchart of the two stage bispectrum QPC estimator	158
Fig. 5.7 Bispectrum contour plot without QPC	159
Fig. 5.8 Bispectrum contour Phase Plot without QPC	159
Fig. 5.9 Magnitude contour plot of Bispectrum	160
Fig. 5.10 Phase contour Plot of	160
Fig. 5.11 3D plot of Bispectrum corresponding to the magnitude plot in Fig. 5.9	160

Fig. 5.12 Mesh Plot for 3 Blade without filtering	161
Fig. 5.13 Contour Plot of 3 Blade without filtering	161
Fig. 5.14 Mesh Plot for 3 Blade with 30 % Filter Threshold	162
Fig. 5.15 Contour Plot for 3 Blade with 30 % Filter Threshold	162
Fig. 5.16 Mesh Plot for Merchant Vessel without filtering	163
Fig. 5.17 Contour Plot for Merchant Vessel without filtering	163
Fig. 5.18 Mesh Plot for Merchant Vessel with 30 % FTL	163
Fig. 5.19 Contour Plot for Merchant Vessel with 30 % FTL	163
Fig. 5.20 Mesh Plot for Humpback Whale without filtering	164
Fig. 5.21 Mesh Plot for Whale without filtering	164
Fig. 5.22 Mesh Plot for Damsel without filtering	164
Fig. 5.23 Mesh Plot for Commercial Vessel without filtering	164
Fig. 5.24 Depicts the procedure for generating the bispectral features	165
Fig. 6.1 Block Schematic of the Classifier	169
Fig. 6.2 Noise spectrum of a typical Surfaced Submarine	172
Fig. 6.3 Noise Spectrum of a Submarine Propeller at 30ft and 50ft	172
Fig. 6.4 Noise Spectrum of an average submarine & destroyer at 20 kHz	173
Fig. 6.5 Comparison of the Noise Spectra of torpedo and submarine	173
Fig. 6.6 Beluga Whale	176
Fig. 6.7 Humpback Whale	176
Fig. 6.8 Harbour Seal	177
Fig. 6.9 Sea Robin	178
Fig. 6.10 Various techniques for extracting the target features	179
Fig. 6.11 Flowchart for generation of TFR	180
Fig. 6.12 Flowchart of class associations prior to HMM design	186
Fig. 6.13 Logarithmic band used	189
Fig. 6.14 The Feature Extraction system using basis projection	191
Fig. 6.15 HMM for a given class i	195
Fig. 6.16 Principle of HMM based Classifier	196
Fig. 6.17 Block Diagram of Classifier Using Spectrum Basis Projection Feature	197
Fig. 6.18 Basic Block Diagram	198
Fig. 6.19 Two channel hydrophone arrangements	199
Fig. 6.20 PSD of the noise data waveform of a surface craft with and without additive ocean wave noise	200

Fig. 6.21 Output screen shot of the Feature Extractor GUI	201
Fig. 6.22 Mesh Plot for Engine without filtering	202
Fig. 6.23 Contour Plot for Engine without filtering	202
Fig. 6.24 Mesh Plot for Engine with 30 % Filter Threshold	202
Fig. 6.25 Contour Plot for Engine with 30 % Filter Threshold	202
Fig. 6.26 Prototype Target Identifier	204
Fig. 6.27 Projection of NSE on Basis Components for Torpedo	205
Fig. 6.28 Projection of NSE on Basis Components for Whale	206
Fig. 6.29 Illustration of the HMM Based Classifier (Torpedo)	207
Fig. 6.30 Illustration of the HMM Based Classifier (Whale)	207
Fig. 6.31 Regeneration of spectra from a composite mixture (Case 1)	207
Fig. 6.32 Regeneration of spectra from a composite mixture (Case 2)	208

List of Tables

	Page No
Table 4.1 Comp. of various algorithms to estimate the AR parameters	94
Table 4.2 Table of MFCC for two different noise sources	137
Table 5.1 Effect of Filter Threshold on the Number of Coupling Frequencies	162
Table 6.1 Edge Frequencies in [Hz] for Logarithmic Bands	188
Table 6.2 Weighting matrix with 12 columns and eight rows.	189
Table 6.3 Spectral features with and without additive ambient noise	200
Table 6.4 Bispectral Features of Engine	203
Table 6.5 Results of comparison of the three Classifiers	204

Abbreviations

ANN	- Artificial Neural Network
AR	- AutoRegressive
ARMA	- AutoRegressive Moving Average
CGF	- Cumulant Generating Function
DARPA	- Defence Advanced Research Projects Agency
DI	- Directivity Index
DT	- Detection Threshold
DUET	- Degenerate Unmixing Estimation Technique
GUI	- Graphical User Interface
HMMs	- Hidden Markov Model
HOS	- Higher Order Spectra
LPC	- Linear Predictive Coding
MGF	- Moment Generating Function
MLSA	- Mel Log Spectrum Approximation
NL	- Self Noise Level; Ambient Noise Level
PSD	- Power Spectral Density
QPC	- Quadratic Phase Coupling
RL	- Reverberation Level
SL	- Projector/ Target Source Level
SNR	- Signal-to-Noise ratio
SSP	- Split Spectrum Processing
TFR	- Target Feature Record
TL	- Transmission Loss
TMA	- Target Motion Analysis
TOA	- Time Of Arrival
TS	- Target Strength
VQ	- Vector Quantization

CHAPTER 1

INTRODUCTION

Sonars, which are devices for remotely detecting and locating objects underwater, play a key role in ocean research. Since its introduction during the early half of the 20th century, it has been undergoing various evolutionary stages and has remained as one of the priority areas of research in developed, developing as well as underdeveloped countries. Sonar uses sound propagation underwater, to navigate, communicate or detect other vessels or targets of interest. This chapter touches upon the different types of sonars and various noise sources in the ocean as well as the need and requirement of a classifier for identifying them. The underlying principle of operation of the proposed classifier, which involves extraction of the various spectral, cepstral and bispectral features, is also briefly introduced in this chapter.

The study of underwater sound or hydro-acoustics, has gained considerable significance due to its strategic as well as commercial importance. Sonars, which are devices for remotely detecting and locating objects underwater, play a key role in ocean research.

1.1 *Definition of Sonar*

The term "SONAR" is defined as the method or equipment that uses underwater sound propagation to explore the presence, location or nature of objects in the sea. It is an acronym for "*SOund NAVigation and Ranging*"

and uses sound propagation underwater, to navigate, communicate or detect other vessels or targets of interest.

1.2 *Types of Sonar Systems*

Sonar, which can be used as a means for the detection and localization of underwater targets, can be classified into two broad categories:

- Active sonars are devices that, generate sound waves of specific, controlled frequencies, and listen for the echoes of these emitted sound signals returned by remote objects underwater.
- Passive sonars are essentially listening devices that record the sounds emitted by the objects underwater. Such devices can be used to detect seismic occurrences, early warning of ships, submarines, torpedoes, etc. and marine creatures that emit characteristic sounds of its own.

Modern naval warfare makes extensive use of both active and passive sonars from various platforms like water-borne vessels, aircrafts and fixed installations. The usefulness of active and passive sonar systems depends on the characteristics of the target of interest. Although in World War II active sonar was mainly used, with the advent of noisy nuclear submarines, passive sonar was preferred for early detection and warning applications.

1.2.1 Active Sonar

Active sonar, as illustrated in Fig.1.1, involves the transmission of an acoustic signal which, when reflected from a target, provides the sonar receiver with a basis for detection, estimation and localization of targets

underwater. A signal, in the form of a sound pulse, called ping, is emitted and the wave then travels in various directions and hits the objects on its propagation path.

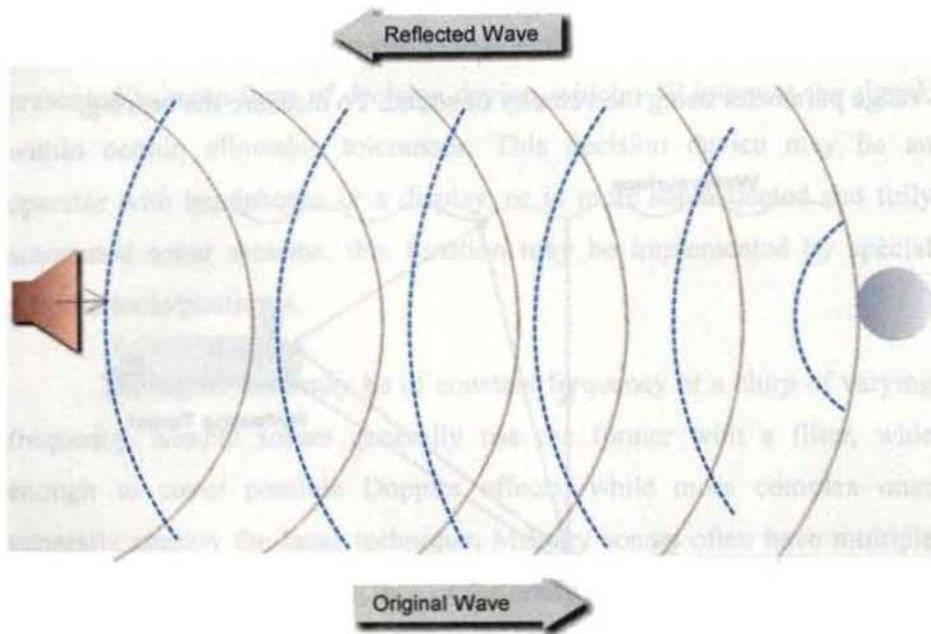


Fig. 1.1 Principle of Active Sonar

The incident wave is then reflected and some of the energy will travel back to the transmitting system. The echo, alongwith other factors such as the frequency, energy of the received signal, depth, water temperature, etc., will enable the sonar system to compute the position of the target of interest, with vanishingly small errors.

Ping of acoustic signals generated using a Sonar Projector working in conjunction with the signal generator, power amplifier and transducer array, possibly with a beam former helps in target detection and estimation

Chapter 1 Introduction

as depicted in Fig.1.2. Acoustic signals can as well be generated underwater by other means such as detonation of explosives.

To estimate the distance of the target of interest, the time elapsed between the transmission and reception of a signal is converted into the range parameter using the velocity of sound. To measure the bearing,

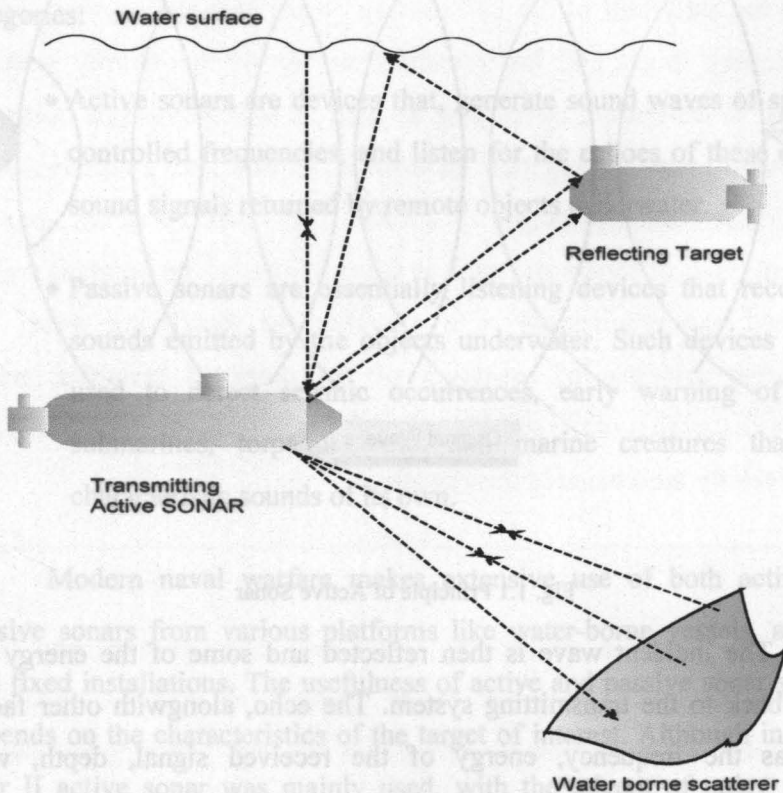


Fig. 1.2 Scenario using Active sonar

several hydrophones are used, which measure the relative time of arrival (TOA) of the reflected signal to each, or by measuring the relative amplitude of beams formed through beamforming, with an array of hydrophones. Beamforming is a technique that is used to manipulate the directionality, or sensitivity of a radiation pattern. When receiving a signal,

Realisation of a Target Classifier for Noise Sources in the Ocean

it can increase the receiver sensitivity in the direction of the desired signals, while it decreases the sensitivity in the direction of interference and unwanted noises. The use of an array reduces the spatial coverage and hence to achieve wider coverage, multi-beam systems are used. The echo returns together with noise is then subjected to various types of signal processing, which for simple sonars may be just energy detectors. It is then presented to some form of decision device, which will interpret the signal, within certain allowable tolerances. This decision device may be an operator with headphones or a display, or in more sophisticated and fully automated sonar systems, this function may be implemented by special purpose tools/platforms.

The signal used may be of constant frequency or a chirp of varying frequency. Simple sonars generally use the former with a filter, wide enough to cover possible Doppler effects, while more complex ones generally employ the latter technique. Military sonars often have multiple beams to perform the surveillance of the entire space, while the simple ones only cover a narrow area.

When single frequency transmission is used, the Doppler effect can be utilized to measure the radial speed of a target. The Doppler shift, which is the difference between the transmitted and received frequencies, is estimated and converted into a velocity term. Since Doppler shifts are caused by either the motions of the receiver or target platforms, appropriate correction terms deemed fit need to be taken into account to compensate for the radial speed of the sonar platform. The use of active transmissions from sonars, especially during war time, need to be analysed on the strategic point of view. Active transmissions from such sonars will help the enemy vessels, around the radiating sonar, to infer the clues as regards to the

Chapter 1 Introduction

presence of active sonar, its transmitting frequency and its position making use of the received acoustic levels.

Since active sonar platforms are very noisy, such sonars will not allow target identifications with significant success rates. Thus, this type of detection is used by fast platforms such as planes and helicopters and by noisy platforms like surface ships, but rarely by submarines. When active sonar is used by surface ships or submarines, it is typically activated very briefly at intermittent periods, to reduce the risk of detection by the enemies.

Depending on the number and position of the transmitters and receivers, the active sonar operation can be classified as

- mono-static
- bi-static
- multi-static

When the transmitter and a receiver are in the same place, the operation is called mono-static, while in bi-static, they are separated. When more transmitters or receivers are used, it is referred to as a multi-static operation. Generally most sonars are used mono-statically with the same array often being used for transmission and reception. In certain mono-static system installations, if the platform is moving, it may be considered as bi-static. Multi-static operation is preferred in active sonobuoy field applications.

1.2.2 Passive Sonar

Passive sonar systems, unlike the active sonars, do not radiate any signals. They detect the targets and perform estimations by analyzing the sound signals emitted by the target itself, as illustrated in Fig. 1.3.

Generally, the passive sonar which is quite frequently referred to as listening sonar, has a much greater detection range than active systems and helps in performing the identification of the targets, estimating the range and bearing as well as tracking of targets. The noise generated by mechanized objects underwater is made use of, for performing the target detection. Once a signal is detected in a certain direction, referred to as broadband detection, it is possible to zoom in and analyze the signal received, referred to as narrow band analysis. Identification of the target is made possible as every target generates its own characteristic noises and Fourier Transform techniques can be used to analyze the various frequency components in it.

Even though passive sonar is stealthy and very useful, performance limitations arise as a result of the propagation loss and additive noise at the receiver, Major limitations result from the imprecise knowledge of the characteristics of the target emanations, and from dispersion in time and frequency of target emissions by the undersea medium. Another use of the passive sonar is to determine the target's trajectory by a technique referred to as Target Motion Analysis (TMA), which will provide the target's range, course, and speed.

1.1 *Sonar Equations*

The sonar equations establish the working relationships between the effects of the medium, target, and equipment and they serve two important practical functions. One of them is the prediction of performance of the sonar equipment of known or existing design, while the other pertains to the design of the sonar system.

The prediction of the performance characteristics, mostly in terms of detection probability, is achieved in sonar by the prediction of range, through the sonar parameter, Transmission Loss (TL). The equations are solved for transmission loss, which is then converted to the range through some assumption concerning the propagation characteristics of the medium.

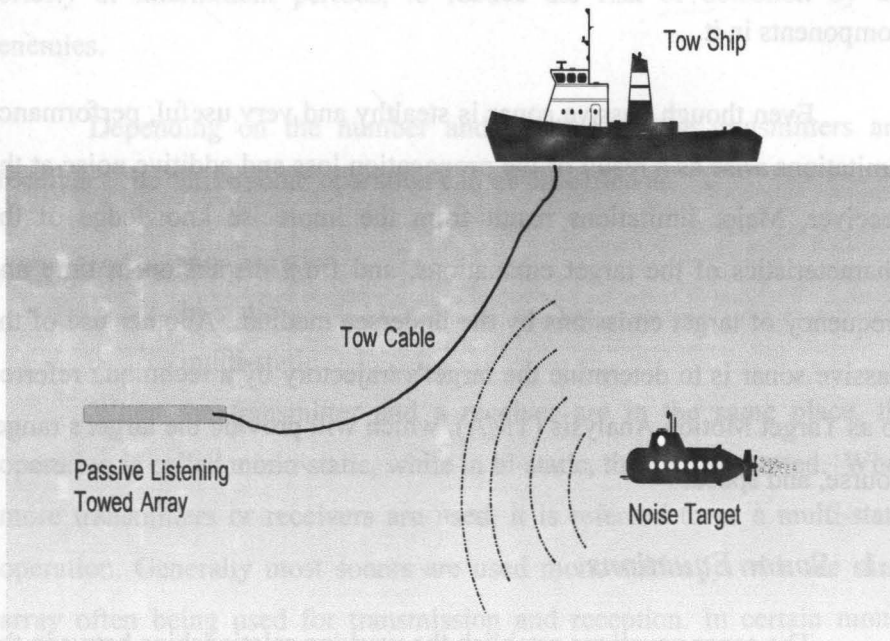


Fig. Error! No text of specified style in document..1 Scenario using Passive sonar

For tackling the sonar design problems, for a given range, the equation is solved for the particular parameter, whose practical realisation is likely to cause difficulty. For example, the equation can be solved for the directivity required, alongwith other probable values of sonar parameters,

to yield the desired range of detection in sonar. After the directivity needed to obtain the desired range has been obtained, the design continues with the trade-offs between the directivity index and other parameters. The design is finally completed through several computations using the equations and the design engineers' intuition and experience.

1.3.1 Active and Passive Sonar Equations

The sonar parameters are referred in units of decibels relative to the standard reference levels. Certain sonar parameters are determined by the equipment, while some others are determined by the medium and the target as detailed below.

- Parameters determined by the equipment
 - Projector Source Level (SL)
 - Self Noise Level (NL)
 - Receiving Directivity Index (DI) and
 - Detection Threshold (DT)
- Parameters determined by the medium
 - Transmission Loss (TL)
 - Reverberation Level (RL) and
 - Ambient Noise Level (NL)
- Parameters determined by the target
 - Target Strength (TS)
 - Target Source Level(SL)

In this context, it may be worth mentioning the fact that one of the parameters on account of the equipment, viz. the self noise level cannot be completely decoupled from the ambient noise level parameter determined by the medium and as such these two parameters are essentially identical and hence represented by the same notation.

Chapter 1 Introduction

A sound source, by appropriate means, produces a *source level* of **SL** decibels at a 1 m. When the radiated sound reaches the target, its level will be reduced by the *transmission loss*, and becomes **SL - TL**. Upon reflection or scattering from the target of target strength **TS**, the reflected or backscattered level will be **SL - TL + TS** at a distance of 1 m from the acoustic centre of the target in the direction back towards the source. In travelling back towards the source, this level is again attenuated by the *transmission loss* and becomes **SL - 2TL + TS**. This is the echo level at the hydrophone terminals. Turning now to the background and assuming it to be isotropic noise rather than reverberation, the *background level* is **NL**. This level is reduced by the *directivity index* of the transducer acting as a receiver or hydrophone so that at the terminals of the hydrophone, the relative noise power is **NL - DI**. Hence, at the hydrophone terminals, the echo-to-noise ratio is **SL - 2TL + TS - (NL - DI)**.

In sonar scenario, a decision will be made by the human observer that a target is present, when the input signal-to-noise ratio is above a certain detection threshold, **DT**, satisfying certain probability criteria, else the decision will be made that the target is not present. If the target is present, just at the point of detection, the signal-to-noise ratio will be equal to the detection threshold, and hence the equation becomes **SL - 2TL + TS - (NL - DI) = DT**. This is the active-sonar equation for the *mono-static* case in which the acoustic returns of the target is back towards the source. In some sonars, a separated source and receiver are employed and the arrangement is said to be *bi-static* and in this case, the two transmission losses, to and from the target, are not the same. Also in some modern sonar, it is not possible to distinguish between **DI** and **DT** and it becomes appropriate to refer to **DI - DT** as the increase in signal-to-background noise ratio generated by the entire receiving system.

Realisation of a Target Classifier for Noise Sources in the Ocean

For a reverberation background we will replace the terms **NL - DI** by an *equivalent plane-wave reverberation level* **RL** observed at the hydrophone terminals. The active-sonar equation then becomes

$$\mathbf{SL} - 2\mathbf{TL} + \mathbf{TS} = \mathbf{RL} + \mathbf{DT}.$$

In the passive case, the target itself produces the signal by which it is detected, and the parameter source level now refers to the level of the radiated noise of the target at 1 m. Also, the parameter target strength becomes irrelevant and as only one way transmission is involved, the *passive sonar equation* becomes

$$\mathbf{SL} - \mathbf{TL} = \mathbf{NL} - \mathbf{DI} + \mathbf{DT}.$$

1.4 Factors Affecting the Sonar Performance

The detection, classification and localization performance of sonar depends on the environmental factors and the receiving equipment. In the case of active sonars, the performance is also determined by the transmitting subsystems, while the radiated noise characteristics also can be a factor that influences the performance of the passive sonar.

1.4.1 Environmental Factors

Sonar operation is affected by variations in sound speed, particularly in the vertical plane. Sound speed is lower in fresh water than in sea water. The speed of sound in water is affected by density, as well and the density in turn is affected by temperature, dissolved molecules, usually salinity, and pressure.

Ocean temperature varies with depth, and for depth ranges between 30 and 100 meters, there is often a significant variation in temperature,

referred to as the thermocline, dividing the warmer surface water from the cold still waters, that make up the rest of the ocean. This will lead to inaccuracies in sonar predictions as a sound originating on one side of the thermocline tends to be bent or refracted off the thermocline.

In sonar, since the wave propagation speed is a time-varying function of depth and range, with significant dependencies on geographic location and season of the year, the estimations turn out to be cumbersome due to complex refractive phenomenon, especially when the propagating energy interacts with the sea surface or bottom. Motions of the water mass, sea surface, sonar platforms and targets lead to a wide variety of channel dispersions in time, frequency and angle.

1.4.2 Reverberation

When active sonar is used, scattering occurs from small objects in the sea as well as from the bottom and surface. This is one of the major sources of interference but does not occur with passive sonar. This scattering is different from that in room reverberation, which is a reflection phenomenon. The reverberation phenomenon in the ocean is analogically similar to the scattering of light from the car's headlights in fog or mist. A high-intensity pencil beam will penetrate the fog and as the main headlights are less directional will result in *white-out*, where the returned reverberation dominates. Hence, to reduce the effect of reverberation, in the ocean, the active sonar needs to transmit in narrow beams.

1.4.3 Target Characteristics

Sonar targets, such as submarines, surface vessels, torpedoes, etc., have two main characteristics that influence the performance of the sonar. For active sonar the sound reflection characteristics of the target, known as

Realisation of a Target Classifier for Noise Sources in the Ocean

its *target strength* and for passive sonar the target's radiated noise characteristics are the critical components that affect the sonar performance. The radiated noise, in general, will consist of an unresolvable continuum of noise with superimposed or resolvable spectral lines on it, the lines aid in classification. Echoes are also obtained from other objects in the sea such as whales, wakes, schools of fish and rocks.

1.4.4 Other Noises

The ocean, as a propagation medium is full of interfering noise sources such as machinery noise from the shipping traffic, flow noise, wave noise, wind noise, noise from biologics and even intentional jammers, which may interfere with the desired target returns and emissions.

1.5 Noise Sources in the ocean

The ocean environment includes a variety of noise sources, which are of natural as well as manmade in origin. The general back ground noise which has the contributions from all the oceanic noise sources is termed as the ambient noise. The ambient noise has a broad frequency range and its characteristics depends on a number of factors including climate, wind speed, presence of aquatic organisms, etc.. The following sections briefly examine the principal sources of ambient noises and their characteristics.

1.5.1 Natural Sources of Ambient Noise

The natural sources of ambient noise can be broadly classified into the following categories:

- Hydrodynamic sources
- Thermal agitations
- Seismic sources
- Ice cracking

Chapter 1 Introduction

- Biological sources

1.5.1.1 Hydrodynamic Sources

Hydrodynamic sources include a large number of sources which generate noise due to various physical phenomena, including movement of water itself due to winds, tides, currents etc.. *Surface waves* are a predominant source of hydrodynamic noise and originate mainly due to wind action and contribute to the low frequency noise spectrum. The *bubbles* are yet another source from which hydrodynamic noise originates. Another source, namely, *turbulence* is commonly formed in the ocean in regions which are near to coastal areas, straits and harbours. Turbulence can occur at the water-ocean floor boundary, at the sea surface and within the water as well.

1.5.1.2 Thermal Agitations

The effects of thermal agitations of the medium determine a minimum noise level for that medium. The minimum ambient noise level at upper frequency limits of ambient noise data, around 20 to 30 kHz, are mainly contributed by thermal agitations.

1.5.1.3 Seismic Sources

Various types of disturbances in the earth's crust (tectonic as well as volcanic actions), can also contribute to the ambient noise in the sea. Even if the sources of these types of disturbances are far away from the sea, those high energy disturbances easily reach the oceans as compression waves. The spectral characteristics of such noises depend on the magnitude and range of the seismic activity, the propagation path, etc. It has been observed that, in general, the spectral peaks due to the seismic activities occur between 2 and 20 Hz, when the disturbances are waterborne.

Realisation of a Target Classifier for Noise Sources in the Ocean

1.5.1.4 Biological Sources

The ocean serves as a habitat for millions of life forms. A large variety of marine organisms like crustaceans, mammals and fishes are good noise makers. Noise from such sources exhibit a wide frequency spectrum from 10 Hz to 100 kHz. The individual sounds are repetitive in nature and of short duration. Generally, noise from various sources blend to form a bewildering mix of noise.

1.5.1.5 Cracking of Ice

Shifting and breaking of ice is a prominent source of noise in the ocean, especially in the Polar Regions. The noise originates from cracking, grinding, sliding and crunching of ice bergs, and covers a wide range of frequencies.

1.5.1.6 Other Sources

Spray of water droplets and hail constitute precipitation. It generally contributes to the ambient noise at frequency above 500 Hz. At low wind speeds, heavy precipitation can generate noise around 100 Hz. Rain also contributes to the increase in ambient noise levels. Heavy rains are found to cause an increase of about 30dB in the 5 to10 kHz range of the noise spectrum.

1.5.2 Manmade Noises

Various types of human activities also contribute greatly towards ambient noise. The main sources include shipping traffic, seismic surveys, oil and gas exploration / production, military operations, sonars. etc.

1.5.2.1 Shipping Traffic

Shipping traffic has been found to be a dominant noise source in the oceans. It has been found that the non-wind dependent component of the

Chapter 1 Introduction

frequency range from 10 Hz to 1000 Hz is contributed mainly by ship traffic noise. The effect is predominant at frequencies between 20 and 500 Hz. The degree to which shipping noise influences the ambient noise depends on various factors like particular combination of transmission loss, number of ships, class of ships and the distribution of ships. It has been found that the effective detectable range for shipping noise in the open ocean can be as high as 1000 miles or more.

1.5.2.2 Seismic Surveys

Seismic surveys are carried out in order to study the structure and composition of geological formation of earth's crust and to detect the presence of natural resources like hydrocarbon reservoirs. Such surveys are carried out by directing high intensity, low frequency sound signals through the earth's crust. The reflected signal is processed to get the required information.

1.5.2.3 Oil and Gas Exploration / Production

Ocean beds have rich source of oil and natural gases. Noise is generated during all phases of oil and gas production, including exploration, pile driving, pipe laying, drilling and platform operations. The noise thus generated may be impulsive or continuous.

1.5.2.4 Military Operations

With newer technologies and innovations which are being developed in the Defence Research and Development Programs, military operations are now-a-days becoming a major source of underwater noise. Naval forces may conduct various experiments, test fire their equipments / gadgets, etc., which could significantly disturb the ocean environment and contribute to short term changes in the ambient noise levels.

Realisation of a Target Classifier for Noise Sources in the Ocean

The use of active sonars also contributes to ocean noise. Sonar systems generally emit short pulses of sound which carries high energy. Submarines and torpedoes are also significant noise sources. Moreover, the explosives used in military tests and exercises can be a considerable source of undesirable noise with typical source levels of 267dB in the frequency band from 1 to 7 kHz.

1.6 Types of Underwater Noises

Various kinds of noises that are generated underwater can be categorised into four groups, when viewed from the sonar signal processing perspective. These are radiated noise, self noise, ambient noise and reverberation noise.

Radiated noise constitutes the acoustic output of surfaced or submerged vessels, weapons or machineries which can reveal the details of the noise sources and as such this type of noise is important in target classification / identification scenarios. Generation of radiated noise can be attributed to propellers, machineries and hydrodynamic effects present in the system.

The self noise mainly gets generated from the vibration of structural parts induced by water flow and rotating as well as reciprocating machineries. Those sources, viz. propellers, machineries and hydrodynamic effects, which contribute to radiated noise also contribute to self noise. Analysis has revealed that the spectrum of self noise has both line spectra as well as continuous spectra and has a steep negative slope at high frequencies.

1.6.1 Sources of Radiated Noise

The radiated noise generated from ships, submarines, oil platforms etc. can be attributed as due to the following components.

- Machineries
- Propellers
- Hydrodynamic sources

1.6.1.1 Machinery Noise

The machinery noise generally originates from the mechanical vibrations of the various parts of the vessel. The vibrations of the structures are coupled to the sea, through the ship's hull or oil platform columns.

The causes for the machinery noise are the following

- Unbalanced rotating parts such as motor armatures
- Repetitive discontinuities. *E.g.* Gear teeth and armature slots
- Reciprocating parts. *E.g.* Compression in engine cylinders.
- Turbulence and cavitation resulting from the flow of fluids through pumps, etc.
- Mechanical friction in machine parts

The machinery noise of the vessel generally contains a continuous spectrum with strong line components. The line components are contributed by the first three causes listed above, while the turbulence and mechanical friction can give rise to the continuous components

1.6.1.2 Propeller noise

When the propeller rotates in water, regions of low or negative pressures are developed on the surface as well as at the tips of propeller blades. The *cavities* thus produced give rise to minute bubbles, which when collapse produce sound. Thus the propeller noise originates outside the hull, while the machinery noises are generated inside the vessel. Radiation

Realisation of a Target Classifier for Noise Sources in the Ocean

patterns of propeller noise reveal that the radiation is not uniformly distributed and has a directional pattern in the horizontal plane around the radiating vessel.

1.6.1.3 Hydrodynamic Noise

This type of noise is generated by the fluctuating and irregular flow of fluid past a physical structure, *viz.* the hull of the vessel. When the fluid irregularly flows, pressure fluctuations arise which induce vibrations in various parts of the vessel, or can be directly transmitted to the ocean. Generally, the contributions due to the hydrodynamic noise are small, and thus get masked by machinery and propeller noises.

1.7 Classifiers

One of the most notable requirements and objectives of sonar is to extract the requisite features of the acoustic space time field from the received signals or echoes and interpret these information legibly, precisely and clearly, without having any ambiguity to the end user. The detection and classification problems generally addressed by the sonar systems are used to detect the presence of targets, by comparing the level of certain statistics with the assumed or estimated statistics, and to classify the targets adopting the joint concepts of estimation, localization and tracking. Tracking of targets also help in extracting invaluable information on the target dynamics. As an example, the information on the target dynamics can be used to identify a school of fish from a freighter target or submarine.

In underwater scenario, it is a usual practice to analyze short term data records as most of the noise signals, or processes of interest to a passive sonar system will be very brief in duration and may have a time varying spectra. These can be considered fairly stable only for short term

Chapter 1 Introduction

data records. As an example, the moving noisy target or a moving receiver platform can cause a time varying spectral responses due to Doppler effects.

In listening sonar, targets are classified on the basis of the tonal components or signatures present in the frequency spectrum of the noise signals emanating from the targets using spectral estimation techniques. For random signals with unknown features and characteristics, as in the case of passive sonar systems, the noise signals emanating from the targets can be assumed to be a Gaussian random process and can be received and processed with suitable energy detectors. In such a scenario the receiver may have a rough knowledge of the spectral bands occupied by the noise signals. Noise power outside the expected spectral range can conveniently be eliminated with the help of bandlimiting filters. Hence, in passive sonar, classification is usually performed on the basis of the tonal components or the signature patterns of the noise data waveforms emanating from the targets by using the technique of template matching.

Fourier analysis approaches implemented in the form of discrete Fourier transforms using Fast Fourier Transform (FFT) techniques were widely being utilized for estimating the power spectral density of noise emanating from underwater targets as well as signals buried in high noise fields. Though the estimation of the power spectral density of deterministic and stochastic processes usually employs FFT, which is computationally efficient and yields satisfactory results for most applications, there are several inherent limitations. Due to the implicit windowing of the data in this conventional approach as well as the limitation in frequency resolution, analysis of short data segments needs a better method. To improve the spectral fidelity, alternative modern spectral estimation procedures are used, based on the approach of fitting the measured data segments to an

20

Realisation of a Target Classifier for Noise Sources in the Ocean

assumed model. Some of the approaches demand significant computational requirements than the conventional methods. The performance of the spectral estimator has to be analysed and a criterion for the selection of a suitable spectral estimator depending on the signal types and data records can be evolved.

The spectrum of any waveform consists of two components, the slowly varying part, referred to as the filter or spectral envelope and the rapidly varying part, referred to as the source or harmonic structure. These two components can be separated by *cepstral analysis*. A more systematic approach for computing the cepstral coefficients can be achieved by estimating the Mel Frequency Cepstral Coefficients (MFCC), which is a measure of the perceived harmonic structure of sound.

The techniques like power spectral analysis are found to have wide applicability and are also robust and time tested. However, many signals, especially those which are generated from nonlinear processes, can not be properly analysed by second order statistical methods. Many of the naturally occurring signals deviate from Gaussianity and linearity. Hitherto, such signals were considered Gaussian or near Gaussian signals and analysis were conducted, which has resulted in loss of valuable information. For these reasons, higher order statistical methods have been developed, which can handle non-Gaussian as well as nonlinear signals. As the phase information is not available in the second order measures such as the power spectrum and autocorrelation functions, it cannot identify non-minimum phase signals and certain types of phase couplings, associated with nonlinearities. Information regarding the phase couplings and nonlinearities can be identified using bispectral estimation.

Chapter 1 Introduction

A classifier system for identifying the noise sources in the ocean using the spectral, cepstral and bispectral features extracted from the noise emissions needs to be implemented for alleviating the inefficiencies in the operator assisted classification system. Though signal analysis can be carried out even in the time domain, most of the target specific signatures are extractable from the frequency domain representation and its variants. The process of feature extraction can be carried out through various signal processing techniques, so that the raw data is transformed into new data sets that can be used by the classifier for the purpose of system identification.

1.8 *Summary*

This chapter throws light on the salient operational and functional features of sonar systems and the various noise sources in the ocean, highlighting the need and requirement of a classifier for identifying them. The underlying principle of operation of the proposed classifier which involves extraction of the various spectral, cepstral and bispectral features is also briefly introduced in this chapter.

CHAPTER 2

REVIEW OF PAST WORK

This chapter is devoted to the review of the research work reported in open literature in the areas of underwater noise, spectral estimation, cepstral analysis, bispectral estimation, target classification, etc.. Classification of targets centred around the statistical classifiers, expert system classifiers, neural network classifiers, etc. have been reported and the results of comparison of the different methods have also been consolidated by various researchers. The target classification is also achieved through energy detection as well as spectral modelling. The functional and operational requirements of the classification systems in use, alongwith the various target specific features as well as the feature selection criteria required to be adopted for realizing the various state-of-the-art classifiers such as the statistical classifiers, expert system classifiers, neural network classifiers, fuzzy classifiers, sonar signal processor based classifiers, etc. are highlighted in this chapter. This chapter also covers the recent trends in the classifier implementation based on the Hidden Markov Model.

2.1 Introduction

In modern Sonar systems, the dry-end comprising of the receiver and the post processing modules performs underwater target detection,

Chapter 2 Review of past work

estimation, localisation, tracking and classification functions. The detection and estimation procedures in sonar involve the computation of various statistics for improving the overall performance of target detection, localisation and classification capabilities of the end system, taking into consideration all the undesirable propagation effects.

Upon judiciously selecting the characteristic features of a target, the relevant features are combined to form a feature vector. In general, such a feature vector forms the input to the classifier. Reports on classifiers based on statistical as well as expert system concepts are available in open literature. Though the results of such activities are reported, most of the papers do not touch upon the implementation details and other related issues to aid the researchers for the practical realisation of such a system. In the area of sonar signal processor based classifiers, many research works have been reported, both in the field of active as well as passive sonars. Some studies even indicate the potential use of broadband sonar as a tool for species and size classification of fish and other marine species.

Yet another major contribution in the field of classification is through the use of neural networks. There are literatures which give an overview of the practical and potential application of neural network models, viz. Hopfield Net, Multilayer Perceptron and Self Organizing Feature maps. Classification schemes implemented using fuzzy logic principles as well as algorithms typically used in pattern recognition systems have also been reported. Of these, the most widely used classifiers are the Neural Network (Multi-layer Perceptron), k-Nearest Neighbours, Gaussian Mixture Model and the Bayes' Classifier.

2.2 Characteristic Signatures of Typical Ocean Noise

Bertilone and Killeen [1], investigated the noise from snapping shrimp, which often dominates the ambient underwater noise environment of warm, shallow waters, at frequencies ranging from 1 kHz to 200 kHz. It is found that the conventional sonars perform poorly in this highly impulsive noise environment, and there is a potential for significant enhancements to detection performance using detectors that are tuned to the non-Gaussian noise. The paper reports the general statistics of band pass snapping shrimp noise data collected from the Timor Sea and investigates the performance of several generalized energy detectors (GEDs) for passive band pass detection of characteristic random processes in the noise data.

A review on the various aspects of radiated noise, self noise and ambient noise has been carried out by Gordon M. Wenz [2]. The review addresses the objectives, accomplishments and basic challenges of underwater noise research. The review also highlights the major problems such as the noise measurements, noise reduction and prevention.

Carey [3] discusses the low-to-mid frequency (LMF) noise characteristics, mechanisms and computations of basin noise based on the breaking wave as a random source of sound. The ambient noise is seen to be attributed as due to the bubble spray and splash produced by wind action and breaking waves at higher frequencies. However, the cause of the low-to-mid-frequency noise (10-500 Hz) remained a puzzle, since large bubbles required to produce low frequency noise are not found at sufficient depths. The LMF ambient noise measurements were often dominated by emissions from ships and industrial activity, making observations of local noise generating mechanisms difficult. Wave-wave interaction, wave-turbulence interaction and the pressure fluctuations due to the turbulent boundary layer

Chapter 2 Review of past work

above the sea surface were all examined as LMF mechanisms but were found to radiate insufficient sound levels. Breaking waves were found to generate microbubble plumes and clouds, while radiating low frequency sound. Recently, cumulative oscillations of these compact microbubble clouds were shown to be responsible for generating LMF noise. Results reported by Williams *et al.* in [4] seem to confirm the theory that the Knudsen region of the ambient noise is produced by breaking waves even at low sea states. It also shows that the main mechanism which produces the noise is the free oscillations of the bubbles. It is concluded that the main source of energy is the radial flow around the proto-bubble at the moment it breaks away to form the actual bubble.

Tan Soo Pieng, *et al.* [5] describe the collection of ambient noise data and the structured compilation of the collected information into a useful database. The data collected spans a frequency range of 11Hz to 8300 Hz. The data has been indexed and stored in a database and accessed through a GUI. A brief summary of the data collected is presented in terms of the power spectral density variations. The observed data is compared with the 'classic' curves reported in open literature.

Potter and Delory [6] studied the ambient noise levels from shipping and other human activities in Northern and Southern Hemisphere sites and concluded that shipping appears to have raised the background noise significantly throughout the Northern Hemisphere. Available evidence and moderate extrapolation of known features of marine mammal hearing leads to the conclusion that the total noise levels are likely to adversely affect several species.

Pflug, *et al.* [7], investigated the stationarity and Gaussianity of ambient shipping noise. To identify the time periods of non-stationarity in

Realisation of a Target Classifier for Noise Sources in the Ocean

the noise, upto fourth moments are analyzed and the summing up of the investigations indicate that the third order moments deviate from Gaussianity more than the fourth order moments. It has been found that, while shipping noise at the deeper waters appear to be somewhat non-Gaussian during certain time periods, the shallow depth data appears Gaussian.

A theoretical model for the prediction of ambient noise levels due to cumulative oscillations of air bubbles under breaking wind waves has been presented by Pavlo Tkalic and Eng Soon Chan [8]. The model uses a budget of the energy flux from the breaking waves to quantify the acoustic power radiation by a bubble cloud and derives good estimates of the magnitude, slope, and frequency range of the noise spectra using the wind speed or height of the breaking waves. In this model, it has been assumed that the wind is the source of the Knudsen spectra only through the mediation of breaking waves, which are themselves the sources of the sound radiating bubbles.

A recent work by Wales *et al.* [9] present an evaluation of the classical model for determining an ensemble of the broadband source spectra of the sound generated by individual ships and propose an alternate model to overcome the deficiencies in the classical model proposed by Ross. The alternate model proposed here represents the individual ship spectra by a modified rational spectrum where the poles and zeros are restricted to the real axis and the exponents of the terms are not restricted to integer values. An evaluation of this model on the source spectra ensemble indicates that the rms errors are significantly less than those obtained with the model where the frequency dependence is represented by a single baseline spectrum. Furthermore, at high frequencies (400 to 1200 Hz), a single-term rational spectrum model is sufficient to describe the frequency

Chapter 2 Review of past work

dependence and, at the low frequencies (30 to 400 Hz), there is only a modest reduction in the rms error for a higher order model. Finally, a joint probability density on the two parameters of the single term model based on the measured histograms of these parameters is proposed. This probability density provides a mechanism for generating an ensemble of ship spectra.

A model has been proposed by Gray and Greeley [10] for the acoustic source strength of blade rate line tonal produced by merchant vessels. These source strengths are based on observed cavitation time histories of merchant vessels and limitations imposed by considerations of propeller design procedures and ship vibration criteria. Relationships are presented for the expected value of the blade rate source strength for ships of different lengths, expressed both as a monopole source strength located at a known depth below a free surface and as a dipole source strength that describes the pressure radiated to the farfield. These relationships are based on a small sample of merchant ship characteristics and are exercised for the estimated population of ships at sea. This calculation yields a statistical description of the distribution of source level and frequency of propeller blade rate acoustic energy for the fleet of single-screw merchant vessels.

Arveson and Vendittis [11] present the results of extensive measurements made on the radiated noise of a bulk cargo ship, powered by a direct-drive low-speed diesel engine, which is a representative design for many modern merchant ships. The radiated noise data show high-level tonal frequencies from the ship's service diesel generator, main engine firing rate, and blade rate harmonics due to propeller cavitation. Radiated noise directionality measurements indicate that the radiation is generally dipole in form at lower frequencies, as expected. There are some departures from this pattern that may indicate hull interactions. Blade rate source level agrees reasonably well with a model of fundamental blade rate radiation

Realisation of a Target Classifier for Noise Sources in the Ocean

previously reported by Gray *et al.*, but agreement in blade rate harmonics is not as good.

Observations obtained from a buoy moored near Alaska have been presented by Hollinberger *et al.* in [12]. The buoy recorded the omnidirectional ambient noise sound pressure level and wind speed. The analysis shows that for a wind speed of about 5 knot, the measured ambient noise level at 900 Hz lies well below the Knudsen curve for open ocean wind generated noise. As the wind speed increases from 5-10 kn, the measured noise level approaches Knudsen curve, and above 10 kn, the measured ambient noise level matches the Knudsen curve.

Michel Bouve *et al.* [13] present a study of statistical modelling of underwater noise using a Gaussian- Gaussian Mixture. Three underwater noise samples are studied with emphasis on noise PDF modeling. The results show that the snapping shrimp noise appears to be non-stationary. The back ground noise is very close to Gaussian while the merchant ship noise seems to be adequately described by a Gaussian-Gaussian Mixture.

The results of an experiment carried out to investigate the relative importance of wind and waves as noise generators are given by Nichols in [14]. Trials were carried out for 40 days to measure wind speed, wave height and noise spectrum levels at three deep water sites. The results suggest that breaking waves are likely to be a source of VLF ambient noise.

The non-Gaussian characteristics of ambient noise have been examined by Webster in [15]. Signal processing algorithms optimized for Gaussian noise may degrade significantly in a non-Gaussian noise environment. A generic distribution suitable for modelling non-Gaussian ambient noise has also been suggested.

Chapter 2 Review of past work

Huynh [16] demonstrates underwater mammal sound classification using a novel application of wavelet time–frequency decomposition and feature extraction using a Bienenstock, Cooper, and Munro (BCM) unsupervised network. Different feature extraction methods and different wavelet representations have been discussed. The system achieves outstanding classification performance even when tested with mammal sounds recorded at very different locations, from those used for training. The results suggest that nonlinear feature extraction from wavelet representations outperforms different linear choices of basis functions.

Certain fish sound recordings and marine mammal vocalizations are available in the archives of certain web sites [17], [18]. Information on some marine life forms like whales is given in [19]. This site also includes few sound files and spectrograms of various sound sources.

2.3 *Classes of features*

The identification and selection of features play a crucial role in the realisation of the classifier with acceptable success rates. A wide range of features extracted from spectral, cepstral, and bispectral methods have been used for implementing various types of classifiers such as statistical classifiers, expert system classifiers, etc..

2.3.1 Spectral Features

The methods and procedures that have been suggested for extracting some of the vital spectrally decomposable features are reported in [20] – [40] and are briefly discussed below.

In [20], Chun Ru Wan *et al.* analysed the statistical property of the power spectrum observations and developed a novel tonal detector by optimally integrating the spectral inferences. The optimal detectors are

Realisation of a Target Classifier for Noise Sources in the Ocean

derived by using the method of maximum likelihood hypothesis test. The results from simulations and open ocean trial data have shown that the proposed detectors have a promising role in detecting tonals.

Marple, in [21] presents a summary of several modern spectral estimation methods. Most of the methods are explained in the context of parametric time series modelling. Non parametric techniques discussed include classical spectral estimation, autoregressive, ARMA, Prony, Maximum likelihood, Pisarenko and MUSIC. The paper also throws some light on current spectral estimation research trends.

Shin, F.B. [22], suggests methods to improve the detection performance of passive emissions from quiet sources in *littoral waters*, focusing on the full spectrum of the target signature. Various noise emissions corrupted with ambient noise are analyzed and the results are presented. A *classify before detect algorithm* is used, which takes advantage of the microstructures present in the aquatic signature for improved performance.

A detailed tutorial on power spectral estimation, periodograms, random signals, fundamental principles of estimation theory, various procedures for power spectral density estimations, etc. are discussed in [23].

In [24], Hinich proposes a method for detecting an unknown periodic signal in additive noise. The period is unknown, but the amplitudes of the fundamental and the first $(M - 1)$ harmonics are known to be nonzero. One application of such a method is the detection of a torpedo by a submarine sonar system from the observed acoustic line spectrum generated by the torpedo's blade motion.

Chapter 2 Review of past work

In the work reported by Cremona *et al.* [25], an approach of Frequency Modulated Continuous Wave (FMCW) radar spectrum analysis with the Auto Regressive parametric estimation is described. The proposed method yields additional information compared to power spectra and a more detailed signal characterization.

A method for estimating signal harmonics in the spectrum is presented by Eftestol in [26]. The method's potential for discriminating between cardiac rhythms organised to different degrees is studied using features based on the signal harmonic frequencies and corresponding amplitudes in a classification system. This study demonstrates that the proposed method for estimating signal harmonics in the spectrum has potential for discriminating between ECGs with different levels of organization.

Ricardo S. Zebulum *et al.*[27] in their work investigate the application of Artificial Neural Network in speech recognition. The performance of a neural network based recognition system when using different spectral analysis models has been compared and different sets of coefficients, such as Autocorrelation and Mel cepstrum, have been extracted. A hybrid system, combining the two different sets of coefficients outperforming the other models, has also been described.

A comparison of different spectrum estimation techniques applied to nonstationary signals has been carried out by Massino Aletto *et al.*[28]. The comparison examines applications in which spectral analysis is applied to nonstationary signals. Different spectral analysis algorithms were tested in order to compare their behaviour in detecting defined harmonic frequencies. The results showed that the chirp-Z transform outperforms

Realisation of a Target Classifier for Noise Sources in the Ocean

other techniques especially when a restricted frequency band has to be analyzed.

Friedlander and Porat [29] present an iterative frequency domain technique, based on minimizing the error between the smoothed sample power spectrum and a spectral model, for estimating AR-plus-noise and autoregressive moving average (ARMA) parameters. The estimation error of this proposed technique, with less computational requirements than maximum likelihood estimators, is found to be close to Cramer-Rao bound, especially for long data records.

A new ARMA model has been proposed by Talkhan *et al.*[30] for the power spectral density function of noisy random ergodic zero mean discrete time signals in which, the residual power not covered by the AR polynomial is represented by a limited order MA polynomial. The residual power which is still not represented by the added limited order MA polynomial has been minimized.. The proposed technique which is computationally efficient has been validated and is found to consume less storage space.

Qi Tian *et al.* [31] made an attempt to enhance the performance of Split Spectrum Processing (SSP) in detecting multiple targets which exhibit different spectral characteristics. An iterative procedure that combines group delay moving entropy and SSP is proposed, whereby the multiple targets are identified one at a time. It has been established that the proposed group delay moving entropy technique can be used to select the optimal frequency region for SSP, when detecting multiple targets. The dominant target is subsequently eliminated using time domain windows, which improves the detection of the remaining weaker targets.

Chapter 2 Review of past work

A high-resolution spectral estimation algorithm based on the approximation to maximum likelihood criterion, has been proposed by Luzin *et al.* [32]. Here, the structure of estimation filter comprises of two-channels, of which the first channel corresponds to a measuring channel like one of Capon's algorithm, while the second channel is used for taking into account and compensating for the non-coherent white noise components. The proposed two beam method allows the design of power spectrum estimating devices having rather simple structure for real time implementations.

A new method for simultaneously estimating a number of power spectra has been suggested in [33]. It is required that a prior estimate of each spectrum is available and new information is obtained in the form of values of the autocorrelation function of their sum. The method is compared with minimum cross-entropy spectral analysis and some basic mathematical properties are discussed. Three numerical examples are included, two based on synthetic spectra, and one based on actual speech data.

The impact of the Fast Fourier transform on the spectrum of time series analysis is discussed in [34]. It is shown that the computationally fastest way to calculate the mean lagged products is to begin by calculating all Fourier coefficients with a Fast Fourier transform and then to fast-Fourier-retransform a sequence made up of $a_k^2 + b_k^2$ (where $a_k + ib_k$ are the complex Fourier coefficients). The paper also discusses the raw and modified Fourier periodograms, bandwidth versus stability aspects, and the aims and computational approaches to complex demodulation.

Arun [35] presents principal components algorithms for the problem of fitting an ARMA model to a given segment of a sample sequence of a

discrete-time stochastic process, and uses the model to estimate the power spectrum of the process. To reduce the effects of finite word length errors, the authors have suggested balanced state-space parameterization of the ARMA model, instead of the more popular difference equation parameterization. Model identification is formulated as a problem of selecting a partial state to approximately span an apparently large dimensional information interface between the past and the future of the process. Different criteria are used to measure the quality of the approximation, and it leads to various Singular Value Decomposition based principal components algorithms for the problem.

Existence of an exact relationship between the maximum likelihood method (MLM) and autoregressive (AR) signal modeling in multidimensional power spectral estimation has been investigated by Dowlal and Lim [36]. For one-dimensional uniformly sampled autocorrelation functions, Burg has shown a relationship between the maximum entropy method and MLM spectral estimates. In this paper the authors have shown a similar relationship between the MLM and AR spectral estimates for m-Dimensional signals sampled uniformly or nonuniformly.

Peretto *et al.* [37] describes power spectrum analysis and a periodic signal estimation whose bandwidth is not limited by the mean sampling time. The procedure relies on the evaluation of the input signal autocorrelation function in different delayed time instants, located at either equispaced or random time instants. A recursive random sampling process in the time domain was used in order to avoid any bandwidth limitation due to the sampling strategy in the evaluation of each autocorrelation function. The signal power spectrum as well as its period can finally be estimated, if the approximate value of the fundamental frequency is known.

Chapter 2 Review of past work

Amin [38] suggests a simple method that provides an access to a set of sliding power spectra with different characteristics. The method is based on the use of cascading-form realisation of the infinite impulse response filter. The filter is employed as a time window to the data samples or their lagged products depending on whether the frequency or the power spectrum is of interest. The choice of the filter's poles and zeros, as well as their cascading order, allows a direct access to a wide range of power-spectrum estimators, each with different trade offs between temporal and spectral resolutions.

The acoustic spectrum of a transiting aircraft, when received by a hydrophone located beneath the sea surface, changes with time due to the Doppler Effect. The traditional method for analysing signals, whose frequency content changes with time is the short-time Fourier transform that selects only a short segment of the signal for spectral analysis at any one time. The short-time Fourier transform requires the frequency content of the signal to be stationary during the analysis window; otherwise the frequency information will be smeared by the transformation. Recently, joint time-frequency distributions, which highlight the temporal localisation of a signal's spectral components, have been used to analyse nonstationary signals whose spectra are time dependent. In this paper Ferguson[39], applied the short-time Fourier transform and the Wigner-Ville time-frequency distribution to a time-series data from the hydrophone so that the instantaneous frequency of the propeller blade rate of a aircraft can be estimated at short time intervals during the aircraft's transit over the hydrophone. The variation with time of the estimates of the Doppler-shifted blade rate is then compared with the corresponding temporal variation predicted using a model that assumes the sound propagation from the

airborne acoustic source to the subsurface receiver through two distinct isospeed media separated by a plane boundary .

Omologo and Svaizer [40] report on the use of cross power spectrum phase (CSP) analysis as an accurate time delay estimation (TDE) technique. It is used in a microphone array system for the location of acoustic events in noisy and reverberant environments. A corresponding coherence measure (CM) and its graphical representation are introduced to show TDE accuracy. Using a two-microphone pair array, experiments show less than 10 cm average location error in a 6 m x 6 m area.

2.3.2 Cepstral Features

Automatic genre classification of music in audio format has gained significant importance as, in addition to automatically structuring large music collections, such classification can be used as a way to evaluate features for describing musical content [41]. A comparison of the automatic results with human genre classifications on the same dataset has been done. The results show that, although there is room for improvement, genre classification is inherently subjective and therefore perfect results can not be expected from either automatic or human classification. The experiments also showed that features derived from an auditory model have similar performance with features based on mel frequency cepstral coefficients (MFCC).

Holmes *et al.* [42] describe the use of subword units based on allophones with an allophone-dependent model structure, to improve subword HMM (hidden Markov model) recognition performance when using vocabulary-independent training. The new system is an extension of an approach based on sub-triphone units called phonicles. The original

Chapter 2 Review of past work

system modelled major phonetic context effects, but did not take account of context effects wider than one immediately adjacent phone or the differences in duration and spectral complexity which exists between different types of phoneme. The recognition system has therefore been extended so that phoneme transcriptions are first converted to allophone transcriptions. Each allophone is then transformed to a sequence of one or more allophonics, where different allophonics can have different numbers of states and one allophonicle may be shared across allophones. Using a Mel cepstrum front end, isolated-word speaker-dependent recognition experiments on six application vocabularies have shown extremely good recognition performance for allophonicle models, with an average error rate of only 0.3%.

A new algorithm of extracting MFCC for speech recognition which reduces the computation power by 53% compared to the conventional algorithm and has an accuracy of 92.93% has been suggested by Han *et al.*[43]. By a reduction of only 1.5%, the number of logic gates required to implement the new algorithm is about half of the MFCC algorithm, which makes the new algorithm very efficient for hardware implementation.

A method for warping the frequency axis of cepstral coefficients in a way analogous to the pre-processing performed by the human ear has been described by Merwe and Preez [44]. The computation is a two-step procedure in which the bilinear transform is used to represent the LPC coefficients on a warped frequency scale. A warping constant determines the degree of transformation. This results in an ARMA representation of the filter transfer function. The second step determines recursively the cepstral coefficients corresponding to this ARMA transfer function

Imai[45] reports a new technique for cepstral analysis-synthesis on the mel frequency scale, the log spectrum on the mel frequency scale is considered to be an effective representation of the spectral envelope of speech. This analysis-synthesis system uses the mel log spectrum approximation (MLSA) filter which was devised for the cepstral synthesis on the mel frequency scale. The filter coefficients are easily obtained through a simple linear transform from the mel cepstrum defined as the Fourier cosine coefficients of the mel log spectral envelope of speech. The MLSA filter has low coefficient sensitivity and good coefficient quantization characteristics. The spectral distortion caused by the interpolation of the filter parameters of two successive frames is small and as such, the data rate of this system is very low. The same quality speech is synthesized at 60-70 % of the data rates in the conventional cepstral vocoder or the LPC vocoder.

New techniques for automatic speaker verification using telephone speech based on a set of functions of time obtained from acoustic analysis of a fixed, sentence-long utterance has been suggested by Furui [46]. Cepstral coefficients are extracted by means of LPC analysis successively throughout an utterance to form time functions. The time functions are expanded by orthogonal polynomial representations and, after a feature selection procedure, brought into time registration with stored reference functions to calculate the overall distance. This is accomplished by a new time warping method using a dynamic programming technique. A decision is made to accept or reject an identity claim, based on the overall distance. Reference functions and decision thresholds are updated for each customer. Results of the experiment indicate that verification error rate of one percent or less can be obtained even if the reference and test utterances are subjected to different transmission conditions.

Chapter 2 Review of past work

Concentrating mainly on the signal processing and physical models behind the algorithms used to classify ships by making use of the radiated noise, the physical model for cavitation is expanded to include the losses by acoustical radiation and the heat transfer from the vapor to the fluid by Lourens [47]. Out of the five algorithms developed for estimating the propeller speed, the performance of the three most promising ones are judged with respect to the ratio of the expected value to the variance of the estimator. A complete Bayes hypothesis test on second-order autoregressive power density spectrum poles are then described for determining the kind of propulsion a vessel uses. The nature of gearbox noise is described and the cepstrum is proposed as a technique to detect this kind of noise.

Xiong *et al.*[48] present a comparison of 6 methods for classification of sports audio. For the feature extraction, the two choices of MPEG-7 audio features and Mel-scale frequency cepstrum coefficients (MFCC) are considered, while for the classification the two choices of maximum likelihood hidden Markov models (ML-HMM) and entropic prior HMM (EP-HMM) are considered. EP-HMM, in turn, have two variations, *viz.* with and without trimming of the model parameters. Thus there exist 6 possible methods, each of which corresponds to a combination. The results show that all the combinations achieve classification accuracy of around 90% with the best and the second best being MPEG-7 features with EP-HMM and MFCC with ML-HMM.

Eronen [49] has compared several features with regard to recognition performance in a musical instrument recognition system. Both mel-frequency and linear prediction cepstral and delta cepstral coefficients were calculated. Linear prediction analysis was carried out both on a uniform and a warped frequency scale, and reflection coefficients were also

Realisation of a Target Classifier for Noise Sources in the Ocean

used as features. The data base consisted of 5286 acoustic and synthetic solo tones from 29 different Western orchestral instruments, out of which 16 instruments were included in the test set. The best performance for solo tone recognition, 35% for individual instruments and 77% for families, was obtained with a feature set consisting of two sets of mel-frequency cepstral coefficients and a subset of the other analysed features. The confusions made by the system were analysed and compared to results reported in a human perception experiment

A vowel system identification using phonological typologies is discussed in [50]. The phonological study of vowel systems shows that a typology of the languages may be issued from the description of their vowel system. The vocalic space has been modelled as a Gaussian mixture and two algorithms, *viz.* LBG and LBG-Rissanen algorithms have been used to estimate it. The success rate of about 75% has been achieved

Molau *et al.* [51] presents a method to derive Mel-frequency cepstral coefficients directly from the power spectrum of a speech signal. Omission of filter bank in signal analysis does not affect the word error rate and it simplifies the speech recognizers front end by merging subsequent signal analysis steps into a single one. It avoids possible interpolation and discretization problems and results in compact implementation. The frequency warping schemes like vocal tract normalization can be integrated easily without additional computational efforts.

Molau *et al.*[52] describes a technique called histogram normalization that aims at normalizing feature space distributions at different stages in the signal analysis front-end, namely the log-compressed filter bank vectors, cepstral coefficients, and LDA (local density approximation) transformed acoustic vectors. Best results are obtained at

Chapter 2 Review of past work

the filter bank, and in most cases there is a minor additional gain when normalization is applied sequentially at different stages. It is shown that histogram normalization performs best if applied both in training and recognition, and that smoothing the target histogram obtained on the training data is also helpful.

Tyagi *et al.* [53] presents new dynamic features derived from the modulation spectrum of the cepstral trajectories of the speech signal. Cepstral trajectories are projected over the basis of sines and cosines yielding the cepstral modulation frequency response of the speech signal. It has been shown that the different sines and cosines basis vectors select different modulation frequencies, whereas the frequency responses of the delta and the double delta filters are only centred over 15 Hz. Therefore, projecting cepstral trajectories over the basis of sines and cosines yield a more complementary and discriminative range of features. In this work, the cepstrum reconstructed from the lower cepstral modulation frequency components is used as the static feature. In experiments, it is shown that these new dynamic features yield a significant increase in the speech recognition performance in various noise conditions when compared directly to the standard temporal derivative features.

Garcia *et al.* [54] presents the development of an automatic recognition system for infant cry, with the objective to classify two types of cry, *viz.* normal and pathological cry from deaf babies. Acoustic characteristics obtained from the mel-frequency cepstrum technique and a feed forward neural network that was trained with several learning methods were used for this classifier and this resulted in a better scaled conjugate gradient algorithm.

Speech and music discrimination has gained much popularity in recent years for efficient coding and automatic retrieval of multimedia sources and Automated Speech Recognition (ASR). Mubarak *et al.*[55] present two novel features that can be concatenated with Mel frequency cepstral coefficients, *viz.* the Delta Cepstral Energy (DCE) and Power Spectrum Deviation (PSDev). Employing a Gaussian mixture model for classification as a back-end to the system, a significant improvement in the error rate was found using these features.

Black *et al.*[56] describe an algorithm for detecting and estimating pitch in acoustic audio signals using the generalized spectrum (GS). A performance evaluation of a GS-based and two classical, autocorrelation- and cepstrum-based, pitch determination algorithms have been conducted on a set of Wavetable synthesized musical signals. The experiment performs the tasks of pitch detection and estimation. Pitch estimation performance is presented in terms of gross pitch errors and mean-squared fine pitch error. The pitch detection performance is evaluated by a receiver operating characteristic analysis of the detection statistics. Results demonstrate that the GS-based estimator generally performs worse than the autocorrelation and cepstrum-based methods. However, the GS-based method performed consistently better for the detection problem, especially at low signal-to-noise ratio levels.

A study on the effectiveness of mel-frequency cepstrum coefficients (MFCCs) and some of their statistical distribution properties such as skewness, kurtosis, standard deviation, etc. as the features for text-dependent speaker identification is presented in [57] by Molla and Hirose. Multi-layer neural network with back propagation learning algorithm is used here as the classification tool. The MFCCs representing the speaker characteristics of a speech segment are computed by nonlinear filter bank

Chapter 2 Review of past work

analysis and discrete cosine transform. The speaker identification efficiency and the convergence speed of the neural network are investigated for different combinations of the proposed features. The result shows that the first MFCC degrades the identification competence and statistical distribution parameters enhance the training speed of the neural network.

Automatic knowledge extraction from music signals is a key component for most music organization and music information retrieval systems. Nielsen *et al.* in [58], consider the problem of instrument modelling and classification from the rough audio data. Two different models on the spectral characterization of musical instruments have been considered. The first assumes a constant envelope of the spectrum (i.e., independent from the pitch), whereas the second assumes a constant relation among the amplitude of the harmonics. The first model is related to the Mel frequency cepstrum coefficients (MFCCs), while the second to harmonic representation (HR). Experiments on a large database of real instrument recordings show that the first model offers a more satisfactory characterization and therefore MFCCs should be preferred to HR for instrument modelling/classification

Hung *et al.* [59], discusses the use of Weighted Filter Bank Analysis (WFBA) to increase the discriminating ability of Mel Frequency Cepstral Coefficients (MFCCs). The WFBA emphasizes the peak structure of the log filter bank energies (LFBEs) obtained from filter bank analysis while attenuating the components with lower energy in a simple, direct, and effective way. Experimental results for recognition of continuous Mandarin telephone speech indicate that the WFBA-based cepstral features are more robust than those derived by employing the standard filter bank analysis and some widely used cepstral liftering and frequency filtering schemes both in channel-distorted and noisy conditions

2.3.3 Bispectral Features

Higher Order Spectral analysis as well as bispectrum concepts have been described in [60] – [76].

An important task in underwater passive sonar signal processing is the determination of target signatures based on the narrow-band signal content in the received signal. To achieve good classification performance it is important to be able to separate the different sources (e.g. engine, hull and drive) present in the signature, and to determine the distinct frequency coupling pattern of each of these sources. Lennartsson, *et al.* [60], attempt to achieve these using bispectral techniques. It was found that the harmonics that propagated through water are engine related at low speeds and drive related at high speeds. The hull vibrations are only present at very low speeds. Moreover, it is found that the normalized bispectrum measures could provide additional coupling information not visible in the standard bispectrum.

Raghuveer and Nikias in [61] provide a detailed study of parametric estimation of bispectrum. Power spectrum estimation essentially contains the same information as the autocorrelation and hence provides a complete statistical description of a process only if it is Gaussian. In cases where the process is non-Gaussian or is generated by nonlinear mechanisms, higher order spectra defined in terms of higher order moments or cumulants provide additional information which cannot be obtained from the power spectrum. This paper concentrates on the third-order spectrum or the bispectrum. The bispectrum of a third-order stationary process can be defined as the double Fourier transform of its third moment sequence. It has the important property of being identically zero for a zero-mean Gaussian process and can thus be used to measure deviations from normality.

Chapter 2 Review of past work

Raghuveer and Nikias in [62], also describes the parametric method for bispectrum estimation which is based on a non-Gaussian white noise driven autoregressive (AR) model. A detailed overview of bispectrum and parametric methods are presented. The paper proposes a parametric approach to bispectrum estimation based on AR modelling of time series. The definition and properties of a parametric bispectrum estimator in the general ARMA case are also presented.

Regazzoni, *et al.* in [63] compare the spectral and bispectral analysis techniques and investigate the acoustical underwater communication problem in the low frequency range, up to 1 kHz, where the shipping noise is dominant and expected to be non-Gaussian. Classical detector performance is found to degrade in the presence of non-Gaussianity. The results indicate that for detection and identification in non-Gaussian environment, HOS based approaches are capable of providing more robust and efficient results.

Another paper which tries to compare the effectiveness of classical spectral analysis as well as modern techniques is given in [64]. The objective of the paper is to ascertain whether passive sonar signals can be classified on the basis of higher order statistics of their time series and whether higher order statistics can have any additional classification information that is not present in the power spectrum. The paper describes the limitations of the conventional higher order spectra (HOS) and defines new higher order spectra called Phase Only Spectra (POS). The studies reveal that conventional HOS could provide no more information than is present in the Power spectra. Higher order analysis should use POS to extract additional information.

Realisation of a Target Classifier for Noise Sources in the Ocean

Bispectrum estimation is found useful in detecting quadratic phase coupling among sinusoids in noise, the phase measurements for non-Gaussian processes, system identification, etc. When the given data records are short, all known methods perform poorly in terms of resolution. Raghuvver and Nikias in [65] presents a method called Constrained Third Order Mean (CTOM), which can perform very well in detecting quadratic phase coupling when the data records are short. The method proposes the estimation of the parameters of an autoregressive (AR) model driven by non-Gaussian White Noise (NGWN) by setting the sample mean of the Third Order Recursion error process to zero.

Papadopoulos, *et al.* [66], suggest a method for transient signal reconstruction using bispectral estimation techniques. The proposed method is capable of reconstructing the transient signal in environments, where the noise is coloured Gaussian with unknown autocorrelation function. The method could out perform the conventional Prony's method whereas the existing methods could not perform well in the presence of significant additive noises.

In [67], Garth and Bresler re-examines many statistical tests for stationary time series, formalizing the consistency requirements for the component HOS estimators. The paper also proposes a new F-test statistic. Studies are carried out on the detrimental factors in Hinich's test and modify this test for coloured scenarios.

In [68], Grassia, *et al.* consider the statistical characterization of non-Gaussian noise, with a particular reference to shipping underwater noise. The bispectrum of sample data are analyzed using both parametric as well as non-parametric methods to obtain useful phase instantaneous information applicable to classification and characterization.

Chapter 2 Review of past work

Nikias and Raghuvver [69] describe the bispectrum estimation in a digital signal processing framework. Definitions and properties of bispectrum is presented. Conventional Power Spectral estimation and its limitations are discussed. General reasons behind the use of bispectrum in signal processing are addressed. Both conventional and parametric models of bispectrum estimations are explained. The paper also briefs various applications of the bispectrum like detection of Quadratic phase coupling, deconvolution, etc.

Hinich, *et al.* [70], describe the bispectrum estimation of a ship radiated noise received using a towed array. The result shows that there exist frequency dependent bispectral components in the ships radiated noise. The ambient noise does not contain any significant bispectral components. Since the existence of a nonzero bispectrum indicates the presence of non-linear components in the noise source, it is estimated that the ship generated noise contains non-linear components. The paper suggests a means for differentiating between ship noise and at least some other forms of ambient noise sources using bispectral analysis. Another significant point to be noted is that the data used was in the narrow band (of bandwidth 130 Hz) and the cavitation noise, which is expected to be a major contributor of the shipping noise, was out of band.

The bispectrum and bicoherence estimates of underwater acoustic signals have been studied by Richardson and Hodgkiss [71]. The properties of bispectrum and bicoherence are described. Bispectra of data collected from a freely drifting swallow float is estimated. The results show how the bispectrum can be used to detect non-Gaussianity, nonlinearity and harmonic coupling. Special stress is given in determining whether the spectral lines are harmonically related.

Mendel in [72], gives an in-depth treatment on higher order statistics. The paper collects some of the most useful theoretical results, making them readily accessible. Various fields of applications of higher order statistics are described. The paper covers various definitions and properties related to higher order statistics and also discuss various results.

Quazi [73] suggests an attempt to utilize the basic quantities of the information theory, *viz.* entropy and mutual information for detection and localization of underwater sources. The entropy of a process having a finite number of sample points is maximum when the received process consists of noise alone and decreases when a correlated signal is present. The paper analyses both active and passive sonar signals and compares them with the results of traditional techniques.

Martin [74], presents a detection statistics, which exploits features in the three dimensional response of the non-stationary bispectrum for an assumed class of transient signals. The results are presented relative to the performance of a conventional power spectrum detector and a detection statistics based on the spectral correlation. The paper also discusses the merits of bispectral detectors relative to other transient detection methods.

Frazer and Boashash [75] have demonstrated the application of the Wigner-Ville time frequency distribution, the bispectrum, the time varying bispectrum and Gerr's third order Wigner distribution, to underwater acoustic data. Use of higher order spectral analysis improves time, frequency and time-frequency analysis methods and provides the analyst with important additional information.

Roy *et al.* [76] in their paper present a novel feature and its estimation method, for the classification of marine vessels using passive

Chapter 2 Review of past work

sonar. A classification feature, namely the coefficient of quadratic nonlinearity (CQNL), which quantifies the quadratic coupling that exists between a pair of running machinery on the target platform, has been proposed. The classification is based on the premise that the degree of nonlinear coupling between the various machineries on a target platform is unique for a particular class of targets and depends on the types of machinery and their placements. The estimation of the CQNL feature uses higher-order spectral analysis in conjunction with a method analogous to matched field processing. The CQNL feature provides unique information about the target platform that is not present in spectrum based features. The performance of the algorithm is good even in low SNR conditions.

2.4 Classifiers

2.4.1 Statistical Classifiers

Statistical classification uses statistical procedure for classification, in which individual items are placed into groups based on quantitative information on one or more characteristics inherently associated with the items (referred to as traits, variables, characters, etc.) and based on a training set of previously labelled items.

In [77], Rajagopal *et al.* describe the classification of marine vessels using Passive Sonar methods. The signals from various surrounding sources are sensed by a receiver. The data is processed and transformed to obtain the input to the classifier, which combines these with any other stored information to make a decision. The paper proposes a scheme for a general classifier and describes the practical constraints on each block of the classifier. Three well known classification techniques, *viz.* statistical,

expert system and neural network are compared and finally combined to give a hybrid classifier.

Shapo and Bethel [78], in their paper introduces *Cell Probability Density Function* (CPDF), a new statistical detecting and tracking algorithm suitable for imaging arrays. The input to the algorithm is the 20 array of intensity levels in all beams as a function of time. CPDF is a three-step algorithm, involving pre-processing, detection, and tracking/bearing estimation. It is found that CPDF has been very successful in detecting and tracking targets on broadband data collected by SONAR arrays, and has excelled in especially challenging scenarios with high bearing rates and multiple crossing targets.

2.4.2 Expert System Classifiers

Rajagopal *et al.* [79] describes an expert system approach for sonar target classification. It deals with passive listening for classification of underwater targets.

There are basically two different techniques of classification, *viz.* the statistical approach which makes use of classical pattern recognition methods and the expert system approach. The paper also identifies and discusses dominant sources of noise such as propeller cavitation noise, blade-rate tonals, piston-slap tonals, gear noise, injector noise and low frequency radiation from the hulls. The structure of the expert system consists of three major parts, *viz.* a knowledge base which deals with rules of inference and facts, a database consisting of the facts made available to the system by the programmer at any given time and the inference engine that guides the reasoning process through the knowledge base by attempting to match the facts in the data base to the rule conditions.

Chapter 2 Review of past work

Algorithms to detect and classify various parameters of ships by analyzing the underwater acoustic noise are presented in [80]. Lourens and Coetzer in this work, discuss the detection of the mechanical features like propeller shaft speed, number of propeller blades and type of propulsion. Classification of the ships into different classes is carried out using a small expert system. The propeller shaft speed and number of blades can be determined by two approaches. The first method consists of computing the Discrete Fourier Transform of the short time power of band pass filtered underwater acoustic noise. The second method determines a two dimensional discrete Fourier transform to extract the required information.

The development of an autonomous sonar classification expert system for AUVs is investigated in [81] by Brutzman, *et al.*. The use of Geometric analysis techniques and an expert system for heuristic reasoning has been examined in this paper. Classification of sonar contacts is performed by comparing the attributes of detected objects with predetermined attributes of known objects of interest.

Adnet and Martin [82] presents the first results of a study of an expert system dedicated to spectral analysis. Spectral analysis methods have been put together with a unification principle stemming from filter bank analysis and the strategy has been applied to generate a Knowledge based system.

2.4.3 Neural Network Classifiers

The various neural network based classifiers reported in open literature are described below.

Jae-Byung Jung, *et al.* [83] discusses the results from a set of experiments conducted on the target classification capabilities of broadband

sonar using targets of differing sizes and materials like Styrofoam balls and hollow plastic bodies. The experiments were carried out by analyzing the spectral components of echoes from the targets using neural networks. The studies indicate the potential use of broadband sonar as a tool for species and size classification of fish and other marine targets.

Several different classification algorithms are tested and benchmarked in [84], by Donghui Li, *et al.* not only for their performance but also to gain insight into the properties of the feature space. Results of a wideband 80-kHz acoustic backscattered data set collected for six different objects are presented in terms of the receiver operating characteristics (ROC) and robustness of the classifiers with respect to reverberation. Classification methods like Multivariate Gaussian Classifier, Evidential K-Nearest Neighbour Classifier, support vector machines, etc. are considered.

In [85], Purnell, *et al.* present the implementation of a classifier which discriminates between ships based on the radar back scatter from the targets. Three different classification methods, *viz.* correlation filters, peak extraction with a feed forward neural network classifier and a feed forward neural network using raw radar data were used. It was concluded that the feed forward neural network method that uses raw radar data showed better performance.

De Yao, *et al.* in [86] propose a classification system which consists of several subsystems including pre-processing, sub-band decomposition using wavelet packets, linear predictive coding, feature selection and neural network classifier. A multi-aspect fusion system is introduced to further improve the classification accuracy. The classification performance of the overall system is demonstrated and benchmarked on two different acoustic backscattered data sets with 40 and 80-kHz bandwidth. A comprehensive

Chapter 2 Review of past work

study has been presented to compare the classification performance using these data sets in terms of the receiver operating curves, error locations, generalization and robustness on a large set of noisy data. Additionally, the importance of different frequency bands for the wideband 80 kHz data is also investigated. For the wideband data, a sub-band fusion mechanism is introduced, which offers very promising result.

[87] – [90] discuss the introductory papers which throw some light on the underlying principles and methodologies of realizing neural network based classifiers [87] outlines the biological neuron structure and its similarity to the artificial neural network (ANN) alongwith a historical overview of ANNs. A brief review of the various components of the network and various training / learning functions is also presented.

Schoonees [88], gives an introduction to artificial neural networks and provides an overview of their potential application in signal processing. A brief survey of three network models, viz. Hopfield Net, Multilayer perceptron and Self Organizing Feature maps is also described.

Richard P. Lippmann [89] in his review paper presents the concepts of artificial neural networks in detail. He reviews six important neural net models that can be used for pattern classification. A comparison of neural nets and traditional classifiers are also presented. Descriptions of Hopfield, Hamming, Single Layer perceptron, Multi layer perceptron, Kohonen's Self Organizing Feature maps, etc. are presented.

Back propagation algorithms are extensively used in almost all applications involving neural networks including pattern as well as target recognition. Paul and Byrne [90] present an efficient learning algorithm for the back propagation networks. Two conditions for reducing the learning

iterations are deduced, without affecting the memory retention or generalization capabilities of the network.

Abdel Allim, *et al.* [91] describe a neural network system which can recognize different types of sonar signals. The work compares the parameters that affect the shape of the echoes returned from different underwater targets like submarines, mines, etc., using fourteen echo signals from three different types of military targets.

A discussion of the real-time digital signal processor based hierarchical neural network classifier, capable of classifying both analog and digital modulation signals is presented in [92]. A high performance DSP processor, *viz.* the TMS320C6701, has been made use for implementing the different kinds of classifiers, including a hierarchical neural network classifier. A total of 31 statistical signal features are extracted and used to classify 11 modulation signals corrupted by white noise.

Martinez Madrid, *et al.* [93], describe a target classification system which uses the measured Doppler signature to excite a neural network. The paper describes the use of Multilayer perceptron based neural network and its training using back propagation algorithm. The paper also points out the advantages of using neural networks, like fault tolerance, learning capabilities, etc.

Eapen, A [94], proposes the use of a neural network for detecting underwater targets in the presence of random noise. Here a neural network is made to adapt to the signal output of a hydrophone. Then the changes triggered by the presence of targets will be detected with the complex classification space of the neural network. Neural networks offer powerful

Chapter 2 Review of past work

collective computational capability for designing special purpose hardware, which can implement automatic detection of targets in real time. The ability to learn is the key property of ANNs. Modern learning procedures fall into two broad categories, *viz.* supervised methods, which require a teacher to specify the desired outputs and unsupervised procedures, which construct internal models that capture regularities in input signals. The work presented in this paper uses a variant of the back propagation rule, which is one of the most widely used algorithms for multilayer perceptron-like networks, called the Modified selective update back propagation algorithm.

A comparison of the relative performance of a number of classical classification methods with the neural network is performed by Patel, *et al.*[95]. Feature data extracted from infrared images are used for the comparison. Classical classification techniques, *viz.* k-Nearest neighbour, Euclidean distance, weighted Euclidean distance and Mahalanobis distance are described and tested. The neural network used was a simple Multilayer perceptron network trained with error back propagation coupled with a gradient descent algorithm. The network consisted of an input layer, a hidden layer and an output layer. A sigmoid function was used as the activation function. The studies show that the neural network and k-nearest neighbor methods could outperform all the other classical techniques. Considering the adaptability and the computational efficiency of Neural Networks, the MLP method is shown to have a distinct advantage.

Chin-Hsing Chen, *et al.* [96] describe the results of four kinds of neural network classifiers that have been used for the classification of underwater passive sonar signals radiated by ships. Classification process is divided into two stages, *viz.* pre-processing feature extraction stage and classification stage. In the pre-processing stage, Two-Pass Split-Windows (TPSW) algorithm is used to extract tonal features from the average power

Realisation of a Target Classifier for Noise Sources in the Ocean

spectral density of the input data. In the classification stage, four kinds of static neural network classifiers are used to evaluate the classification results :

- The probabilistic based classifier-Probabilistic Neural Network (PNN)
- The hyperplane based classifier-Multilayer Perceptron (MLP)
- The kernel based classifier- Adaptive Kernel Classifier (AKC) and
- The exemplar based classifier- Learning Vector Quantization (LVQ).

The data were collected from fishing boats, which were classified into three groups. From each boat, three types of signals (at low speed, at medium speed and at high speed) were recorded. It has been experimentally established that the exemplar classifiers-LVQ have the most efficient learning.

Azimi-Sadjadi, *et al.* [97] describe a new sub band based classification scheme developed for classifying underwater mines and mine like objects from the acoustic backscattered signals. The system consists of a feature extractor using wavelet packets in conjunction with linear predictive coding (LPC), a feature selection scheme and a back propagation neural network classifier. Multi aspect fusion was performed to obtain great improvement in the classification performance of the system.

Roth, M.W in his review paper [98] on Automatic Target Recognition (ATR), highlights the use of neural network technology in the field of ATR. The paper describes ATR sensor development and Multi

Chapter 2 Review of past work

sensor fusion, various issues related to ATR, feature extraction procedures and the scope of neural networks in the field of ATR and its advantages.

Overman and Louri, [99], investigates the design of a neural network architecture that can take noisy serial pixel data as an input and report the detected position of the target with respect to the sensors field of view. The neural network target detection architecture presented is based on Multilayer perceptron neural receiver. The paper describes how a neural network can be implemented as an optimum likelihood ratio receiver and discusses back propagation training process. Preparations in setting up neural net detection architecture for Monte-Carlo simulations against various noise types are also discussed.

Solinsky and Nash [100], in their paper attempt to describe the applications of neural network in sonar. Various neural network classifiers operating on the DARPA Phase I data set has been analyzed using classical decision theory. An important element of the assessment is to include a ground truth of events in the data set. A trained human operator produces such ground truths based on aural analysis of the data.

The use of hybrid neural approaches for passive sonar recognition and analysis using both unsupervised and supervised network topologies are investigated by Howell and Wood [101]. The results presented demonstrate the ability of the network to classify biological, man made, and geological noise sources. The capabilities of the networks to identify the complex vocalizations of several fish and marine mammalian species are also described. Basic structure, processor requirements, training and operational methodologies as well as application to autonomous observation are described. For training the network, Self Organising Map(SOM) - Kohonen maps are used, since it is efficient for unsupervised

learning. It also contains a review of various types of source files (.wav, MP3 etc) and the issues arising out of over sampling data in these types of files.

Hallinan and Jackway [102], describes a novel feature selection algorithm which utilizes a genetic algorithm to simultaneously optimize a feature subset and the weights for a three-layer feed-forward neural network classifier. It has been shown that this method needs only fewer input features and simpler neural network architecture. The results indicate that tailoring a neural network classifier to a specific subset of features has the potential to build a classifier with low classification error and relatively low computational overheads.

The design and evaluation of a comprehensive classifier for short duration oceanic signals obtained from passive sonar is described in [103]. The paper highlights the importance of selecting appropriate feature vectors for efficient classification. Wavelet based feature extractors are examined. A number of static neural network classifiers are evaluated and compared with traditional statistical techniques. The paper highlights the fact that each algorithm is designed to handle only a few set of problems and may have many limitations and a synergistic approach can lead to better results. It is found that a judicious combination of several classifiers will yield higher accuracy, since it can overcome the limitations of a single type of network and the system was tested with DARPA data set.

Yanning Zhang, *et al.* in [104], discuss a local adaptive neural network based classifier to classify ship noises. Combining wavelet theory with neural network to form adaptive wavelet neural network has the advantage of feature automatic compression, extraction and classification from signal. The neural network consists of input layer, adaptive wavelet

Chapter 2 Review of past work

feature extraction layer, hidden layer and output layer. A modified Back propagation algorithm is used to train the network.

Adams, *et al.* [105], present the statistical properties of underwater acoustic ambient noise fields obtained by analyzing the acoustic output of a single hydrophone in the 75-200 Hz band. The analysis demonstrates the non-stationarity of the noise power in 0.78 Hz bands. In addition, the correlation between the noise power fluctuations in 0.78 Hz bands is shown as a function of time and frequency separation of the bands. The fluctuations appear to consist of a slow broadband power increase and a smaller amplitude fluctuation process which has small correlation across frequency and time.

John R. Potter [106], establishes that a feed forward ANN is very effective in self training the system to recognize the end notes of bowhead whale songs. A three layer feed forward network is used for testing.

2.4.4 Fuzzy Classifiers

Argenti, *et al.* [107], address the problem of detecting ships in SAR images in a fully automated way. A classification scheme implemented using fuzzy logic principles is also discussed in this paper.

Amo *et al.* [108], suggests an algorithm for terrain matching, leveraging an existing fuzzy clustering algorithm, and modifying it to its supervised version for apply the algorithm for georegistration as well as pattern recognition. Georegistration is the process of adjusting one drawing or image to the geographic location of a "known good" reference drawing, image, surface or map. The terrain matching algorithm will be based on fuzzy set theory as a very accurate method to represent the imprecision of the real world, and presented as a multicriteria decision making problem.

The energy emitted and reflected by the Earth's surface has to be recorded by relatively complex remote sensing devices that have spatial, spectral and geometrical resolution.

2.4.5 Sonar Signal Processor based Classifiers

Gaunard, in [109], describes the bistatic and mostly monostatic techniques that are useful for target classification by means of active sonar. The echoes returned by any submerged elastic body contain features caused by the poles of the scattering amplitude of the problem. These poles are studied and it was shown that they naturally split into two large sets from which one can separately extract shape or material composition information. The composition information seems easier to determine than details about the shape. Together these sets of poles unambiguously characterize any scatterer.

A filter structure has been proposed for target signal enhancement in reverberation limited environment by Kim *et al.* [110]. The proposed structure consists of an adaptive filter and a non-adaptive filter. The input signal is filtered by the non-adaptive filter whose coefficients are obtained from the adaptive filter working with the delayed signal. The investigations were carried out on the data from an active sonar system for target signal enhancement problem and the results have shown that the proposed method can yield fairly acceptable performance in a time varying channel and is robust to target cancellation effects.

Dwyer [111], discusses the processing technology that enables the classification of target echoes from very wide bandwidth transmitted signals, which can reduce the complexity of classifiers. Implementation of two types of sequential classifiers is discussed. One of the sequential

Chapter 2 Review of past work

classifier used the spectrum of the data while the other used the fourth order cumulant spectrum of the data.

A new method for target localization and classification has been discussed in [112]. Firing of pulses from two closely spaced transmitters, with a time separation of the order of 1 ms is the basic tool for this approach. Maximum Likelihood Estimation (MLE) method is used for the implementation.

A tutorial illustrating some interactive demos, tips and tricks of Digital Signal Processing are described in the website [113].

2.4.6 Recent Trends

A classification algorithm using Hidden Markov Models (HMMs) is presented in [114]. Recognition of three classes of targets such as personnel, tracked and wheeled vehicles can be carried out using this algorithm. The procedure described is based on target Doppler signatures. While conventional Doppler based methods consider the Doppler signature to be stationary, the suggested method utilizes the time-varying nature of Doppler signature as well for efficient classification. One of the advantages of this technique is that the classifier requires only a modest amount of data for training.

Lourens [115] considers an improved cavitation model and proposes algorithms for determining propeller speed and number of blades. The new model takes into account the acoustic losses and heat losses. Gear box identification is also addressed in this paper. A complete Bayes hypothesis test is also described for determining the kind of propulsion the vessel uses.

Paul Chestnut, Helen Landsman and Robert W. Floyd, [116], present a study carried out on an active sonar target recognition system. The data were obtained from 16 targets, submerged in a salt water pool. The frequency responses from the echoes were analyzed and the information is extracted by energy detection in a bank of filters and Spectral modelling. The classification techniques use methods in conventional pattern recognition.

Chan, *et al.* [117] present a new bearings-only method of detecting and tracking low signal-to-noise ratio (SNR) wideband targets on a constant course and velocity trajectory. A track-before-detect strategy based on matched velocity filtering is adopted using spatial images constructed from a sequence of power bearing map (PBM) estimates accumulated during tracking. To lower the threshold SNR for detection, a discrete bank of matched velocity filters integrates the PBM images over a range of hypothesized trajectories. The distribution of the matched filter output is derived based on a single point target in diffuse noise conditions. Receiver operating characteristic curves show a definite detection gain under low SNR conditions for matched velocity filtering over detection from a single PBM.

Attempts by Chen Xiangdong and Wang Zheng [118], throw light on a non-linear signal processing technique called the Similar Sequence Repeatability to analyze the ship radiated noise and indicate its use for the acoustic target recognition. Here, the local similarity of the ship radiated noise data is studied based on the temporal behaviour of the time series itself. According to the local similarity property of the time domain acoustic signal, a phase space is constructed. From this, repeatability parameters are calculated and repeatability (RPT) curves are drawn, from which the entropy information is extracted. The RPT curves and the

Chapter 2 Review of past work

entropy can effectively represent the time domain features of the ship radiated noise and aids in underwater target recognition and classification.

Guo Guirong, *et al.* [119] discuss the problem of ship recognition and a suitable method is proposed. The paper focuses on algorithms for target recognition from radar video returns. The method mainly uses the Fourier transform and Mellin transform for feature extraction. Fourier Transform is invariant to shifting. This property provides a useful means for extracting features insensitive to the time delay of radar returns, that is, the target range. The Mellin transform produces a set of features invariant to scaling changes. This implies that the features extracted from the MT are insensitive to the aspect angle of the radar.

Pezeshki, *et al.* in [120], suggest a feature extraction method for underwater target classification that exploits the linear dependence between two sonar returns. Canonical co-ordinate decomposition is applied to resolve two consecutive acoustic backscattered signals into their dominant canonical coordinates. The hypothesis behind this feature extraction method is that for certain aspect separations linear dependence of coherence between the sonar returns reveals common target/non-target attributes, whereas linear independence reveals bottom reverberation features.

A work that discusses the nonlinear regularities in ship-radiated signals is presented by Su Yang and Zhishun Li [121]. They propose a chaotic feature for classification. Certain classes that cannot be classified effectively by using spectra can be satisfactorily classified using the chaotic features. Experimental results show that this feature is effective and outperforms the spectrum feature in identifying some classes. It can augment current solutions by providing complementary information.

Fractal based approaches for the recognition of ships from the radiated noise is being considered in [122]. The methods proposed by Yang, *et al.* include fractal Brownian motion based analysis, fractal dimension analysis and wavelet analysis, to augment existing feature extraction methods that are based on spectral analysis. The results show that fractal approaches are effective and when used to augment two traditional features, line and average spectra, fractal approaches lead to better classification results. This implies that fractal approaches can capture some information not detected by traditional approaches alone.

A sequential decision feedback approach for target classification of underwater mine-like objects in a changing environment is described by Azimi-Sadjadi *et al.*[123]. An adaptive target classification system developed using the decisions of multiple aspects of an object through a tapped delay line mechanism to impact the final decision of the current aspect is also discussed here. This system minimizes the error of the classifier while it maps the new feature vector to a familiar feature space for the classifier. The test results presented are obtained on a wideband acoustic backscattered data set collected using four different objects with 1 degree of aspect separation for two different bottom (smooth and rough) conditions.

Paul Gaunard *et al.*[124] discuss the automatic classification of environmental noise sources from their acoustic signatures, recorded at the microphone of a noise monitoring system (NMS), using Hidden Markov Models. The performance of the proposed system, which is based on a time frequency analysis of the noise signal, was evaluated experimentally for the classification of five types of noise events, *viz.* car, truck, moped, aircraft and train. The HMM based approach is found to outperform human

Chapter 2 Review of past work

listeners as well as previously proposed classifiers based on the average spectrum of noise event with success rates as high as 95%.

Transformation of a segment of acoustic signal, by processing into a vectorial representation such as the spectrum, can permit the identification of the constituent phonemes within spoken speech according to Grant [125]. A comparison with stored replicas of the data segments using techniques such as dynamic time warping or hidden Markov modelling then permits a speech recognition operation to be accomplished. These signal processor intensive transform and graph-search-based pattern matching techniques are reviewed and currently achievable recognition accuracies are reported.

Existing concepts of Walsh power spectra for wide sense stationary stochastic processes are restricted to the case of auto power spectra because they are based on real Walsh functions. Blaesser [126], describe a Walsh power spectrum, which is based on a system of complex Walsh functions for wide-sense stationary stochastic processes and the concepts have been extended to auto and cross power spectra as well.

2.5 Summary

An attempt has been made in this chapter to present a state-of-the-art literature in the topic covered by the thesis highlighting the characteristic signatures of typical ocean noise as well as the classes of features that have been considered for realizing the various types of classifiers as reported in open literature. The literature survey has also brought out the operational features of various classifiers such as statistical, expert system, neural network and fuzzy k-NN classifiers.

CHAPTER 3

METHODOLOGY

This chapter addresses the methodology adopted for the realisation of the proposed target classifier, which primarily involves the extraction of source features by analysing the composite noise data waveforms and compilation of the knowledge base, which forms the backbone of the classifier. The detection and estimation processor computes the various statistics for improving the target classification capabilities. The output of the estimation processor is compared with the earlier estimations, which are stored in the target feature record and the relevant target features are updated. In case, if a target feature is not updated over a significant period, the concerned feature will be dropped from the target feature record. In many situations, the system may have to backtrack or retrack through the stored feature record to establish the links with the most recent data. As and when the required classification clues are available in the target feature record, the most matching feature vector is identified from the known target feature vectors in the knowledge base, depending on the allowable percentage of mismatch, chosen by the user. For making the system fool proof and full-fledged one, the knowledge base has to be updated with the feature vectors and target dynamics for all the class and type of the targets. The target feature record or the target feature vector is generated from the spectral, cepstral and bispectral features.

Chapter 3 Methodology

3.1 Introduction

Sonar has been in wide spread practical use for underwater target detection, estimation, localization, tracking and classification applications. The recent advancements in microelectronics has created an indelible impact in sonar manufacturing industry, resulting in a rapid transition from hardware based processing systems to software based and fully automated computer controlled systems. Sonar data can be judiciously used to identify and classify underwater targets. Target detection addresses the problem of determining whether the target is present, while classification addresses the problem of identifying or categorising the detected target. To facilitate this, knowledge about the way in which typical isolated individual bodies interact with sound wave is essential. In active sonar, such information are quantified by the parameter *Target Strength* and the process of classification is correlated to the localisation and tracking functions as the target dynamics is severely affected and controlled by the target types and class. Passive sonars are the listening sonar systems which use sound, usually unwillingly, radiated by the target.

The propagation effects, responsible for the performance limitations in sonar systems are summarised below. The undersea propagation medium is a time-varying channel, which shows clear significant functional dependencies on geographic location, depth, range and season. Moreover, the temperature profile, multiple reflections and inhomogeneties present in the ocean cause a wide variety of channel dispersion effects on time, frequency and angle. The adverse effect of time spreading is due to multipath, while frequency spreading is caused by the wave motion of the sea surface, movement of water masses, underwater currents as well as the motions of the transmitter, receiver and targets.

Doppler spread of upto one percent or more are common in sonar. The sonar detection and estimation problems for signals of considerable spreading are much more cumbersome than the ones for simple systems, due to reasons that are obvious. A wide range of interfering noises are also present in the ocean such as the sea state noise, biological noise, machinery and cavitation noise from the shipping traffic, in addition to the thermal noise.

The underwater environment is characterised by a diverse range of *noise-like signals* and *signal-like noises*. In passive listening scenario, the sources and kind of noises from the targets are used to identify the targets. The noise signals generated by such noisy targets will form the basis for passive sonar detection and classification. The noise signals are characteristics of target concerned and may vary a great deal with time as well as class and type of target. Targets can be distinguished on the basis of the noise frequency spectrum or other signatures by performing the spectral analysis, bispectral analysis, cepstral analysis and Hidden Markov Modelling, which in turn can be compared with known signature patterns, and the matching pattern which has a good degree of acceptability can be identified.

The detection and estimation procedures in sonar involve the computation of various statistics for improving the overall performance of the target detection, localization and classification capabilities of the end system, taking into consideration all the undesirable propagation effects mentioned above.

3.2 Basic Model of the Proposed Classifier

In order to interpret most effectively and efficiently the vast amount of data furnished by the signal processor, especially in situations where the detectable range of the system is very large, it is essential to have a fully automated and intelligent classifier, as most of the target information, in all probability, may not be of much interest to the user. Operator assisted classifier turns out to be inappropriate and highly inefficient in such situations. The generalized block schematic of the proposed target classifier is shown in Fig. 3.1.

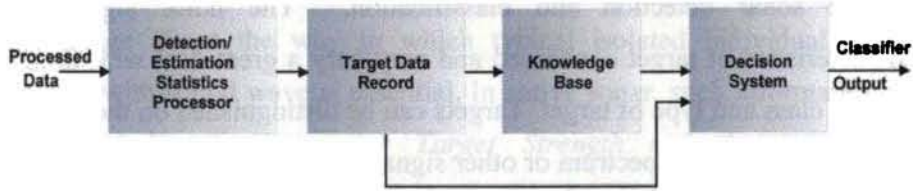


Fig. 3.1 Target Classifier

The detection and estimation statistics processor simply performs the estimation of the signal energy within a finite time interval. The output of the estimation processor is compared with the earlier estimations, which are stored in the target feature record and the relevant target features are updated. In case, if a target feature is not updated over a significant period, the concerned feature will be dropped from the target feature record. In many situations, the system may have to backtrack or retrack through the stored feature record to establish the links with the most recent data. As and when the required classification clues are available in the target feature record, the most matching feature vector is identified from the known target feature vectors in the knowledge base, depending on the allowable percentage of mismatch, chosen by the user. For making the system self contained and full-fledged one, the knowledge base has to be updated with

the signature patterns and target dynamics for all the class and types of targets.

3.3 Extraction of source signatures

3.3.1 Spectral Features

A totally random process with unknown features is normally modelled as a Gaussian random process, in a practical environment for decision-making purposes. Though the features are unknown, the receiver can have a rough knowledge of the spectral region that the signals may occupy, so that band-limiting filters turn out to be a very powerful tool for regenerating the noise signal, devoid of noise power outside the predicted spectral region.

This section presents a summary of some of the features that can be computed from the spectrum of a signal. Some of these features relate directly to some perceptual characteristics of sound, such as loudness, pitch, etc. Most of the features are generated from the spectrogram on a frame-by-frame basis.

3.3.1.1 Spectral Centroid

The spectral centroid, which may also be referred to as the spectral brightness, gives an indication of the spectral shape and is defined as the amplitude-weighted average or centroid of the spectrum [127], [128]. It is a simple, yet efficient parameter, estimated by summing together the product of each frequency component of the spectrum and its magnitude, which is further normalized by dividing with the sum of all the magnitudes. Thus the spectral centroid SC is given by

$$SC = \frac{\sum_{k=0}^{N/2-1} f_k S_k}{\sum_{k=0}^{N/2-1} S_k} \quad (3.1)$$

where S_k is the magnitude spectrum of the k^{th} frequency component f_k and N is the record size.

3.3.1.2 Spectral Range

The spectral range or bandwidth refers to the range of frequencies that are present in the signal. It is computed using the spectral magnitude weighted average of the difference between each frequency component and the centroid, SC . Thus the spectral range, SR is expressed as

$$SR = \frac{\sum_{k=0}^{N/2-1} S_k |f_k - SC|}{\sum_{k=0}^{N/2-1} S_k} \quad (3.2)$$

3.3.1.3 Spectral Roll off

Another spectral feature, which gives a measure of the spectral shape, is the spectral roll off and is defined as the frequency below which 85% of the magnitude distribution of the signal is concentrated [127].

i.e. $RO = \text{Minimum}(R)$, such that

$$\sum_{k=0}^R S_k \geq 0.85 \sum_{k=0}^{N-1} S_k \quad (3.3)$$

3.3.1.4 Spectral Flux

This is a measure of the amount of local spectral change. This is defined as the squared difference between the normalized magnitude spectra of successive frames.

$$Flux = \sum (norm_f[i] - norm_{f-1}[i])^2 \quad (3.4)$$

where $norm_f$ is the magnitude spectrum of the current frame, scaled to the range 0 to 1 and $norm_{f-1}$ is the normalised magnitude spectrum of the previous frame. Spectral flux is a measure of how quickly the power spectrum of the signal is changing and computed by comparing the power spectrum of one frame with that of the previous frame

3.3.1.5 Spectral Slope

The spectral slope is also identified as one of the prominent signatures in the suggested algorithm and refers to the average slope of the power spectral density variation.

3.3.1.6 Number of Peaks and the Peaking frequencies

The total number of peaks in the power spectral density variation, which will help in identifying the tonal as well as continuous frequency components, is treated as one of the significant spectral features. For better results, only the significant peaks above a certain preset threshold value are taken into account. The peaking frequencies, rising as well as falling slopes of the power spectral response of the target emanations are also considered for fine tuning the classification clues.

3.3.2 Cepstral Features

The target specific features extracted using spectral estimation of the noise emissions alone cannot always perform reliable classification especially, in the presence of composite ambient noise and varying environmental parameters. To make the identification process more robust and reliable, additional feature components are incorporated by exploiting the other unexplored features of the noise sources. A variety of signal processing applications use the collection of nonlinear techniques known as cepstral analysis which is capable of yielding potential features that can aid

Chapter 3 Methodology

in the process of classification. One of the important properties of the cepstrum is that it is a homomorphic transformation in which the output is a superposition of the input signals.

The spectrum of a waveform consists of two components, the slowly varying part, referred to as the filter or spectral envelope and the rapidly varying part, referred to as the source or harmonic structure. Separation of these two components can be achieved by taking the cepstrum, an anagram of the word spectrum. The cepstrum is defined as the inverse Fourier transform of the log magnitude Fourier spectrum of the signal and is said to be in the quefrequency domain, an anagram of frequency [129]. The cepstral values are stored as discrete components referred to as the cepstral coefficients, where the n^{th} cepstral coefficient is the amplitude of the n^{th} component along the quefrequency axis.

3.3.2.1 Mel Frequency Cepstral Coefficients

A more systematic approach for extracting the cepstral features makes use of the estimation of Mel Frequency Cepstral Coefficients (MFCC), which is a measure of the perceived harmonic structure of sound [130], [131]. A Mel is a psychoacoustic unit of frequency which relates to the human perception and is approximated using the expression

$$m = 2595 \log_{10} \left[1 + \frac{f}{700} \right] \quad (3.5)$$

where f is the frequency in Hz. The spectrum can be transformed into a spectrum emphasized at Mel intervals using Mel filter banks, which is a row of triangular filters overlapping at Mel-spaced intervals [132]. The cepstrum of this transformed spectrum yields Mel frequency cepstral coefficients.

3.3.3 Bispectral Features

Conventionally, techniques like power spectral estimation is widely being used for the analysis of various acoustic sources in the ocean including that of marine origin. However, power spectral analysis is phase blind and cannot fully characterize the nonlinear signals as well as the noise generating mechanisms. Thus most of the signals are approximated as linear and analysis is carried out, which results in loss of many valuable information in the signal. As the demand for more detailed and accurate analysis as well as modelling has increased, researchers are now mainly focusing on techniques based on higher order spectra [69].

Analysis using Higher Order Spectra, in particular the third order spectra called bispectrum, is being evolved as a powerful technique in the field of digital signal processing and allied areas. Bispectrum is a third order frequency domain measure, capable of providing more information than the conventional tools like power spectrum. While power spectrum can efficiently estimate the power of different frequency components of a signal, it in general fails to quantify any non-linear interactions between the component frequencies. Such interactions induced by the second order nonlinearities give rise to certain phase relations called Quadratic Phase Coupling (QPC). Bispectral analysis can reveal the presence of phase couplings as well as can provide a measure to quantify such couplings.

Bispectrum is the two-dimensional Fourier Transform of the expected value of a signal at three time points. The use of bispectrum is highly motivated by the fact that it can provide information regarding deviations from Gaussianity as well as presence of nonlinearities and phase information.. In situations where the stationary signals has non-Gaussian properties and the additive noise process is stationary Gaussian, the use of

Chapter 3 Methodology

bispectral analysis become advantageous in estimating the signal features. Such an analysis is important, since all periodic, quasi-periodic as well as many of the signals emitted from various machineries and mechanical systems can be considered as non-Gaussian.

Bispectral analysis can play a key role in the analysis of acoustic noise sources. A normalized form of bispectrum, called the bicoherence is found to be more appealing since its variance is independent of the energy content of the signal. Analysis of noise data wave forms generated by the noise sources in the ocean using bicoherence can reveal the deviation of the signals from Gaussianity as well as linearity, which is usually hidden in the traditional spectral analysis. Such information may be effectively utilized for generating certain target specific features, which can aid in the identification and classification of underwater targets.

3.4 Compilation of Knowledge Base

The performance of the classifier relies on the target features available in the knowledge base. To generate the features of a target, the long-term spectra of the specific target class are to be collected and averaged. The average spectrum so obtained is the characteristic spectrum for the specific target class or type under consideration.

The information bearing signals sensed by the hydrophone array, on an average, is white in nature, comprising of a wide range of frequencies. By computing the noise spectral level, over the available frequency range, one can infer the nature of the noisy target and by correlating this information with the available classification clues, it is possible to effectively identify the targets, within the limits of the variances of the classification clues.

3.5 Inference System

3.5.1 Feature Vector

A feature vector is an n -dimensional vector of numerical features that represent an object and facilitates processing and statistical analysis. The vector space associated with these vectors is often called the feature space. In general, feature extraction involves simplifying the amount of resources required to describe a large set of data accurately. When performing analysis of complex data, one of the major problems stem from the number of variables involved. Analysis with a large number of variables generally requires a large amount of memory and computational power. In order to reduce the dimensionality of the feature space, a number of dimensionality reduction techniques can be employed. The feature extraction is a generic term for methods of constructing combinations of the variables to override these problems while describing the data with sufficient accuracy.

3.5.2 Feature Selection

Upon extracting a set of features, which forms the basis for classification, only those features are selected, that can indeed improve the performance of the classifier. This process, known as feature selection, may lead to loss of information and is in many cases based on singular transformations. The feature selection process is significant because of the following reasons.

- **Reduce noise generated by irrelevant features.**

Many classifiers are sensitive to irrelevant features, and will degrade their performance when such features are included. Distance based classifiers, such as the ones used in this work, are

Chapter 3 Methodology

particularly sensitive to this. If a random feature is included, it will contribute to the distance measure just as much as any other feature. If the features were not scaled, they may contribute even more than a relevant feature. Thus, due to this distortion, a pattern may appear as similar to patterns of a different class.

- **The risk of over fitting the training data can be reduced**

The larger the number of features used, the more detailed the classifier will be. But if a classifier has too many degrees of freedom, it may adjust itself perfectly to the training data, but perform poorly when used with other data. By reducing the number of features, and thus the degrees of freedom of the classifier, it is possible to improve generalization for a given scenario.

- **Classifier made computationally feasible.**

The selection of too many features will demand substantial computing power for the purpose of feature extraction, training as well as classification process. Hence, the smaller the number of features the lesser will be the computational complexities of the classifier.

Thus, the classification function operates in a multidimensional space formed by the various components of the feature vector. For the purpose of classification, an efficient inference system, capable of performing template matching by correlating the generated target features with the feature components available in the knowledge base, has to be realized. The classification decision becomes too hard and inappropriate if too many features are considered for the decision-making. The practical

methods for the classification always involve a heuristic approach intended to find a *good-enough* solution to the optimization problem.

3.6 Summary

The methodology suggested to be adopted for realizing the proposed target classifier involving the extraction of target specific features by analysing the composite noise data waveforms followed by template matching of the feature vectors for the purpose of classification has been presented in this chapter. For making the system fool proof and full-fledged one, the knowledge base has to be updated with the feature vectors and target dynamics for all the class and type of the targets.

CHAPTER 4

Spectral and Cepstral Analysis

This chapter highlights the technology involved in extracting the spectral and cepstral feature components required for generating the classification clues. A spectrum is a relationship typically represented by a plot of the magnitude or relative value of some parameter against frequency. Spectral analysis is a frequency domain tool for signal analysis and characterizes the frequency content of a measured signal. Classical spectral estimation methods, in which the Power Spectral Density (PSD) is estimated directly from the signal itself is discussed in detail. In Parametric models, the PSD is estimated from a signal that is assumed to be the output of a linear system driven by white noise. These methods first estimate the parameters of the linear system, from which the signal is assumed to be generated. Such methods are found to give better results for short data segments. They also give better frequency resolutions than conventional estimators. The various algorithms used for the PSD estimations are discussed in detail in this chapter. This chapter also touches upon the concepts of cepstral analysis, which belongs to an area of signal processing known as *homomorphic analysis* and can be accomplished by using a cascade of forward and inverse operations with a linear time invariant operation sandwiched in between. A more systematic approach for computing the cepstral coefficients can be achieved by estimating the Mel Frequency Cepstral Coefficients (MFCC), which is a measure of the perceived harmonic structure of sound.

4.1 Introduction

The widespread and prevailing characteristics of ambient noise, which can be due to a variety of sources, often pose various problems in characterizing the noise data waveforms without subjecting it to various analytical procedures. Investigations on ambient noise carried out in the ocean over the band of frequencies from 1 Hz to 100 kHz show that ambient noise has different characteristics at different frequencies, and with a different spectral slope and a different behavior with varying environmental conditions, such as wind speed. It is also found that one or more of the source noises are dominant over the others in any one region of the spectrum.

The measurements have shown that above 150Hz, ambient noise in the deep ocean is principally surface generated and depends upon the sea surface in the vicinity of the receiver. Time periods of fluctuations in noise spectral level correspond to changes in local weather patterns. Over the band of frequencies 20 to 150 Hz, the ambient noise is highly variable and shipping as well as mining operations are the principal noise contributors. Time scales of fluctuations are much shorter than at higher frequencies and depend upon the proximity of the receiver to shipping channels, ship traffic density and the length of time, the passing ships spend in acoustic convergence zones.

Short-term fluctuations may be superimposed upon seasonal variations arising from variations in the speed of sound in the mixed layer. Characterizations of the noise processes as a stationery zero mean, Gaussian field may be adequate to describe the noise processes during short intervals of time, but do not describe the fluctuations in noise spectral level

which are observed experimentally and are not sufficient for the design of signal processing systems or for the prediction of system performance.

4.1.1 Sources of Ambient Noise

A conceptual diagram depicting some of the sources of deep water ambient noise is shown in Fig 4.1.

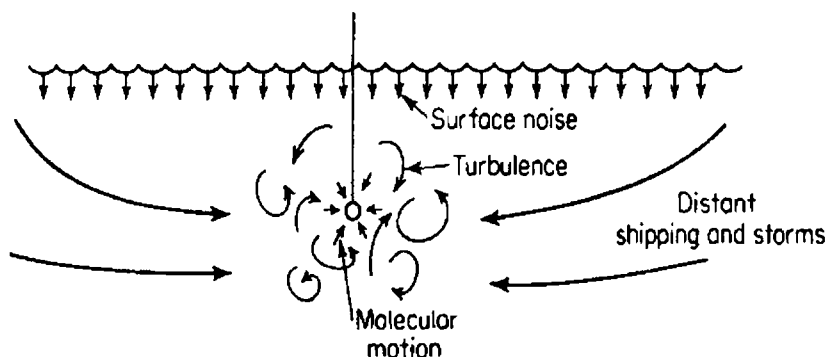


Fig. 4.1 Conceptual Diagram of sources of Ambient Noise

Tides and waves cause hydrostatic pressure variations of relatively large amplitude at the low-frequency end of the spectrum. Surface waves are also a source of hydrostatic pressure variations at a depth in the sea. However, they have pressure amplitude, which falls off rapidly with increasing depth and with decreasing wavelength of the surface waves. Another important contribution of ambient noise is due to seismic activities. The micro seismic disturbances and perhaps earth seismicity, in general, are likely sources of ocean noise at very low frequencies. In addition, intermittent seismic sources such as individual earthquakes and distant volcanic eruptions are undoubtedly the transient contributors to the low-frequency background of the deep sea.

The role of turbulence in the sea as a source of ambient noise is significant as the contribution to ambient noise can be in many forms. It

can contribute in the form of self-noise or can appear as part of the background at places far away from the turbulence itself. The third and the most important, acoustic effect of turbulence is the turbulent pressure variations created inside the turbulent region. The turbulence gives rise to varying dynamic pressures that are picked up by a pressure sensitive hydrophone located in the turbulent region.

The ambient noise measurements in areas of high shipping activities are higher and less wind dependent at frequencies from 50 to 500 Hz than they are in areas where shipping is sparse. Ship traffic, which may occur even at distances of 1,000 miles or more from the measurement hydrophone, can be a principal source of noise in the decade 50 to 500 Hz.

At higher frequencies, ambient noise is governed by the roughness of the sea surface. A direct correlation between the sea state or wind force and the level of ambient noise was found, with a better correlation of noise with local wind speed. The processes by which the sea surface generates the major portion of the ambient noise can be *breaking whitecaps, flow noise, cavitations, wave-generating action of the wind on the surface of the sea, second order effect of sea surface wave motion, etc..*

4.2 *Power spectral estimation*

A spectrum is a relationship typically represented by a plot of the magnitude or relative value of some parameter against frequency. Spectrum analysis is a frequency domain tool for signal analysis and characterizes the frequency content of a measured signal. The spectral density of the wave, when multiplied by an appropriate factor, will give the power carried by the wave per unit frequency.

Chapter 4 Spectral and Cepstral Analysis

The most commonly used method to estimate the PSD is using the Fast Fourier Transform (FFT). FFT based methods are comparatively easy and computationally efficient, though the frequency resolution is minimal. Windowing can also adversely affect the results of the FFT based methods. These limitations are particularly important when analyzing short data records. In order to overcome these limitations, alternate spectral estimation techniques including parametric techniques have been developed.

4.2.1 Definitions and Basics

4.2.1.1 Energy Spectral Density

The energy spectral density describes how the energy or variance of a signal/ time series is distributed with frequency. If $f(t)$ is a finite-energy signal, the spectral density $\Phi(\omega)$ of the signal is the square of the magnitude of the continuous Fourier transform of the signal.

$$\begin{aligned}\Phi(\omega) &= \left| \frac{1}{\sqrt{2\pi}} \int_{-\infty}^{\infty} f(t) e^{-j\omega t} dt \right|^2 \\ &= \frac{F(\omega) F^*(\omega)}{2\pi}\end{aligned}$$

where ω is the angular frequency and $F(\omega)$ is the continuous Fourier transform of $f(t)$, and $F^*(\omega)$ is its complex conjugate.

If the signal is discrete with values f_n , over an infinite number of elements, then the energy spectral density can be defined as:

$$\begin{aligned}\Phi(\omega) &= \left| \frac{1}{\sqrt{2\pi}} \sum_{-\infty}^{\infty} f_n e^{-j\omega n} \right|^2 \\ &= \frac{F(\omega) F^*(\omega)}{2\pi}\end{aligned}$$

where $F(\omega)$ is the discrete-time Fourier transform of f_n .

If the number of defined values is finite, the sequence does not have an energy spectral density as such, and the sequence can be treated as periodic, using a discrete Fourier transform to make a discrete spectrum, or it be extended with zeros and a spectral density can be computed as in the infinite sequence case.

4.2.1.2 Power Spectral Density

The above definitions of energy spectral density require that the Fourier transforms of the signals exist, *i.e.*, that the signals are square integrable or square summable. A more often used alternative is the Power Spectral Density (PSD), which describes the distribution of power of a signal or the time series with frequency. Here power can be the actual physical power, or more often, for convenience with abstract signals, can be defined as the squared value of the signal, if the signal was a voltage applied to a 1 ohm load. This instantaneous power (the mean or expected value of which is the average power) is then given by:

$$P = s(t)^2$$

Since, a signal with nonzero average power is not square integrable, the Fourier transforms do not exist in this case. The PSD is the Fourier transform of the autocorrelation function $R(\tau)$ of the signal, if the signal can be treated as a stationary random process. This results in the formula,

$$S(f) = \int_{-\infty}^{\infty} R(\tau) e^{-2\pi f\tau} d\tau$$

The power of the signal in a given frequency band can be computed by integrating over the positive and negative frequencies,

$$P = \int_{F_1}^{F_2} S(f)df + \int_{-F_2}^{-F_1} S(f)df$$

The power spectral density of a signal exists if and only if the signal is a wide-sense stationary process.

4.3 Spectral Estimation Methods

Various methods of spectrum estimation can be broadly classified into two, viz. Classical and Parametric Methods.

4.3.1 Classical Methods

In the classical spectrum estimation method, the PSD is estimated directly from the signal itself. There are two main estimation techniques based on the Fourier Transform. One is the Correlogram method as suggested by Blackman and Tukey and the other is the Periodogram method.

4.3.1.1 Correlogram Method

According to Blackman and Tukey, the spectral estimate of a finite data sequence x_0, x_1, \dots, x_{N-1} is given by

$$P(f) = \Delta t \sum_{n=-M}^M R_{xx}(m) \exp(-j2\pi f m \Delta t) \quad (4.1)$$

where $-1/(2\Delta t) \leq f \leq 1/(2\Delta t)$ and $R_{xx}(m)$ is given by

$$R_{xx}(m) = \frac{1}{N-m} \sum_{n=0}^{N-m-1} x_{(n+m)} x_n^*$$

4.3.1.2 Periodograms

Periodograms compute power spectral density directly as,

$$P(f) = \frac{1}{N\Delta t} \left| \sum_{n=0}^{N-1} x_n \exp(j2\pi f n \Delta t) \right|^2 \quad (4.2)$$

FFT can be used to evaluate Eq. (4.2) at discrete set of N equally spaced frequencies,

$$f_m = m\Delta f \text{ Hz, for } m = 0, 1, \dots, N-1$$

$$\text{where } \Delta f = \frac{1}{N\Delta t}.$$

Hence,

$$P_m(f_m) = \frac{1}{N\Delta t} |X_m|^2$$

where X_m is the DFT of the series.

The P_m is similar to the energy spectral density, the only difference being that it is divided by a time factor $N\Delta t$, which makes it Power Spectral Density. Now, the total power of the process is given by

$$\text{Power} = \sum_{m=0}^{N-1} P_m \Delta f$$

If the factor Δf is incorporated into P_m ,

$$\overline{P}_m = P_m \Delta f = \frac{1}{(N\Delta t)^2} |X_m|^2$$

$$= \left| \frac{1}{N} \sum_{n=0}^{N-1} x_n \exp(-j2\pi mn / N) \right|^2 \quad (4.3)$$

Eq. (4.3) can be referred to as the periodogram. The performance of periodogram estimators can be improved by applying pseudo ensemble averaging, which will in effect smoothen the PSD estimate.

4.3.2 Parametric Estimators

In parametric models, the PSD is estimated from a signal that is assumed to be the output of a linear system driven by white noise. These

methods first estimate the parameters of the linear system, from which the signal is assumed to be generated. Such methods are found to give better results for short data lengths. They also give better frequency resolutions than conventional estimators.

Parametric approaches take the advantage of the *a priori* knowledge about the process from which the data samples are taken. Thus the parametric methods basically have 3 steps, viz. selecting a time series model, estimating the parameters of the model assumed and generating the spectral estimate by substituting the estimated model parameters in the theoretical PSD, suitable for the model.

4.3.2.1 Random Process Models

A rational transfer function model is found to be useful for approximating many of the commonly encountered, deterministic as well as stochastic, discrete time processes. This model, with an input sequence $u[n]$ and an output sequence $x[n]$, can be represented by a linear difference equation of the type

$$\begin{aligned} x[n] &= -\sum_{k=1}^p a[k]x[n-k] + \sum_{k=0}^q b[k]u[n-k] \\ &= \sum_{k=0}^{\infty} h[k]u[n-k] \end{aligned} \quad (4.4)$$

The system function $H(z)$ between the output and the input has the form

$$H(z) = \frac{B(z)}{A(z)}$$

where

$$A(z) = 1 + \sum_{k=1}^p a[k]z^{-k}$$

$$B(z) = 1 + \sum_{k=1}^q b[k]z^{-k} \quad \text{and}$$

$$H(z) = 1 + \sum_{k=1}^{\infty} h[k]z^{-k}$$

The coefficients $a[k]$ are referred to as Auto Regressive (AR) parameters, while $b[k]$ are the Moving Average (MA) parameters.

4.3.2.1.1 AR Processes

If all the MA parameters, $b[k]$ are zero, except $b[0]=1$, then the process can be expressed as

$$x[n] = -\sum_{k=1}^p a[k]x[n-k] + u[n]$$

Such a process is referred to as AR process of order p and the model is called as an all-pole model. Thus, the AR process assumes that each value of the series depends only on the weighted sum of the previous values of the same series and the input.

4.3.2.1.2 MA Processes

If all the AR parameters, $a[k]$ are zero, except $a[0]=1$, then the process can be expressed as

$$x[n] = \sum_{k=1}^q b[k]u[n-k]$$

Such a process is referred to as MA process of order q and the model is called as an all-zero model. Thus, the MA processes can be thought of as the output of a filter with all-zero transfer function and an input, which is a white noise process.

4.3.2.1.3 ARMA Processes

When both AR and MA terms are present, the process is termed as an ARMA process. Thus, in effect, ARMA model can be thought of as the

output obtained when white noise is passed through a filter with p pole and q zero filter. While the zeros of the filter may be anywhere in the z -plane, the poles are expected to be within the unit circle in the z -plane.

4.3.2.2 Spectrum of ARMA, AR and MA Processes

As described in the previous section, we have 3 types of random processes, viz. AR, MA and ARMA. Each model has its own advantages and limitations. Apart from the theoretical properties of the estimators like consistency, efficiency, etc., practical issues like the speed of computation and the size of the data must also be taken into account in choosing an appropriate method for a given problem. Often, one method in conjunction with others can be used to obtain the best result. These estimation methods, in general, require that the data be stationary and zero-mean. Failure to satisfy these requirements may result in nonsensical results or a breakdown of the numerical computation.

The Z-transform of the autocorrelation of the input sequence, $P_{uu}(z)$ is related to that of the output sequence $P_{xx}(z)$ of the random process by ,

$$P_{xx}(z) = P_{uu}(z) \frac{B(z)B^*(1/z^*)}{A(z)A^*(1/z^*)}$$

If the driving sequence is a white noise process of zero mean and variance ρ_w , $P_{uu}(z) = \rho_w$. The power spectral density of ARMA can be computed by substituting $z = \exp(j2\pi fT)$ in the above equation and scaling by the sampling interval T .

$$\begin{aligned} \text{i.e., } P_{ARMA}(f) &= T\rho_w \left| \frac{B(f)}{A(f)} \right|^2 \\ &= T\rho_w \frac{e_q^H(f)bb^H e_q(f)}{e_p^H(f)aa^H e_p(f)} \end{aligned} \tag{4.5}$$

where

$$A(f) = 1 + \sum_{k=1}^p a[k] \exp(-j2\pi f k T)$$

$$B(f) = 1 + \sum_{k=1}^q b[k] \exp(-j2\pi f k T)$$

and the complex sinusoidal vectors $e_q(f)$ and $e_p(f)$ are given by

$$e_p(f) = \begin{bmatrix} 1 \\ \exp(j2\pi f T) \\ \vdots \\ \exp(j2\pi f p T) \end{bmatrix} \quad \text{and} \quad e_q(f) = \begin{bmatrix} 1 \\ \exp(j2\pi f T) \\ \vdots \\ \exp(j2\pi f q T) \end{bmatrix}$$

and the vectors \mathbf{a} and \mathbf{b} are given by

$$\mathbf{a} = \begin{bmatrix} 1 \\ a[1] \\ \vdots \\ a[p] \end{bmatrix} \quad \text{and} \quad \mathbf{b} = \begin{bmatrix} 1 \\ b[1] \\ \vdots \\ b[q] \end{bmatrix}$$

If all the autoregressive parameters except $a[0] = 1$,

i.e., By setting $p=0$, then

$$P_{MA}(f) = T\rho_w |B(f)|^2 \tag{4.6}$$

$$= T\rho_w e_q^H(f) b b^H e_q(f) .$$

which gives the spectrum of the MA Model.

Similarly if all the moving average parameters except $b[0] = 1$

i.e., by setting $q=0$, then

$$P_{AR}(f) = \frac{T\rho_w}{|A(f)|^2} \quad (4.7)$$

$$= \frac{T\rho_w}{e_p^H(f)aa^H e_p(f)}$$

which gives the spectrum of the AR model.

4.3.3 AR Spectral Estimation

Various algorithms to estimate the AR parameters are available in the open literature. The following sections provide brief descriptions of the different algorithms like Yule Walker, Burg's, Covariance and Modified Covariance.

4.3.3.1 Yule-Walker Method

The Yule-Walker method is one of the most widely used methods to compute the AR parameters, due to its applicability to short data records. For PSD estimations, this method uses auto-correlation function estimates for solving the Yule-Walker equations. A biased estimate of the autocorrelation function of the signal is computed and the least squares minimization of the forward prediction error is solved.

The AR parameters and the autocorrelation sequence are related by the equation,

$$R_{xx}[m] = \begin{cases} -\sum_{k=1}^p a[k]R_{xx}[m-k] & \text{for } m > 0 \\ \rho_w - \sum_{k=1}^p a[k]R_{xx}[-k] & \text{for } m = 0 \\ R_{xx}^*[-m] & \text{for } m < 0 \end{cases}$$

where ρ_w is the variance and p is the model order.

In matrix form, the above equation can be expressed as,

$$\begin{bmatrix} R_{xx}(0) & R_{xx}(-1) & \dots & R_{xx}(-p) \\ R_{xx}(1) & R_{xx}(0) & \dots & R_{xx}(-p+1) \\ \vdots & \vdots & \vdots & \vdots \\ \vdots & \vdots & \vdots & \vdots \\ R_{xx}(p) & R_{xx}(p-1) & \dots & R_{xx}(0) \end{bmatrix} \begin{bmatrix} 1 \\ a[1] \\ \vdots \\ a[p] \end{bmatrix} = \begin{bmatrix} \rho_w \\ 0 \\ \vdots \\ 0 \end{bmatrix}$$

By solving this matrix equation, which relates the AR model with the autocorrelation sequence, AR parameters can be estimated. This procedure of estimation of AR parameters is referred to as the Yule-Walker method.

4.3.3.2 The Burg's Algorithm

The burg's algorithm is based on minimizing the forward and backward prediction errors while satisfying the Levinson-Durbin recursion. The method estimates the reflection coefficients directly. Burg's method is found especially useful in resolving closely spaced sinusoids when low noise levels are present.

4.3.3.3 Covariance Method

The covariance model fits an AR model to the signal by minimizing the forward prediction error in the least squares sense. The covariance based model of spectral estimators can give a better resolution than the Yule Walker equations, for short data lengths. However, it can give rise to unstable models. It also exhibits frequency bias for estimates of sinusoidal signals present in the noise.

4.3.3.4 Modified Covariance Method

Though this method is similar to covariance method, it takes into account minimizations of both forward as well as backward prediction errors. In addition to providing high resolution, this method is immune to

Chapter 4 Spectral and Cepstral Analysis

spectral line splitting. The comparison between the different algorithms is discussed in the Table 4.1.

Table 4.1 Comp. of various algorithms to estimate the AR parameters

	Burg	Covariance	Modified Covariance	Yule-Walker
Characteristics	Does not apply window to data	Does not apply window to data	Does not apply window to data	Applies window to data
	Minimizes the forward & backward prediction errors in the least-squares sense	Minimizes the forward prediction error in the least-squares sense	Minimizes the forward and backward prediction errors in the least-squares sense	Minimizes the forward prediction error in the least-squares sense.
Conditions for Non-singularity		Order must be less than or equal to half the input frame size	Order must be less than or equal to 2/3 the input frame size	Due to the biased estimate, the autocorrelation matrix is guaranteed to positive-definite, hence nonsingular
Advantages	High resolution for short data records. Always produces a stable model	Better resolution than Y-W for short data records (more accurate estimates). Able to extract frequencies from data consisting of p or more pure sinusoids	High resolution for short data records. Able to extract frequencies from data consisting of p or more pure sinusoids. Does not suffer spectral line-splitting	Performs as well as other methods for large data records. Always produces a stable model

	Burg	Covariance	Modified Covariance	Yule-Walker
Disadvantages	<p>Peak locations highly dependent on initial phase.</p> <p>May suffer spectral line-splitting for sinusoids in noise, or when order is very large.</p> <p>Frequency bias for estimates of sinusoids in noise</p>	<p>May produce unstable models.</p> <p>Frequency bias for estimates of sinusoids in noise</p>	<p>May produce unstable models.</p> <p>Peak locations slightly dependent on initial phase.</p> <p>Minor frequency bias for estimates of sinusoids in noise</p>	<p>Performs relatively poorly for short data records.</p> <p>Frequency bias for estimates of sinusoids in noise</p>

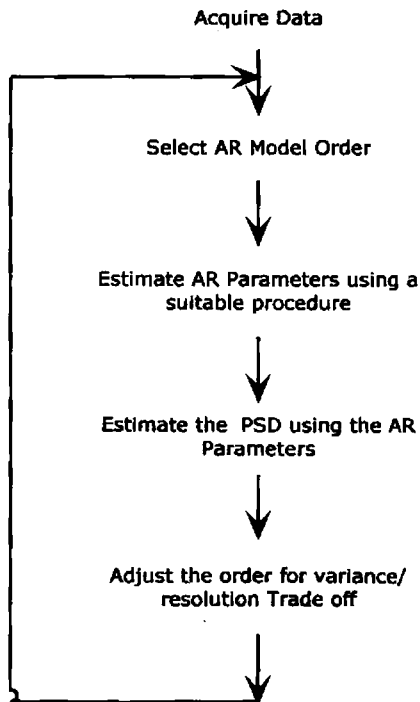


Fig. 4.2 Flow chart for the generic estimation of AR PSD

Chapter 4 Spectral and Cepstral Analysis

A general flowchart for AR PSD estimation is given in the Fig. 4.2. Let the N data samples be acquired with a sample interval of T seconds. A suitable AR order is then selected and the AR parameters are obtained from the sampled data by any one of the methods. The PSD can then be obtained using Eq.(4.7). The analysis may be carried out by selecting various orders till a satisfactory result is obtained.

The MA parameters can be estimated by a technique commonly known as the *method of moments*. Here, the MA parameters of a q^{th} order process are calculated by solving the set of non-linear equations (which is the autocorrelation function of the MA process), given by the following equation.

$$R_{xx}[m] = \begin{cases} 0 & \text{for } m > q \\ \rho_w \sum_{k=m}^q b[k]b^*[k-m] & \text{for } 0 \leq m \leq q \\ R_{xx}^*[-m] & \text{for } m < 0 \end{cases} \quad (4.8)$$

In order to obtain the spectral estimate, there is no need to solve for the MA parameters, since the PSD can be directly estimated from the Autocorrelation sequence as

$$P_{MA}(f) = T \sum_{k=-q}^q R_{xx}[k] \exp(-j2\pi f k T).$$

A flowchart of a generic MA PSD estimator is given in Fig. 4.3. Another approach which is relatively simple and relies on linear operations is to use higher order AR Approximation to the MA process. Let $B(z)$ and $1/A_{\infty}(z)$ be the system functions of an $MA(q)$ process and $AR(\infty)$ process equivalent to the $MA(q)$ process respectively, which are defined as,

$$B(z) = 1 + \sum_{k=1}^q b[k]z^{-k}$$

$$A_{\infty}(z) = 1 + \sum_{k=1}^{\infty} a[k]z^{-k}$$

$$\text{i.e., } B(z)A_{\infty}(z) = 1.$$

The inverse z-transform of the transform product, $B(z) A_{\infty}(z)$ is the convolution of the MA parameters with the AR parameters and that of constant 1 is the sample function $\delta[m]$.

Equivalently,

$$a[m] + \sum_{n=1}^q b[n]a[m-n] = \delta[m] \quad (4.9)$$

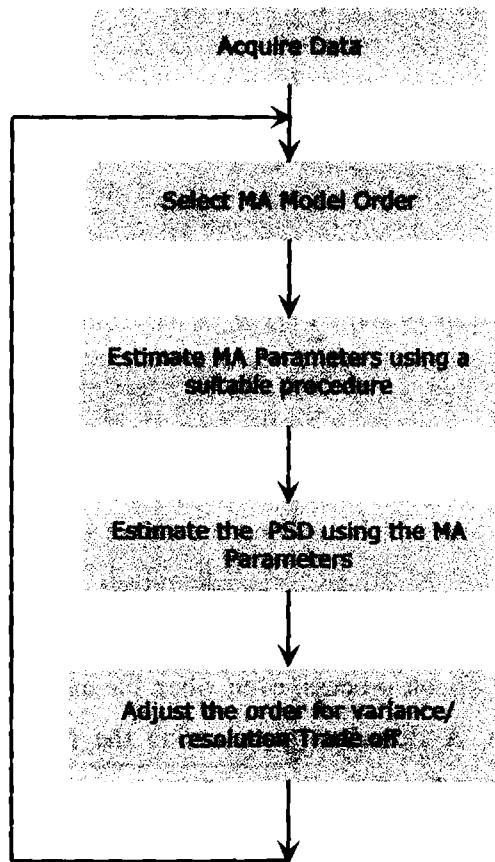


Fig. 4.3 Flowchart for the Generic MA PSD Estimation

$$\text{where } \delta[m] = \begin{cases} 1 & \text{for } m = 0 \\ 0 & \text{for } m \neq 0 \end{cases} \quad \text{and } a[0] = 1 \text{ and } a[k] = 0 \text{ for } k < 0.$$

Thus, one can estimate the MA parameters from an equivalent infinite order AR model using Eq (4.9).

4.3.4 ARMA Spectral Estimation

The ARMA process model is given by

$$x[n] = -\sum_{k=1}^p a[k]x[n-k] + \sum_{k=0}^q b[k]u[n-k] \quad (4.10)$$

The ARMA parameters $b[k]$ and $a[k]$ are related to the autocorrelation of the process $x[k]$ by

$$R_{xx}[m] = \begin{cases} -\sum_{k=1}^p a[k]R_{xx}[m-k] & \text{for } m > q \\ \rho_w \sum_{k=m}^q b[k]h^*[k-m] - \sum_{k=1}^p a[k]R_{xx}[m-k] & \text{for } 0 \leq m \leq q \\ R_{xx}^*[-m] & \text{for } m < 0 \end{cases} \quad (4.11)$$

Thus, the ARMA parameters can be estimated by obtaining the autocorrelation values and by solving the above equations. However, the non-linear nature of the above equation and the need to simultaneously estimate the MA and AR parameters, make the ARMA estimation comparatively a difficult process, even when the autocorrelation sequence is exactly known. A flowchart representing the procedures for ARMA estimation is given in Fig. 4.4.

4.4 Analysis of Noise Signals on the Spectral Perspective

It has been found that the various noise sources can be effectively classified and identified by analyzing the frequency spectrum of the noise

signals emanating from the targets using various spectral estimation techniques. As envisaged in section 4.3.2, using certain *a priori* information on the general characteristics of the spectrum, parametric spectral estimation techniques are seen to yield better results when compared to classical estimation techniques.

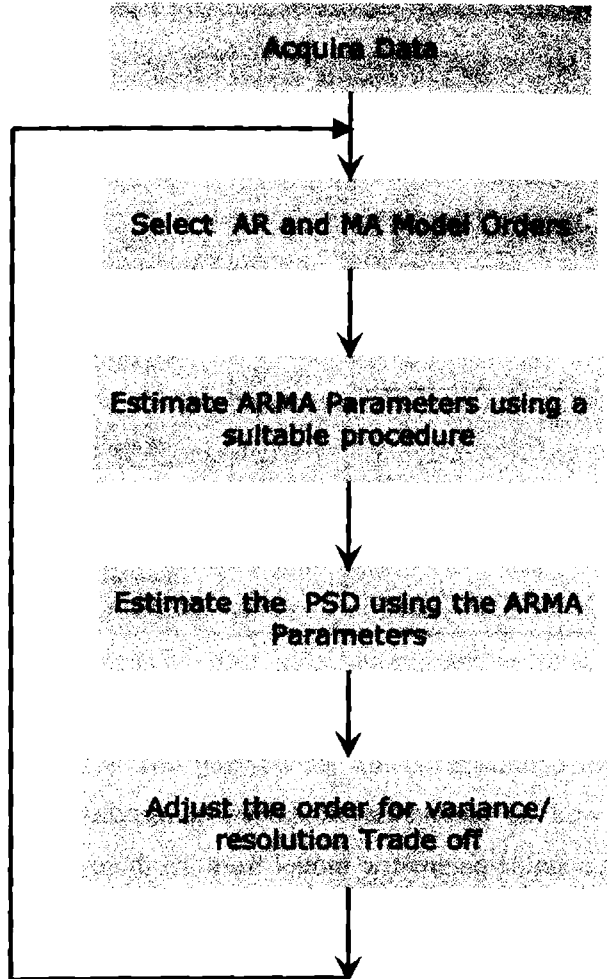


Fig. 4.4 Flowchart for the Generic ARMA PSD Estimation

The various types of spectral estimators have been implemented in Matlab and the front end of the estimator is the graphical user interface (GUI) shown in Fig.4.5.

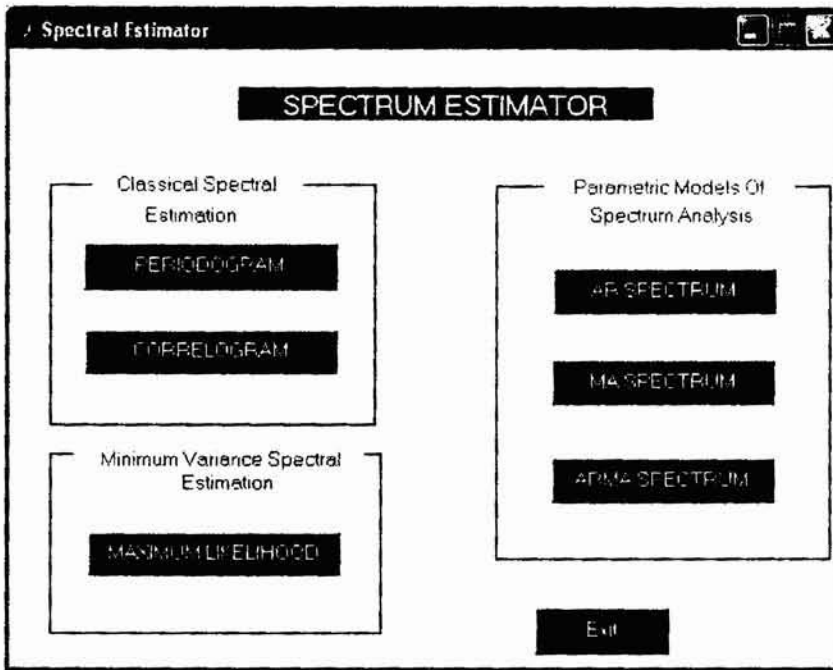


Fig. 4.5 GUI of the Spectral Estimator

This GUI has a provision for carrying out the classical, minimum variance as well as parametric model based spectral estimations. The selection of a suitable parametric model from the three established models, viz. AR, MA and ARMA, should be carried out by analyzing the spectral shape and computational efficiency. AR models give the spectra with sharp peaks, but with no deep nulls. In the MA model spectrum, the reverse is true, *i.e.*, there are deep nulls but no sharp peaks. The ARMA model can, in general, represent both the extremes. Also, the model which gives a satisfactory result with the use of fewer numbers of parameters should be selected. From a thorough analysis of the data samples and the models, it

has been observed that the AR model, which has less computational burden, can be a best choice for analysis of ocean noise data waveforms.

The performance of the AR estimator making use of the Yule-Walker, Burg, Covariance and Modified Covariance algorithms implemented in Matlab have been studied in detail for various types of signals as well as noise types usually encountered in underwater scenario. All the files are segmented into records of one second in duration for analysis. The plots indicate that the spectra of different sources differ in many aspects while there is a notable similarity between the samples of the same signal. The results of the analysis are furnished in Figs. 4.6 through 4.27, with the spectra plotted for four different orders, *viz.* 20, 40, 60 and 80 as well as different algorithms discussed above.

For evaluating the performance of the time series AR estimator, the noise data waveforms generated by a merchant vessel approaching a monitoring station from 1.7 kms as well as that of a large commercial vessel cruising at approximately 20 knots and 3.2 kms away were considered. The performance validation of the model estimators based on these algorithms revealed that an Autoregressive time series model estimator making use of the Yule-Walker algorithm is the optimum one in terms of the computational complexity as well as the spectral fidelity for processing the noise types described above.

Figs. 4.6 to 4.8 depict the spectra for the merchant vessel using the Yule-Walker algorithm for three parametric models, *viz.* AR, MA and ARMA. In order to study the effect of the order selection, the spectra are plotted for the orders of 20, 40, 60 and 80. The Figs. 4.9 to 4.11 depict the PSD plotted for AR models in respect of the noise generated by the merchant vessel using the other three algorithms with the four different

orders. Figs. 4.12 to 4.15 depict the PSD of the commercial vessel for the various AR algorithms, while Fig. 4.16 depicts the MA spectrum using Yule Walker algorithm.

It can be observed that the MA spectrum shown in Figs. 4.7 and 4.16 has broad peaks around the peaking frequency. In addition, as the order increases, the broadness of the peaks decreases while the sharpness of the nulls is getting increased. The ARMA spectrum in Fig. 4.8 has sharp nulls and peaks and for low orders, the sharpness tends to decrease, especially for the peaks.

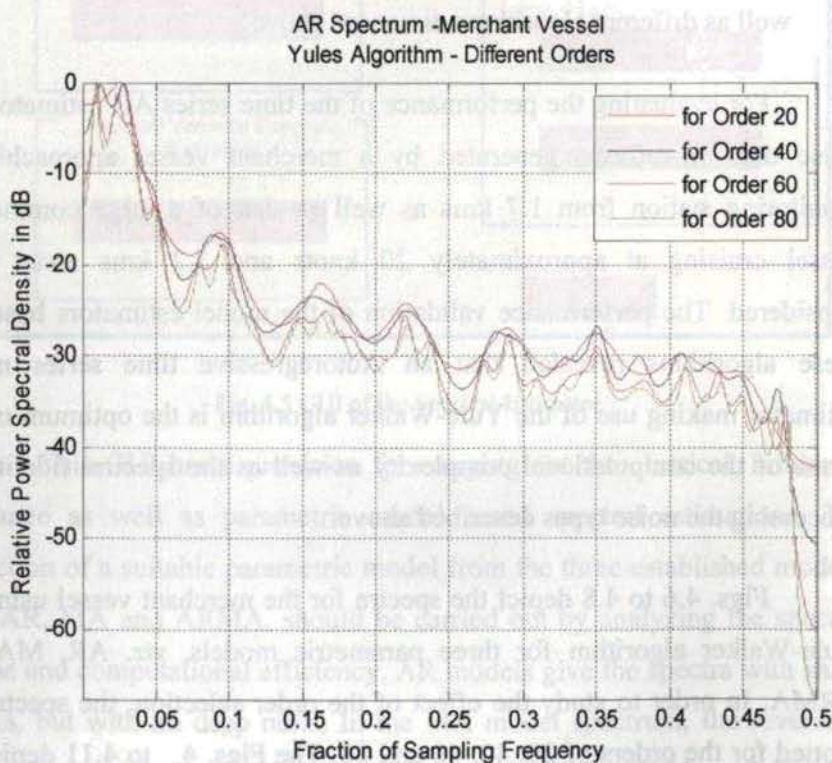


Fig. 4.6 AR Spectrum of a Merchant Vessel using Yule Walker

The AR spectra in Figs. 4.6 and 4.9 to 4.15 have moderate peaks and nulls and are found to give a smooth spectral profile. As the order increases, there is an increase in the number of peaks and nulls.

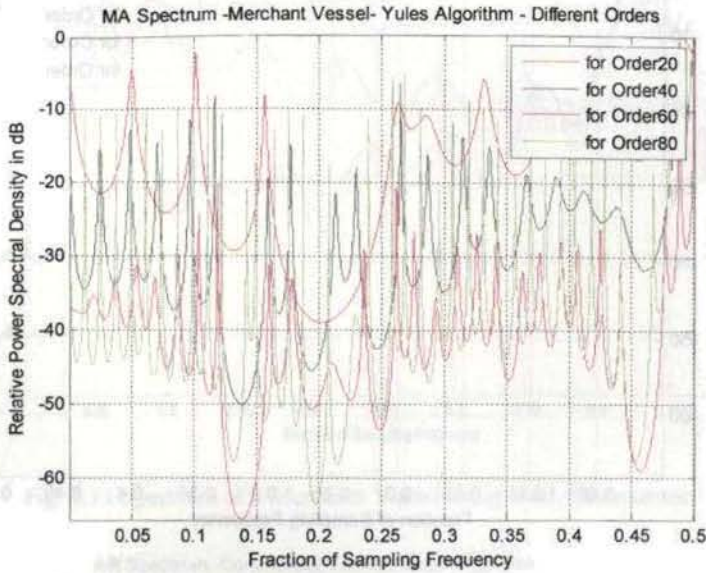


Fig. 4.7 MA Spectrum of a Merchant Vessel using Yule Walker

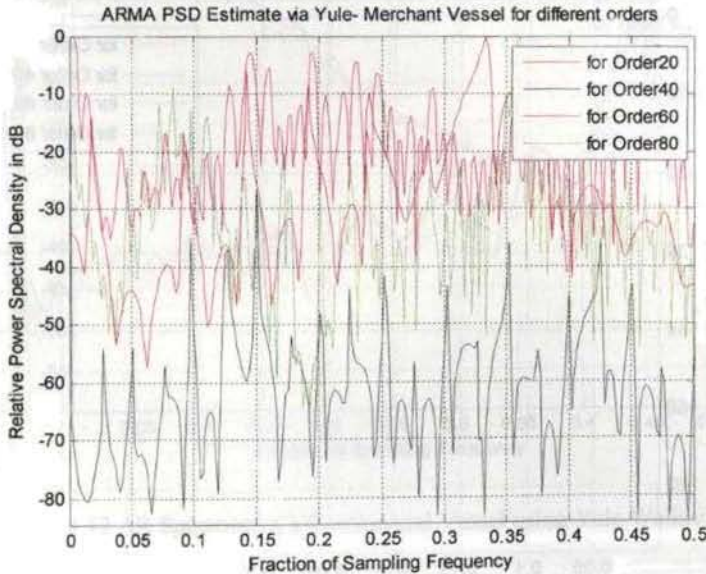


Fig. 4.8 ARMA Spectrum of Merchant Vessel using Yule Walker

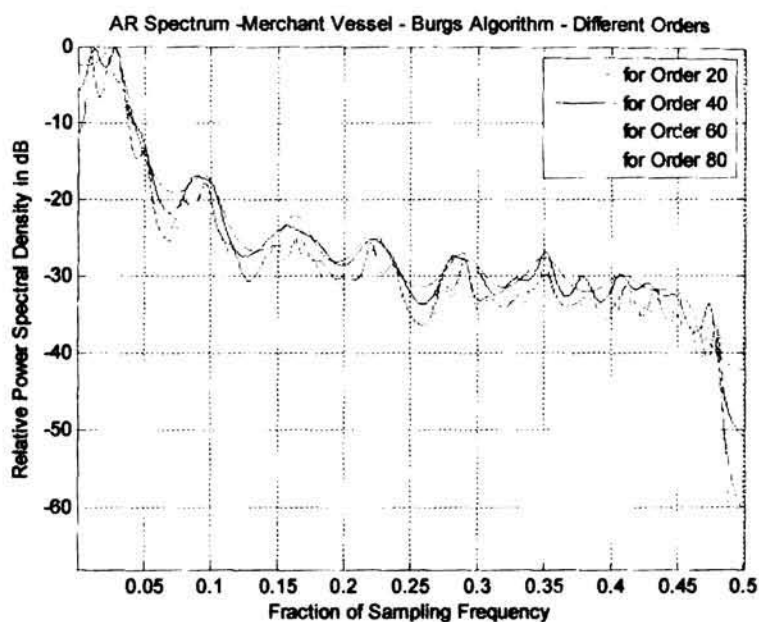


Fig. 4.9 AR Spectrum of a Merchant Vessel using Burg

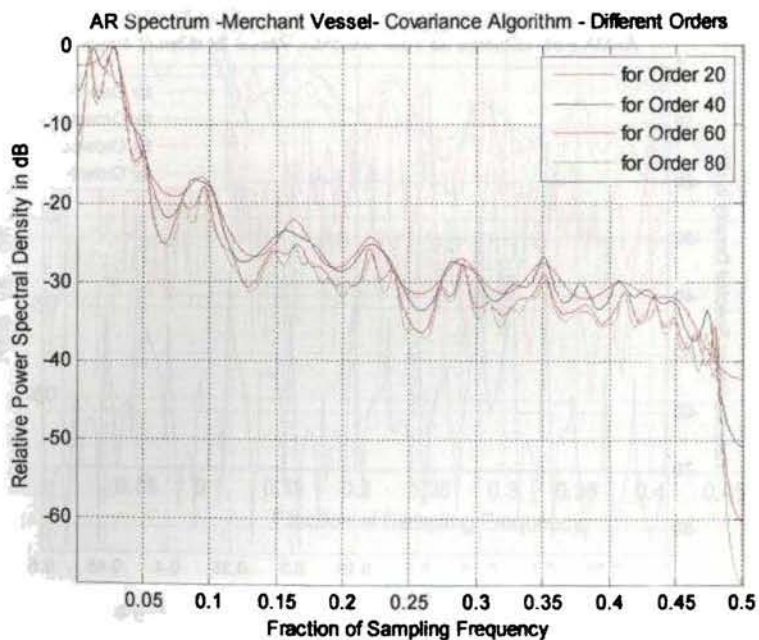


Fig. 4.10 AR Spectrum of a Merchant Vessel using Covariance

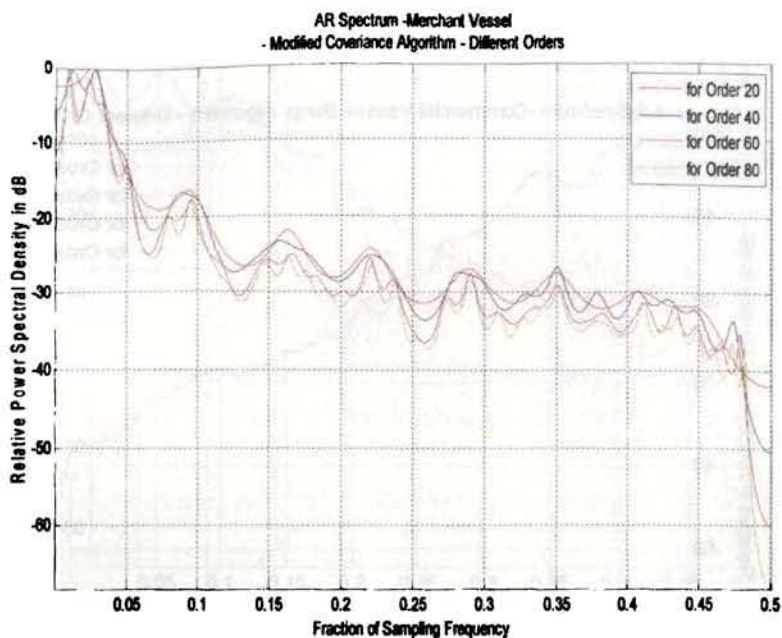


Fig. 4.11 Spectrum of a Merchant Vessel using Mod. Covariance

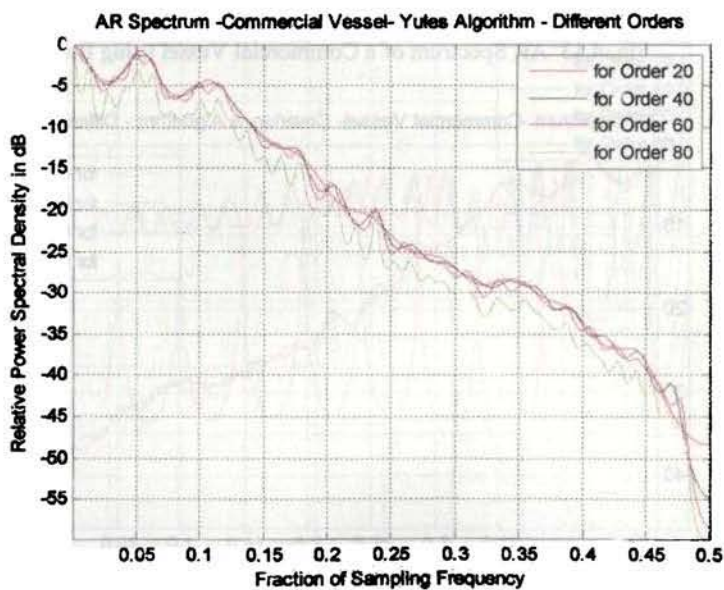


Fig. 4.12 AR Spectrum of a Commercial Vessel using Yule Walker

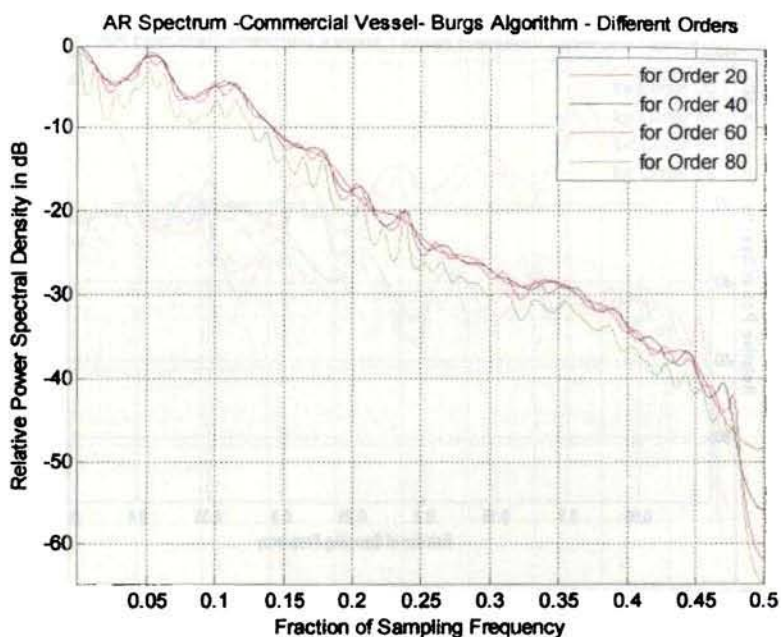


Fig. 4.13 AR Spectrum of a Commercial Vessel using Burg

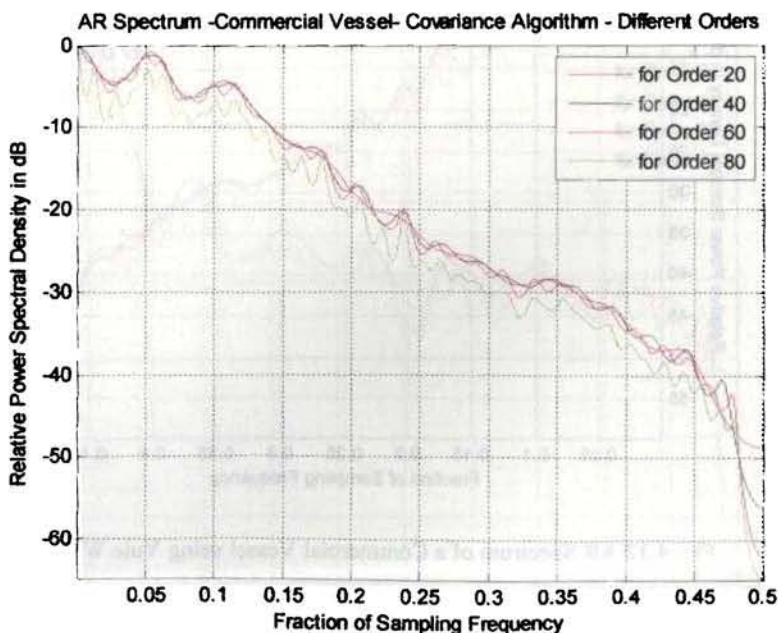


Fig. 4.14 AR Spectrum of a Commercial Vessel using Cov.Algo

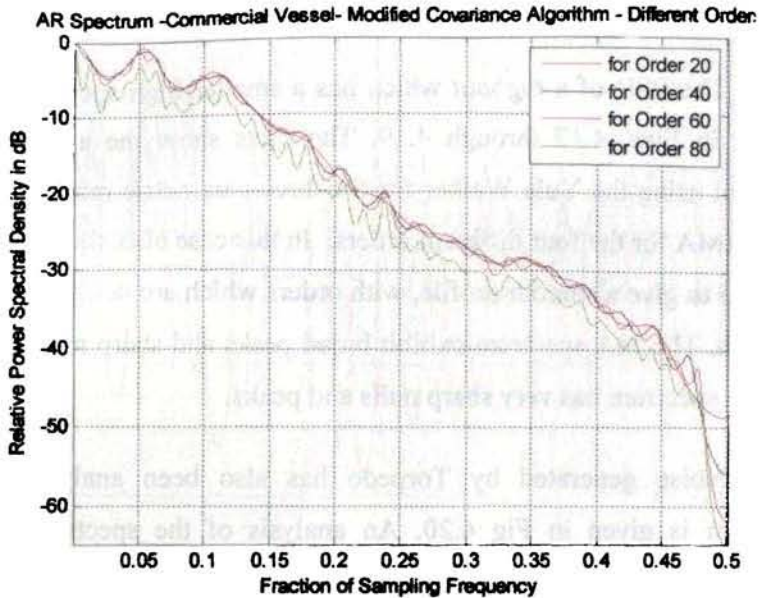


Fig. 4.15 AR Spectrum of a Commercial Vessel using Mod. Cov

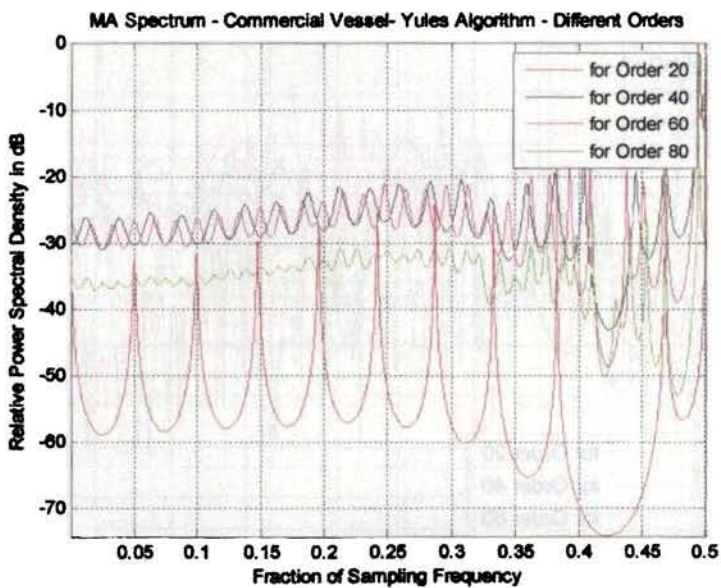


Fig. 4.16 MA Spectrum of a Commercial Vessel using Yule-Walker

The PSD of a *tugboat* which has a smaller high speed propeller is plotted in Figs. 4.17 through 4.19. The plots show the analysis results obtained using the Yule Walker for the three parametric models, AR, MA and ARMA for the four different orders. In this case also, the AR spectrum is found to give a smooth profile, with orders which are neither too low nor too high. The MA spectrum exhibit broad peaks and sharp nulls, while the ARMA spectrum has very sharp nulls and peaks.

Noise generated by Torpedo has also been analysed and the spectrum is given in Fig 4.20. An analysis of the spectra has clearly indicated that the AR model is the ideal one for characterizing the Torpedo.

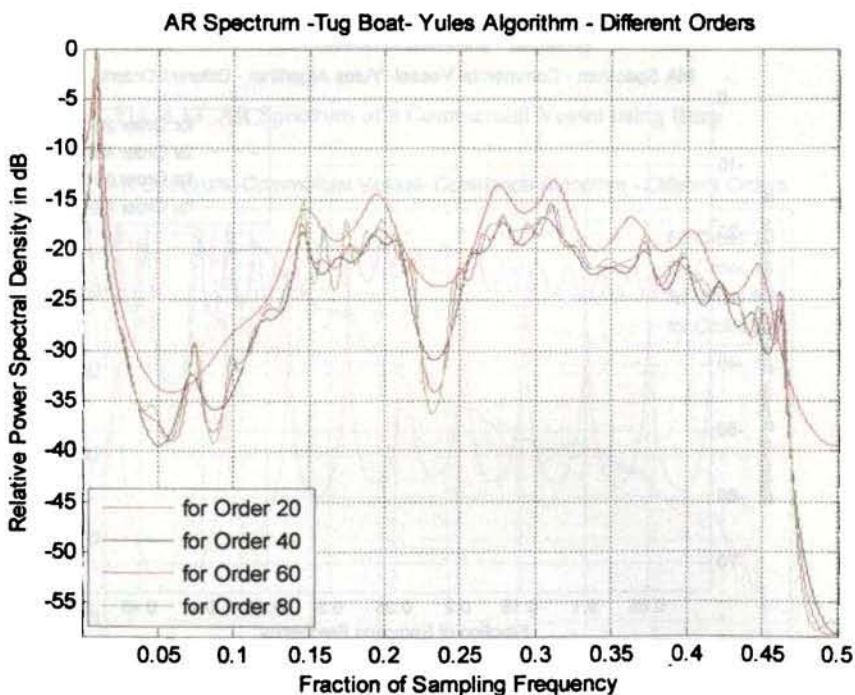


Fig. 4.17 AR Spectrum of a Tug Boat using Yules

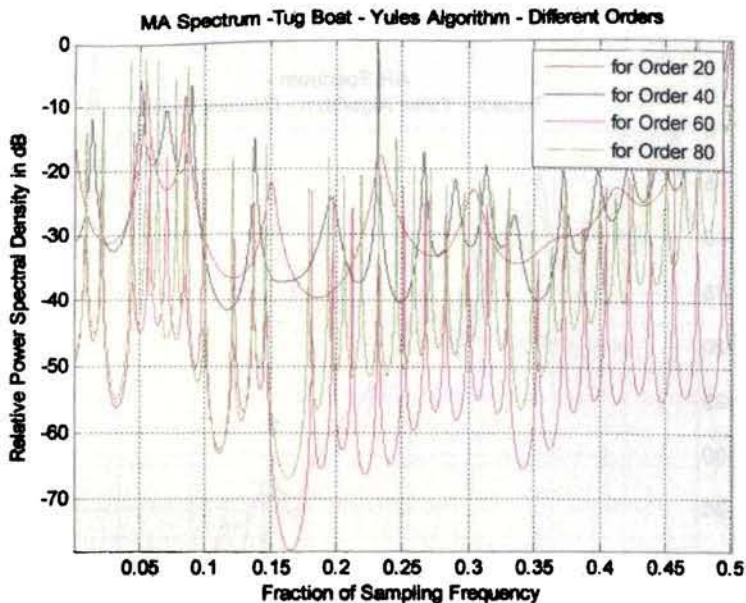


Fig. 4.18 MA Spectrum of a Tug Boat using Yules

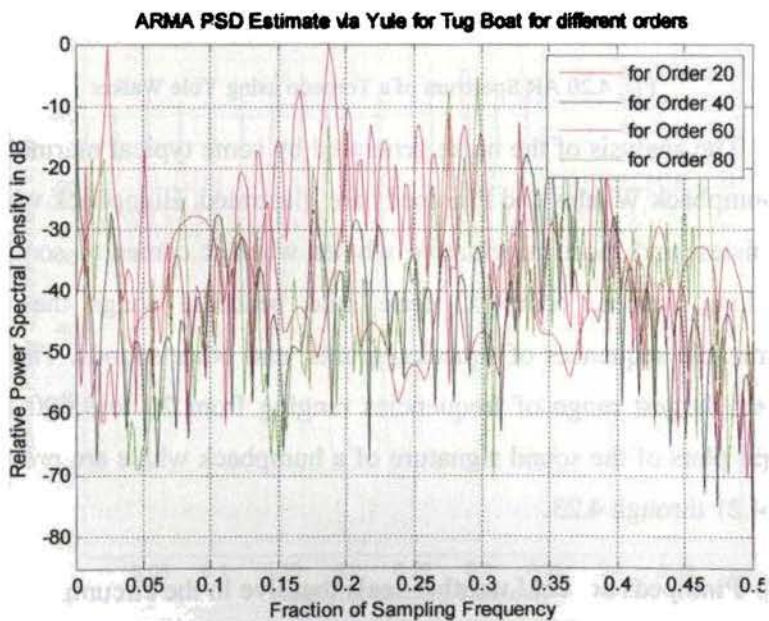


Fig. 4.19 ARMA Spectrum of a Tug Boat using Yules

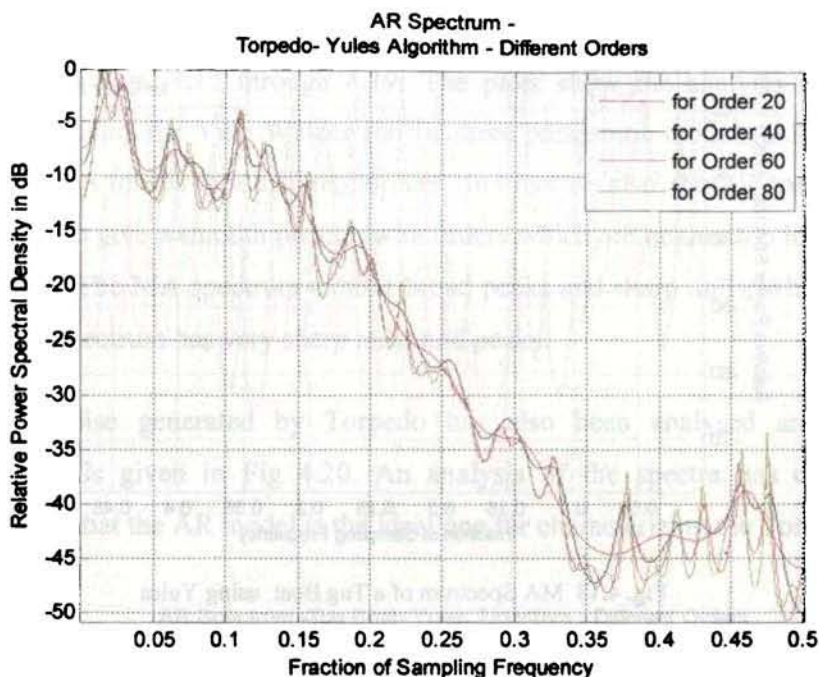


Fig. 4.20 AR Spectrum of a Torpedo using Yule Walker

The analysis of the noise generated by some typical marine species, viz. Humpback Whales and Pinnipeds are illustrated. Humpback whales are the noisiest and most imaginative whales when it comes to songs. They have long, varied, complex, eerie, and beautiful songs that include recognizable sequences of squeaks, grunts, and other sounds. Their songs have the largest range of frequencies ranging from 20 to 9,000 Hz. The spectral plots of the sound signature of a humpback whale are presented in Figs. 4.21 through 4.23.

Pinnipeds are cold weather seals that live in the circumpolar regions of the northern hemisphere. These animals produce a distinctive song ranging from 0.02 to 6 kHz in frequency. These complex songs consist of long, spiralling trills and short, low frequency moans. Results of the spectral analysis carried out using Yule Walker algorithm for the noise

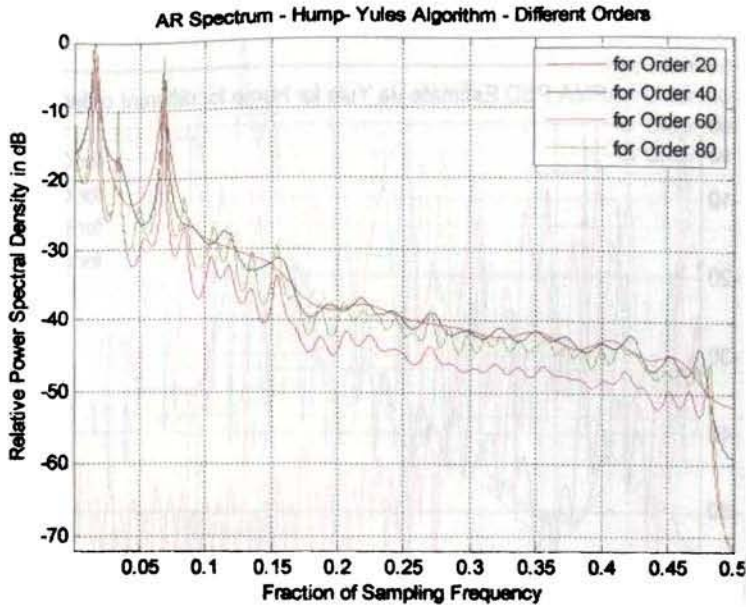


Fig. 4.21 AR Spectrum of a Humpback Whale using Yule Walker

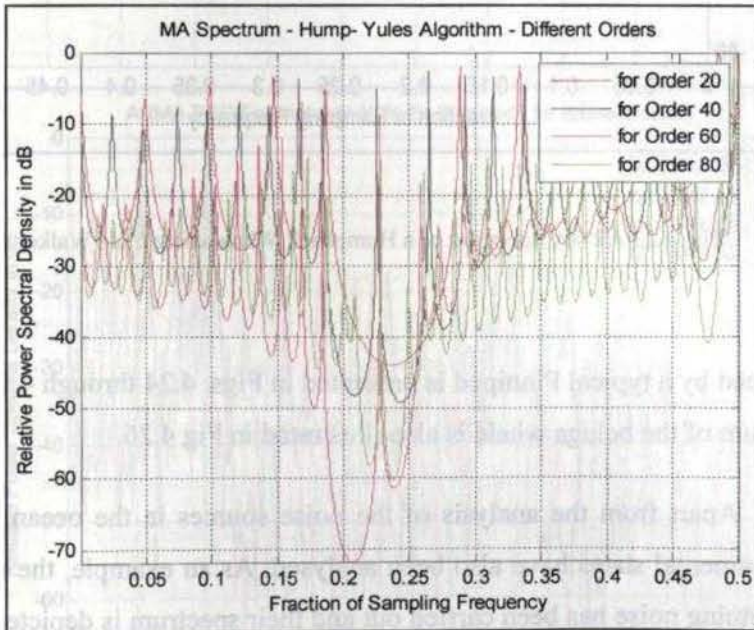


Fig. 4.22 MA Spectrum of a Humpback Whale using Yule Walker

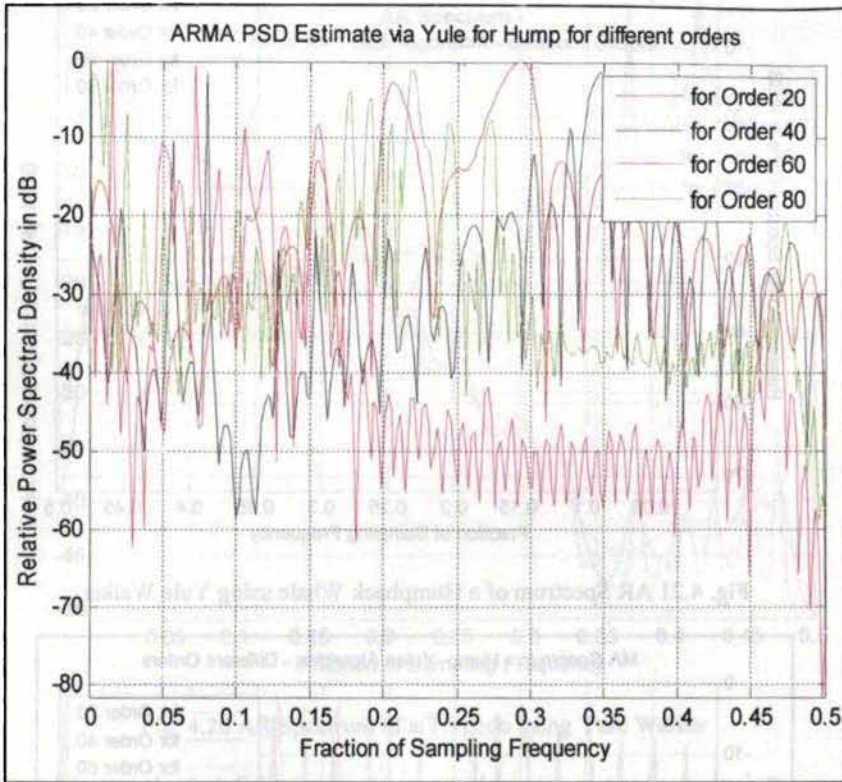


Fig. 4.23 ARMA Spectrum of a Humpback Whale using Yule Walker

produced by a typical Pinniped is presented in Figs. 4.24 through 4.25. The spectrum of the beluga whale is also illustrated in Fig 4.26.

Apart from the analysis of the noise sources in the ocean, certain environmental states have also been analysed. As an example, the analysis of lightning noise has been carried out and their spectrum is depicted in Fig 4.27.

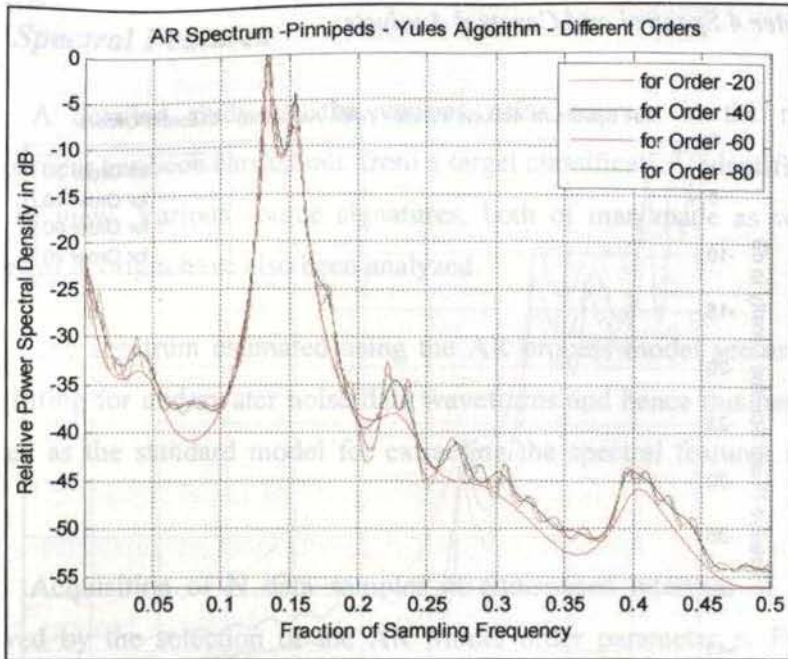


Fig. 4.24 AR Spectrum of a Pinnipeds using Yule Walker

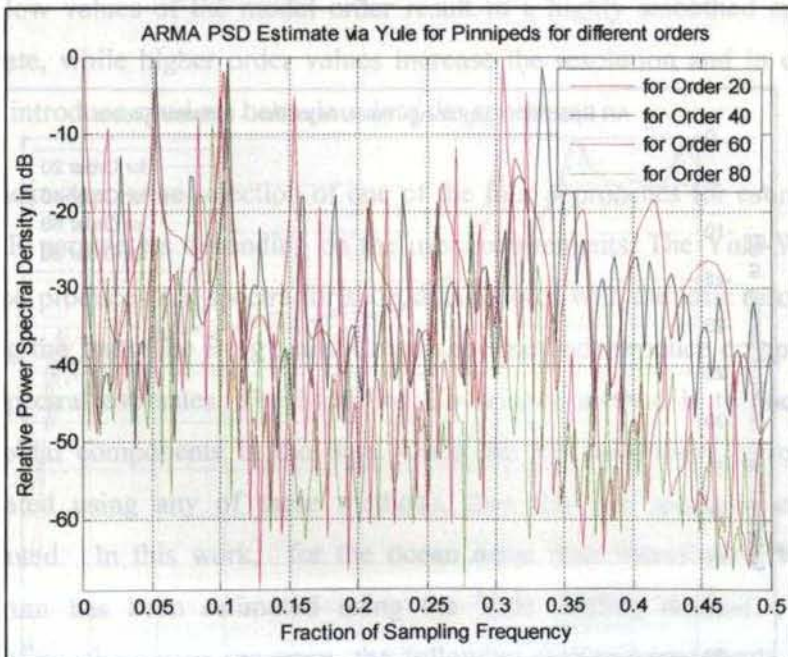


Fig. 4.25 ARMA Spectrum of a Pinnipeds using Yule Walker

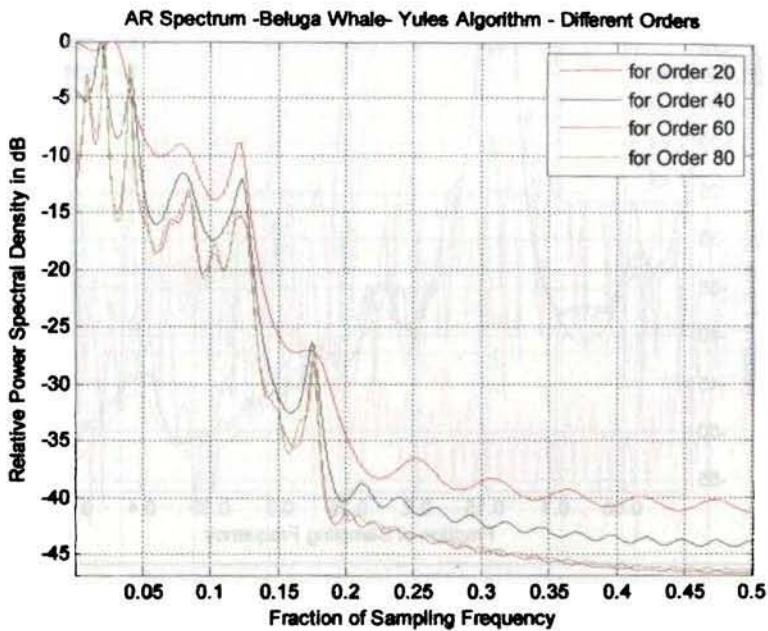


Fig. 4.26 AR Spectrum of a Beluga Whale using Yule Walker

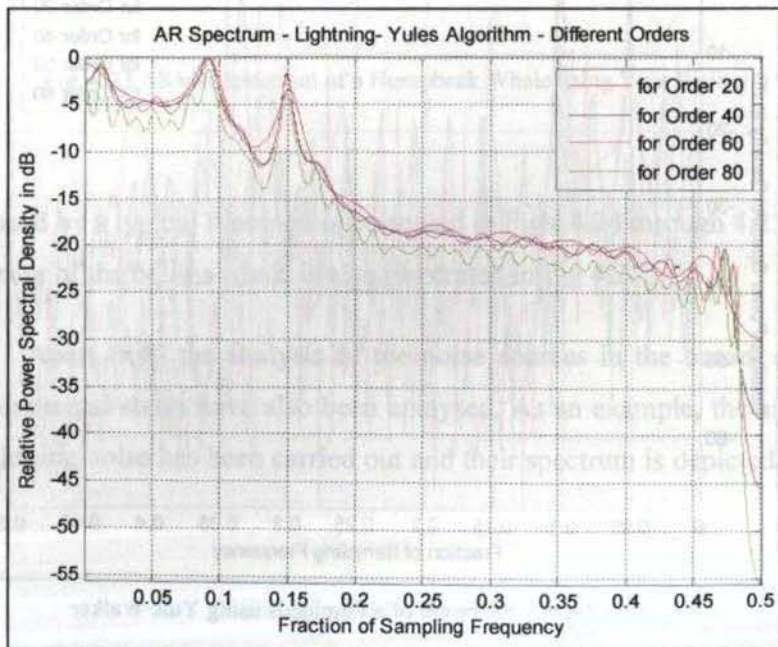


Fig. 4.27 AR Spectrum of a Lightning using Yule Walker

4.5 Spectral Features

A detailed study on the various noise sources in the marine environment has been carried out, from a target classification/ identification point of view. Various source signatures, both of man made as well as biological in origin have also been analyzed.

The spectrum estimated using the AR process model seems to be more fitting for underwater noise data waveforms and hence this has been adopted as the standard model for extracting the spectral features in this work.

Acquisition of N data samples at equispaced intervals of Δt is followed by the selection of the AR Model order parameter p . From a knowledge of certain error criterion, it is possible to select the required model order. The significance of the model order in AR model is such that, very low values of the model order result in a highly smoothed spectral estimate, while higher order values increase the resolution and in certain cases introduce spurious behaviour into the spectrum.

The next step is the selection of one of the four approaches for estimating the AR parameters depending on the user requirements. The Yule-Walker method produces AR spectra for short data records with the least resolution among the four. The Burg's and Covariance methods produce comparable AR spectral estimates. The Modified Covariance method is the best for sinusoidal components in the data. Once the AR parameters have been estimated using any of these methods, then the AR spectrum can be computed. In this work, for the ocean noise data waveforms, the AR spectrum has been estimated using the Yule Walker method. Upon estimating, the power spectrum, the following feature components which

reveal the significant spectral characteristics, considered for the realisation of the proposed classifier, is computed as shown in Fig. 4.28.

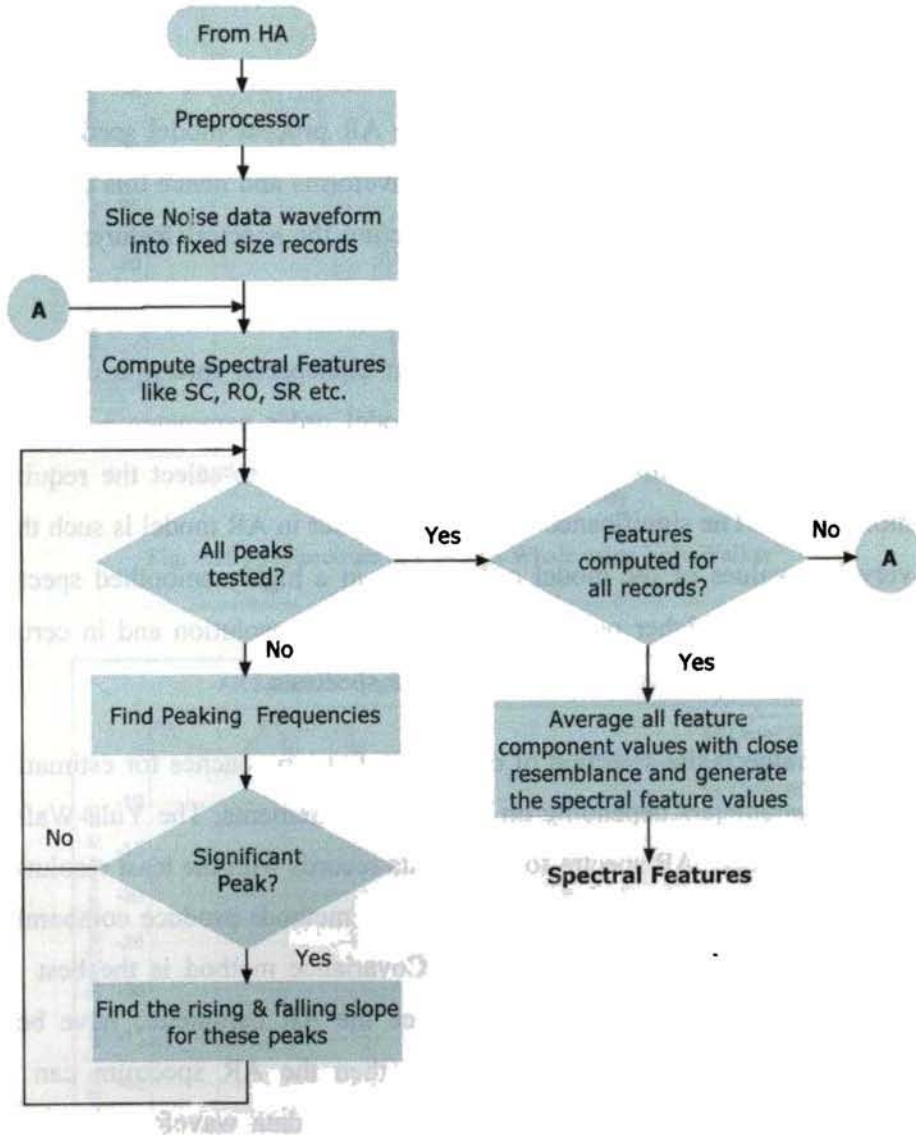


Fig. 4.28 Illustration of Extraction of Spectral Features

- Spectral Centroid, which may also be referred to as the spectral brightness, gives an indication of the spectral shape.
- Spectral Range, which refers to the range of frequencies that are present in the signal.
- Spectral Roll off, which gives a measure of the spectral shape.
- Spectral flux, which is a measure of how quickly the power spectrum of the signal changes
- Spectral Slope, which refers to the average slope of the power spectral density variation.
- Number of Peaks and the Peaking frequencies, which will help in identifying the tonal as well as continuous frequency components.

4.6 Cepstral Analysis

Cepstral analysis belongs to an area of signal processing known as *homomorphic analysis*. The attraction of the homomorphic analysis is that, it can be accomplished using cascade of forward and inverse operations with a linear time invariant operation sandwiched in between.

The spectrum of any waveform consists of two components, the slowly varying part, referred to as the filter or spectral envelope and the rapidly varying part, referred to as the source or harmonic structure. Separation of these two components can be achieved by taking the *cepstrum*, an anagram of the word *spectrum*. The Cepstrum is defined as the inverse Fourier transform of the log magnitude Fourier spectrum of the signal and is said to be in the *quefrequency* domain, an anagram of *frequency*.

The convolution of any two signals in the time domain is transformed into simple multiplication of DFTs in the frequency domain. Thus, Fourier transform of any signal is actually a multiplication of the

Chapter 4 Spectral and Cepstral Analysis

frequency transform of the source and the filter signals. Hence, by applying the operation of logarithm to this Fourier transform, we get the convolution in the time domain transformed into a sum of log-magnitude components in the frequency domain. Now applying an inverse Fourier transform to the log spectrum takes the function back into the time domain, and is a measure of the rate of change of the spectral magnitudes [129]. The idea of the log spectrum or cepstral averaging is found useful in many applications such as speech processing, echo detection and noise source recognition.

Consider a signal $s(t)$ consisting of the convolution of the two components, $x(t)$ and $y(t)$, so that $s(t) = x(t) \otimes y(t)$.

Then, taking Fourier transforms of both sides,

$$S(\omega) = X(\omega)Y(\omega)$$

The magnitude spectrum of the signal can be written as

$$|S(\omega)| = |X(\omega)||Y(\omega)|$$

By taking the logarithms of both sides,

$$\ln|S(\omega)| = \ln|X(\omega)| + \ln|Y(\omega)|$$

Thus, a convolution in time has been transformed into a sum of log-magnitude components in the frequency domain. For separating the components $x(t)$ and $y(t)$, the inverse Fourier transform can be applied. However, it should be noted that the phase information from the original signal has been lost, as a result of the magnitude operation on the complex spectra.

Applying an inverse Fourier transform to the log spectrum gives

$$F^{-1} \{ \ln|S(\omega)| \} = F^{-1} \{ \ln|X(\omega)| \} + F^{-1} \{ \ln|Y(\omega)| \}$$

For the signal $s(t) = x(t) \otimes y(t)$, $c_s(n)$ is given by

$$c_s(n) = c_x(n) + c_y(n),$$

where $c_s(n)$, $c_x(n)$ and $c_y(n)$ are the cepstra of signals $s(t)$, $x(t)$ and $y(t)$, respectively. The various steps involved in the computation of the cepstral coefficients are depicted in Fig. 4.29.

The cepstrum so derived is the real cepstrum, as it is derived from the power spectrum of the signal, which is always a real function of frequency and is an even function of the independent variable, lag or quefrequency. Because the log-magnitude spectrum is real and symmetrical for real signals, the final IFT can be replaced with a *cosine transform*.



Fig. 4.29 Steps involved in computing Real Cepstrum

Using a suitable cepstral filter normally referred to as lifter, the components may be separated from each other and then they can be transformed back into log-magnitudes or magnitudes in the frequency domain as required.

- Low order cepstral coefficients are sensitive to spectral slope, glottal pulse shape, etc.
- High order cepstral coefficients are sensitive to the analysis window position and other temporal artefacts.

- The variations in these coefficients can be reduced by using a raised sine window that emphasizes the coefficients at the centre of the window

One of the drawbacks of the real cepstrum concerns with the loss of phase information. By taking the complex logarithm of the Fourier transform, it is possible to generate the complex cepstrum. The various steps involved in the computation of the complex cepstrum are depicted in Fig. 4.30.

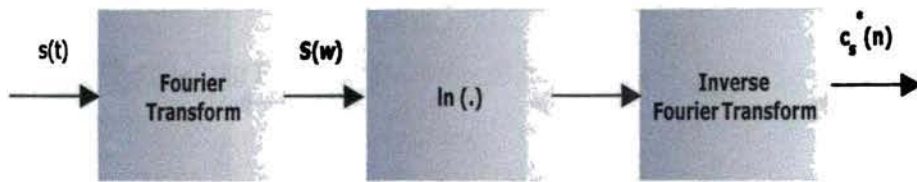


Fig. 4.30 Steps involved in getting the complex cepstrum

4.6.1 Cepstral Plots

It can be seen that most of the details occur near the origin and in peaks higher up the cepstrum. Thus, the lower numbered coefficients provide the envelope information, while the remaining information are mostly confined to the peaks which are separated by the pitch period. The windowed noise waveforms, its cepstrum, the spectral envelope and the spectral details of various noise sources in the ocean are depicted in Figs. 4.31 to Fig. 4.42.

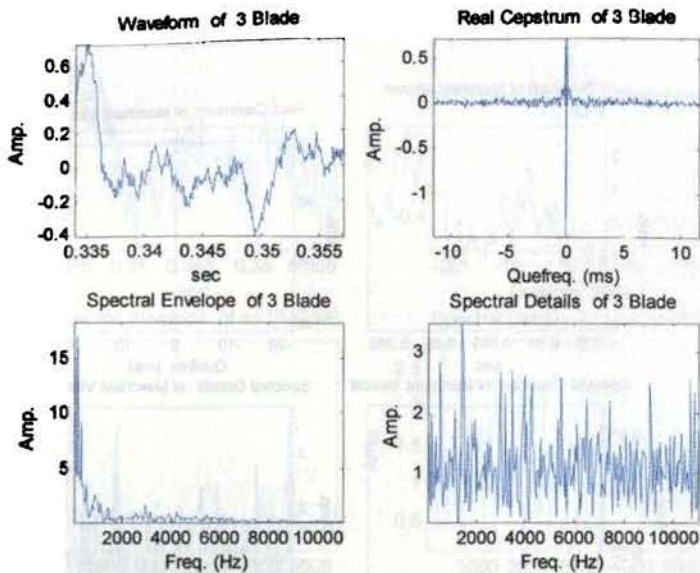


Fig. 4.31 Characterisation of 3 Blade Engine Noise

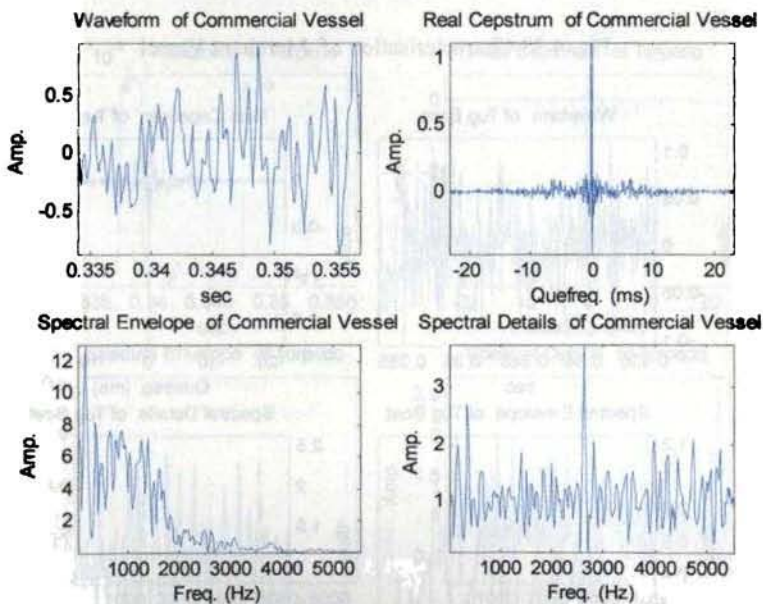


Fig. 4.32 Characterisation of a Commercial Vessel

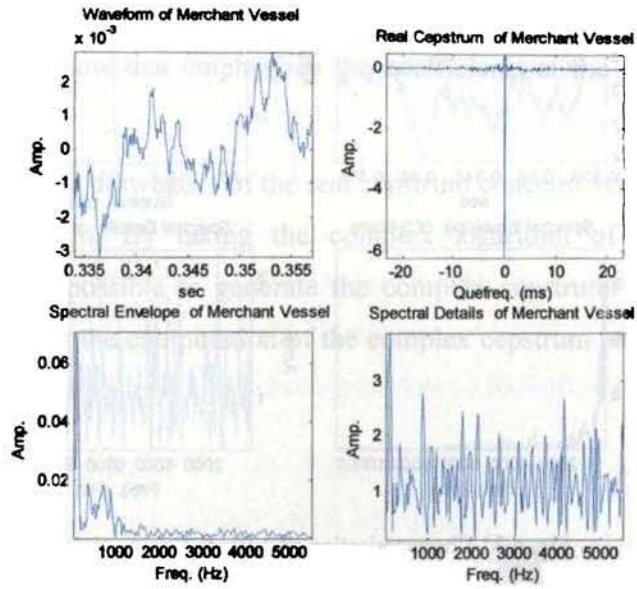


Fig. 4.33 Characterisation of Merchant Vessel

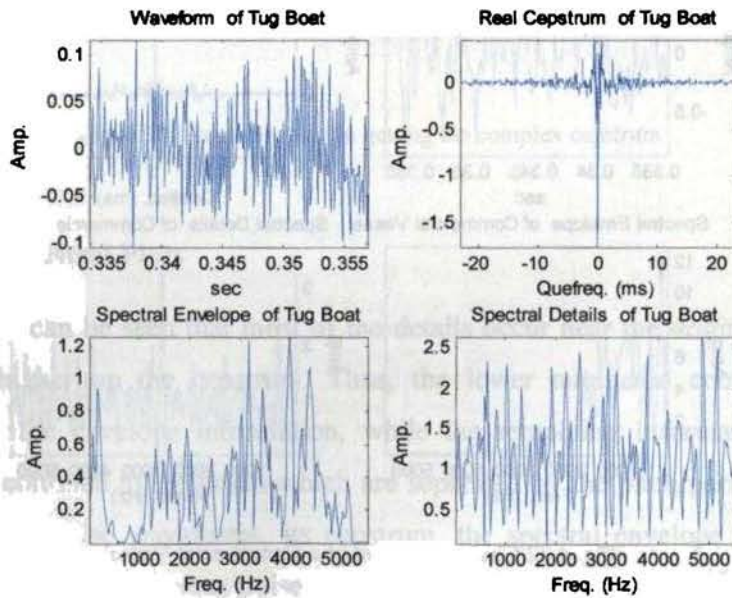


Fig. 4.34 Characterisation of Tug Boat

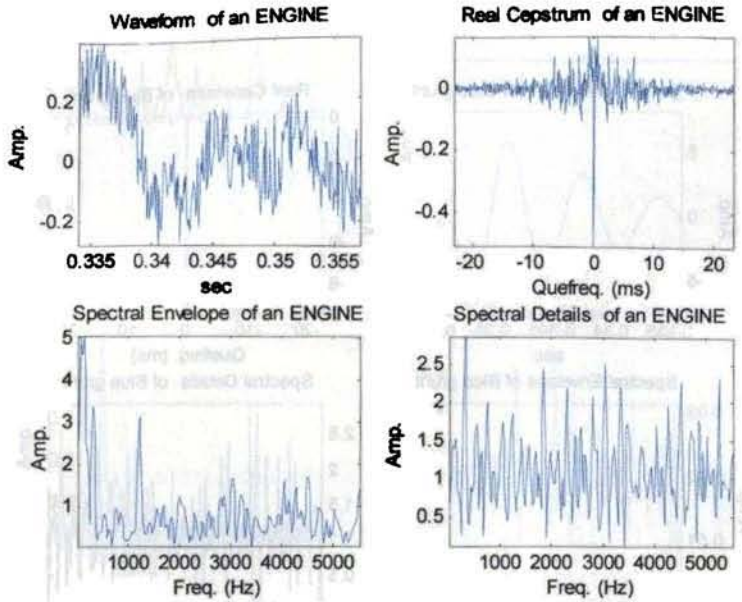


Fig. 4.35 Characterisation of an Engine

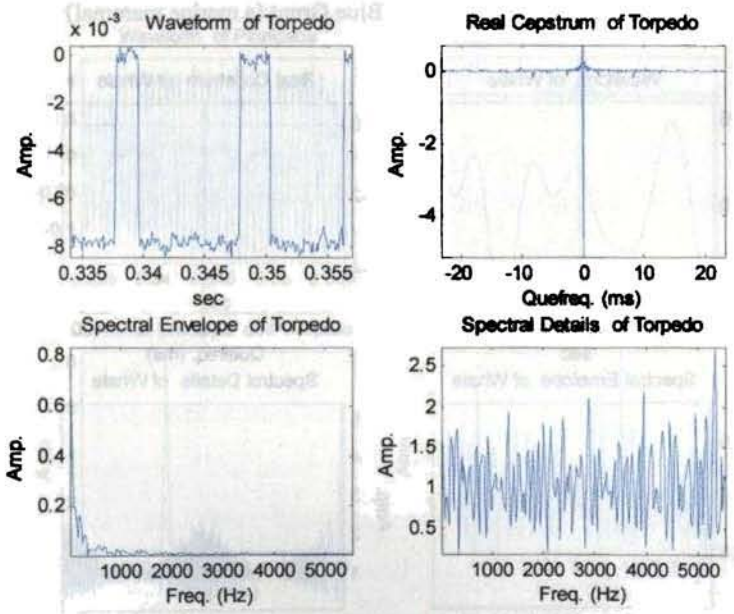


Fig. 4.36 Characterisation of Torpedo

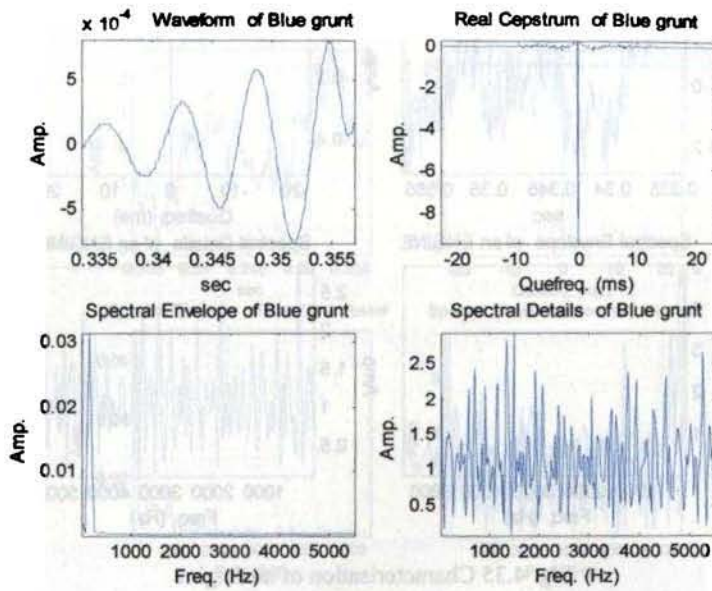


Fig. 4.37 Characterisation of Blue Grunt (a marine mammal)

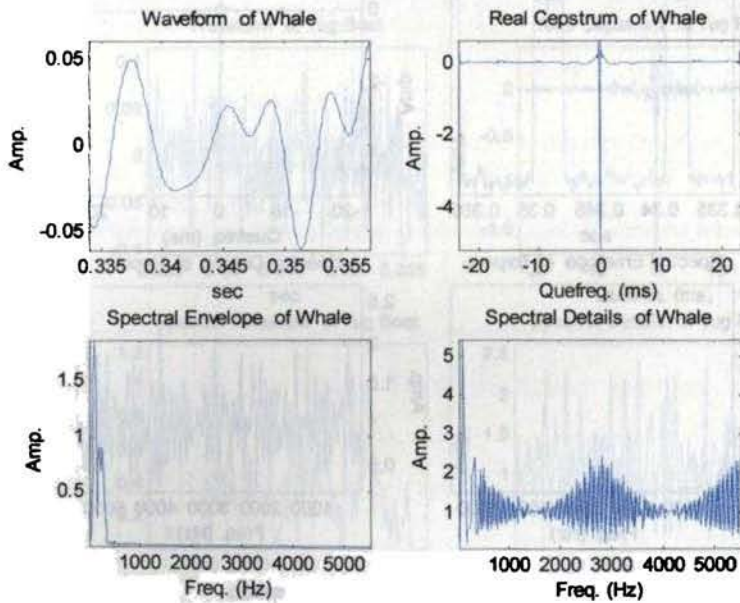


Fig. 4.38 Characterisation of Whale (a marine mammal)

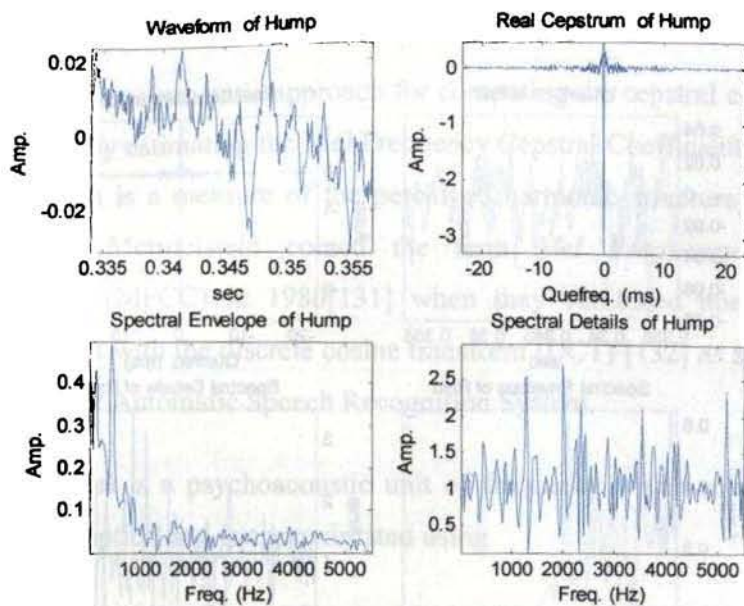


Fig. 4.39 Characterisation of Humpback Whale (a marine mammal)

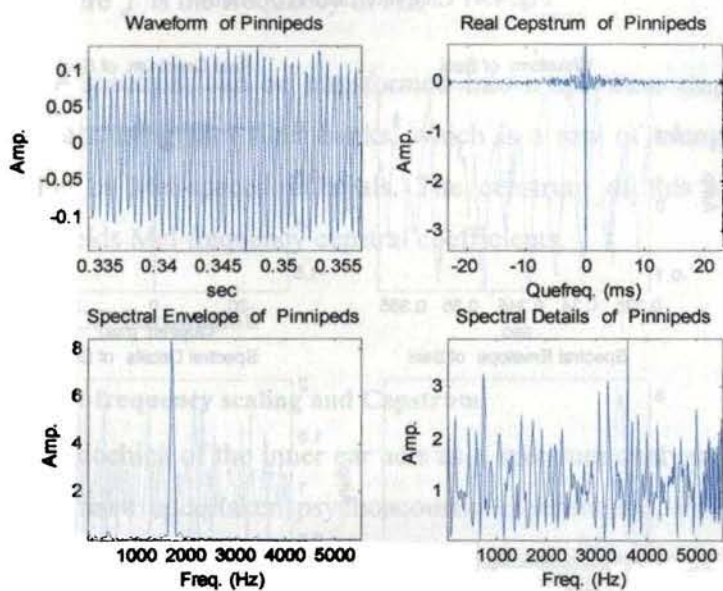


Fig. 4.40 Characterisation of Pinnipeds

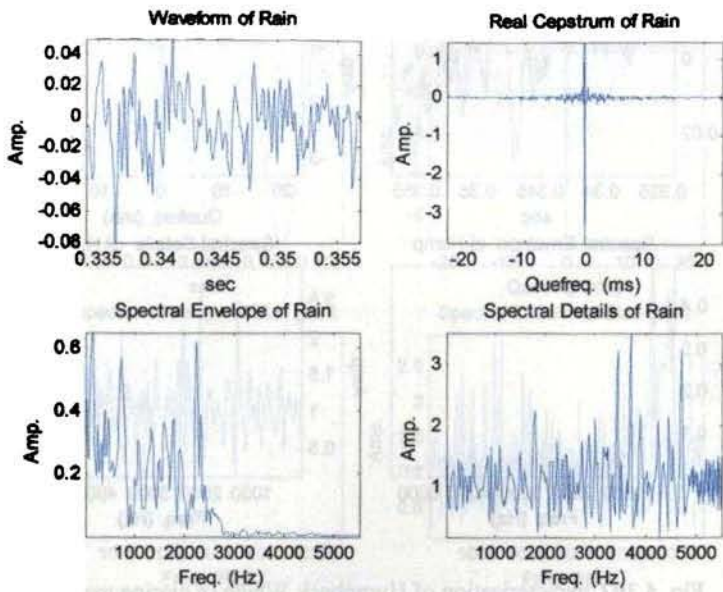


Fig. 4.41 Characterisation of Rain

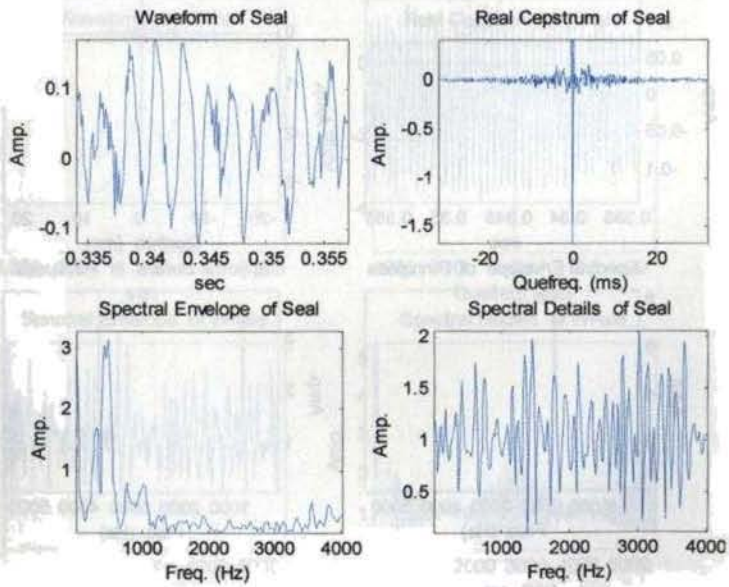


Fig. 4.42 Characterisation of Seal

4.7 *Mel Frequency Cepstral Coefficients*

A more systematic approach for computing the cepstral coefficients is achieved by estimating the Mel Frequency Cepstral Coefficients (MFCC) [130], which is a measure of the perceived harmonic structure of sound. Davis and Mermelstein coined the term *Mel Frequency Cepstral Coefficients* (MFCC) in 1980[131] when they combined nonuniformly spaced filters with the discrete cosine transform (DCT) [132] as a front-end algorithm for Automatic Speech Recognition System.

A Mel is a psychoacoustic unit of frequency which relates to the human perception and is approximated using

$$m = 2595 \log_{10} \left[1 + \frac{f}{700} \right]$$

where f is the frequency in Hz.

The spectrum can be transformed into a spectrum emphasized at Mel intervals using Mel filter banks, which is a row of triangular filters overlapping at Mel-spaced intervals. The cepstrum of this transformed spectrum yields Mel frequency cepstral coefficients.

4.7.1 MFCC Estimation

4.7.1.1 Mel-frequency scaling and Cepstrum

The cochlea of the inner ear acts as a spectrum analyzer and hence researchers have undertaken psychoacoustic experimental work to derive frequency scales that attempt to model the natural response of the human perceptual system. The complex mechanism of the inner ear and auditory nerve implies that the perceptual attributes of sounds at different frequencies may not be entirely simple or linear in nature. The cochlea in

the auditory system acts, as if it is made up of overlapping filters having bandwidths equal to the critical bandwidth. Hence the method of frequency scaling is used to map the linear frequencies into human perception. Mel-frequency scale as shown in Fig 4.43 is such a kind of perceptually motivated scale, which is linear below 1 kHz, and logarithmic at higher frequencies.

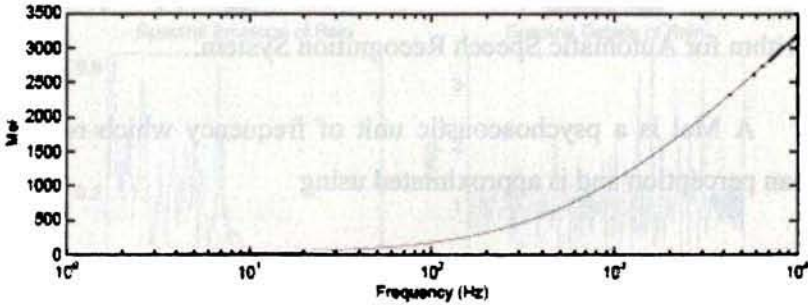


Fig. 4.43 The Mel-scale

The Mel scale more closely models the sensitivity of the human ear than a purely linear scale and provides for greater discriminatory capability between audio segments. The Mel-scale frequency analysis has been widely used in current speech recognition system and can be used for target emissions also.

The DFT of the input signal $x(n)$ is given by

$$X(k) = \sum_{n=0}^{N-1} x(n) \exp(-j2\pi nk / N) \quad k = 0, 1, 2, \dots, N-1$$

Hence the Mel-frequency filter bank [132],[133] comprising of p filters can be represented as shown in the Fig. 4.44 with the energy in each band given by m_j ($j=1, 2, \dots, p$), and is computed as detailed below.

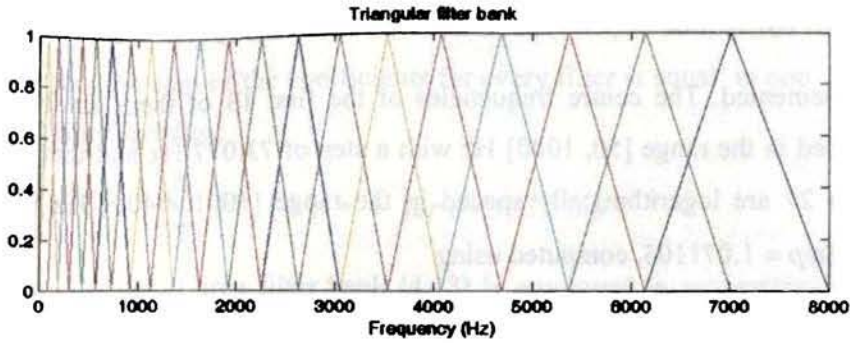


Fig. 4.44 Mel-Frequency filter bank on a linear frequency (Hz) scale

Each Fourier Transform magnitude coefficient is multiplied by the corresponding filter gain and the results are accumulated. It can be computed as

$$m_j = \sum_{k=0}^{N-1} |X(k)|^2 H_j(k) \quad 0 \leq j \leq p$$

where $H_j(k)$ is the transfer function of j^{th} filter.

The Mel-frequency cepstrum is then the discrete cosine transform [55] of the p filter outputs and is represented as

$$c_i = \sqrt{\frac{2}{N}} \sum_{j=1}^p m_j \cos\left(\frac{\pi i j}{p}\right) \quad (4.12)$$

where c_i is the i^{th} MFCC coefficient .

Mel-cepstral coefficients are extracted from the noise data waveforms. The key difference between MFCCs and cepstral coefficients lies in the process involved in extracting the characteristics of a noise signal [134].

With a sampling frequency of 11025, a filter bank of 40 equal area filters, which cover the frequency range [50, 6400] Hz has been

implemented. The centre frequencies of the first 13 of them are linearly spaced in the range [50, 1000] Hz with a step of 73.077 Hz and that of the next 27 are logarithmically spaced in the range [1001, 6400] Hz with a $\logStep = 1.071103$, computed using

$$\logStep = \exp \left(\frac{\ln \left(\frac{f_{c40}}{1000} \right)}{NumLogFilt} \right)$$

where f_{c40} , the centre frequency of the last one in the logarithmically spaced filters is 6400, and $NumLogFilt = 27$, the number of logarithmically spaced filters..

Each one of these equal area triangular filters is defined as

$$H_i(k) = \begin{cases} 0 & \text{for } k < f_{b_{i-1}} \\ \frac{2(k - f_{b_{i-1}})}{(f_{b_i} - f_{b_{i-1}})(f_{b_{i+1}} - f_{b_{i-1}})} & \text{for } f_{b_{i-1}} \leq k \leq f_{b_i} \\ \frac{2(f_{b_{i+1}} - k)}{(f_{b_{i+1}} - f_{b_i})(f_{b_{i+1}} - f_{b_{i-1}})} & \text{for } f_{b_i} \leq k \leq f_{b_{i+1}} \\ 0 & \text{for } k > f_{b_{i+1}} \end{cases} \quad (4.13)$$

where $i = 1, 2, \dots, p$ and stands for the i^{th} filter, f_{b_i} are $p + 2$ boundary points that specify the p filters, and $k = 1, 2, \dots, N$ corresponds to the k^{th} coefficient of the N point DFT. The boundary points f_{b_i} are expressed in terms of the position. The key to equalization of the area below the filters lies in the term

$$\frac{2}{f_{b_{i+1}} - f_{b_{i-1}}} \quad (4.14)$$

On account of this term the filter bank (4.13) is normalized in such a way that the sum of the coefficients for every filter is equal to one. Thus, the i^{th} filter satisfies:

$$\sum_{k=1}^N H_i(k) = 1 \text{ for } i = 1, 2, \dots, p$$

The equal area filter bank (4.13) is employed in generating of the log-energy output. Finally, the Discrete Cosine Transform (DCT) provides the MFCC-FB40 parameters.

The Discrete Cosine Transform performed on the log of the Mel-spectral coefficients provides the Mel-Frequency Cepstral Coefficients [135]. Of the many MFCCs, only the first 20 coefficients of each frame are considered, since most of the features of the noise source can be extracted from these coefficients. The use of DCT minimizes the distortion in the frequency domain and is efficient in computation, since an N-point DCT can be carried out using a symmetric 2N-point FFT.

4.7.2 Window function

When the spectral analysis techniques like the Fast Fourier Transform are applied to the segments as a whole, it behaves as if it is operating on a data signal waveform that is zero just before the segment and then abruptly jumps to the signal during the segment and then back to zero when the segment ends. This introduces significant distortion of the signal and warrants the need for windowing.

The motivation behind the function of windowing is to remove the undesirable undulations and smoothen the edges of each data record, so as to reduce the spectral distortion as well as discontinuities or abrupt changes at the end points. More specifically, if the original signal level is $s(i)$ at time

i , then the windowed signal can be represented as $s(i) * W(i)$ where $W(i)$ is the window function.

A window function that works well is the *Hamming window* and is defined by

$$W(n) = 0.54 - 0.46 \cos\left(\frac{2\pi n}{N-1}\right)$$

When the cepstral coefficients are extracted, using the procedures already formulated it has been observed that the MFCCs for various records vary over a wide range of values. Hence, the optimum set of values for the cepstral coefficients are to be synthesized by a technique referred to as *vector quantization* [136].

4.7.3 Vector Quantization

Vector quantization is a lossy data compression method based on the principle of block coding, which codes the values from a multidimensional vector space into values in a discrete subspace of lower dimension. In the work reported here, the LBG (Linde, Buzo, Gray) design algorithm [137] for vector quantization by trimming the cepstral coefficients to the nearest value is adopted for finding out the optimum match.

4.7.3.1 Implementation

The MFCC matrix is vector quantized by passing each column of this matrix through a vector quantizer. In vector quantization, the columns of the MFCC matrix are taken as source vectors, which will generate the quantized code vectors comprising of the various cepstral coefficients at different frequencies.

If the source vectors are k -dimensional, then X_m can be represented as

$$X_m = (x_{m1}, x_{m2}, \dots, x_{mk}) \text{ where } m = 1, 2, \dots, M.$$

Let P be the number of code vectors which are synthesized from the M source vectors, by following an iterative procedure for trimming the cepstral coefficients, starting with a column vector, obtained by taking the average of the entire elements in a row of the MFCC matrix.

$\{C\} = \{c_1, c_2, \dots, c_P\}$ represents the set of k -dimensional code vectors with the various components of each c_p given by $c_p = (c_{p1}, c_{p2}, \dots, c_{pk})$ where $p = 1, 2, \dots, P-1, P$ being the number of code vectors that are to be synthesized from the source vectors, as specified at the time of initialization.

The LBG algorithm requires an initial code book containing one code vector obtained by taking the row wise mean of the MFCC matrix. The initial code vector is split into two column vectors by adding and subtracting an error term. From these column vectors, the minimum distance to the various columns of the MFCC matrix is computed by the Euclidean distance technique using the equation,

$$D = \sqrt{\sum_{m=1}^M (\vec{X}_m - \vec{Y}_m)^2}$$

where D is the Euclidean distance, \vec{X}_m is the source vector and \vec{Y}_m is the code vector. The stipulated procedure for trimming the cepstral coefficients using vector quantization is illustrated in the flowchart shown in Fig. 4.45.

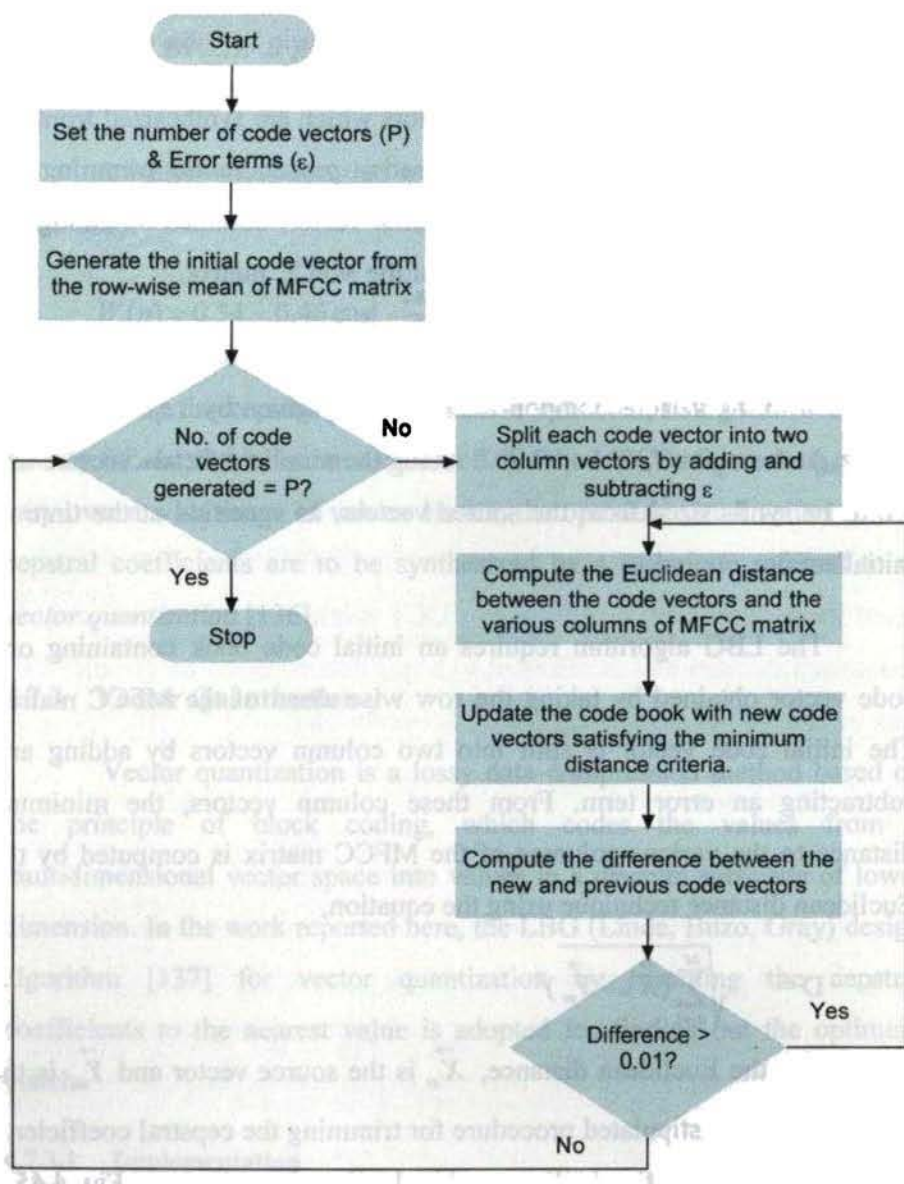


Fig. 4.45 Procedure for vector quantization

Using this minimum distance and its index, the corresponding column vectors of the MFCC matrix are identified and from the average values, new code vectors are generated.

The new code vectors so generated are compared with the previous code vectors. If the difference is greater than the error term, minimum distances between these code vectors and MFCC matrix is again computed by the same method and the code book is being updated until the difference is less than the error term. The process of splitting the code vectors is continued till the number of iterations specified at the time of initialisation is reached. As the number of iterations in the vector quantizer has to be an integer, the number of code vectors specified at the time of initialization has to be a power of two.

4.8 Cepstral Features

For the extraction of cepstral features the signals collected from the hydrophone are pre-processed which mainly includes framing, windowing and pre-emphasis. The various processes involved in the extraction of the cepstral features are illustrated in Fig.4.46.

Framing is used to segment the long-time signal to the short-time signal in order to get relatively stable frequency characteristics. Thus the noise data is sliced into different records of fixed length N and each data record is windowed using a Hamming window. The windowed data record is then transformed into the frequency domain by taking FFT, which is applied to the Mel-scale filter bank. The MFCCs are computed by taking the discrete cosine transform (DCT) of the log-scaled filter bank output and is further subjected to vector quantisation.

In an attempt to extract the cepstrally decomposable features, 20 MFCCs have been generated. The Table 4.2 summarizes the MFCCs with

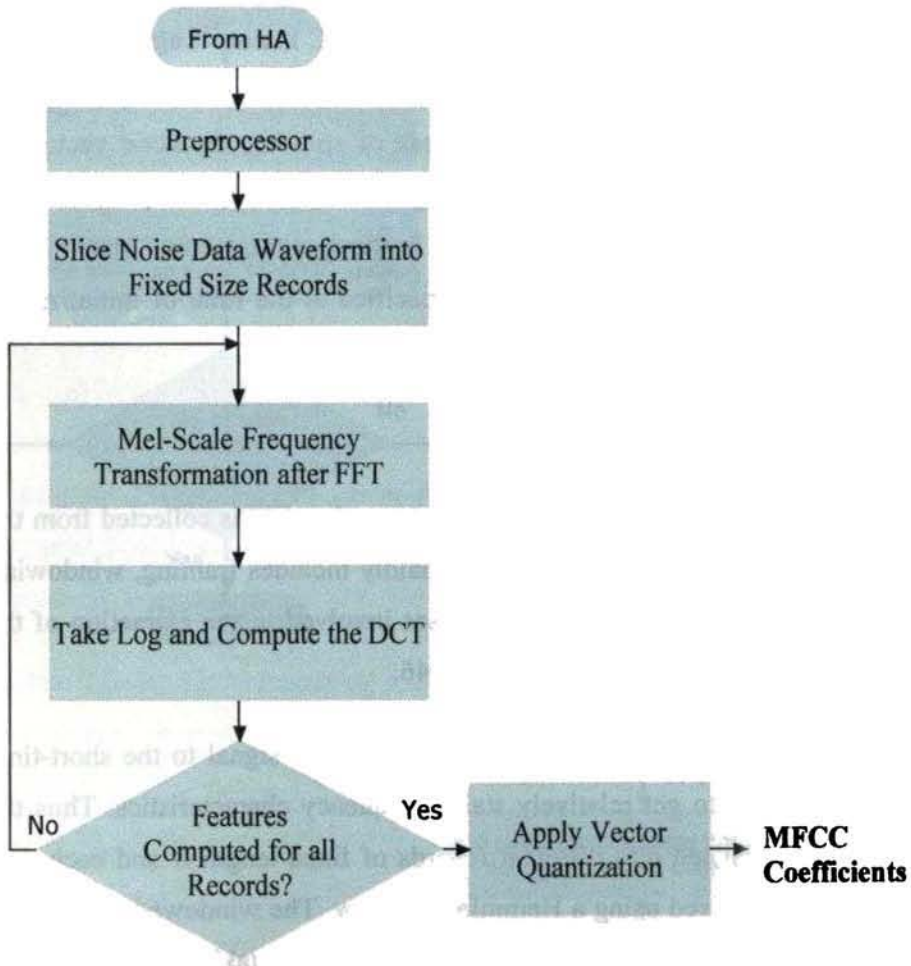


Fig. 4.46 Illustration of the steps involved in estimation of MFCC

and without noise for two different noise sources , viz. engine and a surface craft. In underwater scenario, as man made noise data contain certain valuable low frequency information, the Mel filter banks have been extended to the low frequency cut off value of 50 Hz.

Table 4.2 Table of MFCC for two different noise sources

ENGINE				BOAT			
MFCC(without noise)	VQ(without noise)	MFCC(with noise)	VQ(with noise)	MFCC(without noise)	VQ(without noise)	MFCC(with noise)	VQ(with noise)
-10.03600	-10.00500	-9.27650	-9.27200	-9.40760	-9.39900	-8.94210	-9.41910
-1.91800	-1.91980	-1.29340	-1.28690	1.94420	1.94580	1.39010	1.33860
-0.12247	-0.11614	0.01102	0.01729	-1.81440	-1.80390	-1.48920	-1.45380
0.00562	0.01932	-0.00326	0.00547	-0.03919	-0.02978	-0.13143	-0.1133
0.17826	0.16857	0.02445	0.02279	-0.53635	-0.52936	-0.36691	-0.36104
0.38255	0.38257	0.15368	0.14744	0.07886	0.07321	-0.01608	-0.01083
0.32239	0.32903	0.11544	0.11892	-0.35154	-0.35473	-0.27156	-0.24204
0.12236	0.13344	-0.03715	-0.02744	-0.12932	-0.13455	-0.21963	-0.21028
-0.03592	-0.02889	-0.13080	-0.12722	-0.03189	-0.03388	-0.05134	-0.04338
0.01818	0.00330	-0.05365	-0.05629	-0.13503	-0.12872	-0.05672	-0.05774
0.13244	0.11247	0.05403	0.05924	0.28481	0.28800	0.21459	0.19267
0.12084	0.12221	0.07212	0.07549	-0.22155	-0.21884	-0.06984	-0.07290
-0.06611	-0.05528	-0.04210	-0.03955	0.22930	0.22831	0.13303	0.12586
-0.18141	-0.18559	-0.11832	-0.11294	-0.26006	-0.25951	-0.16329	-0.15808
-0.14267	-0.13664	-0.08246	-0.08612	0.29963	0.29593	0.10468	0.10566
0.01217	0.01636	0.03863	0.03664	-0.28433	-0.28325	-0.13267	-0.12409
0.06414	0.06597	0.07923	0.07641	0.08896	0.08946	0.03609	0.03009
-0.04586	-0.04916	0.00470	-0.00424	-0.20589	-0.20540	-0.11799	-0.12153
-0.14250	-0.13556	-0.06930	-0.06846	0.14926	0.14848	0.06515	0.06923
-0.08870	-0.08474	-0.04470	-0.04260	-0.20498	-0.20398	-0.06682	-0.06192

4.9 Summary

This techniques and procedures involved in extracting the various feature components required for generating the classification clues are highlighted in this chapter. The classical as well as parametric model based power spectral estimators for extracting the spectral features have also been presented in this chapter. It has been observed that parametric model based estimators give better results for short data segments and yield better frequency resolutions than conventional estimators. In this context it is also worth mentioning the fact that parametric approaches take the advantage of the *a priori* knowledge about the process from which the data samples are taken.

This chapter also touches upon the concepts of cepstral analysis, which belongs to an area of signal processing known as *homomorphic analysis* and can be accomplished by using a cascade of forward and inverse operations with a linear time invariant operation sandwiched in between. The spectrum of any waveform consists of two components, the slowly varying part, referred to as the filter or spectral envelope and the rapidly varying part, referred to as the source or harmonic structure. Separation of these two components can be achieved by taking the *cepstrum*. A more systematic approach for computing the cepstral coefficients can be achieved by estimating the Mel Frequency Cepstral Coefficients (MFCC), which is a measure of the perceived harmonic structure of sound.

CHAPTER 5

BISPECTRAL ESTIMATION

In the analysis and handling of random signals, the first and second order statistics have gained significant importance and is used in a wide variety of applications. For many signals, which are generated from nonlinear processes, second order statistical methods are not sufficient for analysis. Many of the naturally occurring signals deviate from Gaussianity and linearity. Hitherto, such signals were considered Gaussian or near Gaussian signals and analysis were conducted, which has resulted in loss of valuable information. For these reasons, higher order statistical methods have been developed, which can handle non-Gaussian as well as non-linear signals. Phase information is not available in the second-order measures such as the power spectrum and autocorrelation functions because of which, non-minimum phase signals and certain types of phase couplings, associated with nonlinearities, cannot be correctly identified by second order statistics. The Gaussian signals can be completely characterized by its mean and variances. Different types of nonlinearities results in different types of phase couplings. If a signal composed of two sinusoids is passed through a non linear system, then the output will contain components at the sum and difference frequencies as well. Quadratic Phase Coupling is the term used to describe the coupling which results from such type of nonlinearities. The procedures to be adopted for generating the bispectrally extractable features such as the mutual coupling frequencies, self coupling frequencies, the peak at the bifrequencies, etc. are described in this chapter.

5.1 Introduction

As the applicability of the signal processing technology is increasing, a number of techniques based on certain statistical approaches have been developed to analyze and handle random signals. The first and second order statistics have gained significant importance and is used in a variety of applications. The technique of power spectral analysis is found to have wide applicability and are also robust and time tested. However, many signals, especially those which are generated from nonlinear processes, can not be properly analysed by second order statistical methods.

Many of the naturally occurring signals deviate from Gaussianity and linearity. Until recently, such signals were considered Gaussian or near Gaussian signals and analysis were conducted, which has resulted in loss of valuable information. For handling such signals, higher order statistical methods have been developed, which can handle non-Gaussian as well as non-linear signals.

During the 1970s, for the first time, Higher Order Spectrum (HOS) techniques were applied to signal processing problems, and since then HOS has been continuing to expand into different fields as speech, seismic data processing, plasma physics, optics, etc..

5.1.1 Theory and Definitions

Consider a discrete time real valued random signal $x(n)$. The probability density function (PDF) of $x(n)$ gives an insight into the distribution of the amplitudes of $x(n)$. The shape of the PDF can be characterized by a set of measures called *moments*. Another measure called *cumulants*, which are very similar to moments,, has also been coined and the higher order spectra are defined in terms of these cumulants.

5.1.1.1 Moments

The moments are defined as the coefficients of the Taylor's expansion of the Moment Generating Function (MGF). The first moment, the *mean*, gives a measure of the location of the PDF, while the second moment, the *variance*, gives a measure of the spread of the PDF. The third and fourth order moments are called *skewness* and *kurtosis*, which gives a measure of the asymmetry and sharpness of the PDF, respectively.

The k^{th} order moment, about the mean, of the process can be estimated by computing the expected value of product of itself with $(k-1)$ lagged versions. Thus, the second and third order moments can be written as

$$m_2(\tau_1) = E[x(n)x(n + \tau_1)]$$

$$m_3(\tau_1, \tau_2) = E[x(n)x(n + \tau_1)x(n + \tau_2)]$$

In general, the k^{th} order moment can be estimated as

$$m_k(\tau_1, \dots, \tau_{k-1}) = E[x(n)x(n + \tau_1) \dots x(n + \tau_{k-1})] \quad (5.1)$$

5.1.1.2 Cumulants

The natural logarithm of MGF is the Cumulant Generating Function (CGF) and the coefficients of the Taylor's expansion of the CGF are termed as the *cumulants*. One of the notable features of the cumulants is that, for a Gaussian process, all cumulants of order greater than two are identically zeroes and this helps in distinguishing a non-Gaussian process from a Gaussian one.

Cumulants are closely related to moments and can be estimated by first computing the moments of the process and then applying some simple relations, which exist between the cumulants and moments.

Chapter 5 Bispectral Analysis

$$c_1 = m_1$$

$$c_2 = m_2 - m_1^2$$

$$c_3 = m_3 - 3m_2m_1 + 2m_1^3$$

$$c_4 = m_4 - 4m_3m_1 - 3m_2^2 + 12m_2m_1^2 - 6m_1^4$$

where m_i and c_i are the i^{th} order *moment* and *cumulant* respectively.

Hence, for zero mean processes, the second and third order cumulants will be equal to the respective moments. Even for zero mean processes, for orders greater than three, the moments and cumulants are distinct,

$$\text{i.e., } m_n(\tau_1, \dots, \tau_n) \neq c_n(\tau_1, \dots, \tau_n) \text{ for } n > 3.$$

Cumulants have certain attractive properties, that make it more useful over moments and because of which the expressions involving cumulants are much simpler and easier to manipulate than expressions involving moments.

5.1.1.3 Polyspectrum

Fourier transform of a real discrete zero-mean process $x(n)$ is given by

$$X(f) = \sum_{n=-\infty}^{\infty} x(n) \exp(-j2\pi fn) \quad (5.2)$$

The polyspectrum, or the n^{th} order cumulant spectrum, is defined as the Fourier Transform of the n^{th} order cumulant sequence. Thus, the first member of the polyspectrum family is the well known power spectrum $P(f)$ and is expressed as the Fourier transform of the second order cumulant or the autocorrelation sequence [69].

$$\text{i.e., } P(f) = \sum_{k=-\infty}^{\infty} C_x(k) \exp(-j2\pi f k) \quad (5.3)$$

where C_x is the second-order cumulant of $x(n)$, given by

$$C_x(k) = E[x(n)x^*(n+k)] \quad (5.4)$$

Similar to the power spectrum, the third order spectrum or the *bispectrum* $B(f_1, f_2)$ is defined as

$$B(f_1, f_2) = \sum_{k=-\infty}^{\infty} \sum_{l=-\infty}^{\infty} C_{xx}(k, l) \exp(-j2\pi f_1 k) \exp(-j2\pi f_2 l) \quad (5.5)$$

where $C_{xx}(k, l)$ is the autobicorrelation, which is the third order cumulant and is expressed as,

$$C_{xx}(k, l) = E[x(n)x(n+k)x^*(n+l)] \quad (5.6)$$

Fourier transform of the fourth order cumulant sequence is called the *trispectrum* and is given by

$$T(f_1, f_2, f_3) = \sum_{k=-\infty}^{\infty} \sum_{l=-\infty}^{\infty} \sum_{m=-\infty}^{\infty} C_{xxx}(k, l, m) \exp(-j2\pi f_1 k) \exp(-j2\pi f_2 l) \exp(-j2\pi f_3 m) \quad (5.7)$$

It may be noted that the bispectrum is a function of two frequencies, whereas the trispectrum is a function of three frequencies. In contrast with the power spectrum which is real valued and nonnegative, bispectra and trispectra are complex valued. In general, Higher Order Spectra, $H(f_1, f_2, \dots, f_k)$ is complex for order k greater than two.

An outstanding property of polyspectrum is that all polyspectra of higher order (order greater than two) vanish when the process is Gaussian. This property is a direct consequence of the fact that all the cumulants of order greater than 2 are identically zero. Thus higher-order spectra measure

the deviation of a stochastic process from Gaussianity. Higher order statistics such as skewness, kurtosis, etc. are now widely being used in applications like speech processing, source identification/classification, etc..

A random signal $x(n)$ can be completely characterized by its autocorrelation function (ACF) only if it originates from a random process with Gaussian characteristics. In non Gaussian processes, the higher order moments carry information that can not be found in the ACF. Such non-Gaussianities can be found, for example, in speech, radar, sonar, bio-medical, seismology, etc.. The extra information provided by HOS leads to better estimates of the parameters and throws light on the non-linearities in the source of the signal.

Some of the notable advantages of such techniques over the traditional second-order techniques are the following:

- ❖ The phase information is not available in the second-order measures such as the power spectrum and autocorrelation functions. Because of this, non-minimum phase signals and certain types of phase couplings associated with nonlinearities cannot be correctly identified by second order techniques.
- ❖ The Gaussian signals can be completely characterized by its mean and variances. Consequently, the HOS of Gaussian signals are zero. Since, many signals encountered in practice are non-Gaussian and many measurement noises are Gaussian in nature, HOS are less affected by Gaussian background noise than the second order measures.

The second feature becomes very attractive in classification or identification scenarios. For example, the power spectrum of a deterministic signal and Gaussian noise is very different from the power spectrum of the signal alone. However the bispectrum of the signal and noise is, at least in principle, the same as that of the signal.

Thus, the general motivations behind the use of higher order spectra are to extract information due to deviation from Gaussianity, to detect and characterize the non-linear properties of signal generating mechanisms and to estimate the phase of non-Gaussian parametric signals.

5.2 *Bispectrum*

As already established, the traditional power spectrum is the Fourier transform of the autocorrelation sequence, while the bispectrum is the Fourier transform of the third-order cumulant sequence or the autobicorrelation sequence. The bispectrum is a member of the category of *higher order spectra*, or *polyspectra* and can provide additional information than the power spectrum.

Among the higher order spectra, the third order polyspectrum or the bispectrum can be computed very easily and hence is attracting more and more researchers. The bispectrum can be thought of as a frequency decomposition of the third-order cumulant and it follows that the process skewness γ_3 which is the zero-lag cumulant $C_3(0,0)$ is equal to the bispectrum summed over all the frequencies. This can be compared with the way in which the variance of a process is related to its power spectrum and second-order cumulant or autocorrelation function. Bispectral analysis can reveal the deviation of the processes from Gaussianity, since all

polyspectra of order greater than two is identically zero for Gaussian process.

5.2.1 Energy Dependence of Bispectrum

The bispectrum is asymptotically consistent. However, at the bifrequency (f_1, f_2) , the complex variance is proportional to the product of the power of the signals at the frequencies f_1 , f_2 and $(f_1 + f_2)$.

$$\text{i.e. } \text{var}[B(f_1, f_2)] \propto P(f_1)P(f_2)P(f_1 + f_2)$$

So the value of the bispectrum at a particular bifrequency depends on the energy content at those frequencies. This energy dependency can lead to erroneous results. As an illustration consider the bispectrum of a Gaussian signal as shown in Fig. 5.1. Though theoretically, the bispectrum of the Gaussian signal should be identically zero. In practical scenario bispectral values are found to have smaller values (nearly zero) as shown in the Fig 5.1.

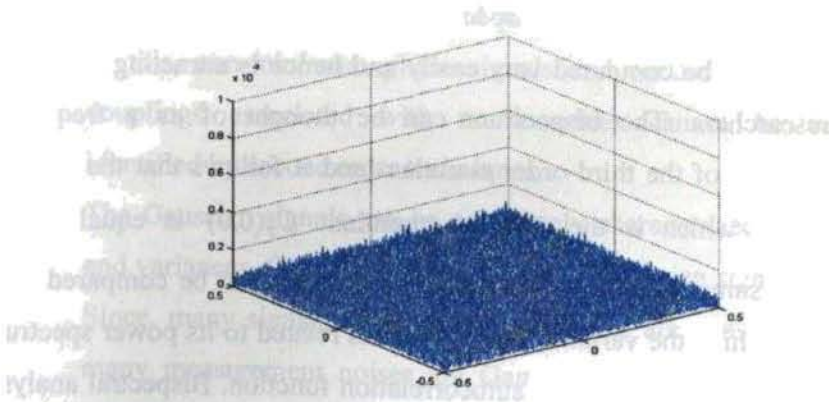


Fig. 5.1 Bispectrum of Gaussian Noise

However, as the amplitude of the signal gets increased, the bispectral plot also shows false peaks, indicating the signal as non-Gaussian

even though the signal is purely Gaussian. Figs. 5.2 (a) and (b) shows the bispectral plots of the Gaussian signal amplified by a factor of 2 and 100 respectively.

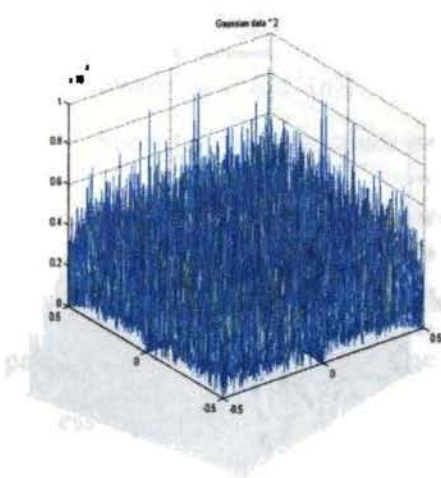


Fig. 5.2 (a) Bispectrum of the Gaussian signal amplified by 2

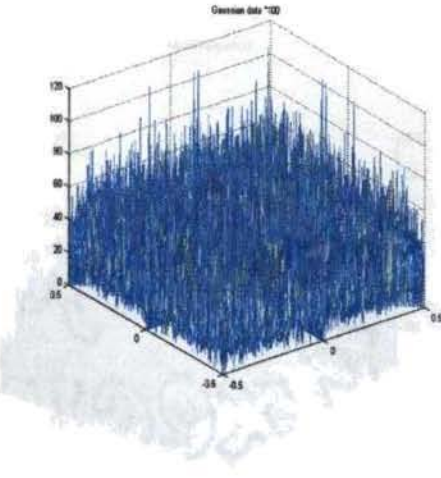


Fig. 5.2 (b) Bispectrum of the Gaussian signal amplified by 100

5.3 Bicoherence

It can be seen that the magnitude of the bispectrum plot, on a large scale, depends on the amplitude of the signal under consideration. Thus, in order to make the bispectrum independent of the energy content at the bifrequencies, another parameter called bicoherence is used.

Bicoherence $bic(f_1, f_2)$ is defined as

$$bic(f_1, f_2) = \frac{|B(f_1, f_2)|}{[P(f_1)P(f_2)P(f_1 + f_2)]^{1/2}} \quad (5.8)$$

Since the bicoherence is independent of the energy or amplitude of the signal, it can be used as a convenient test statistics for the detection of non Gaussian, nonlinear and coupled processes.

From Figs.5.3 (a) and (b), it is clear that the bicoherence is independent of the energy content or the amplitude of the signal.

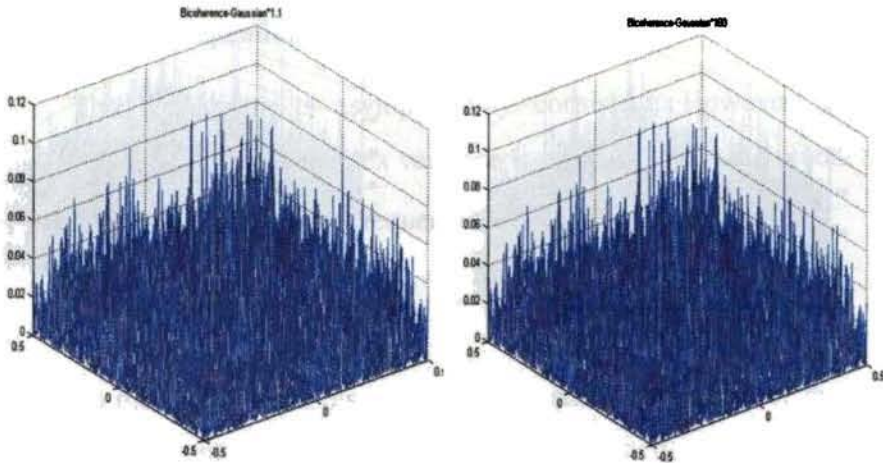


Fig. 5.3(a) Bicoherence of the signal amplified by 2.

(b) Bicoherence of the signal amplified by 100

5.3.1 Linear and Gaussian Models

A time series is said to be stationary, if the mean, covariance and the third moment do not change with the shift of time. A stationary time series $x(n)$ is said to be linear, if it can be expressed in the form

$$x(n) = \sum_m h(m)\varepsilon(n-m)$$

where $\varepsilon(n)$ is a pure noise process and $h(m)$ is the *volterra* kernel. If $\varepsilon(n)$ happens to be Gaussian, then $x(n)$ is also Gaussian. Thus it is evident that all Gaussian processes are linear while the converse need not be true.

The power spectrum $P(f)$ is given by

$P(f) = \sigma^2 |H(f)|^2$ where

$H(f) = \sum_m h(m) \exp(-j2\pi f m)$ and the bispectrum is given by

$$B(f_1, f_2) = \mu_3 H(f_1) H(f_2) H(f_1 + f_2)$$

where $\mu_3 = E[\varepsilon^3(n)]$.

Substituting these values in Eq. (5.8),

$$bic^2 = \frac{\mu_3^2}{\sigma^6}, \text{ which will be a constant.} \quad (5.9)$$

Hence, the bicoherence will be a constant for all frequency pairs (f_1, f_2) , if $x(n)$ is linear. Since the higher order moments of a Gaussian process is zero *i.e.* $\mu_3 = 0$, the bicoherence is also zero. Thus, one can easily show that if the process is linear then its bicoherence is constant. Hence, if the bispectrum or bicoherence is not zero, then the process is non-Gaussian; if the bicoherence is not constant then the process is nonlinear. Consequently we have the following hypothesis testing procedures:

H_1 : The bispectrum of $x(n)$ is nonzero

H_0 : The bispectrum of $x(n)$ is zero

If hypothesis H_1 holds, we can test for linearity, that is, we have a second hypothesis testing problem:

H_1' : The bicoherence of $x(n)$ is not constant

H_1'' : The bicoherence of $x(n)$ is a constant

If hypothesis H_1'' holds, the process is linear.

5.4 Properties of Bispectrum

Let $\{X(k)\}$ be a real, discrete, zero-mean stationary process. The power spectrum $P(\omega)$, can be defined as

$$P(\omega) = \sum_{\tau=-\infty}^{\infty} r(\tau) \cdot \exp(-j\omega\tau) \quad \text{for } |\omega| < \pi \quad (5.10)$$

where $r(\tau) = E[X(k)X(k + \tau)]$ is its autocorrelation sequence. If $R(m, n)$ denotes the third moment sequence of $\{X(k)\}$,

i.e., $R(m, n) = E[X(k)X(k + m)X(k + n)]$, then its bispectrum is defined as

$$B(\omega_1, \omega_2) = \sum_{m=-\infty}^{\infty} \sum_{n=-\infty}^{\infty} R(m, n) \cdot \exp[-j(\omega_1 m + \omega_2 n)] \quad (5.11)$$

Since the third-order moments and cumulants are identical, the bispectrum is a third-order cumulant spectrum.

The physical significance of the power spectrum and bispectrum becomes apparent when expressed in terms of the components $dZ(\omega)$ of the Fourier – Stieltjes representation of $X(k)$ (Cramer spectral representation).

$$X(k) = \frac{1}{2\pi} \int_{-\infty}^{\infty} \exp(j\omega k) dZ(\omega) \quad \text{for all } k, \quad (5.12)$$

where $E[dZ(\omega)] = 0$

$$E[dZ(\omega_1)dZ^*(\omega_2)] = \begin{cases} 0 & \omega_1 \neq \omega_2 \\ 2\pi P(\omega)d\omega & \omega_1 = \omega_2 = \omega \end{cases}$$

and

$$E[dZ(\omega_1)dZ(\omega_2)dZ^*(\omega_3)] = \begin{cases} 0, (\omega_1 + \omega_2 \neq \omega_3) \\ B(\omega_1, \omega_2)d\omega_1 d\omega_2, (\omega_1 + \omega_2 = \omega_3) \end{cases}$$

It is therefore apparent that the power spectrum $P(\omega)$ represents the contribution to the mean product of two Fourier components whose frequencies are the same, whereas the bispectrum $B(\omega_1, \omega_2)$ represents the

contribution to the mean product of three Fourier components, where one frequency equals the sum of the other two.

The important symmetry conditions that follow from the above definitions are:

$$r(\tau) = r(-\tau)$$

$$P(\omega) = P(-\omega)$$

$$P(\omega) \geq 0 \text{ (real, nonnegative function).}$$

The third moments obey the symmetry properties

$$R(m, n) = R(n, m)$$

$$= R(-n, m - n)$$

$$= R(n - m, -m)$$

$$= R(m - n, -n)$$

$$= R(-m, n - m).$$

Consequently, knowing the third moments in any one of the six sectors, (I) through (VI) shown in Fig.5.4, would enable to find the entire third moment sequence. These sectors include their boundaries so that, for *example*, sector (I) is an infinite wedge bounded by the lines $m = 0$ and $m = n$; $m, n \geq 0$.

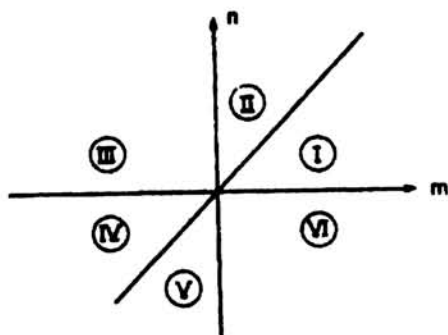
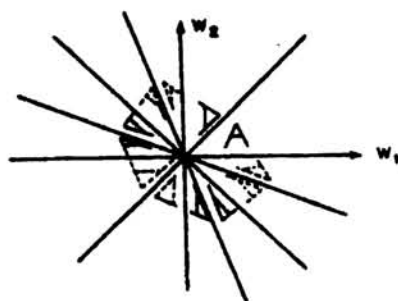


Fig. 5.4 (a) Symmetry regions of third-order moments



(b) Symmetry regions of the bispectrum

From the definition of the bispectrum and the properties of third moments, it follows that

$B(\omega_1, \omega_2)$ is generally complex, *i.e.*, it has magnitude and phase

$$B(\omega_1, \omega_2) = |B(\omega_1, \omega_2)| \exp [j\psi_B(\omega_1, \omega_2)]$$

$B(\omega_1, \omega_2)$ is doubly periodic with period 2π

$$B(\omega_1, \omega_2) = B(\omega_1 + 2\pi, \omega_2 + 2\pi).$$

$$\begin{aligned} B(\omega_1, \omega_2) &= B(\omega_2, \omega_1) \\ &= B^*(-\omega_2, -\omega_1) \\ &= B^*(-\omega_1, -\omega_2) \\ &= B(-\omega_1 - \omega_2, \omega_2) \\ &= B(\omega_1, -\omega_1 - \omega_2) \\ &= B(-\omega_1 - \omega_2, \omega_1) \\ &= B(\omega_2, -\omega_1 - \omega_2). \end{aligned}$$

Thus, a knowledge of the bispectrum in the triangular region $\omega_2 \geq 0$, $\omega_1 \geq \omega_2$, $\omega_1 + \omega_2 \leq \pi$ shown in Fig.5.4 (b) is enough for a complete description of the bispectrum. It is worth noting that the computation of $B(\omega_1, \omega_2)$ is carried out over one of the twelve sectors shown in Fig. 5.4(b) and the symmetries are then utilized, for completely characterizing the bispectral behaviour of the process.

Additional significant properties of the bispectrum that make it very attractive in practical application are outlined below.

- (i) **Gaussian Processes:** If $\{X(k)\}$ is a stationary zero-mean Gaussian process, its third-moment sequence $R(m, n) = 0$ for all (m, n) and therefore its bispectrum $B(\omega_1, \omega_2)$ is identically zero

(ii) **Linear Phase Shifts:** Given $\{X(k)\}$ with power spectrum $P_X(\omega)$ and bispectrum $B(\omega_1, \omega_2)$, the process $Y(k) = X(k - N)$, where N is a constant integer, has power spectrum $P_Y(\omega) = P_X(\omega)$ and bispectrum $B_Y(\omega_1, \omega_2) = B_X(\omega_1, \omega_2)$, i.e., the second- and third-order moments suppress *linear* phase information. However, the power spectrum suppresses *all* phase information, while the bispectrum does not.

(iii) **Non-Gaussian White Noise:** If $\{W(k)\}$ is a stationary non-Gaussian process with $E[W(k)] = 0$, $E[W(k)W(k + \tau)] = Q\delta(\tau)$, and $E[W(k)W(k + \tau)W(k + \rho)] = \beta\delta(\tau, \rho)$, then its power spectrum and bispectrum are both flat, i.e., $P(\omega) = Q$ and $B(\omega_1, \omega_2) = \beta$.

(iv) **Quadratic Phase Coupling:** There are situations in practice where because of interaction between two harmonic components of a process there is contribution to the power at their sum and/or difference frequencies. Such a phenomenon, which could be due to quadratic nonlinearities, gives rise to certain phase relations called quadratic phase coupling. In certain applications it is necessary to find out, if peaks at harmonically related positions, in the power spectrum are, in fact, coupled. Since the power spectrum suppresses all phase relations it cannot provide the answer while bispectrum, is capable of detecting and quantifying phase coupling.

5.5 Bispectral Estimators

Bispectral estimation techniques can be broadly classified into Conventional and Parametric Methods.

In the conventional method, direct type algorithms estimate the bispectrum directly from the data, while the indirect methods compute the

bispectrum from an estimate of the autocorrelation. Parametric estimators use a model for the process under investigation and obtain an estimate of the bispectrum by first computing the parameters of the model, while conventional estimators make no assumptions about the model of the process. Parametric techniques can provide better estimates of the bispectrum than conventional techniques in situations, where an assumption about the underlying model is valid.

5.5.1 Conventional Bispectral Estimators

The conventional bispectrum estimation can further be classified as Direct method and Indirect method.

5.5.1.1 Direct Method

Consider a series comprising of N samples, $\{x(1), x(2), \dots, x(N)\}$. The series is divided into K segments/records ($i = 1, 2, 3, \dots, K$) each of length M ($K \geq M$), so that $N = KM$.

Let the i^{th} segment be denoted as $x^{(i)}(k)$, $k=0, 1, \dots, M-1$ and $i = 1, 2, \dots, K$. The mean μ_i of the i^{th} segment is calculated and is subtracted from each sample of that segment.

$x^{(i)}(k) = x^{(i)}(k) - \mu_i$. The Discrete Fourier Transform of each segment $x^{(i)}(k)$ is calculated as :

$$X^{(i)}(f) = \frac{1}{M} \sum_{k=0}^{M-1} x^{(i)}(k) \exp(-j2\pi kf / M) \quad f = 0, 1, \dots, M/2 \quad (5.13)$$

$$i = 1, 2, \dots, K$$

Now, the bispectrum of the i^{th} segment is given by,

$$B^{(i)}(f_1, f_2) = X^{(i)}(f_1) X^{(i)}(f_2) X^{(i)*}(f_1 + f_2) \quad (5.14)$$

Finally, the $B^{(i)}(f_1, f_2)$ of all segments are averaged to get the bispectrum.

$$B(f_1, f_2) = \frac{1}{K} \sum_{i=1}^K B^{(i)}(f_1 + f_2) \quad (5.15)$$

5.5.1.2 Indirect Method

As already mentioned, using the indirect method, the bispectrum is computed from an estimate of the autocorrelation sequence. The following steps can be adopted for estimating the bispectrum for a data set, $\{x(1), x(2), \dots, x(N)\}$. Now,

- 1) Segment the data into K records of M samples each *i.e.*, $N = KM$.
- 2) The mean μ_i of the i^{th} segment is calculated and is subtracted from each sample of that segment.
- 3) Assuming that $\{x^{(i)}(k), k = 0, 1, \dots, M-1\}$ is the data per segment, obtain an estimate of the third-moment sequence

$$r^{(i)}(m, n) = \frac{1}{M \sum_{l=s_1}^{s_2} x^{(i)}(l)x^{(i)}(l+m)x^{(i)}(l+n)}$$

where, $i = 1, 2, \dots, K$

$$s_1 = \max(0, -m, -n)$$

$$s_2 = \min(M-1, M-1-m, M-1-n)$$

- 4) Average $r^{(i)}(m, n)$ over all segments

$$\hat{R}(m, n) = \frac{1}{K} \sum_{i=1}^K r^{(i)}(m, n).$$

- 5) Generate the bispectrum estimate

$$B'_{IN}(\omega_1, \omega_2) = \sum_{m=-L}^L \sum_{n=-L}^L \hat{R}(m, n) W(m, n) \cdot \exp\{-j(\omega_1 m + \omega_2 n)\}$$

where $L < M-1$ and $W(m, n)$ is a two-dimensional window function. The computational requirements of the *bispectrum* estimate may be substantially reduced if symmetry properties of third moments are taken into account for the computation of $r^{(i)}(m, n)$. In the case of conventional bispectrum estimation, to get better estimates, suitable windows should be used.

5.6 Quadratic Phase Coupling (QPC)

Different types of nonlinearities result in different types of phase couplings. If a signal composed of two sinusoids is passed through a squarer, then the output will contain components at the sum and difference frequencies of the two sinusoids. Quadratic phase coupling is the term used to describe the coupling which results from this type of nonlinearity.

5.6.1 Theoretical Background

If $x(n)$, the sum of two sinusoids $x_1(n) = \cos(2\pi f_1 n + \phi_1)$ and $x_2(n) = \cos(2\pi f_2 n + \phi_2)$ are passed through a nonlinear system as shown in Fig. 5.5, then the output signal $y(n)$ is $x_1(n) + x_2(n) + [x_1(n) + x_2(n)]^2$.

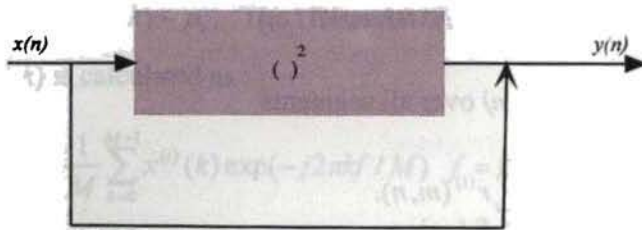


Fig. 5.5 Model of a Nonlinear System

$$y(n) = \cos(2\pi f_1 n + \phi_1) + \cos(2\pi f_2 n + \phi_2) + \cos^2(2\pi f_1 n + \phi_1) + \cos^2(2\pi f_2 n + \phi_2) + 2 \cos(2\pi f_1 n + \phi_1) \cos(2\pi f_2 n + \phi_2)$$

$$\begin{aligned}
y(n) = & \cos(2\pi f_1 n + \phi_1) + \cos(2\pi f_2 n + \phi_2) + 1 + \frac{1}{2} \cos(4\pi f_1 n + 2\phi_1) + \\
& \frac{1}{2} \cos(4\pi f_2 n + 2\phi_2) + \cos[2\pi(f_1 + f_2)n + (\phi_1 + \phi_2)] + \\
& \cos(2\pi(f_1 - f_2)n + (\phi_1 - \phi_2))
\end{aligned}$$

As evident from the above equation, the output signal $y(n)$ contains the components at $2f_1$, $2f_2$, $(f_1 + f_2)$ and $(f_1 - f_2)$ along with f_1 and f_2 . $y(n)$ also exhibits certain phase relations and such nonlinear interactions would give rise to a quadratic phase coupling at the bifrequencies (f_1, f_2) .

Bispectrum plots will show peaks at bifrequencies wherever there are frequency couplings, even if there is no phase coupling. This issue may be resolved by considering the phase of the bispectrum at the required bifrequencies.

$$B(f_1, f_2) = X(f_1)X(f_2)X^*(f_1 + f_2)$$

Now,

$$\text{abs}[B(f_1, f_2)] = |X(f_1)X(f_2)X^*(f_1 + f_2)|$$

$$\angle B(f_1, f_2) = \phi_1 + \phi_2 - \phi_{12}$$

Thus,

$$\angle B(f_1, f_1) = \phi_1 + \phi_1 - 2\phi_1 = 0$$

$$\angle B(f_2, f_2) = \phi_2 + \phi_2 - 2\phi_2 = 0$$

$$\angle B(f_1, f_2) = \phi_1 + \phi_2 - (\phi_1 + \phi_2) = 0$$

$$\angle B(f_1, -f_2) = \phi_1 - \phi_2 - (\phi_1 - \phi_2) = 0$$

Hence, the phase of the bispectrum, for the bifrequency for which QPC exists should be zero. This feature is made use of in a two stage bispectrum estimator to detect the QPC. The advantage of the two stage QPC detector is that, it doesn't require the phase randomization concept,

which is otherwise necessary for the reliable estimation of the bispectrum. A flowchart of the two stage bispectrum QPC estimator is as shown in Fig.5.6.

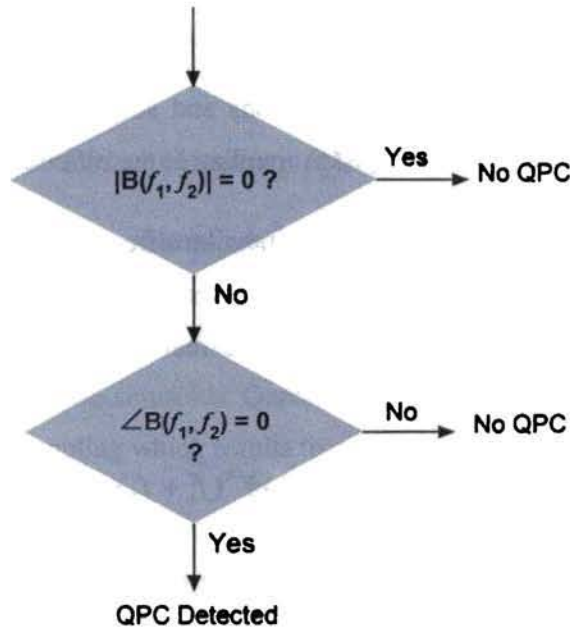


Fig. 5.6 Flowchart of the two stage bispectrum QPC estimator

As an illustration, consider a signal containing three sinusoidal waves at frequencies $f_1 = 5$, $f_2 = 10$ and $f_3 = 15$ and phases $\phi_1 = 0.5$, $\phi_2 = 0.8$ and $\phi_3 = 2.0$. Here, $f_3 = f_1 + f_2$. But $\phi_3 \neq \phi_1 + \phi_2$. Thus at the bifrequency (f_1, f_2) , there is frequency coupling, with no phase coupling. However, as shown in Fig. 5.7, the bispectrum contour plot has a peak at the bifrequency (f_1, f_2) , even though there is no phase coupling.

Fig. 5.8 show the phase contour plot of the above illustration. It may be noted that there is no peak at the phase plot corresponding to the bifrequency (f_1, f_2) , which leads to the conclusion that there is no QPC at

the bifrequency (f_1, f_2) , and indicates that QPC can be reliably detected using both magnitude and phase plots.

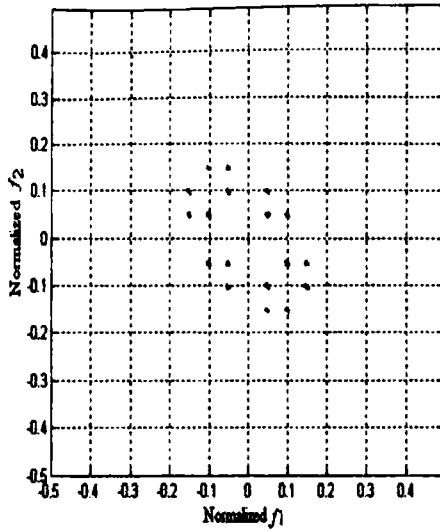


Fig. 5.7 Bispectrum contour plot without QPC

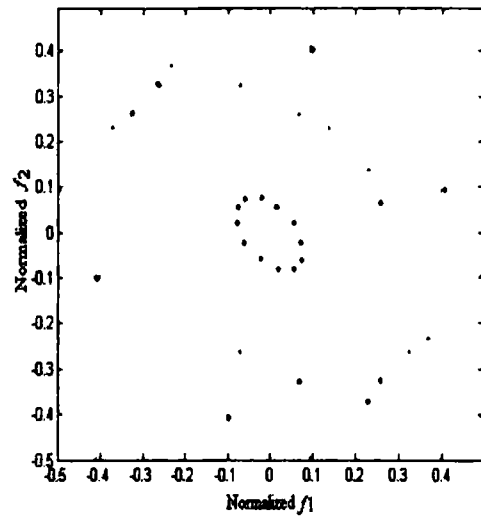


Fig. 5.8 Bispectrum contour Phase Plot without QPC

On the other hand, if $\phi_3 = 1.3$, then $\phi_3 = \phi_1 + \phi_2$ and $f_3 = f_1 + f_2$. In this case, there is both frequency and phase couplings and thus the presence of QPC is implied as indicated by the plots shown in Figs.5.9 and 5.10 where there is a peak at both the frequency as well as the phase plots of the bispectrum corresponding to the bifrequency (f_1, f_2) . The 3-Dimensional plot of the magnitude bispectrum is shown in Fig. 5.11.

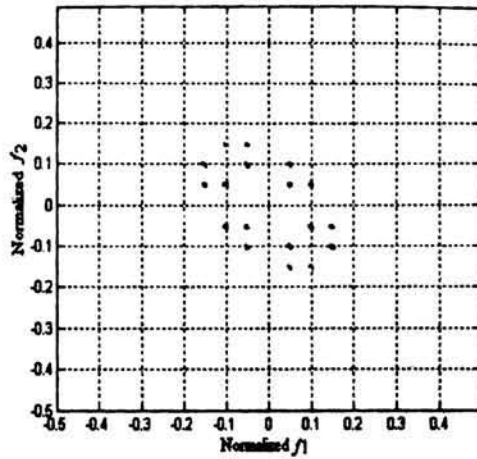


Fig. 5.9 Magnitude contour plot of Bispectrum (where QPC is present)

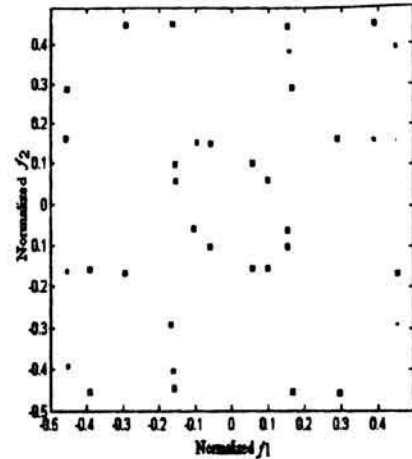


Fig. 5.10 Phase contour Plot of Bispectrum (where QPC is present)

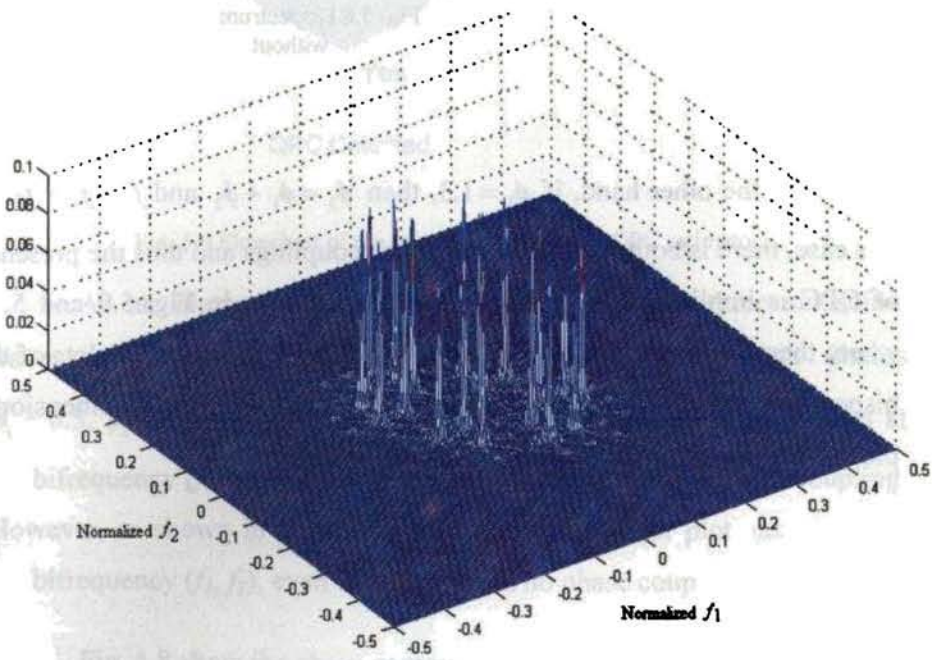


Fig. 5.11 3D plot of Bispectrum corresponding to the magnitude plot in Fig. 5. 9

5.7 Data Analysis and Results

The Bispectrally extractable features of the targets have been generated making use of the procedures formulated in the preceding sections. Since the bispectrum depends on the amplitude of the signal under consideration, the bicoherence measure has been used as a convenient test statistics for the detection of non-Gaussian, nonlinear and coupled processes. The bicoherence mesh and contour plots for the noise waveforms generated by 3 Blade are shown in Figs. 5.12 and 5.13.

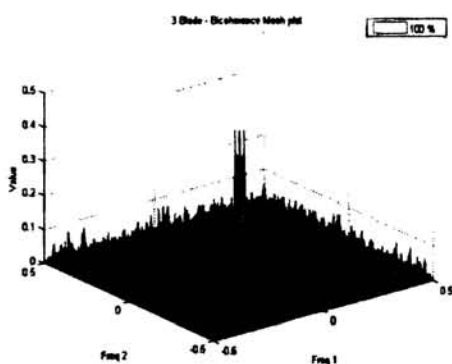


Fig. 5.12 Mesh Plot for 3 Blade without filtering

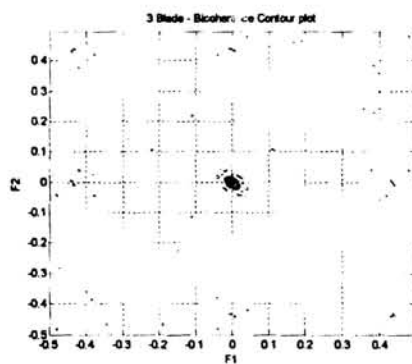


Fig. 5.13 Contour Plot of 3 Blade without filtering

In these plots, it has been noticed that there are certain undesirable spurious frequency components which needs to be filtered out for identifying the coupling frequencies. It has been further observed that by adopting certain threshold statistics, it is possible to extract these frequencies and the peaks at the bifrequencies to an acceptable level of reproducibility. In this work, bicoherence levels below 30% of the highest bicoherence level has been adopted for the purpose of filtering out the unwanted components leading to the extraction of certain target specific

bispectral features. With a threshold level of 30%, the bicoherence mesh and contour plots of 3 Blade noise source for the same data record are depicted in Fig.5.14 and 5.15. It was further noticed that when the filter threshold is varied the number of coupling frequencies also vary as summarized in Table 5.1.

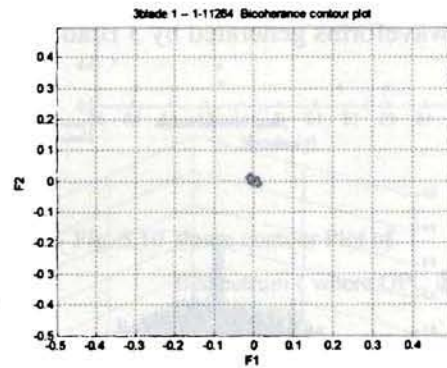
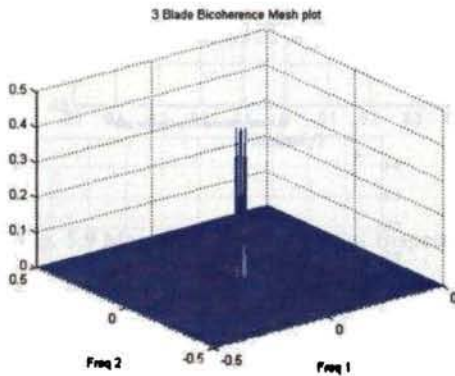


Fig. 5.14 Mesh Plot for 3 Blade with 30 % Filter Threshold Fig. 5.15 Contour Plot for 3 Blade with 30 % Filter Threshold

Table 5.1 Effect of Filter Threshold on the Number of Coupling Frequencies

Filter Threshold Level (FTL)	30 %	40%	50 %	60 %	70%
Num of Coupling Frequency	61	42	24	18	18

Figs. 5.16, 5.17, 5.18 and 5.19 depict the bicoherence mesh and contour plots for the noise emanations from a merchant vessel for the entire range of frequencies and in the filtered scenario with the filter threshold level of 30%.

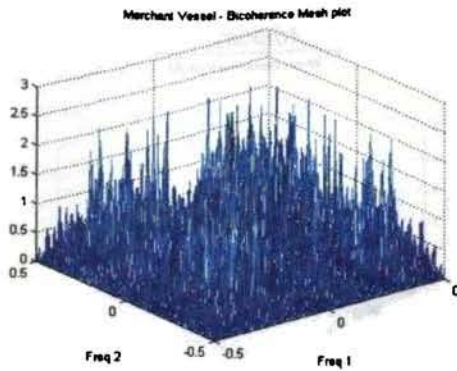


Fig. 5.16 Mesh Plot for Merchant Vessel without filtering

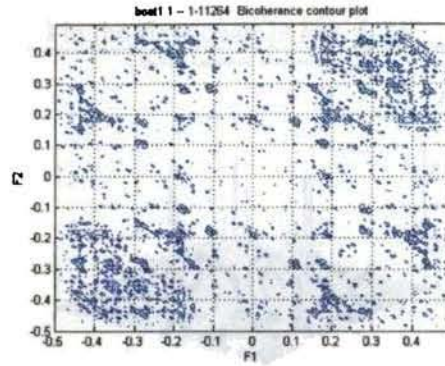


Fig. 5.17 Contour Plot for Merchant Vessel without filtering

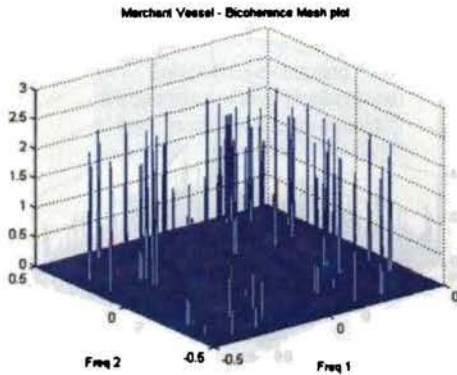


Fig. 5.18 Mesh Plot for Merchant Vessel with 30 % FTL

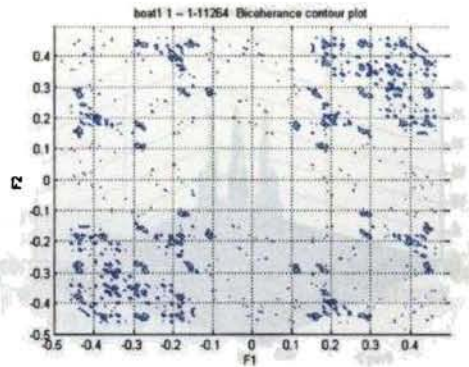


Fig. 5.19 Contour Plot for Merchant Vessel with 30 % FTL

The bicoherence mesh plots without filtering for the a commercial vessel as well as that of marine species like whale, hump back whale and damsel are also illustrated in Figs 5.20, 5.21,5.22 and 5.23 respectively.

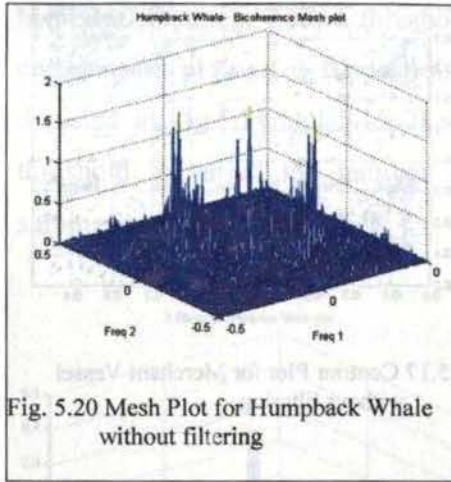


Fig. 5.20 Mesh Plot for Humpback Whale without filtering

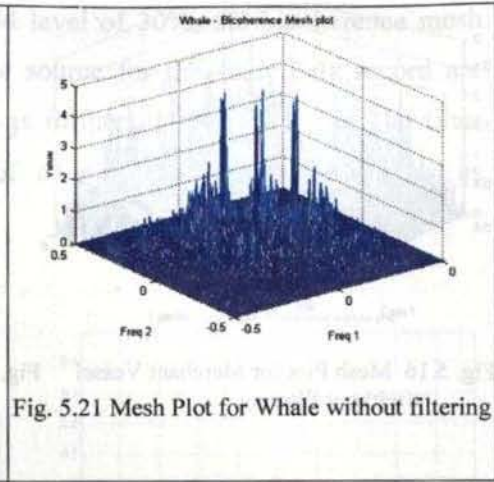


Fig. 5.21 Mesh Plot for Whale without filtering

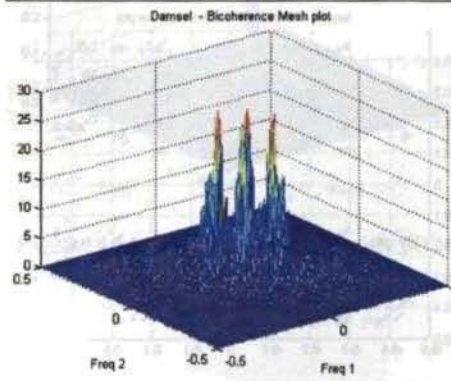


Fig. 5.22 Mesh Plot for Damsel without filtering

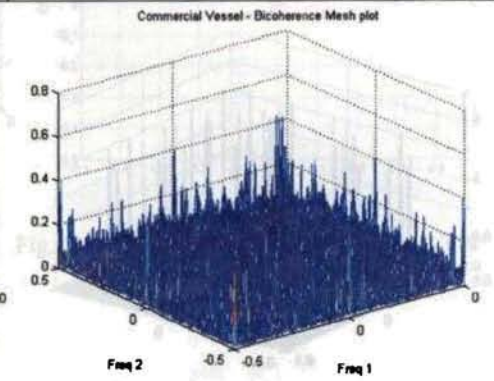


Fig. 5.23 Mesh Plot for Commercial Vessel without filtering

5.8 Bispectral Features

As with power spectrum estimators, there are two main approaches for estimating the bispectrum, *viz.* conventional and parametric approaches. The conventional method is based on the direct application of Fourier transforms and may be further classified into direct and indirect methods. The direct class of bispectral estimators has been implemented, due to its simplicity as well as the ease in the implementation.

The procedures that are to be followed for generating the bispectrally extractable features depicted in the flow chart in Fig. 5.24.

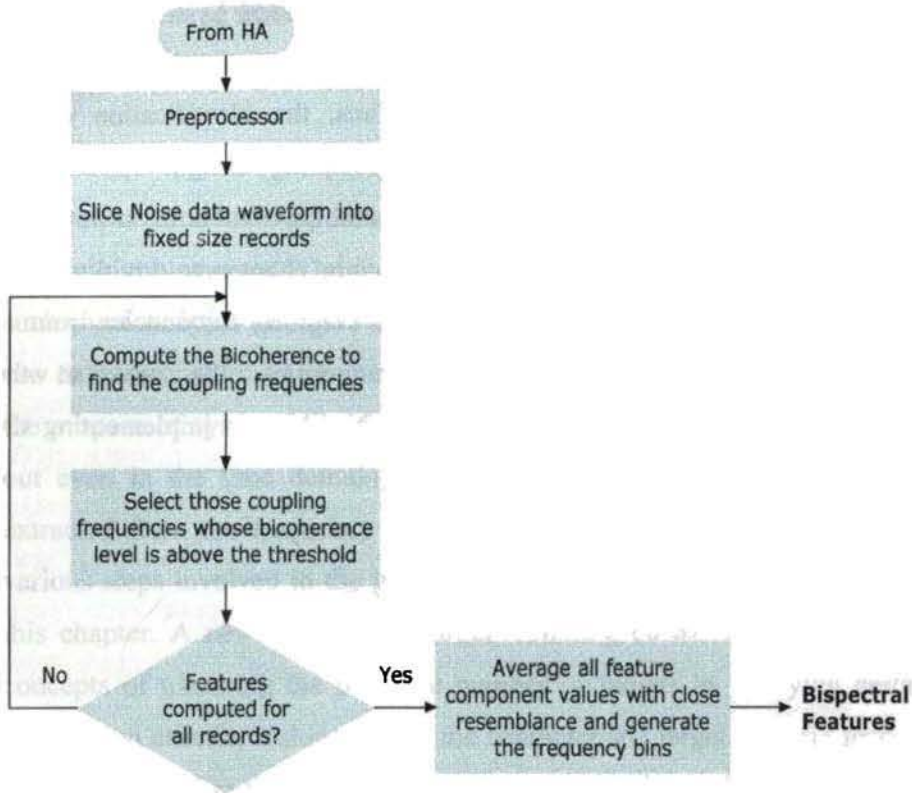


Fig. 5.24 Depicts the procedure for generating the bispectral features

5.9 Summary

The bispectrum which is based on the third order statistics can characterize non-Gaussian as well as nonlinear signals. Since, many signals encountered in practice are non-Gaussian and many measurement noises are Gaussian in nature, the bispectrum are less affected by Gaussian background noise than the second order measures, as the bispectrum of Gaussian signals are zero. Moreover, different types of nonlinearities results in different types of phase couplings.

QPC has been identified as an invaluable tool in non-linear system identification. It is based on the fact that a nonlinear system excited by independent sinusoidal sources produces a harmonic signal that has quadratically coupled frequency pairs. Thus, the identification of the coupled frequencies and the corresponding coupling strength enables us to identify some of the features of the system and the number of independent sources. An attempt has been made in this chapter to highlight the bispectral features such as the number of coupling frequencies, mutual coupling frequencies, self coupling frequencies, the peak at the bifrequencies etc. which can be effectively utilized in implementing the target classifier.

CHAPTER 6

THE TARGET CLASSIFIER

A prototype system for identifying the noise sources in the ocean using the spectral, cepstral and bispectral features extracted from the noise emissions has been implemented. The process of feature extraction involves obtaining such characteristics through various signal processing techniques, so that the raw data is transformed into new data sets that can be used by a classifier for the purpose of system identification. Though signal analysis can be carried out even in the time domain, most of the target specific signatures are extracted from the frequency domain representation and its variants. The various steps involved in the generation of feature vectors are described in this chapter. A new hierarchical target trimming classifier centred on the concepts of trimming the probable number of targets by applying certain elimination criteria, making use of the characteristic target specific features is also proposed in this chapter. The performance of this classifier has been compared with that of the Euclidean distance as well as the more sophisticated Fuzzy K-Nearest Neighbour model classifiers. In the proposed target classification system, the feature vector based hierarchical target trimming classifier works in conjunction with the Hidden Markov Model (HMM) based classifier. In situations where the decisions of the Feature Vector based classifier differs from the HMM based classifier, the DUET algorithm can be resorted to for resolving the contentions. The various steps involved in implementing the HMM based classifier and the DUET algorithm are also described in this chapter.

6.1 Introduction

The problem of identification of noise sources in the ocean is of prime importance because of its diverse practical applications. The noise waveforms emanating from the sources will certainly disclose the general characteristics of the noise generating mechanisms. The composite ambient noise containing the noise waveforms from the targets, received by the hydrophone array systems are processed for extracting the target specific features. Though quite a large number of techniques have been evolved for the extraction of source specific features, none of them are capable of providing the entire set of classification clues. Of these, many of the techniques are complex and some of them often yield complementary results, leading to ambiguities in the decision making process. Since classification of certain noise sources with acceptable confidence levels, using traditional spectral estimation techniques yield low success rates, many techniques centred on the concept of parametric modelling have been reported in open literature. These modern parametric approaches for the extraction of spectral profiles give more emphasis to spectral resolutions and enhanced signal detection capabilities than conventional techniques.

In order to interpret most effectively and efficiently the vast amount of data furnished by the signal processor, especially in situations where the detectable range of the system is very large, it is essential to have a fully automated and intelligent classifier, as most of the target information, in all probability, may not be of much interest to the user. Operator controlled classifier turns out to be inappropriate and highly inefficient in such situations. Automatic detection and classification algorithm attempts to alleviate this operability problem by taking over the operator's role of

picking out targets from a background of noise and interferences. The generalized structure of the proposed classifier is shown in Fig. 6.1.

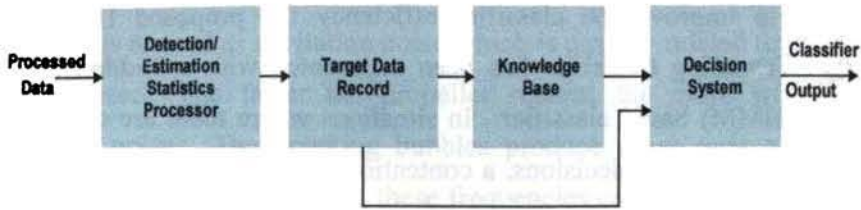


Fig. 6.1 Block Schematic of the Classifier

The detection and estimation statistics processor simply performs the estimation of the signal energy within a finite time interval. The output of the estimation processor is compared with the earlier estimations, which are stored in the Target Feature Record (TFR) and the relevant target features are updated. In case if a target feature is not updated over a significant period, the concerned data will be dropped from the target feature record. In many situations, the system may have to backtrack/retrack through the stored TFRs to establish the links with the most recent data. As and when the required classification clues are available in the target feature record, the most matching signature pattern is identified from the known target signatures in the knowledge base, depending on the allowable percentage of mismatch, chosen by the user.

A prototype system for identifying the sources using the spectral, cepstral and bispectral features extracted from the noise emissions has been implemented. The various steps involved in the generation of feature vectors are described in this chapter. A new hierarchical target trimming classifier centred on the concepts of trimming the probable number of targets by applying certain elimination criterion, making use of the characteristic target specific features is also proposed. The performance of

this classifier has been compared with that of the Euclidean distance as well as the more sophisticated Fuzzy K-Nearest Neighbour models. In an attempt to improve the classifier efficiency the proposed Hierarchical Target Trimming Classifier has been augmented with a Hidden Markov Model (HMM) based classifier. In situations where there are chances for conflicting classifier decisions, a contention resolving mechanism has also been proposed by effectively utilizing the concepts of blind source separation with the help of the Degenerate Unmixing Estimation Technique (DUET).

6.2 Knowledge Base

For the realisation of the proposed classifier, it is essential to have a powerful knowledge base comprising of the relevant parameters of different class and types of targets. The raw data collected has to be processed for gathering the relevant parameters for creating the knowledge base.

6.2.1 Noise Data

The noise data used for creating the knowledge base mainly comprises of the man made noises and noise that are of biological in nature. Some of the data sets used in developing the knowledge base were collected during scheduled cruises off Cochin and Mangalore.

6.2.1.1 Man Made Noises

Surfaced and submerged vessels create noise from their propellers, motors and gears. The noise generated by the motor is continuous and caused by the mini-explosions that occur, as the fuel burns rapidly inside the engine cylinders and by the rotating gears and shafts. Sound is also generated due to the formation of bubbles during the rotation of propellers

and, to a lesser extent, by the wake of waves produced due to the movement of the vessels. As the vessel moves and the propellers rotate, bubbles are formed in the water and the formation of these bubbles is known as cavitation. The breaking of these bubbles create a loud acoustic noise and is termed as cavitation noise which is directly related to the speed of the vessel. The faster the propeller rotates, the more will be the cavitation noise. The breaking bubbles produce noise over a range of frequencies, and at high speeds, these frequencies can be as high as 20,000 Hz. On the other extreme, a large ship with slowly turning propellers can generate very low frequencies to the extent of 10 Hz or even less. The rotation of the propellers creates bands of noise at more or less constant frequencies that are proportional to the rate of rotation of the propeller. The noise created by these rotations, called *blade-rate lines*, can help to distinguish between different sizes of ships and even a particular ship in certain cases. Low frequency noise generated by ships contributes significantly to the amount of low-frequency ambient noise in the ocean, particularly in regions with heavy ship traffic. In fact, because of the increase in propeller-driven vessels, low-frequency ambient noise has increased 10-15 dB during the past 50 years.

Some of the representative typical target signatures are depicted in Figs 6.2 through 6.5. The main engine noise spectrum of a typical surfaced submarine at moderate speed is shown in Fig. 6.2.

The long-term averaged noise spectral response of a typical submarine propeller is shown in Fig.6.3. As the depth is increased, the bump in the noise spectrum, which is a feature of the cavitation gets shifted towards the high frequency of the spectrum.

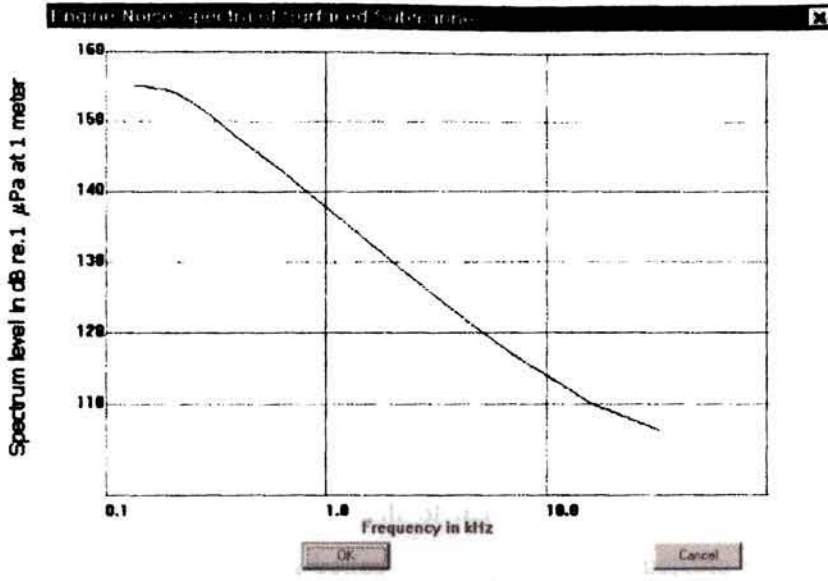


Fig. 6.2 Noise spectrum of a typical Surfaced Submarine

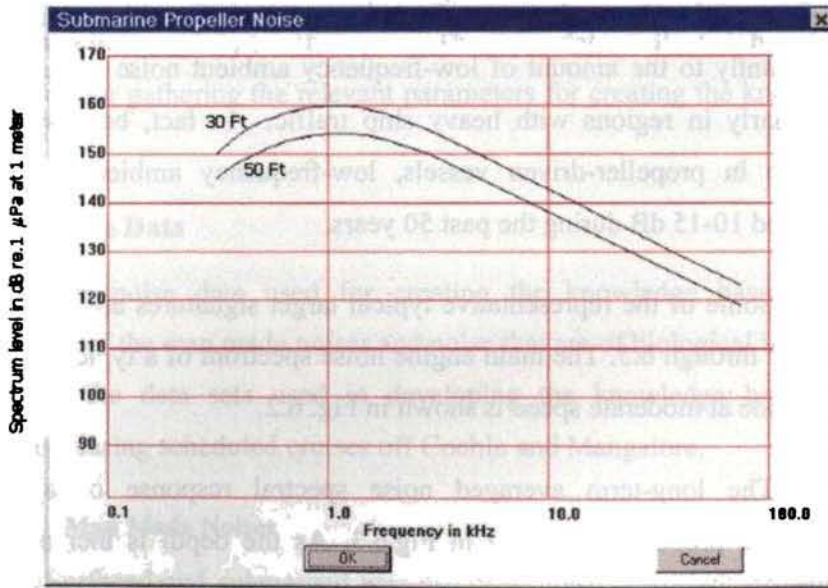


Fig. 6.3 Noise Spectrum of a Submarine Propeller at 30ft and 50ft

Fig. 6.4 depicts the variation of noise spectrum for an average submarine and destroyer at 20 kHz with speed, while Fig.6.5 depicts a comparison of the noise spectra of a torpedo and a submarine.

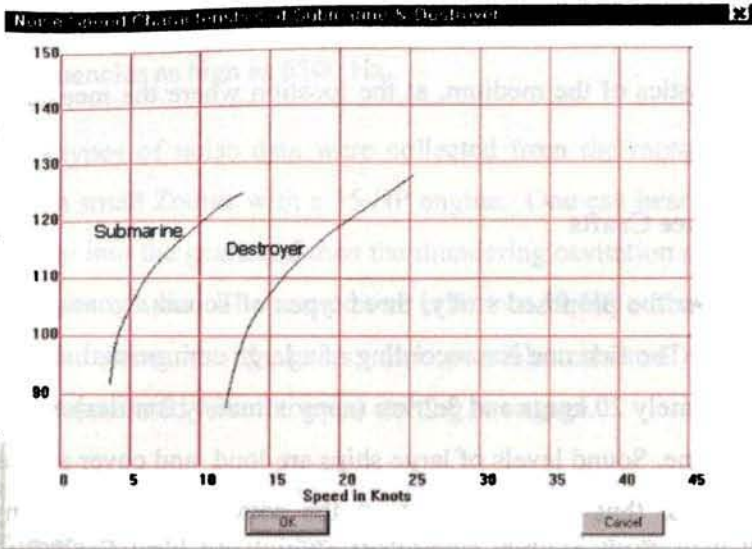


Fig. 6.4 Noise Spectrum of an average submarine & destroyer at 20 kHz

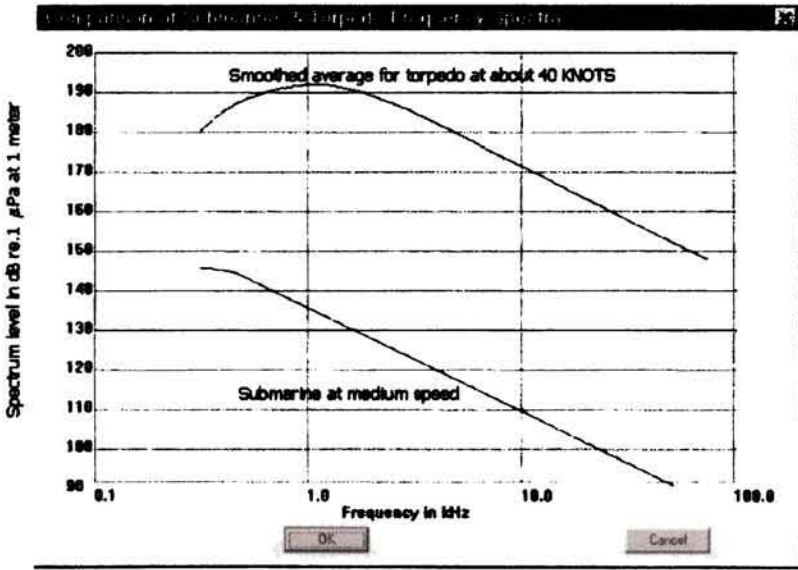


Fig. 6.5 Comparison of the Noise Spectra of torpedo and submarine

Results of observations, which deviate from the variations shown above, have also been reported. Such differences can be attributed as due to the variations in the vessel features in a particular class and propagation

characteristics of the medium, at the location where the measurements are taken.

(a) Surface Crafts

For the proposed study, three types of sound signatures have been collected. The first one is a recording of a large commercial ship cruising at approximately 20 knots and 3.2 km (approximately 2 miles) away from the hydrophone. Sound levels of large ships are loud and cover a broadband of frequencies, thus masking most of the sounds made by many marine mammals, as well as other life in the oceans, such as various fishes. Second was of a Merchant vessel in the Cochin Shipyard and the noise data were recorded, as the vessel was approaching from 1.7 km (approximately 1 mile) away. The third noise data was of a tug boat, which has a smaller high speed propeller than larger ships.

Tugs with barges typically produce less near surface sound than other ships. This is not because they are quieter, but rather the propellers of a typical tugboat are recessed to reduce propeller cavitation and to protect the propeller from damage in case of grounding. With the propeller in this position, the sound rays from the propellers are blocked by the ship's hull. Thus, propeller noise cannot be heard ahead of the tugs and barges. This effect is called *acoustic shadowing*.

(b) Outboard Motor

Outboard motors are found on small boats, such as a zodiac, that are popular in coastal waters. The propeller of an outboard motor is what creates sound. On smaller boats, like a zodiac, the small propeller produces a cavitation noise which is at higher frequencies than larger vessels. The smaller propellers also produce higher rotation rates which also causes the

propeller to make high frequency noises. A zodiac, for example, can produce frequencies as high as 6300 Hz.

Two types of noise data were collected from the motor boat, the first is from a small Zodiac with a 35 HP engine. One can hear the engine starting, going into the gears and then the thundering cavitation noise as the propeller begins to spin. The second one is from a 50 HP outboard engine starting up and going into the gears. It is possible to hear a *ratchet* like sound that is associated with the gears starting to engage.

(c) Torpedo

Torpedoes used for military operations produce more than just an explosive sound upon detonation. After an initial firing, the sound of the outer hatch can be heard closing. The torpedo can then be heard moving through the water to the target. The length of this sound is dependant upon the distance of the target. Finally, a large explosion is heard. Torpedoes are also associated with a pinging noise used by the sonar for torpedoes before firing. The recording of this sound is of a live torpedo shot downloaded from the website. The signatures include the sounds of the launch, the closing of the torpedo hatch and the explosion of the torpedo.

6.2.1.2 Biological Noise Data

A variety of biological noise data has been used for the purpose of creating the knowledge base. Some typical biological data, which have been used in developing the knowledge base were the noises generated by the following species.

(a) Beluga Whale

The beluga, a medium sized toothed whale, which is white in colour has an adaptation to its environment and it lives primarily in the Arctic. Its

name is derived from the Russian word for white. Thick blubber makes it possible for the Beluga to live in extremely cold water, and a back with no dorsal fin allows it to move freely under ice. The beluga's body is thick, muscular and tapered at both the ends, with a small head and a narrow caudal peduncle (tail stock). Its head is round and has a short beak and a prominent, protruding forehead called the *melon*.



Fig. 6.6 Beluga Whale

Beluga Whale are amongst the loudest animals in the sea. They exhibit a wide range of vocalizations including clicks, squeaks, whistles, squarks and a bell-like clang. The sounds recorded are mostly in the range of 0.1 to 12 kHz.

(b) Humpback Whale:

The humpback whale is one of rorquals which have two characteristics in common, viz. dorsal fins on their back, and ventral pleats running from the tip of the lower jaw back to the belly area.

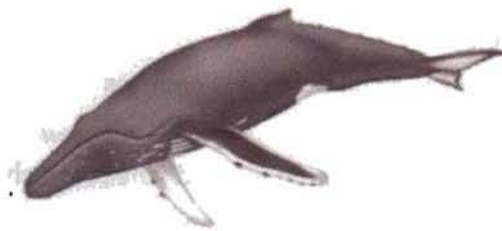


Fig. 6.7 Humpback Whale

The body is black on the dorsal side and mottled black and white on the ventral side. Humpbacks are best known for their vocalizations that are arranged in complex, repeating sequences with the characteristics of *song* and contain both tonal and pulsed sounds.

(c) Harbour Seal :

The harbour seal resides in North Pacific, North Atlantic, and Arctic waters. These seals have no external ears like those found on otariid seals (eared seals). Instead, only a small ear opening behind the eyes is visible.



Fig. 6.8 Harbour Seal

The furred hind flippers of true seals are shorter than those of the fur seals and sea lions, and extend behind their body to provide propulsion during swimming. The short, furry front flippers act mainly as rudders when the seals are swimming and help in their movement on land or ice. Some of the different types of seal calls are: trill, chirp, multiple whistle, single whistle, growl, whoop, chug, and grunt.

(d) Sea robin

Sea robins are the only local fish that "walk". They use their unique, detached, finger-like fin rays to feel their way across the bottom. The body of the sea robin is elongated, nearly round, and tapers to the tail. They also use these fins to burrow into the sediments, so that their eyes and the tops

of their heads are exposed, a tactics for avoiding predators, to ambush prey, or to wait out the tidal currents.



Fig. 6.9 Sea Robin

The fins are also used to agitate the bottom and help sense food in the area. They are very noisy fishes and make sounds like grunting, growling and grumbling.

6.2.2 Data Analysis

For creating the knowledge base, the noise data waveforms of various targets are analysed following the procedures for extracting the spectral, cepstral and bispectral features described in chapters 4 and 5. The performance of the classifier depends on how extend and vast the knowledge base is. In the prototype system all the available noise data waveforms were analysed and a representative knowledge base has been developed. The knowledge base for the prototype classifier comprise of the spectral, cepstral and bispectral features of different classes like ships, boats, marine mammals, environmental conditions, etc.

6.2.3 Updating of Knowledge Base

The knowledge base that has been developed for realizing the prototype target classifier is only representative and not complete in all respects. For making the system efficient, the knowledge base has to be

updated with the signature patterns and the target dynamics for all the classes and types of targets.

6.3 Generation of Feature Vector

The pre-processed noise data waveforms are analyzed in different ways in the Estimation Statistics Processor. The different techniques like cepstral analysis, spectral analysis and bispectral estimation techniques used for extracting the various signatures of the targets are illustrated in Fig.6.10.

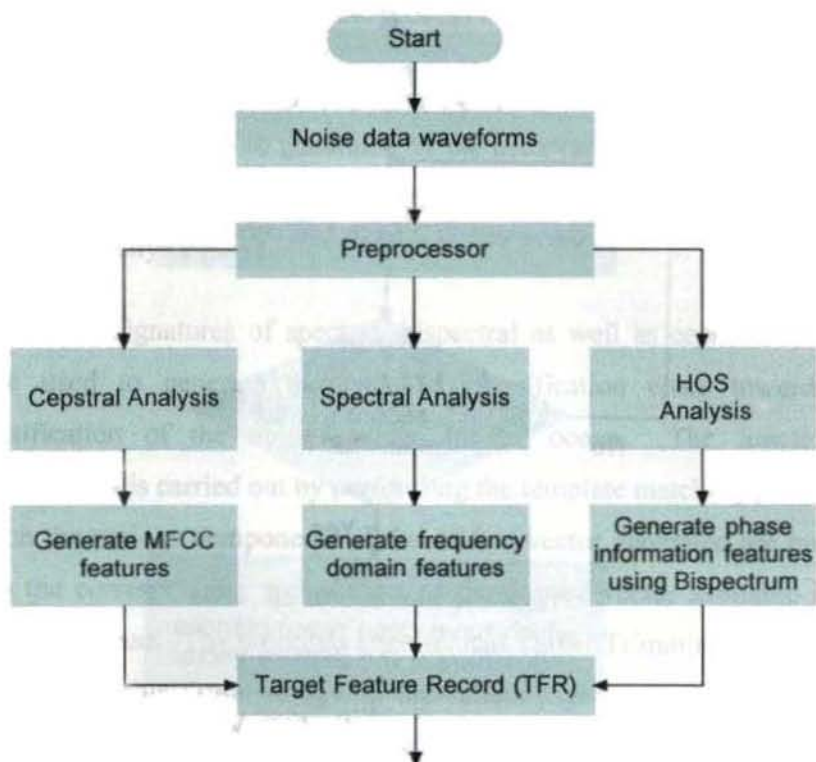


Fig. 6.10 Various techniques for extracting the target features

The various features generated from this analysis are stored in a target feature record (TFR), which is used for the purpose of mapping the target signatures with the signatures available in the knowledge base.

6.4 Generation of Target Feature Record

The generation of the target feature record (TFR), as depicted in Fig. 6.11., plays an important role in the efficiency and success rate of the

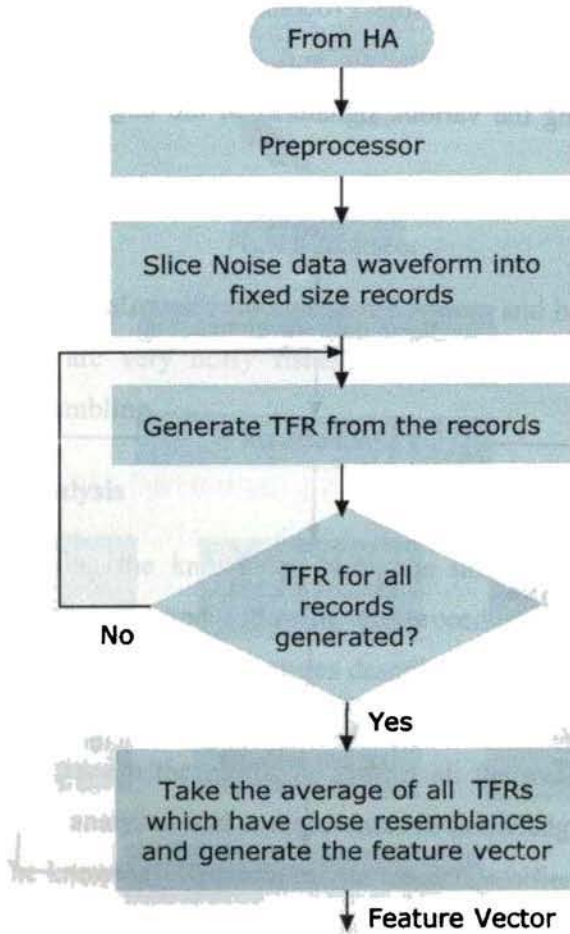


Fig. 6.11 Flowchart for generation of TFR

classifier. As such, when the noise data waveforms are made available to the classifier, it generates the target feature record by performing spectral estimation, cepstral analysis and bispectral estimation. The target feature records for various data records are generated. In case, if a TFR is not

updated over a considerable period of time, the concerned feature record will be dropped and the system takes the average of all the TFRs which have close resemblances and thus generates the TFR.

6.5 *Prototype Target Classifier*

The classification function operates in a multidimensional space formed by the various components of the feature vector. For the purpose of target classification, one has to identify the characteristic features from the representation of an object. Upon generating the various features, those features that can indeed aid in the process of classification are selected.

Though, such a selection will generally lead to loss of information, this will reduce the noise generated by the irrelevant features as well as the risk of over fitting the training data, thus making the classifier computationally efficient.

The signatures of spectral, bispectral as well as cepstral in origin were used to generate the required classification clues towards the identification of the noise sources in the ocean. The function of classification is carried out by performing the template matching process, in which the various components of the feature vector generated are mapped with the corresponding components of the feature vector available in the knowledge base. The proposed Hierarchical Target Trimming Approach is described in this thesis alongwith the salient highlights of the Euclidean distance Model, adopted in arriving at the nearest match to a feature vector with approximate weights assigned to the various feature components and the Fuzzy K-Nearest Neighbour model based on the concept of Fuzzy logic. An effort is also made in the thesis to augment the decision of the classifier with a Hidden Markov Model based classifier. In situations where the decisions of both the classifiers differ, a contention resolving

mechanism built around the DUET algorithm for blind source separation (BSS) has been suggested.

6.5.1 Feature Vector based Identifier

6.5.1.1 Euclidean Distance Model

Euclidean distance model is one of the simple yet efficient classifier algorithms and a properly weighted model, making use of the feature vector, could be used to find out the nearest match [139]. The weights for the various components of the feature vector have been selected based on heuristics, the knowledge gained from the training examples as well as trial and error procedures. For the purpose of feature vector based classification, the Euclidean distance between the feature vectors of the unknown target and that of the various targets in the knowledge base is computed. The vector components are normalized by standard deviation or the range of the features, across the whole knowledge base. Further to normalization, each feature is weighted in proportion to its significance in the similarity estimation.

The Euclidean distance D_E is computed as

$$D_E = \sqrt{\sum_{i=1}^l \left(\frac{(x_i - y_i) \times w_i}{v_i} \right)^2} \quad (6.1)$$

where x_i and y_i refers to the i^{th} feature component of the unknown target and that of the various targets in the knowledge base respectively, w_i is the weight assigned to the i^{th} feature component such that, $\sum_{i=1}^l w_i = 1$, v_i represents the normalization vector and l is the total number of features.

6.5.1.2 Fuzzy K-Nearest Neighbour Model

K-Nearest Neighbour is a basic technique of supervised classification and *Fuzzy* K-NN is K-NN with the inclusion of fuzzy concepts. *Fuzzy* K-NN has the advantages of having a wider range of K and is easily tunable.

In K-NN, the matching parameters between the unknown feature vector \hat{x} and all the feature vector components of target signatures are computed and for all the components, k nearest neighbours are identified. From these k nearest neighbours most frequently occurring value is considered to be the probable one. One of the problems encountered in using the K-NN classifier is that normally each of the sample vectors is considered equally important in the assignment of the class label to the input vector. Another difficulty is that once an input vector is assigned to a class, there is no indication of its *strength* of membership in that class. Incorporation of fuzzy set theory into the K-NN rule will resolve these two issues in the K-NN algorithm.

By introducing fuzzy sets, the degree of membership in a set can be specified, which will provide information as regards to the strength with which the object belongs to each class, rather than just the binary decision. The *Fuzzy* K-NN algorithm assigns membership as a function of the distance of the vector from the k -nearest neighbours as well as memberships of the neighbours in the possible classes. The class memberships have been computed using the procedures set out by Keller *et al.*[138]

6.5.1.3 Hierarchical Target Trimming Approach

The proposed algorithm for classification of targets is centred on the concept of template matching within the allowable ambiguity parameter.

Here, the feature vector of the target to be identified is assumed to be composed of many feature components that are extractable using spectral, cepstral and bispectral techniques.

Let the Universal set of targets with known features be $U = \{T, T_2, \dots, T_M\}$. Any member target in this ensemble can be described as T_m where m varies from 1 to M .

Let the feature vector of a member target T_m be F_m with the feature components $\{F_{mS}, F_{mC}, F_{mB}\}$, where F_{mS} refers to the set of spectral features comprising of the components $\{F_{ms1}, \dots, F_{ms6}\}$ where F_{m6} can be mapped to a $q \times r$ array $S_M(q, r)$ of frequency related signatures, F_{mC} refers to the set of cepstral features and F_{mB} refers to the bispectral feature, the number of coupling frequencies, which can be mapped to an array $m \times n$ $B_M(m, n)$ of bifrequency related signatures.

The order in which the various feature components are processed for target trimming leading to the final classification has been so chosen that a subset of as many probable targets as possible is formed during the first level of screening, while the subsequent levels lead to the elimination of targets from this set based on the characteristics of each of the feature components under consideration.

6.5.1.3.1 Algorithm for classification

- a) For the unknown target, the feature vector F_u and the arrays S_u and B_u are estimated first.
- b) F_{uS} , the first component of F_u , is mapped with F_{mS} , allowing a reasonable mismatch parameter Δ_1 . Thus the set S_1 of M_1 probable member targets conforming to $F_{m1} \pm \Delta_1$ is formed.

- c) F_{uC} , the second component of F_u , is then mapped with F_{mC} of all the M_1 targets in the set S_1 , allowing a reasonable mismatch parameter Δ_2 , thus forming a set S_2 of M_2 members. The process is repeated till the mapping of the entire feature components are completed, resulting in a minimum members M_i of probable targets in the set S_i .
- d) From these trimmed target set, target identification is performed by elimination process, making use of the characteristic signature array S_M and B_M of the M_i targets in the set S_i .
- e) For further resolving the ambiguities, if any, in the target identification process, Euclidean minimum distance criteria can be resorted to.

For extracting the spectral features, the power spectral density has been computed using the AR parametric model. The algorithms for extracting the source specific signatures such as, spectral centroid, spectral range, spectral roll off, spectral slope, spectral flux, number of peaks, peaking frequencies, rising slope, falling slope, Mel frequency cepstral coefficients, number of coupling frequencies, mutual coupling frequencies, self coupling frequencies and the peak at the bifrequencies have been developed. These features have been judiciously exploited for the target identification making use of the three classifier algorithms described above, with acceptable reproducibility and repeatability. For validating the performance of the algorithm and methodology proposed here, the noise data waveforms of the entire data set were mixed with the ocean wave noise and fed to all the three classifiers under consideration. During the validation process it has been observed that one of the spectral features, viz., spectral flux, is a redundant feature as far as the target identification process is concerned and as such it can be discarded. The validation results as well as the comparison of the three classifiers are discussed in section 6.7.

6.5.2 Hidden Markov Model Based Classifier

Hidden Markov Models provide an effective architecture for target detection and classification of distinct targets in multiple target scenarios. It is possible to design HMMs to identify target classes where members of a given class may share common physical attributes. Such a strategy may be incorporated into a hierarchical identification framework where a target is first assigned to a class and later with sufficient additional information, it may be identified as a particular target within that class. The class based model approach is summarized in Fig 6.12.

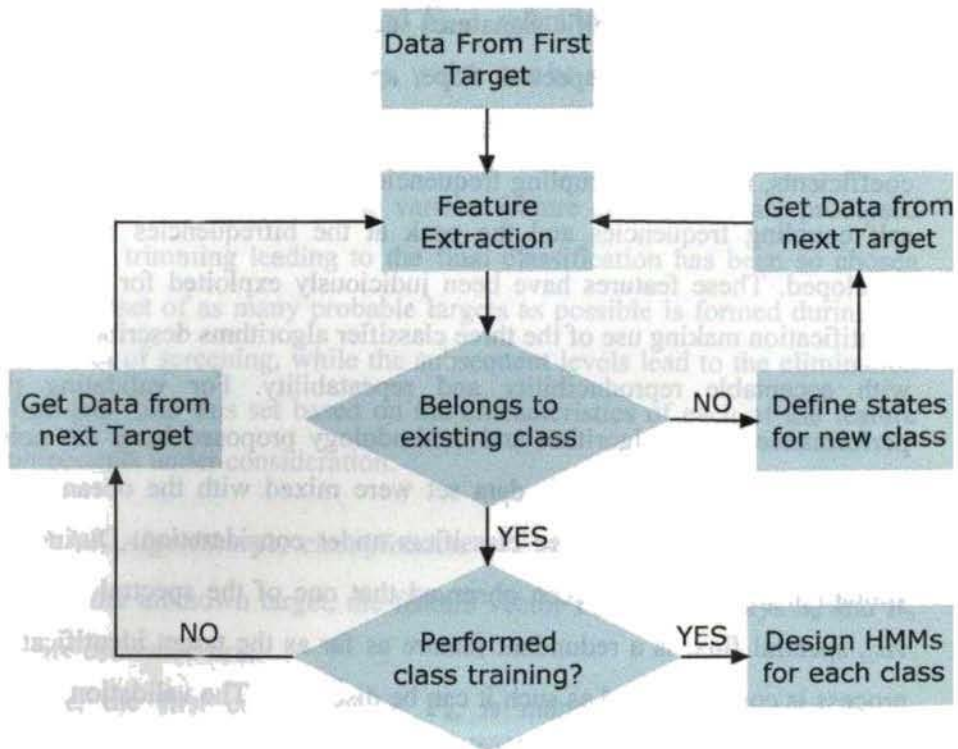


Fig. 6.12 Flowchart of class associations prior to HMM design

In order to train a statistical model for each class, HMMs can be used, which consist of several training states. The class based HMMs can be trained on the target data associated with their respective classes. Though many model based features can be generated for training HMMs, only the NoiseSpectrumEnvelope feature has been adopted in this work.

6.5.2.1 Spectrum Basis Projection

NoiseSpectrumEnvelope is a feature, which is a logarithmic frequency spectrum, spaced by a power-of-two divisor or multiple of an octave. This feature describes the short-term power spectrum of a noise data waveform. It may be used to display a spectrogram, to synthesize a crude *auralization* of the data, or as a general-purpose descriptor for search and comparison.

Let l_w denote the length of the analysis window in samples. The position of each window is described by a shift h , which is the number of samples the Hamming window has to slide over the noise file to obtain the next analysis window position. For Hamming windowed noise signal $x(n)$, the Fourier coefficients $X_w(k)$ are computed as

$$X_w(k) = \sum_{n=0}^{N-1} x(n) \exp(-j2\pi kn / N) \quad 0 \leq k \leq N-1 \quad (6.2)$$

where N is the FFT size, which is chosen such that it is the next power of 2 greater than l_w , due to which the analysis window needs to be enlarged by zero padding, resulting in a larger number of Fourier coefficients and thereby enhancing the frequency resolution.

Each coefficient belongs to one of the N frequencies and as only one half of these frequencies is retained due to the symmetry of the Fourier

Chapter 6 The Target Identifier

transform, the frequency distance DF between two adjacent frequencies can be expressed as $DF = f_s / N$ where f_s , denotes the sampling rate.

A specific grouping of these coefficients can be made to obtain a logarithmic frequency axis and this frequency axis is considered due to the logarithmic frequency response of the human ear. To obtain such a frequency axis, logarithmic frequency bands are defined as shown in Fig.6.13. The edge frequencies of these bands, $f_{edge} = 2^m \cdot 1 \text{ kHz}$, $m \in Z$ where r is the resolution and m determines the number of edge frequencies within the octaves. As an example, for $m = -16, -15, \dots, 7, 8$ and a resolution of $r = 1/4$, the 25 edge frequencies which results in 24 bands have been computed and is given in Table 6.1 .

Table 6.1 Edge Frequencies in [Hz] for Logarithmic Bands

62.5	148.7	353.6	840.9	2000
74.3	176.8	420.4	1000	2378.4
88.4	210.2	500	1189.2	2828.4
105.1	250	594.6	1414.2	3363.6
125	297.3	707.1	1681.8	4000

Each band is represented by a mean value calculated from the Fourier coefficients that refer to this band. The frequencies 62.5 Hz and 4000 Hz are denoted as lo_{edge} and hi_{edge} . Two additional values have to be calculated for the out-of-band energy for 0... lo_{edge} and $hi_{edge}, \dots f_s/2$.

For the computation of a value that represents a logarithmic band, an assignment rule has to be followed, which states that the Fourier coefficients with frequencies farther away than $DF/2$ from a band edge have to be shared between the two bands in such a way that each band retains a part of the coefficient. A linear weighting function can be used to estimate these parts and is illustrated in Fig 6.13. In fact, a logarithmic

frequency band contains Fourier coefficients from $l_{\text{edge}} - DF/2$ to $h_{\text{edge}} + DF/2$, partially weighted using the weighting function.

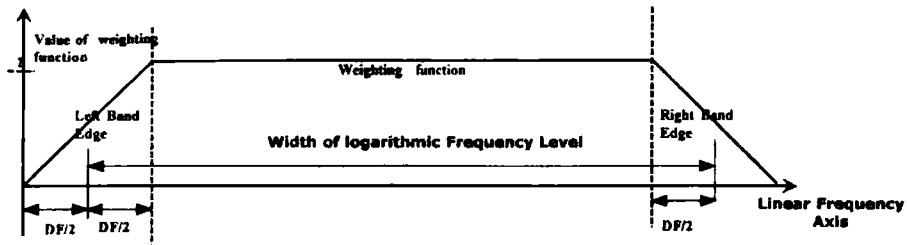


Fig. 6.13 Logarithmic band used

For computational effective realisation of such a method, a weighting matrix, as given in Table 6.2, can be considered. Each row selects Fourier coefficients for a logarithmic band value. Values larger than 0 and smaller than 1 indicate that the Fourier coefficients are shared between adjacent logarithmic bands. Upon computing the short term Fourier coefficients, these coefficients are retained in a matrix C with N rows, the number of Fourier frequencies, and F columns, the number of analysis frames. Each vector of such a matrix contains the Fourier coefficients of one analysis frame.

Table 6.2 Weighting matrix with 12 columns and 8 rows.

	1	2	3	4	5	6	7	8	9	10	11	12
1	0	1	1	1	0.5	0	0	0	0	0	0	0
2	0	0	0	0	0.5	0.2568	0	0	0	0	0	0
3	0	0	0	0	0	0.74317	0.15685	0	0	0	0	0
4	0	0	0	0	0	0	0.84315	0.22717	0	0	0	0
5	0	0	0	0	0	0	0	0.77283	0.5	0	0	0
6	0	0	0	0	0	0	0	0	0.5	1	0.013657	0
7	0	0	0	0	0	0	0	0	0	0	0.98634	0.81371
8	0	0	0	0	0	0	0	0	0	0	0	0.18629

Chapter 6 The Target Identifier

With an appropriate weighting matrix \mathbf{W} , the matrix \mathbf{D} containing L logarithmic band values per column is given as

$$\mathbf{D} = (\mathbf{W} * \mathbf{C}) \cdot \mathbf{W}' \quad (6.3)$$

where \mathbf{W}' denotes a matrix containing the number of Fourier coefficients that are considered for each logarithmic band value. In Eq.(6.3), $*$ denotes a matrix product, whereas \cdot denotes an element by element product. The matrix \mathbf{W}' calculates the mean values from the summed Fourier coefficients and is constructed from the sum of the rows of \mathbf{W} . The resulting vector is F times repeated to construct a L -by- F matrix \mathbf{W}' . A column vector of \mathbf{D} then contains the logarithmic band values that belong to an analysis frame. Each value of such a column is the result of a scalar product between a row of the weighting matrix and a column of the Fourier matrix \mathbf{D} .

Therefore each row of the weighting matrix has to select the appropriate values of a column of the Fourier matrix to construct a logarithmic band value. The weighting matrix must contain as many rows as there are logarithmic bands and as many columns as there are Fourier frequencies. Generally, this methodology to obtain a logarithmic scale is very sensitive to the choice of the logarithmic edge frequencies. Furthermore, the number of coefficients per band increases exponentially. Therefore, the lower bands contain a significantly smaller number of coefficients than the higher bands.

The feature extraction technique using basis projection is illustrated in Fig.6.14 which mainly consists of computation of Short-time Fourier transform (STFT), NoiseSpectrumEnvelope (NSE), Normalized NoiseSpectrumEnvelope (NNSE), basis decomposition algorithm—such as

singular value decomposition (SVD) or ICA followed by basis projection, obtained by multiplying the NNSE with a set of extracted basis functions.

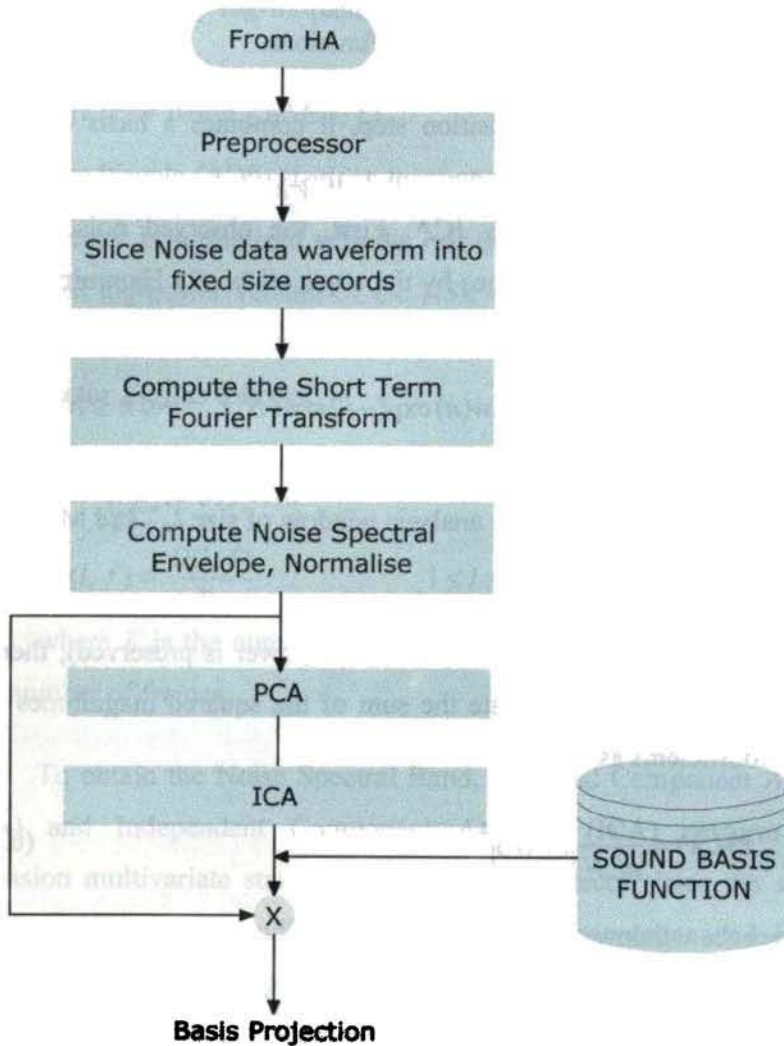


Fig. 6.14 The Feature Extraction system using basis projection

In this feature extraction method, an attempt has been made to obtain from the noise data waveform a low-complex description of its content. A balanced tradeoff between reducing the dimensionality of data and

retaining maximum information content must be achieved, which can be accomplished by using the projection of a spectrum into a low-dimensional representation using decorrelated basis functions.

In the basis decomposition step, it combines a basis dimension-reduction using a principal component analysis (PCA) algorithm with basis information maximization by ICA. First, the observed noise signal is divided into overlapping frames by the application of a Hamming window function and analyzed using the STFT

$$S(l, k) = \sum_{n=0}^{N-1} s(n + lM) \cdot w(n) \exp(-j2\pi kn / N) \quad 0 \leq k \leq N - 1$$

where N is the size of the STFT, k is the frequency bin index, l is the time frame index, w is an analysis window of size l_w , and M is the hop size.

By Parseval's theorem (*i.e.*, so that power is preserved), there is a further factor of $1/N$ to equate the sum of the squared magnitudes of the STFT coefficients as

$$P(l, k) = \frac{1}{nf \cdot N} |S(l, k)|^2 \quad (6.4)$$

where the window normalization factor

$$nf = \sum_{n=0}^{l_w-1} w^2(n)$$

To extract the reduced-rank spectral features, the spectral coefficients $P(l, k)$ are grouped in logarithmic sub bands. Frequency channels are logarithmically spaced in non overlapping 1/4-octave bands spanning between the low edge of 62.5 Hz and high edge of 8 kHz, the band of frequencies occupied by the ocean noise. The spectrum according to a logarithmic frequency scale, which can be referred to as NSE, consists

of a coefficient representing power between 0 Hz and *low edge*, a series of coefficients representing power in logarithmically spaced bands between *low edge* and *high edge*, and a coefficient representing power above *high edge*. The resulting log-frequency power spectrum is converted to the decibel scale.

$$D(l, f) = 10 \log_{10} NSE(l, f) \quad (6.5)$$

where f is the logarithmic frequency range. Each decibel-scale spectral vector is normalized with the *rms* energy envelope, thus yielding a normalized log-power version of the NSE called as NNSE. The full-rank features for each frame consist of both the rms-norm gain value R_l and the NNSE vector $X(l, f)$ as follows:

$$R_l = \sqrt{\sum_{f=1}^F (D(l, f))^2}; \quad 1 \leq f \leq F$$

$$X(l, f) = \frac{D(l, f)}{R_l} \quad 1 \leq l \leq L \quad (6.6)$$

where F is the number of NSE spectral coefficients and L is the total number of frames.

To obtain the Noise Spectral Band, Principal Component Analysis (PCA) and Independent Component Analysis (ICA) perform high-dimension multivariate statistical analysis. PCA decorrelates the second-order moments corresponding to low-frequency properties and extracts orthogonal principal components of variations [141]. ICA, on the other hand, is a linear but not necessarily orthogonal transform, which makes unknown linear mixtures of multidimensional random variables as statistically independent as possible. It not only decorrelates the second-order statistics but also reduces higher order statistical dependencies. It extracts independent components even if their magnitudes are small, whereas PCA extracts only components with the largest magnitudes. Thus,

in the feature extraction process, the ICA representation captures the essential basis functions of the data.

The next step in the feature extraction is generation of a subspace from the NNSE using the PCA algorithm. Then to yield statistically independent or uncorrelated component ICA algorithm can be used.

If X represents the input signal in the form of a $L \times F$ time-frequency matrix, with each row corresponding to a time frame index l and each column corresponding to a frequency range index f , then the columns should be centred by subtracting the mean μ_f value from each one as follows:

$$\hat{X}(f, l) = X(f, l) - \mu_f$$

$$\mu_f = \frac{1}{L} \sum_{l=0}^L X(f, l)$$

where μ_f is the mean of the column f . The next step is the standardization of the rows by removing the dc offset and normalizing the variance as detailed below.

$$\mu_l = \frac{1}{F} \sum_{f=1}^F \hat{X}(f, l)$$

$$\chi_l = \sum_{f=1}^F \hat{X}^2(f, l)$$

$$\Gamma_l = \sqrt{(\chi_l - F \cdot \mu_l^2) / (F - 1)}$$

$$\hat{X}(f, l) = \frac{\hat{X}(f, l) - \mu_l}{\Gamma_l}$$

where μ_l is the mean, $\hat{X}(f, l)$ is the energy of the NNSE and Γ_l is the standard deviation of the row l .

The columns are linearly transformed to remove any linear correlations between the dimensions through eigenvalue decomposition of the covariance matrix. This whitening process established by Hyoung-Gook Kim *et al.*[140] is closely related to PCA.

Following the procedures set out in [140], spectrum projection has been performed and the resulting spectrum projection is the product of the NNSE matrix, the dimension-reduced PCA basis functions and the ICA transformation matrix. The basis function so generated is stored in the basis function database for the purpose of classification.

6.5.2.2 Classification Using Spectrum Projections and HMMs

Spectrum projection is used to represent low dimensional features of a spectrum after projection onto a reduced-rank basis. In order to train a statistical model on the basis projection features for each class, HMMs can be used, which consist of several states [142],[143]. During training, the parameters for each state of the model are estimated by analyzing the feature vectors of the training set. Each state represents a similarly behaving observable process. At each instant in time, the observable symbol in each sequence either stays at the same state or moves on to another state depending on a set of state transition probabilities. Fig. 6.15 illustrates the training process of a HMM for a given class.

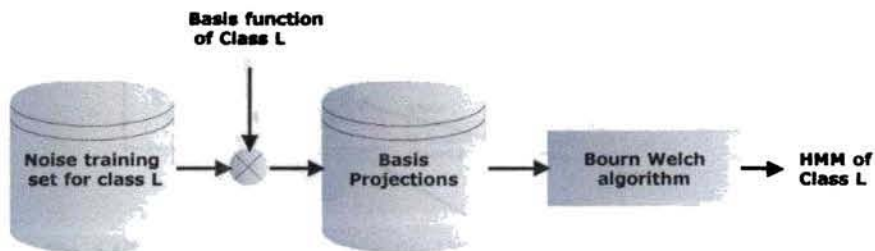


Fig. 6.15 HMM for a given class i

Chapter 6 The Target Identifier

The training data is first projected onto the basis function corresponding to the noise class. The HMM parameters are then obtained using the well-known Baum–Welch algorithm.

The procedure starts with random initial values for all of the parameters and optimizes the parameters by iterative re-estimation. Each iteration runs through the entire set of training data in a process that is repeated until the model converges to satisfactory values. The parameters converge after three training iterations. With the Baum–Welch re-estimation training patterns, one HMM is computed for each class of noise that captures the statistically most regular features of the noise feature space. Fig. 6.16 show an example classification scheme consisting of ships, boats, torpedoes and whales.

Each of the resulting HMMs is stored in the knowledge base. Acoustic signals are modelled according to class labels and represented by a set of HMM parameters. Automatic classification of noise uses a collection of HMMs, class labels, and basis functions.

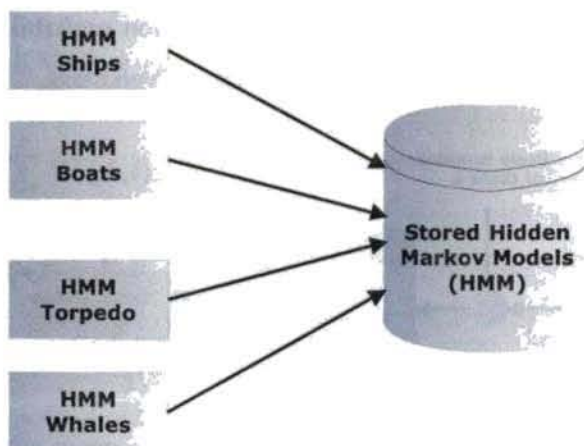


Fig. 6.16 Principle of HMM based Classifier

Automatic classification finds the best-match class for an input sound by presenting it to a number of HMMs and selecting the model having maximum likelihood score. Fig. 6.17 depicts the recognition module used to classify noise input based on pre-trained noise class models. Noise data waveforms are read from a media source format, such as WAVE files. Given an input sound, the NNSE features are extracted and projected against each individual noise model's set of basis functions, producing a low-dimensional feature representation. The HMM yielding the best maximum-likelihood-score is selected, and the corresponding optimal state path is stored.

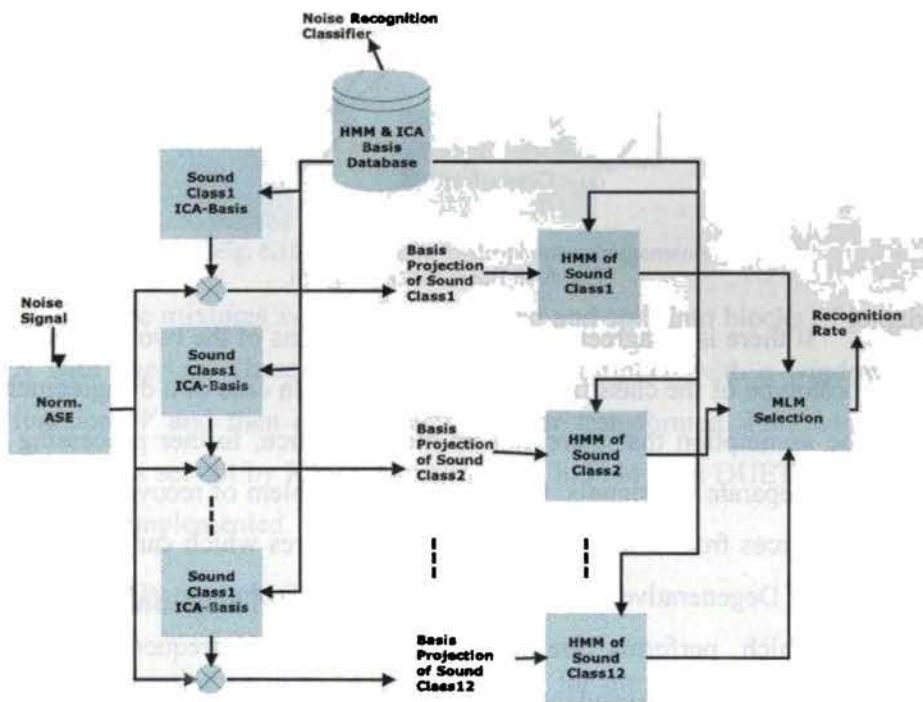


Fig. 6.17 Block Diagram of Classifier Using Spectrum Basis Projection Feature

6.6 Decision System

The processed data furnished by the front end system is fed to the Feature Vector as well as Model based Classifiers. In the Feature Vector Based Classifier, the Hierarchical Target Trimming Approach [144] is adapted and from the classification clues the target is identified. Simultaneously the model-based classifier also works on the pre-processed data and an identification of the target is done as shown in Fig. 6.18.

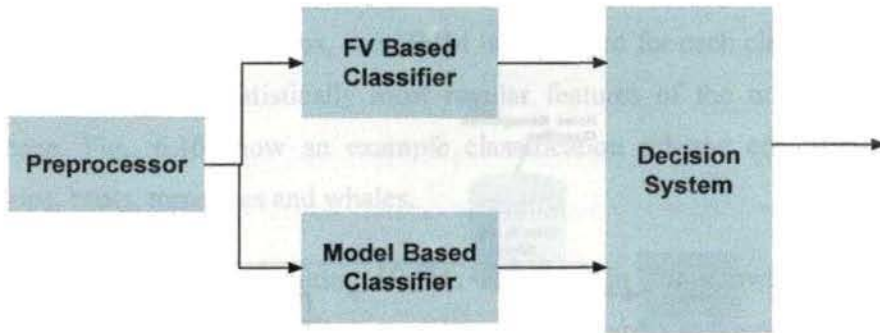


Fig. 6.18 Basic Block Diagram

If there is an agreement among the decisions of the two approaches, the prototype of the classifier displays the target. In case of a disagreement, on the assumption that there can be more a source, further processing is done to separate the signals. It is treated as a problem of recovering two or more sources from a number of unknown mixtures which can be handled with the Degenerative Unmixing Estimations Technique (DUET)[145], [146] which performs the source separation by frequency domain processing and is independent of the number of mixed sources.

6.6.1 Degenerative Unmixing Estimations Technique

Let the sources be positioned at different locations, as shown in Fig. 6.19.

For a two-channel hydrophone arrangement with K sources, the incoming mixed signals x_1 and x_2 can be described as

$$x_1(n) = \sum_{i=1}^K s_i(n)$$

$$x_2(n) = \sum_{i=1}^K a_i s_i(n - \delta_i)$$

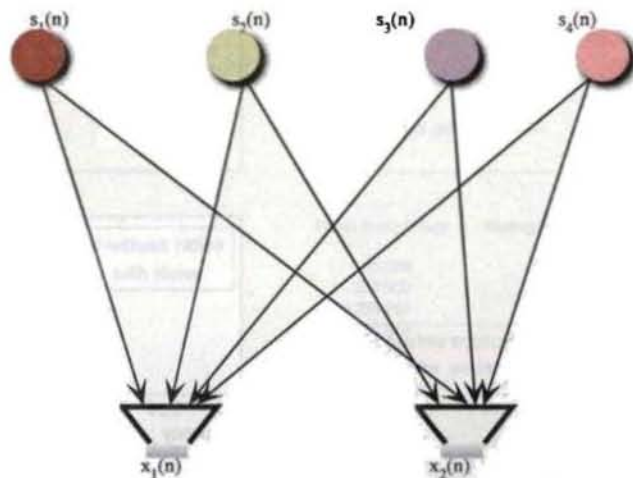


Fig. 6.19 Two channel hydrophone arrangements

The mixtures x_1 and x_2 are sampled and split into blocks of length N with overlap. These sample blocks are multiplied with a windowing function W and then discrete time Fourier transformed. Following the procedures set out by Robert Gavelin *et al.* in [144], the DUET algorithm has been implemented.

6.7 Results and Discussions

The variation of power spectral density for the noise waveforms of a surface craft with and without additive ocean noise are shown in Fig. 6.20 and the various spectral features extracted using the noise emissions from

three typical targets including the surface craft are summarized in Table 6.3.

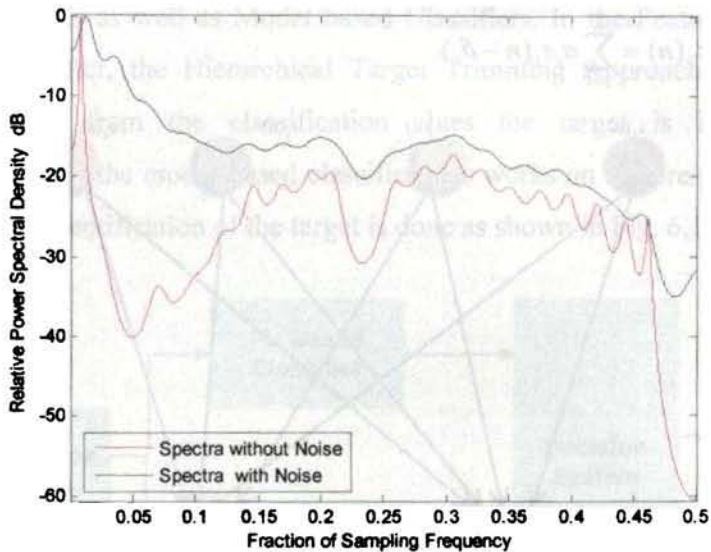


Fig. 6.20 PSD of the noise data waveform of a surface craft with and without additive ocean wave noise

As can be seen from this table, the enlisted spectral features are different for the various noise sources and each of these spectral features can be treated as the characteristics of the corresponding noise sources.

Table 6.3 Spectral features with and without additive ambient noise

Spectral Features	Surface Craft		Engine		Beluga	
	Without Noise	With Noise	Without Noise	With Noise	Without Noise	With Noise
Spectral Centroid	3731	3722	2824	2954	13097	13067
Spectral Range	1084	1048	1333	1293	4674	4993
Spectral Roll off	5145	5095	4694	4750	19488	19781
Spectral Slope	-114	-75	-41	-44	-88	-50
Number of Peaks	11	8	18	17	17	11

The output screen shot of the spectral feature extractor GUI when used for the engine as test case is shown in Fig 6.21.

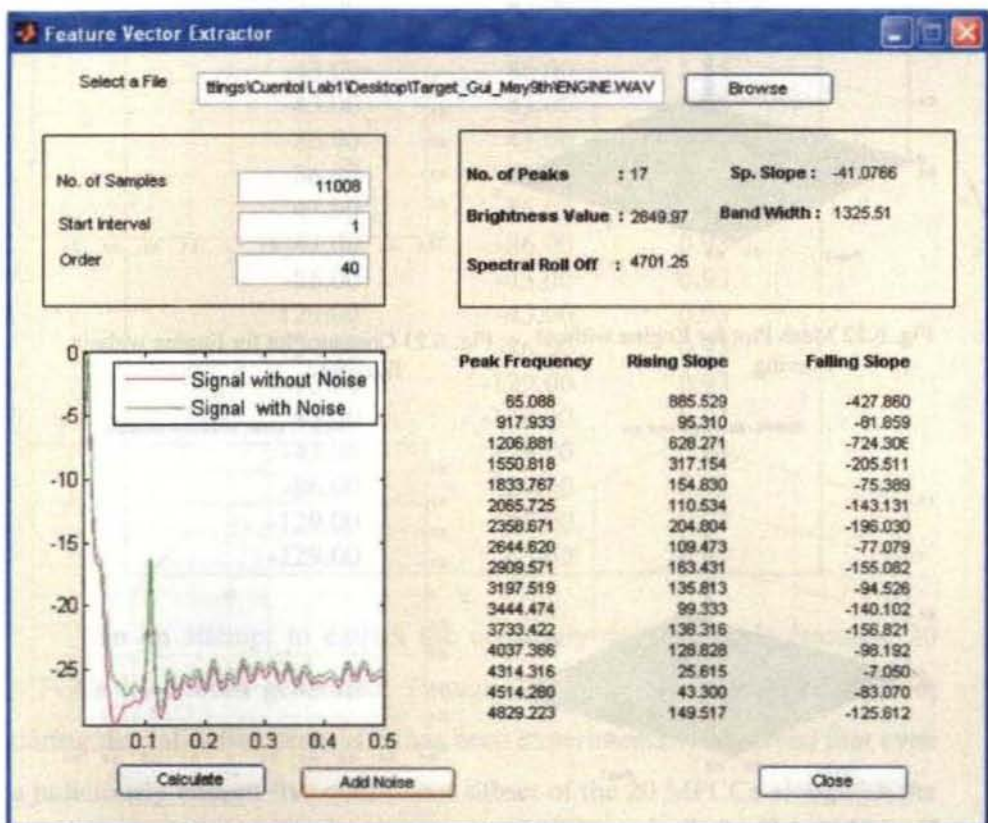


Fig. 6.21 Output screen shot of the Feature Extractor GUI

The 3-dimensional bicoherence plot and the corresponding contour plot of the same signal are shown in Figs 6.22 and 6.23 while Figs. 6.24 and 6.25 depicts the plots for a filtered output of 30 % threshold respectively.

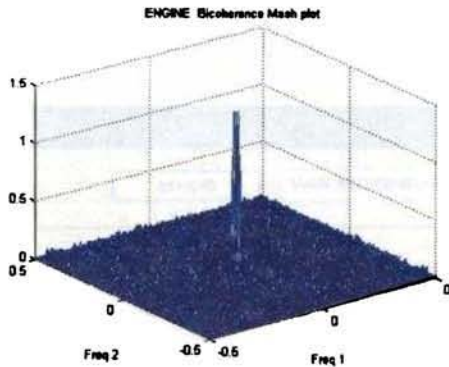


Fig. 6.22 Mesh Plot for Engine without filtering

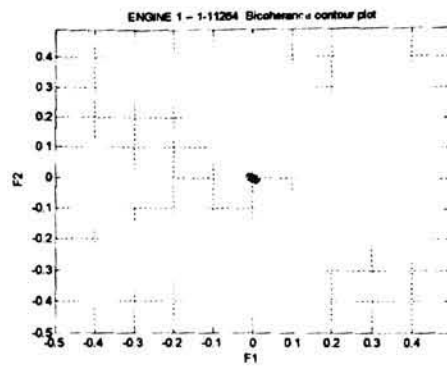


Fig. 6.23 Contour Plot for Engine without filtering

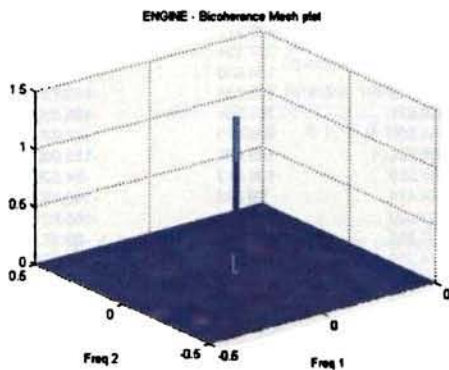


Fig. 6.24 Mesh Plot for Engine with 30 % Filter Threshold

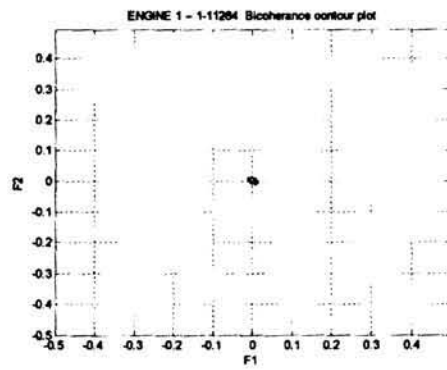


Fig. 6.25 Contour Plot for Engine with 30 % Filter Threshold

The bicoherence plot clearly brings out the non-Gaussian nature of the noise signal. From the contour plots, it is clear that there are certain nonlinear interactions between some of the constituent frequencies. Many prominent peaks can be observed at various bifrequencies, some of which are due to self couplings while others are due to mutual couplings, With a filter threshold of 30% eighteen characteristic coupling frequencies with varying bicoherence levels have been obtained and are as summarized in Table 6.4.

Table 6.4 Bispectral Features of Engine

Frequency f_1	Frequency f_2	Bic (f_1, f_2)
86.00	-43.00	1.35
43.00	43.00	1.35
43.00	-86.00	1.35
-43.00	86.00	1.35
-43.00	-43.00	1.35
-86.00	43.00	1.35
86.00	43.00	0.93
43.00	86.00	0.93
-43.00	-86.00	0.93
-86.00	-43.00	0.93
129.00	-43.00	0.93
129.00	-86.00	0.93
86.00	-129.00	0.93
43.00	-129.00	0.93
-43.00	129.00	0.93
-86.00	129.00	0.93
-129.00	86.00	0.93
-129.00	43.00	0.93

In an attempt to extract the cepstrally decomposable features, 20 MFCCs have been generated. Though 20 MFCCs have been computed, during the validation process, it has been experimentally observed that even a judiciously chosen five coefficient subset of the 20 MFCCs alongwith the spectral and bispectral features are capable of identifying the targets with success rates as high as 92% for the Hierarchical Target Trimming Model.

It has also been observed that any further increase in the MFCCs does not improve the success rates of the identifier any further. Moreover, with the inclusion of 20 MFCCs for the realisation of the classifier the computational complexity has increased considerably. The adaptability of the suggested algorithm has been further established through some of the basic test statistics carried out with the Euclidean distance(ED) and Fuzzy K-Nearest Neighbour (FKNN) Models. The success rates of all the three

classifiers have been validated with 110 noise sources and the results are summarized in Table 6.5. The output screen shot of the Target classifier with the target identified as Engine is as shown in Fig 6.26.

Table 6.5 Results of comparison of the three Classifiers

Success Rate of					
ED Model		FKNN-NN Model		Proposed Model	
Without Noise	With Noise	Without Noise	With Noise	Without Noise	With Noise
0.9363	0.8909	0.9545	0.9090	0.9545	0.9181

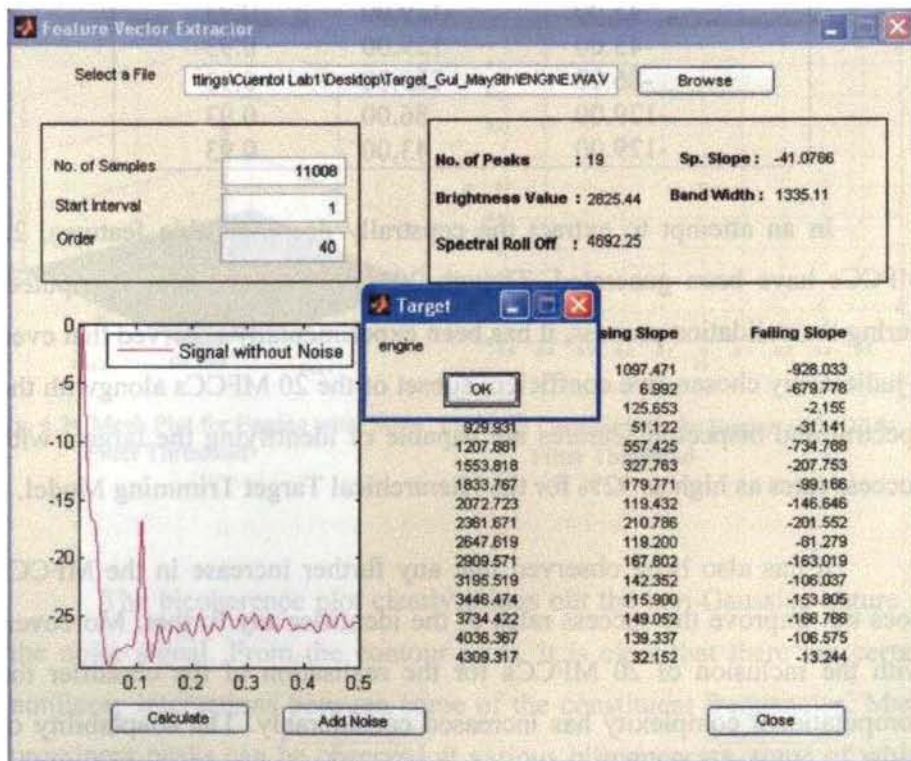


Fig. 6.26 Prototype Target Identifier

The following figures Figs. 6.27 and 6.28 depicts the projection of NoiseSpectrumEnvelope on the basis components in respect of two typical

noise sources namely Torpedo and Whale while the screen shots shown in Figs.6.29 and 6.30 demonstrate the HMM Based Prototype Underwater Target Classifier using the NSE vector.

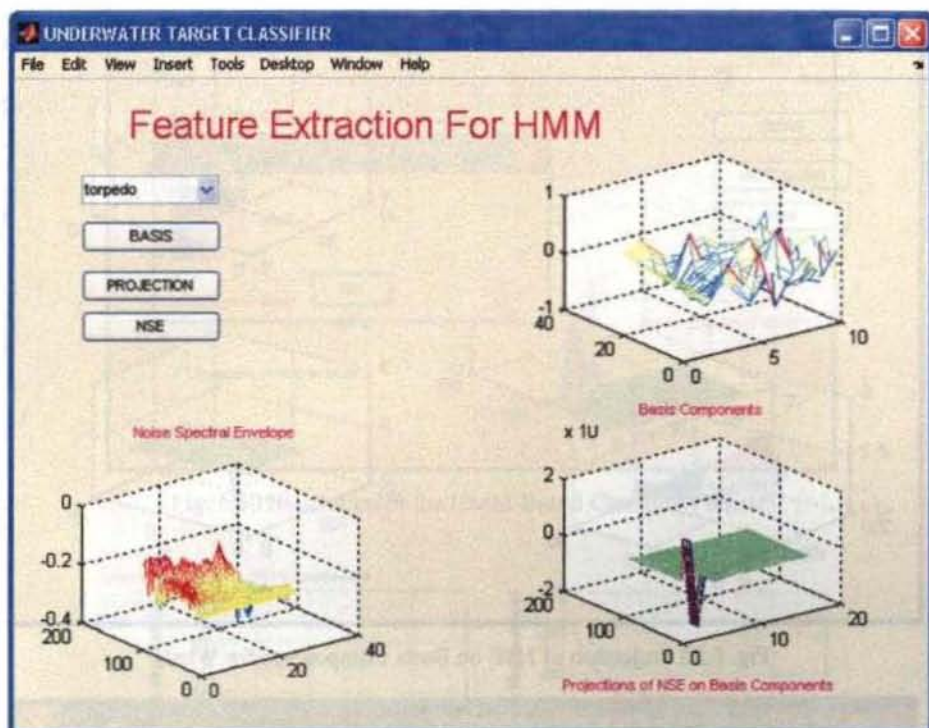


Fig. 6.27 Projection of NSE on Basis Components for Torpedo

The capability of the DUET algorithm for resolving contentions, in case the decisions of the feature vector based classifier differs from the HMM based classifier has been evaluated with a few test cases and is found to yield encouraging results. The simulated composite signal comprising of noise data waveforms generated by two sources Source 1 and Source 2 has been used as the input to the DUET algorithm. Adopting suitable demixing techniques suggested in [144], the characteristic source emanations could be separated from the mixture. The mixed signal comprising of the

Chapter 6 The Target Identifier

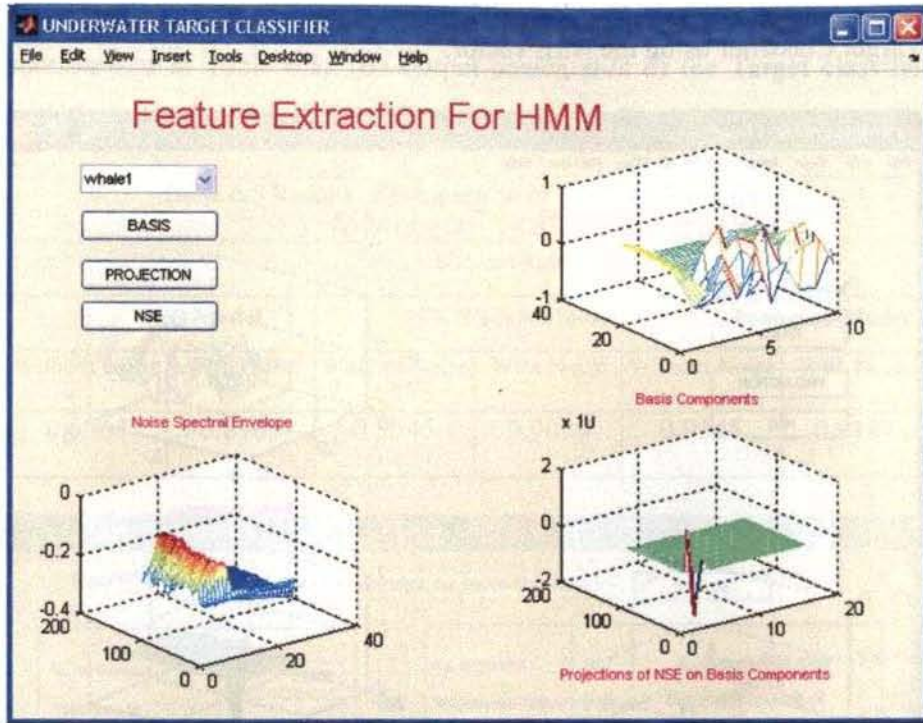


Fig. 6.28 Projection of NSE on Basis Components for Whale

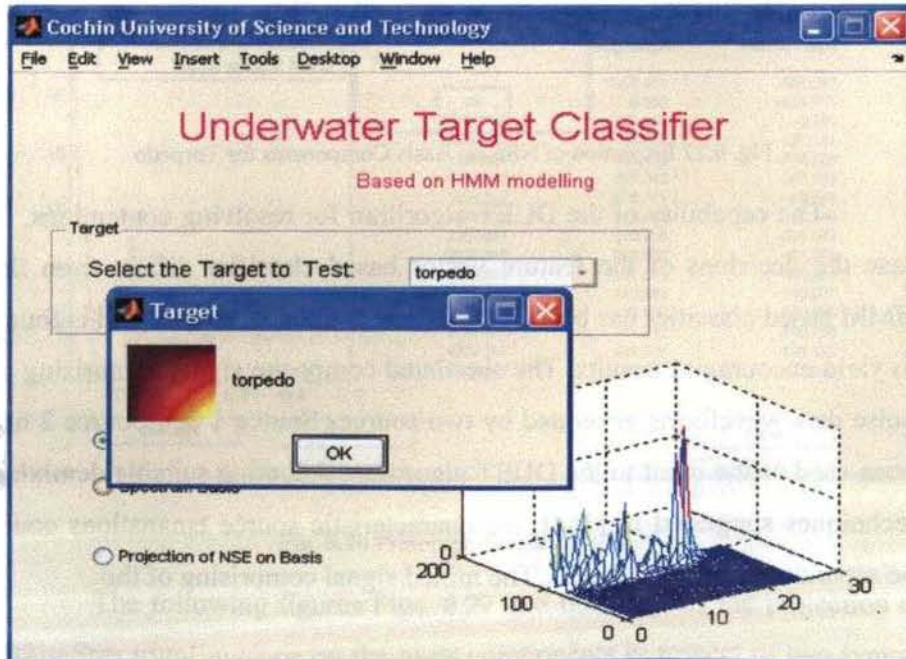


Fig. 6.29 Illustration of the HMM Based Classifier (Torpedo)

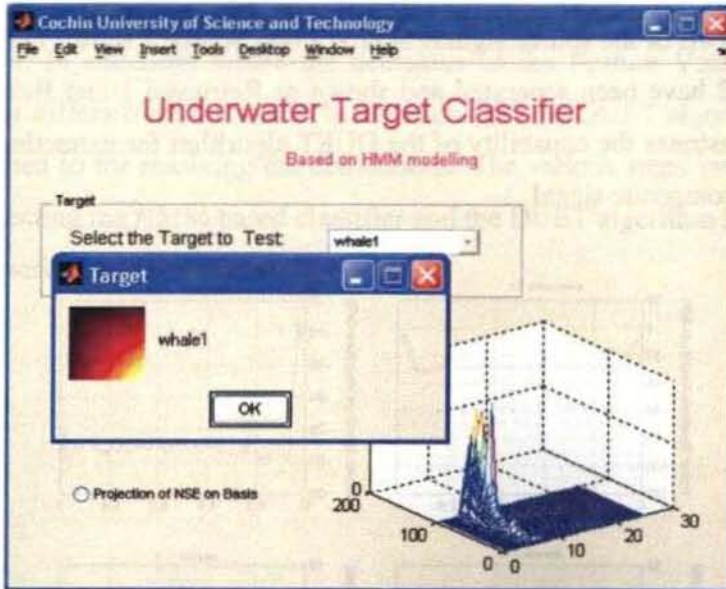


Fig. 6.30 Illustration of the HMM Based Classifier (Whale)

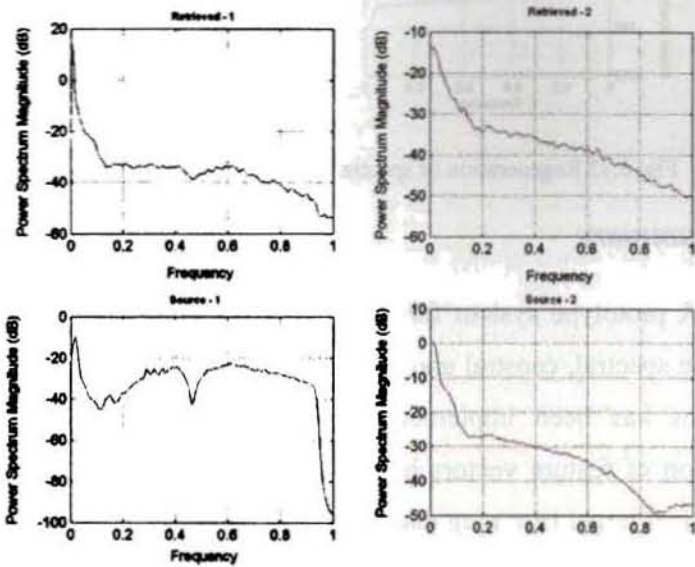


Fig. 6.31 Regeneration of spectra from a composite mixture (Case 1)

components of the source signals Source 1 and Source 2 shown in Figs 6.31 and 6.32 have been separated and shown as Retrieved 1 and Retrieved 2. This illustrates the capability of the DUET algorithm for extracting signals from a composite signal.

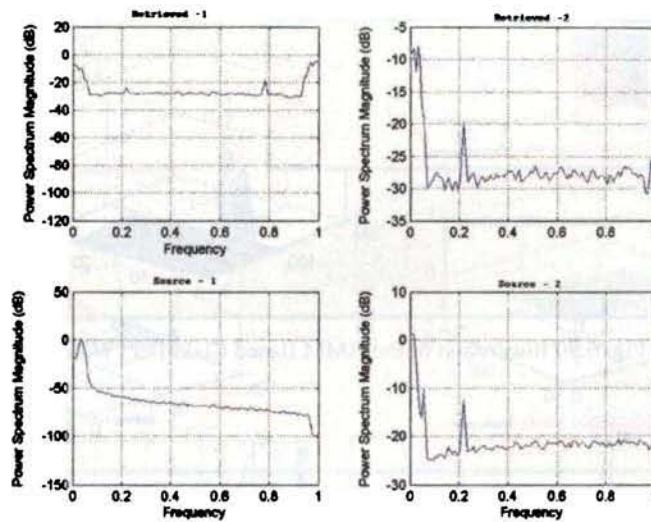


Fig. 6.32 Regeneration of spectra from a composite mixture (Case 2)

6.8 Summary

A prototype system for identifying the noise sources in the ocean using the spectral, cepstral and bispectral features extracted from the noise emissions has been implemented. The various steps involved in the generation of feature vectors have been described in this chapter. A new hierarchical target trimming classifier centred on the concepts of trimming the probable number of targets by applying certain elimination criteria, making use of the characteristic target specific features has also been proposed in this chapter. The performance of this classifier has been compared with that of the Euclidean distance as well as the more sophisticated Fuzzy K-Nearest Neighbour model classifiers. In the

proposed target classification system, the feature vector based classifier works in conjunction with the Hidden Markov Model (HMM) based classifier. In situations where the decisions of the Feature Vector based classifier differs from the HMM based classifier, the DUET algorithm can be resorted to for resolving the contentions. The various steps involved in implementing the HMM based classifier and the DUET algorithm have also been described in this chapter.

CHAPTER 7

Conclusions

This thesis addresses one of the emerging topics in Sonar Signal Processing, *viz.* the implementation of a target classifier for noise sources in the ocean, as the operator-assisted classification turns out to be tedious, laborious and time consuming. In the work reported in this thesis, various judiciously chosen components of the feature vector are used for realizing the newly proposed Hierarchical Target Trimming Model. The performance of the proposed classifier has been compared with the Euclidean distance and Fuzzy K-Nearest Neighbour Model classifiers and is found to have better success rates. The procedures for generating the Target Feature Record or the Feature Vector from the spectral, cepstral and bispectral features have also been suggested. The Feature Vector, so generated from the noise data waveform is compared with the feature vectors available in the knowledge base and the most matching pattern is identified, for the purpose of target classification. In an attempt to improve the success rate of the Feature Vector based classifier, the proposed system has been augmented with the HMM based Classifier. In situations where both the classifier decisions disagree, a contention resolving mechanism built around the DUET algorithm has been suggested. This chapter also brings out the salient highlights of the work and the general inferences gathered alongwith enlisting of the scope and direction for future research in this area.

7.1 *Highlights of the Thesis*

The study of underwater sound has gained considerable significance due to its strategic as well as commercial importance. The ocean, as a propagation medium is full of interfering noise sources such as machinery noise from the shipping traffic, flow noise, wave noise, wind noise, noise from biologics and even intentional jammers. The ambient noise in the ocean is composite in nature comprising of the components emanating from a variety of noise sources. The studies carried out on the noise in the ocean reveal that its spectrum extends over the frequency range from a few hertz to about 100 kHz. The work reported in the thesis entitled *Realisation of a Target Classifier for Noise Sources in the Ocean* addresses one of the emerging topics in Sonar Signal Processing, viz. the implementation of a target classifier for noise sources in the ocean, as the operator assisted classification turns out to be tedious, laborious and time consuming. The following are the salient highlights of this thesis.

7.1.1 Need and Requirement of a Computer Assisted Classifier

The introductory chapter of the thesis throws light on the various noise sources in the ocean as well as the need and requirement of a computer assisted classifier for identifying them. The underlying principle of operation of the proposed classifier which involves extraction of the various spectral, cepstral and bispectral features is also briefly introduced in this chapter.

7.1.2 Preparation of a State-of-the-art Literature

As a part of the work, a state-of-the-art literature has been prepared in the topic covered in the thesis highlighting the characteristic signatures of different noise sources in the ocean and various classifiers such as the

Chapter 7 Conclusions

statistical classifiers, expert system classifiers, neural network classifiers, fuzzy classifiers, sonar signal processor based classifiers, etc..

7.1.3 Feature Vector Based Classifier

The methodology suggested to be adopted for realizing the proposed classifier involves the extraction of source features by analyzing the composite noise data waveforms and identifying the most matching feature vector using template matching technique leading to the identification of the target. For making the system fool proof and full fledged one, the knowledge base has to be updated with the feature vectors and target dynamics for all the class and type of the targets.

7.1.4 Extraction of Spectral Features

Though the thesis addresses both the classical and parametric model based power spectral estimators for extracting the spectral features, the model based estimators are found to give better performance as well as frequency resolution for short data segments than conventional estimators. The parametric model based estimation techniques require a prior knowledge of the process from which the data samples are taken.

7.1.5 Extraction of Cepstral Features

The cepstral features are extracted using cepstral analysis, which is accomplished by using a cascade of forward and inverse operations with a linear time invariant operation sandwiched in between. A more systematic approach for computing the cepstral coefficients can be achieved by estimating the MFCCs. Though 20 MFCCs have been computed, it has been experimentally observed that even a judiciously chosen five coefficient subset of the 20 MFCCs alongwith the spectral features are capable of identifying the targets with acceptable confidence levels.

7.1.6 Extraction of Bispectral Features

The bispectrum, which is based on the third order statistics, can characterize non-Gaussian as well as nonlinear signals. Different types of nonlinearities results in different types of phase couplings. QPC is considered as an invaluable tool in nonlinear system identification. Some of the bispectral features which can be effectively utilized in realizing the target identifier have been brought out in this thesis. Moreover, the procedures to be adopted for generating the bispectrally extractable features such as the self coupling frequencies, mutual coupling frequencies, the peak at the bifrequencies, etc. are also described in the thesis.

7.1.7 Generation of Target Feature Record

The thesis also addresses the various steps involved in the generation of target feature records. If the target feature record so generated from the various data records, are not updated over a considerable period, the relevant feature records will be dropped and the average of all the feature records that have close resemblances will be used for generating the *feature vector*.

7.1.8 Classifier Based on Hierarchical Target Trimming Approach.

A new classifier approach centred on the concept of trimming the probable number of targets by applying certain elimination criteria, making use of the feature vectors, which are assumed to be composed of many feature components that are extractable using spectral, cepstral and bispectral techniques has also been presented in this thesis. The performance of this classifier has been compared with the Euclidean distance and fuzzy k -NN classifiers and the results of the comparison yielded encouraging results.

Chapter 7 Conclusions

7.1.9 Towards Improving the Performance of the Classifier

In the Target Classifier System proposed in this thesis, the feature vector based Hierarchical Target Trimming System works in conjunction with the Hidden Markov Model based classifier. In situations, where the decisions of the feature vector based classifier differ from the HMM based classifier, the DUET algorithm can be resorted to for resolving contentions.

7.1.10 DUET Algorithm for Resolving Contentions

The thesis also addresses the principle and working of the Degenerative Unmixing Estimations Technique (DUET), which is capable of resolving the issues arising out of multiple sources scenarios. Here the noise emanations from the various sources are separated by frequency domain processing and its performance is seen to be independent of the number of sources.

7.2 Future Scope for Research

The work presented in this thesis has a significant role to play in view of its practical applications. This work also has substantial scope for further research for improving the overall system performance. Some of the possible proposals for future work in this area are enlisted below.

7.2.1 Prototype System

The proposed prototype system for identifying the noise sources in the ocean works on a simulated environment with the sample data sets obtained from some of the web sites and open literatures. In the simulated environment, the system has been validated by mixing these noise data waveforms with ocean wave noise data. The performance of the systems needs to be validated with realistic data for the Indian Seas.

7.2.2 Realistic Field Data

During the course of implementation of the target classifier suggested in this thesis, though attempts were made to obtain the realistic data for the Indian seas, from some of the National Laboratories in the Country, the efforts did not succeed to the expectations. Due to reasons that are obvious, the field collection of realistic data as a part of Ph.D. thesis is beyond its scope, as it involves massive efforts and substantial investments. Hence, it was not attempted. This will be taken up as a separate major project from appropriate funding agencies.

7.2.3 Real-time Target Classifiers

As already brought out, the classifier system reported in this thesis works on a simulated environment. In order to make the system more reliable, robust and fool proof, the knowledge base of the system needs to be updated with the feature vectors and target dynamics for all the class and type of the targets. This demands massive investments and efforts. Moreover, in order to make the system a real time, the classifier needs to be augmented with the requisite hardware comprising of the hydrophone array, receiving electronics subsystems and pre-processing modules, so that the processed data is made available to the estimation statistics processor. As this proposal also demands massive investment, this will be taken up separately later.

7.2.4 Hardware Based Feature Vector Generator

The classifier system reported in this thesis works on a simulated environment and the modules have been developed in *Matlab*. In order to reduce the processing time, it is proposed to generate the feature vectors

Chapter 7 Conclusions

with dedicated hardware using DSP boards which will also be taken up separately later.

7.2.5 Handling Multiple Target Scenario

For improving the classifier performance, the feature vector based Hierarchical Target Trimming System is made to work in conjunction with the Hidden Markov Model based Classifier. In case the decision system encounters with contentions in the inferences gathered by these systems, appropriate contention resolving mechanisms built around the DUET algorithm needs to be invoked. In the work reported in this thesis, the DUET algorithm has been implemented in a simulated environment. In real time target classifier proposed to be realized with specific funding from appropriate Government Agencies/Departments, the Degenerate Unmixing Estimation Technique (DUET) is also suggested to be implemented in real time.

7.2.6 Modeling other features using HMM

The HMM based classifier has been implemented by modelling only one of the features, *viz.* the NoiseSpectrumEnvelope. The reliability and success rate of the HMM based classifier can be improved by incorporating more training vectors on to the model.

7.3 Summary

An attempt has been made in this chapter to bring out the salient highlights of the work and the general inferences gathered along with enlisting of the scope and direction for future research in this area. When the real-time classifier system augmented with a full fledged backbone knowledge base becomes a reality, the system can outperform the state-of-the-art classifiers with amazing high success rates.

References

- [1]. Bertilone, D.C. and Killeen, D.S.; *Statistics of biological noise and performance of generalized energy detectors for passive detection*, IEEE Journal of Oceanic Engineering, 26(2), 2001, pp:285 – 294.
- [2]. Gordon M. Wenz; *Review of Underwater Acoustic Research: Noise*, J. Acoust. Soc. Am. 51(3), 1972
- [3]. Carey, W.M.; *Oceanic Low frequency Ambient Noise*, Proceedings of the MTS/IEEE Conference and Exhibition on OCEANS, 1, 2000, pp: 453 - 458
- [4]. Pumphrey, H.C. and Ffowcs Williams, J.E.; *Bubbles as sources of ambient noise*, IEEE Journal of Oceanic Engineering, 15(4), 1990, pp: 268 – 274
- [5]. Tan Soo Pieng, Koay Teong Beng, P. Venugopalan, Mandar A Chitre and John R. Potter; *Development of a Shallow Water Ambient Noise Database*, Proceedings of the International Symposium on Underwater Technology, 2004, pp: 169 - 173
- [6]. Potter, J.R. and Delory, E.; *Noise sources in the sea and the impact for those who live there*, Proceeding of the Conference on Acoustics and Vibration Asia'98, 1998 (Downloaded from <http://www.arl.nus.edu.sg/web/pub>)
- [7]. Pflug, I.A.; Jackson, P.M.; Ioup, J.W. and Ioup, G.E.; *Moment analysis of ambient noise dominated by local shipping*, Proceedings of the IEEE Signal Processing Workshop on Statistical Signal and Array Processing, 1996, pp: 271 – 274
- [8]. Pavlo Tkalich and Eng Soon Chan; *Breaking wind waves as a source of ambient noise*, J. Acoust. Soc. Am. 112 (2), 2002.
- [9]. Stephen C. Wales and Richard M. Heitmeyer, *An ensemble source spectra model for merchant ship-radiated noise*, J. Acoust Soc. Am., 111(3), 2002, pp: 1211-1231
- [10]. Leslie M. Gray and David S. Greeley, *Source level model for propeller blade rate radiation for the world's merchant fleet*, J. Acoust Soc. Am.; 67(2), 1980, pp: 516-522
- [11]. Arveson, P.T. and Vendittis, D.J.; *Radiated noise characteristics of a modern cargo ship*, J. Acoust Soc. Am. 107(1), 2000, pp:118-129

References

- [12]. Hollinberger, D.E. and Bruder, D.W.; *Ambient noise data logger buoy*, IEEE Journal of Oceanic Engineering, 15(4) , 1990, pp:286 – 291
- [13]. Michel Bouvet and Stuart C. Schwartz; *Underwater noises : statistical modelling, detection and normalization*, J. Acoust Soc. Am., 83(3), 1988, pp:1023-33
- [14]. Rudolph H. Nichols, *Infrasonic ocean noise sources: Wind versus Waves*, J. Acoust Soc. Am. 82(4), 1987
- [15]. Webster, R.J.; *Ambient noise statistics*, IEEE Transactions on Signal Processing, 41(6), 1993, pp: 2249 – 2253
- [16]. Huynh, Q.Q.; Cooper, L.N.; Intrator, N. and Shouval, H.; *Classification of underwater mammals using feature extraction based on time-frequency analysis and BCM theory*, IEEE Transactions on Signal Processing, [see also IEEE Transactions on Acoustics, Speech, and Signal Processing,] , 46(5), 1998, pp:1202 – 1207
- [17]. <http://www.fishecology.org/index.htm>
- [18]. <http://birds.cornell.edu/brp/SoundsMarMamm.html>
- [19]. <http://www.pmel.noaa.gov>
- [20]. Chun Ru Wan; Joo Thiam Goh and Hong Tat Chee; *Optimal tonal detectors based on the power spectrum* IEEE Journal of Oceanic Engineering, 25(4), 2000, pp: 540 - 552
- [21]. Marple, S.L., Jr.; *A tutorial overview of modern spectral estimation*, International Conference on Acoustics, Speech, and Signal Processing, 4, 1989, pp:2152 - 2157
- [22]. Shin, F.B. and Kil, D.H.; *Full spectrum signal processing*, Proceedings of the MTS/IEEE Conference on Challenges of Our Changing Global Environment, 1, 1995, pp:397 - 403
- [23]. *Power Spectral Estimation*, National Semiconductor Application Note 255, 1980
- [24]. Hinich M.; *Detecting a hidden periodic signal when its period is unknown*, IEEE Transactions on Acoustics, Speech and Signal Processing, 30(5), 1982, pp:747 – 750
- [25]. Cremona, P.; Kunert, M. and Castanie, F.; *Parametric spectrum analysis for target characterization*, Proceedings of the Symposium on Intelligent Vehicles, 1994, pp:149 - 154

- [26]. Eftestol, T. and Vatland, E.; *A method for detection of signal harmonics in the spectrum*, Computers in Cardiology, 1999, pp: 547 – 550
- [27]. Ricardo S. Zebulum, Marley Vellascot, Guy Perelmuter and Marco Aurelio, *A Comparison of Different Spectral Analysis Models For Speech Recognition Using Neural Networks*, Proceedings of the IEEE 39th Midwest symposium on Circuits and Systems, 3, 1996 pp:1428-1431
- [28]. Massimo Aiello, Antonio Cataliotti, and Salvatore Nuccio; *A Comparison of Spectrum Estimation Techniques for Nonstationary Signals in Induction Motor Drive Measurements*, IEEE Transactions on Instrumentation and Measurement, 54(6), 2005, pp:2264 – 2271
- [29]. Benjamin K. Friedlander and Boaz Porat, *A Spectral Matching Technique for ARMA Parameter Estimation*, IEEE Transactions On Acoustics, Speech and Signal Processing, 32(2), 1984 pp:313 - 316
- [30]. E.A. Talkhan, A.F. Hassan, and N.A. Pmin; *An ARMA Model for Power Spectrum Estimation*, Proceedings of the IEEE International Conference on Acoustics, Speech and Signal Processing, 1983, pp:1080 – 1083.
- [31]. Qi Tian, Nihat m. Bilgutay and Xing; *An Iterative Spectral Method For Multiple Target Detection*, Proceedings of the IEEE Symposium on Ultrasonics, 1995, pp:721 - 724
- [32]. Igor Luzin, Maxim Dubinsky, and Magistant; *High Resolution Spectrum Estimating Algorithm*, Proceedings of the IEEE OCEANS Conference, 3, 1998, pp:1409 - 1412
- [33]. R. Rodney W. Johnson and John E. Shore; *Minimum Cross-Entropy Spectral Analysis of Multiple Signals*, IEEE Transactions On Acoustics, Speech and Signal Processing, 31(3), 1983, pp:574 - 582
- [34]. Christopher Bingham, Michael D. Godfrey, and John W. Tukey; *Modern Techniques of Power Spectrum Estimation*, IEEE Transactions on Audio and Electroacoustics, 2, 1967, pp:56 - 66
- [35]. K. S. Arun, *Principal Components Algorithms for ARMA Spectrum Estimation*, IEEE Transactions On Acoustics. Speech, And Signal Processing, 37(4), 1989, pp:566 – 571.
- [36]. Farid U. Dowla And Jae S. Lim; *Relationship Between Maximum Likelihood Method and Autoregressive Modelling in*

References

- Multidimensional Power Spectrum Estimation*, IEEE Transactions On Acoustics, Speech and Signal Processing, 32,(5), 1984, pp:1083 – 1087.
- [37]. Lorenzo Peretto, Gaetano Pasini and Carlo Muscas; *Signal Spectrum Analysis and Period Estimation by Using Delayed Signal Sampling*, Proceedings of the IEEE International Conference on Acoustics, Speech and Signal Processing, 2, 1994, pp:1035 – 1040.
- [38]. Moeness G. Amin; *Sliding Spectra: A New Perspective*, Proceedings of the Fourth Annual ASSP Workshop on Spectrum Estimation and Modeling, 1988, pp: 55 - 59.
- [39]. Brian G. Ferguson; *Time-Frequency Signal Analysis of Hydrophone Data*, IEEE Journal Of Oceanic Engineering, 21(4), 1996, pp:537 – 544
- [40]. M. Omologo and P. Svaizer; *Use of the Crosspower-Spectrum Phase in Acoustic Event Location*, IEEE Transactions on Speech and Audio Processing, 5(3) 1997, pp:288 – 292.
- [41]. Lippens, S.; Martens, J.P. and De Mulder, T.; *A comparison of human and automatic musical genre classification*, Proceedings of the IEEE International Conference on Acoustics, Speech and Signal Processing, 4, 2004, pp:233 -236
- [42]. Holmes, W.J.; Wood, L.C. and Pearce, D.J.B.; *Allophone modeling for vocabulary-independent HMM recognition*, Proceedings of the IEEE International Conference on Acoustics, Speech and Signal Processing, 2, 1993, pp:487 - 490
- [43]. Wei Han, Cheong-Fat Chan, Chiu-Sing Choy and Kong-Pang Pun.; *An Efficient MFCC Extraction Method in Speech Recognition*, Proceedings of the IEEE International Symposium on Circuits and Systems, 2006, pp:145-148
- [44]. Van Der Merwe, C.J. and Du Preez, J.A.; *Calculation of LPC-based cepstrum coefficients using mel-scale frequency warping*, Proceedings of South African Symposium on Communications and Signal Processing, 1991, pp:17 - 21
- [45]. Imai, S.; *Cepstral analysis synthesis on the mel frequency scale*, Proceedings of the IEEE International Conference on Acoustics, Speech and Signal Processing, 8, 1983, pp: 93 - 96
- [46]. Furui, S.; *Cepstral analysis technique for automatic speaker verification*, IEEE Transactions on Acoustics, Speech and Signal

- Processing [see also IEEE Transactions on Signal Processing], 29(2), 1981, pp:254 - 272
- [47]. Lourens, J.G.; *Classification of ships using underwater radiated noise*, Proceedings of Southern African Conference on Communications and Signal Processing, 1988, pp:130 - 134
- [48]. Ziyong Xiong; Radhakrishnan, R.; Divakaran, A. and Huang, T.S.; *Comparing MFCC and MPEG-7 audio features for feature extraction, maximum likelihood HMM and entropic prior HMM for sports audio classification*, Proceedings of the International Conference on Multimedia and Expo, 3, 2003, pp:397-400
- [49]. Eronen, A.; *Comparison of features for musical instrument recognition*, Proceedings of the IEEE Workshop on Applications of Signal Processing to Audio and Acoustics, 2001, pp:19 - 22
- [50]. Francois Pellegrino and RkGINE Andre-Obrecht , *Vocalic System Modeling: A VQ Approach*, Proceedings of the IEEE International Conference on Digital Signal Processing, 2, 1997. pp: 745 –748
- [51]. Molau, S.; Pitz, M.; Schluter, R. and Ney, H.; *Computing Mel-frequency cepstral coefficients on the power spectrum*, Proceedings of the IEEE International Conference on Acoustics, Speech, and Signal Processing, 1, 2001, pp:73 - 76
- [52]. Molau, S.; Pitz, M. and Ney, H.; *Histogram based normalization in the acoustic feature space*, Proceedings of the IEEE Workshop on Automatic Speech Recognition and Understanding, 2001, pp:21 - 24
- [53]. Tyagi, V.; McCowan, I.; Misra, H. and Bourlard, H.; *Mel-cepstrum modulation spectrum (MCMS) features for robust* Proceedings of the IEEE Workshop on Automatic Speech Recognition and Understanding, 2003, pp:399 - 404
- [54]. Garcia, J.O. and Reyes Garcia, C.A.; *Mel-frequency cepstrum coefficients extraction from infant cry for classification of normal and pathological cry with feed-forward neural networks*, Proceedings of the International Joint Conference on Neural Networks, 4, 2003, pp:3140 - 3145
- [55]. Mubarak, O.M.; Ambikairajah, E. and Epps, J.; *Novel Features for Effective Speech and Music Discrimination*, Proceedings of the IEEE International Conference on Engineering of Intelligent Systems, 2006, pp:1 - 5

References

- [56]. Black, T.R. and Donohue, K.D.; *Pitch determination of music signals using the generalized spectrum*, Proceedings of the IEEE Southeastcon, 2000, pp:104 - 109
- [57]. Molla, K.I. and Hirose, K.; *On the effectiveness of MFCCs and their statistical distribution properties in speaker identification*, Proceedings of the IEEE Symposium on Virtual Environments, Human-Computer Interfaces and Measurement Systems, 2004, pp:136 - 141
- [58]. Nielsen, A.B.; Sigurdsson, S.; Hansen, L.K. and Arenas-Garcia, J.; *On the Relevance of Spectral Features for Instrument Classification*, Proceedings of the IEEE International Conference on Acoustics, Speech and Signal Processing, 2, 2007, pp: 485 - 488
- [59]. Wei-Wen Hung and Hsiao-Chuan Wang; *On the use of weighted filter bank analysis for the derivation of robust MFCCs*, IEEE Signal Processing Letters, 8(3), 2001, pp:70 - 73
- [60]. Lennartsson, R.K.; Robinson, J.W.C.; Persson, L.; Hinich, M.J. and McLaughlin, S.; *Passive Sonar Signature Estimation Using Bispectral Techniques*, Proceedings of the IEEE Workshop on Statistical Signal and Array Processing, 2000, pp:281 – 285
- [61]. Raghuv eer, M. and Nikias, C.; *Bispectrum Estimation: A Parametric Approach*, IEEE Transactions on Acoustics, Speech, and Signal Processing [see also IEEE Transactions on Signal Processing], 33(5), 1985, pp: 1213 – 1230
- [62]. Raghuv eer, M. and Nikias, C.; *A Parametric Approach to Bispectrum Estimation*, Proceedings of the IEEE International Conference on Acoustics, Speech and Signal Processing, 9, 1984, pp:120 - 123
- [63]. Regazzoni, C.S.; Tesei, A. and Tacconi, G.; *A comparison between spectral and bispectral analysis for ship detection from acoustical time series*, Proceedings of the IEEE International Conference on Acoustics, Speech and Signal Processing, 2, 1994, pp:289 - 292
- [64]. Lyons, A.R.; Newton, T.J.; Goddard, N.J. and Parsons, A.T.; *Can passive sonar signals be classified on the basis of their higher order statistics?* IEE Colloquium on Higher Order Statistics in Signal Processing: Are They of Any Use?, 6, 1995, pp:1 - 6
- [65]. Raghuv eer, M. and Nikias, C.; *Bispectrum estimation for short length data* Proceedings of the IEEE International Conference on

- Acoustics, Speech and Signal Processing, 10, 1985, pp:1352 - 1355
- [66]. Papadopoulos, C.K. and Nikias, C.L.; *Bispectrum estimation of transient signals*, Proceedings of the IEEE International Conference on Acoustics, Speech and Signal Processing, 4, 1988, pp:2404 - 2407
- [67]. Garth, L.M. and Bresler, Y.; *A comparison of optimized higher order spectral detection techniques for non-Gaussian signals*, Proceedings of the IEEE International Conference on Signal Processing, [see also IEEE International Conference on Acoustics, Speech, and Signal Processing,], 44(5), 1996, pp:1198 - 1213
- [68]. Grassia, F.; Tacconi, G.; Tiano, A. and Borghini, F.; *On non-Gaussian character-ization of shipping traffic underwater noise*, Proceedings of the Oceans Conference on Engineering in Harmony with Ocean. 3, 1993, pp: 285 - 292
- [69]. Nikias, C.L. and Raghuveer, M.; *Bispectrum Estimation : A digital Signal processing frame work*, Proceedings of the IEEE, 75(7), 1987, pp. 869-891
- [70]. Melvin J. Hinich, Davide Marandino and Edmund J. Sullivan; *Bispectrum of ship radiated noise*, J, Acoust. Soc. Am.; 85(4), 1989
- [71]. A.M Richardson and W. S Hodgkiss; *Bispectral analysis of underwater acoustic data*, J, Acoust. Soc. Am.; 96(2), 1994
- [72]. Mendel, J.M.; *Tutorial on higher-order statistics (spectra) in signal processing and system theory: theoretical results and some applications*, Proceedings of the IEEE , 79(3), 1991, pp: 278 - 305
- [73]. Quazi, A.H.; *Nonlinear sonar signal processing*, Proceedings of the International Conference on Signal Processing, 1, 1996, pp:264 - 267
- [74]. Martin L. Barlett, Kevin W. Baugh and Gary R. Wilson, *Transient detection using non stationary bispectrum*, J, Acoust. Soc. Am. 99(5), ,1996, pp: 3018-3028
- [75]. Gordon J. Frazer and Boualem Boashash, *Detection of Underwater Transient Acoustic Signals using Time Frequency Distributions and Higher-Order Spectra*, Proceedings of the IEEE Twenty-Fifth Asilomar Conference on Signals, Systems and Computers, 1991, pp:1103 - 1107.

- [76]. Tanmay Roy, Arun Kumar, and Rajendar Bahl , *Estimation of a coupling feature for target classification using passive sonar*, Proceedings of MTS/IEEE International conference on OCEANS, 1, 2005, pp: 148 – 153
- [77]. R. Rajagopal, K. Anoop Kumar and P Ramakrishna Rao, *An Integrated Approach to Passive Target Classification*, Proceedings of IEEE International Conference on Acoustics, Speech, and Signal Processing, 2(2), 1994, pp: 313 - 316
- [78]. Shapo, B. and Bethel, R.; *A novel passive broadband Bayesian detector/tracker*, Proceedings of the IEEE Workshop on Sensor Array and Multichannel Signal Processing. 2000, pp: 92 – 96
- [79]. Rajagopal, R.; Sankaranarayanan, B. and Ramakrishna Rao, P., *Target Classification in Passive Sonar – An Expert System Approach*, Proceedings of the IEEE International Conference on Acoustics, Speech, and Signal Processing, 5, 1990, pp:2911 - 2914
- [80]. Lourens, J. and Coetzer, M., *Detection Of Mechanical Ship Features From Under-water Acoustic Sound*, Proceedings of the IEEE international Conference on Acoustics, Speech, and Signal Processing, 12, 1987, pp: 1700 - 1703
- [81]. Brutzman, D.P.; Compton, M.A. and Kanayama, Y.; *Autonomous Sonar Classification Using Expert Systems*, Proceedings of IEEE International Conference of OCEANS on Mastering the Oceans Through Technology, 2, 1992, pp:554 – 559
- [82]. C.Adnet and N.Martin, *Unified And Intelligent Spectral Analysis*, Proceedings of IEEE International Conference on Acoustics, Speech and Signal Processing, 1990, pp:2599 - 2602
- [83]. Jae-Byung Jung; Jacobs, J.H.; Denny, G.F. and Simpson, P.K., *Broadband Sonar Target Classification: Pool Experiments*, Proceedings of the International Joint Conference on Neural Networks, 2, 2003, pp:1307 - 1312
- [84]. Donghui Li; Azimi-Sadjadi, M.R. and Robinson, M.; *Comparison of different classification algorithms for underwater target discrimination*, IEEE Transactions on Neural Networks, 15(1), 2004, pp. 189 – 194
- [85]. Purnell, D.W.; Botha, E.C. and Nieuwoudt, C.; *Classification of two ship targets using radar backscatter*, Proceedings of the South African Symposium on Communications and Signal Processing, 1998, pp:187 – 192.

- [86]. De Yao; Azimi-Sadjadi, M.R.; Jamshidi, A.A. and Dobeck, G.J.; *A study of effects of sonar bandwidth for underwater target classification*, IEEE Journal of Oceanic Engineering, 27(3), 2002, pp:619 – 627
- [87]. Robert E. Uhrig, *Introduction to artificial neural networks*, Proceedings of the Electronic Technology Directions to the Year 2000, 1995, pp:36 – 62
- [88]. Schoonees, J.A.; *Parallel distributed processing: practical applications of neural networks in signal processing*, Proceedings of the Southern African Conference on Communications and Signal Processing, 1988, pp: 76 – 80
- [89]. Richard P. Lippmann, *An Introduction to Computing with Neural Nets*. IEEE Acoustics, Speech, and Signal Processing Magazine, 4(2.1), 1987, pp: 4-22
- [90]. Paul, A.L. and Byrne, P.C.; *An efficient learning algorithm for the back propagation artificial neural network*, Proceedings of the IEEE Conference on Southeastcon, 1, 1990 pp:61 - 63, 63a
- [91]. Abdel Allim, O. and Fahmy Hashem, H.; *Automatic recognition of the sonar signals using neural network*, Proceedings of the URSI Fifteenth National Radio Science Conference, 1998, pp:C34/1 - C34/8
- [92]. Namjin Kim; Kehtarnavaz, N.; Yeary, M.B. and Thornton, S.; *DSP-based hierarchical neural network modulation signal classification*, IEEE Transactions on Neural Networks, 14(5), 2003, pp:1065 - 1071
- [93]. Martinez Madrid, J.J.; Casar Corredera, J.R. and de Miguel Vela, G.; *A Neural Network approach to Doppler based Target Classification*, Proceedings of the International Conference on Radar, 1992, pp:450 – 453
- [94]. Eapen, A.; *Neural Network For Underwater target Detection*, Proceedings of the IEEE Conference on Neural Networks for Ocean Engineering, 1991, pp:91 - 98
- [95]. Patel, A.K.; Wright, W.A. and Collins, P.R.; *Target Classification using Neural and Classical Techniques* Proceedings of the Third International Conference on Artificial Neural Networks, 1993, pp:238 – 242
- [96]. Chin-Hsing Chen, Jiann-Der Lee and Ming-Chi Lin, *Classification of Underwater Signals Using Neural Networks*,

References

- Tamkang Journal of Science and Engineering, 3(1), 2000, pp: 31-48
- [97]. Azimi-Sadjadi, M.R.; De Yao; Qiang Huang and Dobeck, G.J.; *Underwater target classification using wavelet packets and neural networks* IEEE Transactions on Neural Networks, 11(3), 2000, pp:784 - 794
- [98]. Roth, M.W.; *Survey of Neural Network Technology for Automatic Target Recognition*, IEEE Transactions on Neural Networks, 1(1), 1990, pp:28 - 43
- [99]. Tim. L Overman and Ahmed Louri; *Target Detecting Neural network Architecture for Serial Sensor Data streams*, Proceedings of the International Conference on Electro/94, 1994, pp: 393-403
- [100]. Solinsky, J.C. and Nash, E.A; *Neural-network performance assessment in sonar applications*, Proceedings of the IEEE Conference on Neural Networks for Ocean Engineering, 1991, pp:1 - 12
- [101]. Howell, B.P. and Wood, S.; *Passive sonar recognition and analysis using hybrid neural networks*, Proceedings of the Conference on OCEANS, 4, 2003, pp: 1917 - 1924
- [102]. Jennifer Hallinan and Paul Jackway; *Simultaneous Evolution of Feature Subset and Neural Classifier on High dimensional Data*, Proceedings of the Conference on Digital Image Computing and Applications, 1999,
- [103]. Ghosh, J.; Deuser, L. and Beck, S.D.; *A neural network based hybrid system for detection, characterization, and classification of short-duration oceanic signals*, IEEE Journal of Oceanic Engineering, , 17(4), 1992, pp: 351 - 363
- [104]. Yanning Zhang; Licheng Jiao and Hu Songhua, *An efficient method of target classification*, Proceedings of the Fourth International Conference on Signal Processing, 2, 1998, pp:1181 - 1184
- [105]. Adams, S. and Jobst, W.; *Statistical properties of underwater acoustic ambient noise fields*, Proceedings of the IEEE International Conference on Acoustics, Speech, and Signal Processing, 1, 1976, pp: 656 - 659
- [106]. John R. Potter, David K. Mellinger and Christopher W. Clark; *Marine mammal call discrimination using artificial neural networks*, J. Acoust Soc Am. 96(3), 1994.

- [107]. Argenti, F.; Benelli, G.; Garzelli, A. and Mecocci, A.; *Automatic ship detection in SAR images*, Proceedings of the International Conference on Radar, 1992 , pp:465 – 468
- [108]. Del Amo, A.; Gomez, D. and Montero, J.; *Spectral Fuzzy Classification System for Target Recognition*, Proceedings of the 22nd International Conference of the North American Fuzzy Information Processing Society, 2003, pp: 495 – 499.
- [109]. Guillermo C. Gaunard, *Techniques for Sonar Target Identification*, IEEE Journal Of Oceanic Engineering, 12(2), 1987, pp: 419 - 422
- [110]. Kim, K.M.; Youn, D.H.; Doh, K.C. and Oh, W.C.; *An adaptive signal processing for enhanced target detection in active sonar systems*, Proceedings of the MTS/IEEE International OCEANS Conference on Riding the Crest into the 21st Century, 1 , 1999, pp: 295 - 298
- [111]. Dwyer, R.F.; *Classification of very wide bandwidth acoustic signals*, Proceedings of the MTS/IEEE Conference on OCEANS, 1, 1997, pp: 496 - 499
- [112]. Heale, A. and Kleeman, L.; *Fast target classification using sonar*, Proceedings of the IEEE/RSJ International Conference on Intelligent Robots and Systems , 3, 2001, pp: 1446 - 1451
- [113]. <http://www.dspguru.com/info/tutor/index.htm>
- [114]. M. Jahangir, K.M. Ponting and J.W. O’Loghlen, *Robust Doppler classification technique based on hidden Markov models*, IEE Proceedings Radar, Sonar and Navig., 150(1), 2003, pp: 33 - 36
- [115]. Lourens, J.G.; *Classification of ships using underwater radiated noise*, Proceedings of the Southern African Conference on Communications and Signal Processing, 1988, pp: 130 – 134
- [116]. Paul Chestnut, Helen Landsman and Robert W. Floyd, *A Sonar Target recognition experiment*, J. Acoust. Soc. Am. 66(1), 1979.
- [117]. Y. T. Chan, G. H. Niezgoda and S. P. Morton, *Passive Sonar Detection and Localization by Matched Velocity Filtering*, IEEE Journal Of Oceanic Engineering, 20(3), 1995, pp: 179 - 189
- [118]. Chen Xiangdong and Wang Zheng; *Time Domain characteristic Study of Ship Radiated Noise based on the Similar Sequence Repeatability*, Proceedings of the Fourth International Conference on Signal Processing, 2, 1998, pp: 1447 - 1450

References

- [119]. Guo Guirong, Zhang Wei and Yi Wenxian, *An Intelligence Recognition Method of Ship Targets*, Proceedings of the IEEE Aerospace and Electronics Conference, 1989, pp: 1088 - 1096
- [120]. Pezeshki, A.; Azimi-Sadjadi, M.R.; Scharf, L.L. and Robinson, M.; *Underwater target classification using canonical correlations*, Proceedings of the IEEE International Conference on OCEANS, 4, 2003, pp:1906 - 1911
- [121]. Su Yang and Zhishun Li; *Classification of ship-radiated signals via chaotic features*, Electronics Letters, 39(4), 2003, pp: 395 – 397.
- [122]. Yang S, Li Z and Wang X; *Ship recognition via its radiated sound: the fractal based approaches*, J. Acoust Soc. Am. 2002, pp: 112(1):172-7.
- [123]. Azimi-Sadjadi, M.R.; Robinson, M.; Jamshidi, A.A. and Dobeck, G.J.; *A biologically inspired adaptive underwater target classification using a multi-aspect decision feedback unit*, Proceedings of the MTS/IEEE International Conference on OCEANS, 1, 2002, pp: 38 - 45
- [124]. Paul Gaunard, Corine Ginette Mubikangiey, Christophe Couvreur and Vincent Fontaine, *Automatic Classification of Environmental Noise Events by Hidden Markov Model*, Proceedings of the IEEE International Conference on Acoustics, Speech, and Signal Processing, 6, 1998, pp:3609 – 3612.
- [125]. Grant, P. M.; *Speech recognition techniques*, IEE Journal of Electronics & Communication Engineering, 3(1), 1991, pp:37 – 48
- [126]. Linus M. Blaesser, *Walsh Power Spectrum for Wide-Sense Stationary Stochastic Processes*, IEEE Transactions on Information Theory, 32(5), 1986, pp:716 – 724
- [127]. George Tzanetakis and Perry Cook, *Musical Genre Classification of Audio Signals*, IEEE Transactions On Speech And Audio processing, 10(5), 2002, pp: 293-302.
- [128]. Sujay Phadke, Rhishikesh Limaye, Siddharth Verma and Kavitha Subramanian, *On Design and Implementation of an Embedded Automatic Speech Recognition System*, Proceedings of the 17th IEEE International Conference on VLSI Design, 2004, pp: 127-132.

- [129]. R.C.Kemerait and D.G.Childers, *Signal Detection and Extraction by Cepstrum Techniques*, IEEE Transactions on Information Theory, 18(6), 1972, pp: 745-757.
- [130]. Li Tan and Montri Karnjanadecha, *Modified Mel-Frequency Cepstrum Coefficient*, Proceedings of the Information Engineering Postgraduate Workshop, 2003, pp. 127-130
- [131]. Davis S. and Mermelstein, P., *Comparison of parametric representations for monosyllabic word recognition in continuously spoken sentences*, IEEE Transactions on Signal Processing, 28(4), 1980, pp: 357 - 366
- [132]. Sirko Molau, Michael Pitz, Ralf Schluter and Hermann Ney, *Computing Mel-Frequency Cepstral Coefficients on the Power Spectrum*, Proceedings of the IEEE International Conference on Acoustics, Speech and Signal Processing, 1, 2001, pp: 73-76.
- [133]. Mark D. Skowronski and John G. Harris, *Improving the Filter Bank of a Classic Speech Feature Extraction Algorithm*, Proceedings of the IEEE International Symposium on Circuits and Systems, 4, 2003, pp: 281- 284
- [134]. Sabato M. Siniscalchi, Fulvio Gennaro, Salvatore Andolina, Salvatore Vitabile, Antonio Gentile, and Filippo Sorbello, *Embedded Knowledge-based Speech Detectors for Real-Time Recognition Tasks* Proceedings of the 2006 International Conference on Parallel Processing Workshops, 2006, pp 6.
- [135]. Guido Bertocci, Brian W. Schoenherr and David G. Messerschmitt, *An approach to the Implementation of a Discrete Cosine Transform*, IEEE Transactions on Communications, 30(4), 1982, pp: 635 - 641
- [136]. Yoseph Linde, Andres Buzo, and Robert Gray, *An Algorithm for Vector Quantizer Design*, IEEE Transactions On Communications, 28(1), 1980, pp: 84 - 95
- [137]. Yih-Chuan Lin and Shen-Chuan Tai; *A fast Linde-Buzo-Gray algorithm in image vector quantization* IEEE Transactions on Circuits and Systems II: Analog and Digital Signal Processing, 45(3), 1998, pp: 432-435.
- [138]. James M. Keller, Michael R. Gray and James A. Givens. JR, *A Fuzzy K-Nearest Neighbour Algorithm*, IEEE Transactions on System, Man and Cybernetics, 15(4), 1985, pp: 580 - 585.
- [139]. Perfecto Herrera, Xavier Amatriain, Eloi Battle and Xavier Serra, *Towards Instrument Segmentation for Music Content Description:*

References

- A Critical Review of Instrument Classification Techniques*, Proceedings of the International Symposium on Music Information Retrieval, 2000
- [140]. Hyoung-Gook Kim, Moreau, N. and Sikora, T, *Audio classification based on MPEG-7 spectral basis representations*, IEEE Transactions on Circuits and Systems for Video Technology, 14(5), 2004, pp: 716 - 725
- [141]. Lindsay I Smith; *A Tutorial on Principal Components Analysis* , downloaded from <http://kybele.psych.cornell.edu/~edelman/Psych-465-Spring-2003/PCA-tutorial.pdf>
- [142]. Lawrence R. Rabiner; *A Tutorial on Hidden Markov Models and Selected Applications in Speech Recognition*, Proceedings of IEEE, 77(2), 1989, pp: 257- 286
- [143]. Ziyou Xiong, Regunathan Radhakrishnan, Ajay Divakaran and Thomas S. Huang; *Comparing MFCC and MPEG-7 Audio Features for Feature Extraction, Maximum Likelihood HMM and Entropic Prior HMM for Sports Audio Classification*, Proceedings of the IEEE International Conference on Acoustics, Speech, and Signal Processing, 5, 2003, pp: 628 - 631
- [144]. Supriya M.H., Shaheer K., Mahendran M.G. and P.R. Saseendran Pillai: *Towards Improving the Target Recognition Using a Hierarchical Target Trimming Approach*: WSEAS Transactions on Signal Processing, Vol 3(5), 2007, pp. 340- 345.
- [145]. Robert Gavelin, Harald Klomp, Clinton Priddle and Mats Uddenfeldt; *Blind Source Separation, 2004, pp 1- 19*
- [146]. A. Jourjine, S. Rickard, and O. Yilmaz., *Blind Separation of Disjoint Orthogonal Signals: Demixing N Sources from 2 Mixtures*, Proceedings of the 2000 IEEE International Conference on Acoustics, Speech, and Signal Processing, Istanbul, Turkey, June 2000, vol. 5, pp. 2985--88.

Publications brought out in the field of research

1. Supriya M.H. and P.R. Saseendran Pillai : *Implementation of an Intelligent Target Classifier*: Proc. ICONS-2002 (International Conference on Sonar Sensors and Systems), Allied Publishers, New Delhi, Vol .1, 2002, pp. 313 – 318.
2. Supriya M.H. and P.R. Saseendran Pillai: *Development of an Underwater Target Classifier Using Target Specific Features*: J. Acoust. Soc. Am., 113 (4, Pt. 2), 2003, p. 2261.
3. Supriya M.H. and P.R. Saseendran Pillai: *Implementation of an Estimation Processor for the Extraction of Spectral Components*: Proc. SYMPOL-2003 (National Symposium on Ocean Electronics), Allied Publishers Pvt. Ltd., New Delhi, 2003, pp.117-123.
4. Supriya M.H. and P.R. Saseendran Pillai: *Implementation of Algorithms for Extracting Tonal Components in Underwater Noise*: J. Acoust. Soc.Am.115 (5, Pt. 2), 2004, p. 2613.
5. Supriya M.H., Mohan Kumar K. and P.R. Saseendran Pillai: *Bispectral Estimation for Detecting Phase Coupled Noises in the Ocean*: J. Acoust. Soc. In, Vol 33, 2005, pp.551- 556
6. Supriya M.H. and P.R. Saseendran Pillai: *An Optimized Autoregressive Spectral Estimator for Vessel Generated Noise*: J. Acoust. Soc. In , Vol 33, pp.584 - 590.
7. Supriya M.H. and P.R. Saseendran Pillai: *Analysis of Variable Length Data Records for Generating Spectrally Decomposable Target Specific Features*: J. Acoust. Soc. Am, Vol 118(3, Pt. 2), 2005, p.1967.
8. Mohan Kumar K., Supriya M.H. and P.R. Saseendran Pillai: *Detection of Nonlinear Noise Sources in the Ocean Using Bicoherence*: Proc. SYMPOL-2005 (National Symposium on Ocean Electronics), Allied Publishers Pvt. Ltd., New Delhi, 2005, pp.207 – 213.
9. Supriya M.H., Shaheer K., Mahendran M.G. and P.R. Saseendran Pillai: *Towards Improving the Target Recognition Using a Hierarchical Target Trimming Approach*: WSEAS Transactions on Signal Processing, Vol 3(5), 2007, pp. 340- 345.
10. Supriya M.H., and P.R. Saseendran Pillai: *Towards Improving the Target Recognition Using Spectral and Cepstral Features*: J. Acoust. Soc.Am. 121(5, Pt. 2), 2007, p. 3046.

Publications

11. Supriya M.H., and P.R. Saseendran Pillai: *Hidden Markov Model Based Underwater Target Classifier*: Accepted for presentation at the International Symposium on Ocean Electronics (SYMPOL 2007)
12. Mohan Kumar K., Supriya M.H. and P.R.Saseendran Pillai : *Extraction of Bispectral features using Principal Component Analysis*: Accepted for presentation at the International Symposium on Ocean Electronics (SYMPOL 2007).

Other Publications

1. James Kurian, Supriya M.H. and P.R. Saseendran Pillai.: *Design and Implementation of a Computer Controlled Transducer Positioning System for an Acoustic Tank*: Proc. NICE 2001 (National Conference on Technology Convergence for Information Communications & Environment), 2001, pp 221- 224.
2. James Kurian, Supriya M.H. and P.R.Saseendran Pillai: *Development of an Automated Transducer Positioning System for an Underwater Test Facility*: Proc. SYMPOL-2001(National Symposium on Ocean Electronics), 2001, pp.84-88.
3. Anil Kumar C.P., Sajith N.Pai, Soniraj N., James Kurian, Supriya M.H., Madhavan.C., and P.R. Saseendran Pillai.: *Studies of Target Strengths of Fishes Under Captive Condition* : Proc.SYMPOL-2001(National Symposium on Ocean Electronics), 2001, pp.124-129.
4. Anil Kumar C.P., Sajith.N.Pai, Soniraj.N., Saseendran Pillai.P.R., James Kurian, Supriya M.H., Madhavan.C., and Mani.T.K.: *Studies on Geometrical Backscattering Models of Marine Bodies* : J. Acoust. Soc. Am., 113 (4, Pt. 2), 2003, p. 2236.
5. Mani.T.K., P.R Saseendran Pillai, James Kurian and Supriya M.H.: *Rain Parameter Estimation Using Impact Generated Low Frequency Acoustic Signals* : J. Acoust. Soc. Am., 113 (4, Pt. 2), 2003, p. 2278.
6. Binu George, Anand Raj, Supriya M.H., James Kurian and P.R Saseendran Pillai. : *Development of a Spread Spectrum Communication System for Underwater Telemetry Applications* : Proc. SYMPOL-2003 (National Symposium on Ocean Electronics), Allied Publishers Pvt. Limited, New Delhi, 2003, pp.55-61
7. Sajith.N.Pai, Anilkumar C.P., Soniraj N., Balu.N., Supriya M.H., James Kurian, Madhavan.C. and P.R Saseendran Pillai.. : *Backscattering Models of Sardines*, Proc. SYMPOL-2003 (National Symposium on Ocean Electronics), Allied Publishers, Pvt. Limited, New Delhi, 2003, pp.146-149.
8. Anil Kumar C.P., Sajith.N.Pai, Soniraj N., Balu.N., Supriya M.H., James Kurian, Madhavan.C. and P.R Saseendran Pillai.. : *Numerical Analysis for Geometrical Backscattering of Selected Marine Specie*, Proc. SYMPOL-2003 (National Symposium on

Publications

- Ocean Electronics), Allied Publishers, Pvt. Limited, New Delhi, 2003, pp. 157-161.
9. Anil Kumar C.P., Sajith.N.Pai, Soniraj N., Balu.N., Supriya M.H., James Kurian, Madhavan.C., and P.R Saseendran Pillai. : *Development of an Algorithm for Biomass Estimations*, Proc. SYMPOL-2003 (National Symposium on Ocean Electronics), Allied Publishers Pvt. Ltd., New Delhi, 2003, pp.150-156
 10. Anand Raj, Binu George, Supriya M.H., James Kurian and P.R Saseendran Pillai., *Doppler Compensated Underwater Acoustic Communication System* : J. Acoust. Soc. Am. 115(5, Pt. 2), 2004, p. 2507.
 11. Anil Kumar.C.P., Sajith.N.Pai, Soniraj.N., Supriya M.H., James Kurian, Madhavan.C. and P.R Saseendran Pillai. : *An Echo Analysis Technique for Estimating the Fish Population* : J. Acoust. Soc. Am. 115(5, Pt. 2), 2004, p. 2584.
 12. Shery Joseph Gregory, Jinto George, Prajas John, Supriya .M.H. and P.R. Saseendran Pillai: *Development of an Electronic Tag for Monitoring Ocean Temperature*, Proc. SYMPOL-2005 (National Symposium on Ocean Electronics), Allied Publishers Pvt. Ltd., New Delhi, 2005, pp.251 – 256.
 13. Prajas John, Jinto George, Supriya M.H. and P.R.Saseendran Pillai : *Development of a Miniaturised Pressure Tag for Ocean Depth Measurements*, Accepted for presentation at the International Symposium on Ocean Electronics (SYMPOL 2007).
 14. Jinto George, Prajas John, Supriya M.H. and P.R.Saseendran Pillai : *Geolocation Estimation Using Light Intensity Measurements*, Accepted for presentation at the International Symposium on Ocean Electronics (SYMPOL 2007).
 15. Ananthakrishnan V., Supriya M.H. and P.R.Saseendran Pillai : *Development of a Hydrophone Array Controller for Ocean Surveillance Applications*: Accepted for presentation at the International Symposium on Ocean Electronics (SYMPOL 2007).
 16. C.Prabha, Supriya M.H. and P.R.Saseendran Pillai : *Model Studies on the localisation of Underwater Target using Sensor Networks*: Accepted for presentation at the International Symposium on Ocean Electronics (SYMPOL 2007).

17. S.Maheswaran, Supriya M.H. and P.R.Saseendran Pillai: Realisation of an RF link for Sensor *Networks*: Accepted for presentation at the International Symposium on Ocean Electronics (SYMPOL 2007).

Subject Index

Subject Index

A

acoustic levels6
Active sonar2, 3, 5
ambient noise .. 11, 15, 16, 17, 18, 19, 28, 29,
30, 32, 33, 35, 52, 65, 80, 88, 89, 90, 179,
182, 214, 226
Ambient Noisexxi, 10, 15, 89, 233
AR... 36, 37, 39, 50, 51, 96, 97, 99, 100, 101,
102, 103, 104, 105, 106, 107, 108, 109,
110, 111, 113, 114, 115, 116, 117, 119,
120, 122, 123, 124
ARMA 34, 36, 37, 38, 42, 50, 97, 98, 106,
107, 108, 110, 111, 112, 117, 118, 121,
122, 235
autobicorrelation 153, 155
autocorrelation 24, 38, 39, 47, 49, 51, 93, 98,
100, 101, 102, 104, 107, 153, 154, 155,
156, 160, 164, 166
Autocorrelation36, 105

B

beamforming5
Beamforming5
Bicoherence..... 158, 159
Biological sources 16
bispectral estimation 24, 26, 51, 191, 192
Bispectral Features81
bispectrum..... 49, 50, 52, 53, 54, 82, 83, 153,
155, 156, 158, 159, 160, 161, 162, 163,
164, 165, 166, 167, 168, 169, 170, 175,
176, 239
bi-static.....7
bubbles..... 16, 21, 29, 30, 182
Burg ... 39, 100, 101, 102, 109, 113, 115, 124

C

Cepstral ... 23, 41, 43, 46, 47, 48, 80, 81, 126,
129, 136, 140, 145, 148, 191, 236, 237,
245
cepstral analysis.. 23, 26, 42, 75, 80, 87, 148,
192, 228
Cepstral Coefficients..... 23, 48, 81, 136, 140,
148, 245
Classifier ... 28, 54, 55, 57, 58, 62, 65, 76, 85,
180, 181, 193, 198, 211, 242
Classifiers.....21, 54, 66
complex cepstrum 129
Correlogram 93
Covariance 100, 101, 102, 109, 113, 124
Cumulant Generating Function 151
Cumulants 151, 152

D

Detection Threshold 10
directivity index 10, 11
discrete cosine transform.... 47, 136, 139, 145
Doppler
 shift,effect 6, 22, 40, 60, 67, 75, 251
Doppler effects 22
DT 10, 12, 13

E

Euclidean distance..... 61, 143, 194, 229
Euclidean Distance.. 181, 193, 194, 218, 223,
225

Realisation of a Target Classifier for Noise Sources in the Ocean

F

Fast Fourier Transform23, 141
 FFT91
 feature extraction... 24, 33, 44, 61, 62, 64, 69,
 70, 84, 178, 203, 207, 234, 237
 feature selection 26, 43, 58, 62, 64, 84
 Feature Selection..... 84
 feature vector 27, 71, 77, 84, 85, 193, 194,
 195, 196, 197, 219, 223, 225, 227, 229,
 231
 Feature Vector..... 84, 194, 211
 Features..... 34, 41, 49, 77, 80, 124, 145, 175,
 190, 237, 238, 240, 246
 Fuzzy.. 65, 181, 194, 195, 196, 218, 223, 225

G

Gaussian.... 22, 24, 28, 30, 32, 33, 45, 47, 49,
 50, 51, 52, 57, 77, 82, 88, 150, 151, 154,
 155, 156, 157, 158, 159, 163, 164, 176,
 228

H

Hamming59, 145, 200
Hamming window 141
 harmonic structure... 23, 80, 81, 87, 126, 136,
 148
 Hidden Markov models..... 67, 71
 Hidden Markov Models 198
 Hierarchical Target Trimming Approach 193,
 196, 211, 229, 247, 248
 Hydrodynamic..... 15, 16, 20, 21
 Hydrodynamic..... 15
 Hydrodynamic sources..... 16, 20

K

K-Nearest Neighbour 181, 194, 195, 218,
 223, 225

kurtosis.....47, 151, 154

M

MA .. 37, 96, 97, 99, 104, 105, 106, 107, 108,
 110, 111, 112, 116, 117, 118, 120
 Machinery Noise20
 Maximum Likelihood Estimation 67
 Mel Frequency Cepstral Coefficients.81, 136
 MFCC ... 23, 41, 42, 44, 48, 81, 87, 136, 137,
 139, 140, 142, 143, 144, 145, 146, 147,
 148, 236, 237, 246
 Modified Covariance..... 100, 101, 109, 124
 Moment Generating Function 151
 mono-static.....7
 multi-static7

N

NL..... 11
 noise sources 1, 15, 19, 24, 52, 63, 71, 80, 83,
 107, 121, 124, 130, 146, 147, 178, 179,
 193, 214, 218, 219, 223, 225, 226, 227,
 230
 NoiseSpectrumEnvelope..... 199, 203, 232
 Number of Peaks 79, 126

P

Parametric Estimators 95
 Passive sonar 2, 7, 8, 9, 242
 Passive sonars 74
 Peaking frequencies 79, 126
 periodograms.....35, 38
 Periodograms 94
 polyspectrum..... 152, 154, 155
 Power Spectral Density 92
 Projector Source Level
 SL xxi, 10

Subject Index

Propellers20
PSD . 91, 92, 93, 95, 100, 103, 104, 105, 106,
108, 110, 117

Q

QPC.... 82, 167, 168, 169, 170, 171, 177, 228
Quadratic Phase Coupling.....82, 164, 167

R

radiated noise .. 12, 13, 14, 19, 20, 28, 32, 43,
52, 69, 70
real cepstrum..... 128, 129
receiver.... 3, 5, 6, 7, 8, 11, 12, 22, 27, 40, 47,
55, 57, 58, 63, 75, 77, 88
Receiving Directivity Index 10
Reverberation Level 10
reverberation noise 19

S

Seismic sources 15
self noise 11, 19, 28
Self Noise Level..... 10
skewness 47, 151, 154, 156
Sonar. 1, 2, 3, 4, 8, 10, 13, 14, 19, 27, 55, 66,
74, 238, 240, 243, 244
sonar equation 12, 13
sonar parameter9
source level 11, 12, 31, 32
Spectral 34, 49, 52, 57, 68, 77, 78, 79, 91, 92,
93, 94, 99, 106, 107, 108, 109, 124, 126,
184, 191, 192, 234, 235, 238, 240, 243
spectral envelope.... 23, 42, 80, 126, 130, 148
Spectral Flux 79
Spectral Range 78
Spectral Roll off..... 79
Spectral Slope 79

submarines2, 7, 14, 20, 59
succcss rates 7, 34, 71, 179, 217, 225, 232
Surface waves..... 16, 89

T

target 172, 218, 234, 240, 241, 242, 243, 244
identification, classification 2, 3, 4, 6, 7, 8,
10, 11, 12, 13, 14, 15, 19, 22, 24, 26,
27, 35, 37, 46, 49, 54, 56, 57, 59, 60,
63, 66, 67, 68, 69, 70, 71, 73, 74, 75,
76, 77, 80, 83, 85, 86, 124, 138, 177,
178, 179, 180, 181, 183, 187, 190,
191, 192, 193, 194, 195, 196, 197,
198, 199, 211, 212, 223, 225, 226,
227, 228, 230, 231
target feature record 77, 180, 191, 228
Target Motion Analysis..... 8
Target Source Level 11
Target Strength..... 11, 74
Thermal agitations..... 15
time of arrival 5
torpedo 35, 184, 185, 187
Transmission Loss
TL 9, 10
transmitter 7, 75
turbulence 16, 20, 29, 90

V

Vector quantization 142

W

Window..... 141

Y

Yule-Walker..... 100, 101, 102, 109, 110, 124